NASA CR-159,471

A Reproduced Copy

OF

NASA CR-159,471

NASA CR-159471
R79AEG573

QUIET CLEAN SHORT-HAUL EXPERIMENTAL ENGINE (QCSEE) UNDER-THE-WING (UTW) ENGINE COMPOSITE NACELLE TEST REPORT

Volume I - Summary, Aerodynamic and Mechanical Performance

APRIL 1979

by

Advanced Engineering and Technology Programs Department
Aircraft Engine Engineering Division

Prepared For

National Aeronautics and Space Administration

NASA-Lewis Research Center
NAS3-18021

TABLE OF CONTENTS

TABLE OF CONTENTS (Continued)

TABLE OF CONTENTS (Concluded)

LIST OF ILLUSTRATIONS

LIST OF ILLUSTRATIONS (Continued)

LIST OF ILLUSTRATIONS (Continued)

LIST OF ILLUSTRATIONS (Concluded)

LIST OF TABLES

LIST OF TABLES (Concluded)

1.0 SUMMARY

The QCSEE UTW Propulsion System was tested with a composite flight-type nacelle at General Electric's Peebles, Ohio Outdoor Test Site IV-D during the fourth quarter of 1977 and the first and third quarters of 1978. One hundred and six hours of engine operation were completed, including mechanical and performance checkout, baseline acoustic testing with a bellmouth inlet, fully suppressed acoustic testing with a flight-type composite inlet, reverse thrust testing, acoustic technology tests, and limited controls testing. The engine included a variable-pitch fan having advanced composite fan blades and using a ball-spline pitch actuation system.

Acoustic results of the testing were within 2 EPNdB of the 95 EPNdB sideline noise goal at approach and takeoff conditions. A maximum reverse thrust of 27 percent of maximum installed forward thrust was reached, and the sideline noise level at this condition was 5 PNdB above the 100 PNdB goal. Although the engine source noise somewhat exceeded predictions, the suppression performed very close to objectives. Furthermore, the program goal was based on power settings for a 609.6 m (2000 ft) runway, and studies indicated that a 914.4 m (3000 ft) runway would be a more likely requirement. The 95 EPNdB goal could be met at the lower power setting required for a 914.4 m (3000 ft) runway.

Engine performance results verified the data from previous testing, meeting all performance objectives except the 35 percent reverse thrust goal.

The composite blades were known to be satisfactory for test stand operation only, because of inadequate FOD (bird strike) resistance. The blades exhibited a vibratory response in the range of the first flex/two per rev intersection, aggravated by high tailwind and crosswind conditions. Testing was delayed by unusually severe weather conditions during the winter test period. Prolonged snow cover delayed far-field acoustic testing, and high winds restricted engine operation.

Other advanced design features including the main reduction gear, digital control, and composite nacelle components operated satisfactorily throughout the test.

After successful demonstration of most of the contract goals, the engine was removed from the test stand in May 1978. It was reinstalled in July 1978 for acoustic technology tests to investigate the source of higher-than-expected unsuppressed noise levels.

The fully automatic control mode was activated during the final test period, indicating very stable operation at several steady-state power settings, and with limited (five percent) power transients. When larger transients were attempted, a speed overshoot of 300 rpm was observed. This problem is believed to be a result of internal leakage in the hydraulic motor that positions the blades, and could possibly be alleviated by increasing the electrical gain in this control circuit.

Following completion of this testing, the engine was removed from the test stand in July 1978, refurbished, and delivered to NASA-Lewis Research Center for further testing with a wing/flap system.

2.0 INTRODUCTION

The General Electric Company is currently engaged in the Quiet, Clean, Short-Haul Experimental Engine Program (QCSEE) under Contract NAS3-18021 to the NASA-Lewis Research Center. The Under-the-Wing (UTW) engine was designed and built under the program, to develop and demonstrate technology applicable to engines for future externally blown flap short-haul transport aircraft. The engine contained the following advanced technology features:

- Variable-pitch fan
- Composite fan blades
- Ball-spline blade actuation system
- Main Reduction Gear
- Composite fan frame
- Digital control

The initial buildup of the UTW engine was tested with a boilerplate nacelle during the period from September 2 through December 17, 1976, as reported in Reference 1. Uninstalled and installed performance were investigated. Testing was interrupted during initial reverse thrust testing by an exhaust nozzle attachment ring failure.

The engine was repaired, the harmonic drive variable actuation system was replaced with a ball-spline system, and the engine was reinstalled with the complete composite nacelle to resume testing in July 1977. This report covers all testing of the final engine configuration.

3.0 DESCRIPTION OF EQUIPMENT TESTED

The Under-the-Wing propulsion system (Figure 1 and Reference 2) included a variable-pitch, high bypass ratio, gear-driven fan, and a YF101 core engine and low pressure turbine. The fan blades, fan frame, and the entire nacelle were constructed of advanced composite materials. The fan exhaust nozzle was a four-flap variable area composite assembly. The core exhaust nozzle consisted of a shroud and plug with both hardwall and acoustically treated metal parts available. The engine was tested with two inlets: a bellmouth design for performance calibration and a composite high throat Mach number inlet designed to suppress forward-radiated fan noise. A more detailed description of these components follows. A cross-section drawing of the propulsion system is provided in Figure 2.

3.1 FAN ROTOR ASSEMBLY

The UTW engine has 18 composite fan blades mounted in trunnions to allow the fan blade pitch angle to be changed by rotating the trunnions. The blade and trunnion centrifugal loads are carried by single-row ball, grease-lubricated bearings. Secondary and vibratory loads from the trunnions are carried by dry thrust and journal bearings located in the periphery of the machined titanium disk.

The variable-pitch actuation mechanism developed by General Electric, includes an electrohydraulic servovalve, which directs high pressure oil to the hydraulic motor. The motor sends a pitch change command through a differential gear set and a no-back. Motion of the no-back is reduced in a ball screw and ball spline, rotating two opposed ring gears. These gears engage bevel pinions on the bases of the blades to vary blade pitch angle.

3.2 MAIN REDUCTION GEAR

The main reduction gear set for the UTW engine is an epicyclic star configuration developed by Curtiss-Wright Corporation. The low pressure turbine rotor is splined to a sun gear which drives a ring gear through a set of six star gears. The star gears are mounted on tandem, spherical roller bearings which are supported by a fixed carrier. Lubrication requirements for the reduction gear vary between approximately 1134 cc/s (18 gpm) at idle to approximately 1512 cc/s (24 gpm) at takeoff. The gear ratio is 2.4648, and both the input and output are flexibly mounted to prevent engine deflections from influencing the gear operation.

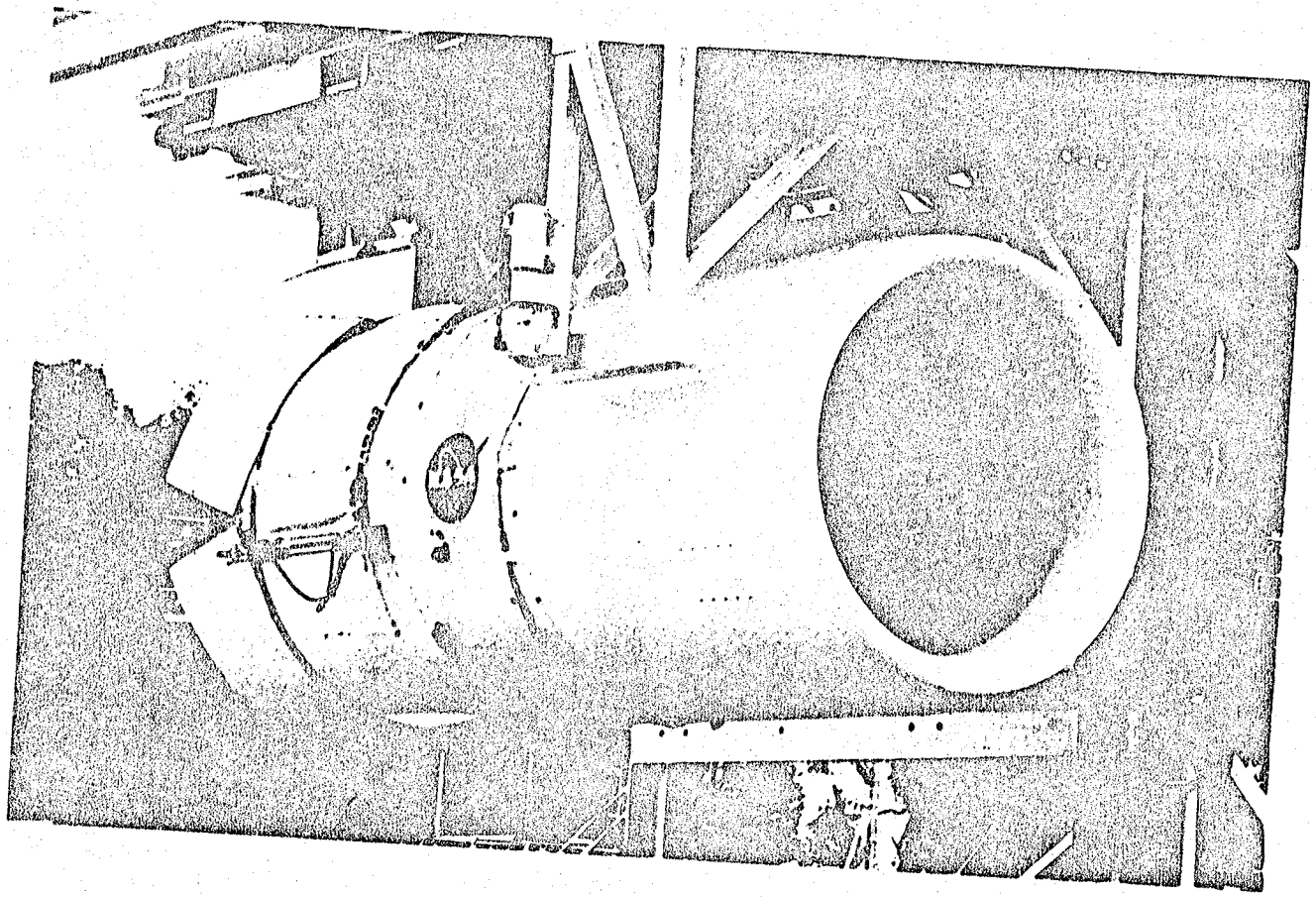

Figure 1. QCSEE Engine on Test.

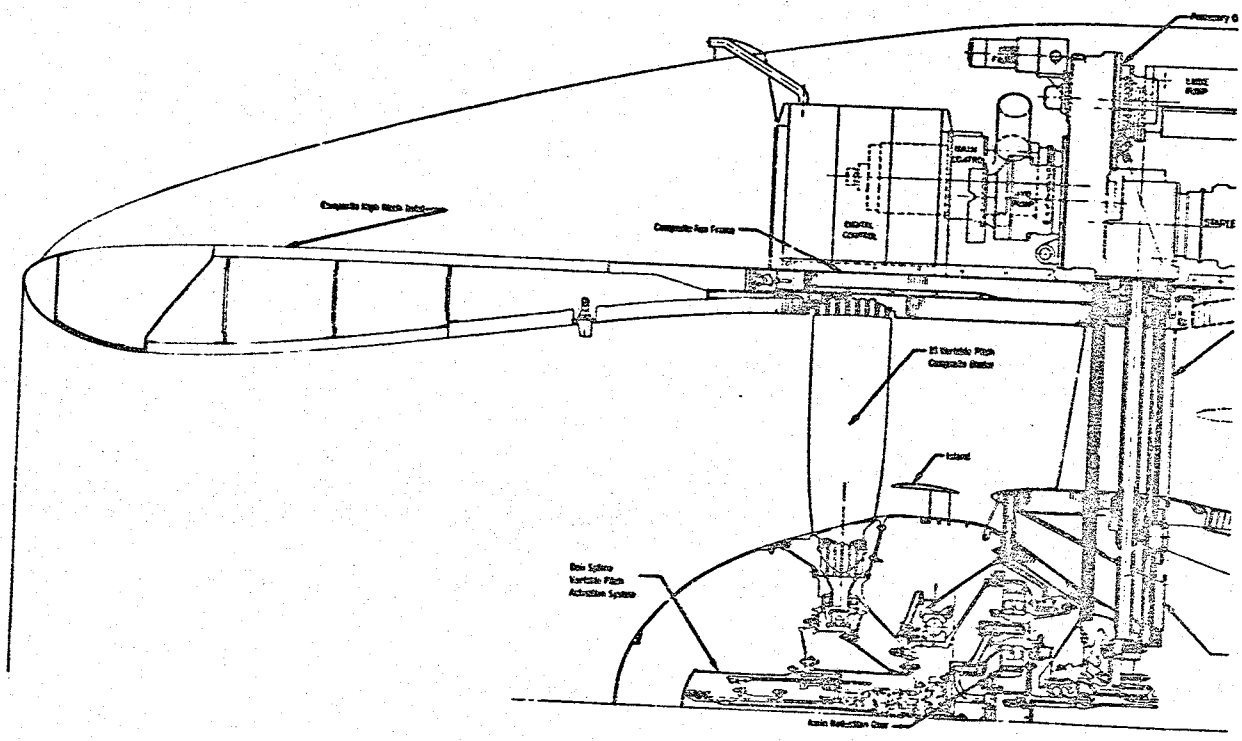

Figure 2. UTW Build-Up N

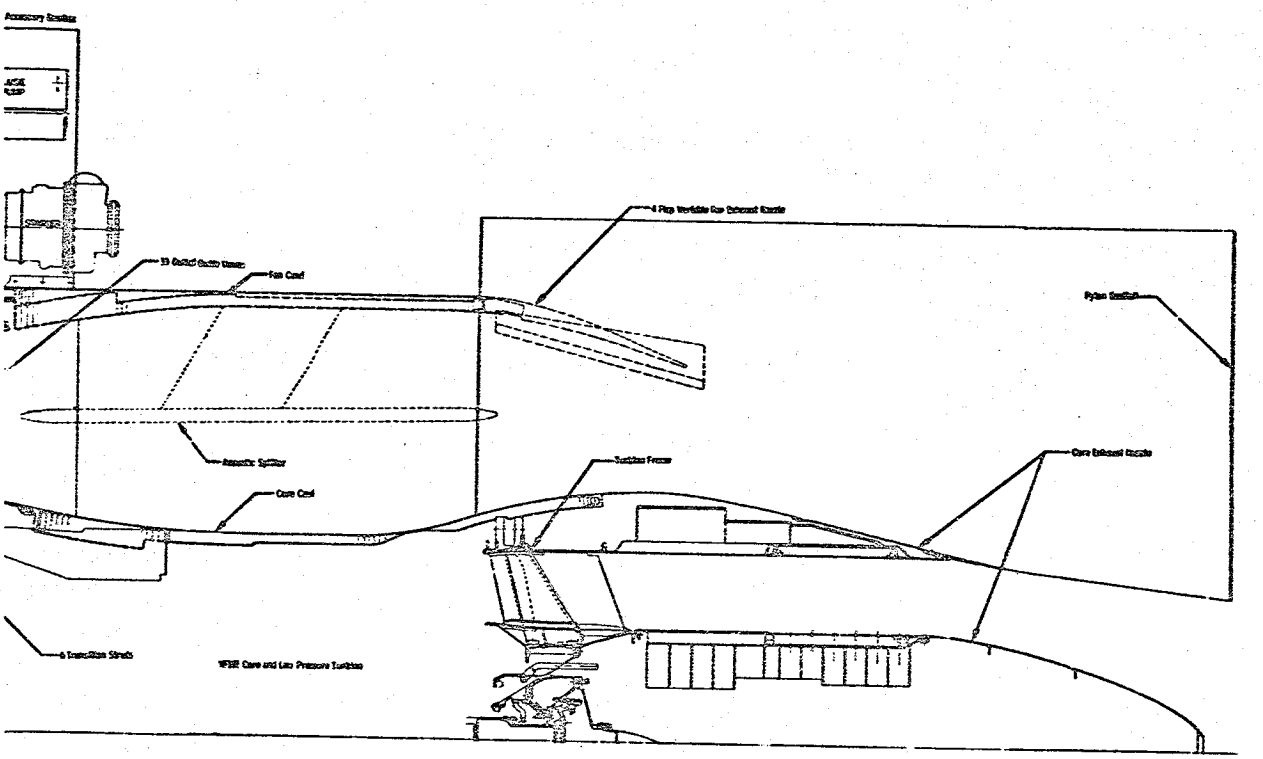

1-Up No. 2 Cross Section.

3.3 FAN FRAME

The fan frame is an all-composite static structure formed from integration of several separate structures, as shown in Figure 3. The outer casing of the frame combines the function of the nacelle with the frame outer shell. This casing provides part of the external nacelle surface as well as the internal fan flowpath. Fan blade tip treatment is provided by a grooved structure integrated into the forward portion of the outer casing. Containment of failed composite airfoils is provided by a felted Kevlar band in the outer casing. Positioning of the fan and core engine relative to the outer casing is provided by 33 vanes which also serve as the fan-bypass stator vanes. The hub of the frame is connected to the frame splitter through six equally spaced struts. The inner shell of the outer casing, the bypass duct and core duct surfaces of the frame splitter, and the pressure faces of the bypass vanes are perforated to provide acoustic suppression within the frame structure. The forward end of the compressor attaches to the rear of the frame at the exit of the frame inner airflow path. The outer cowl doors attach by a tongue-and-groove arrangement to the outer casing at the rear of the frame. The core cowl doors attach in a similar manner to the casing. The frame also provides the major support point for the engine through a uniball and two thrust mounts located at the top of the core cowl.

Flow turning of the fan flow into the core is provided by an independent set of metallic outlet guide vanes attached to the forward flange of the frame hub. The island splitter is formed from sheet metal with stator vanes penetrating and brazed to the skins. The stator vanes are supported at the hub through brazed joints into an inner casing that is bolted to the fan frame.

3.4 ENGINE

The QCSEE UTW engine utilized the YF101 core with modifications described as follows.

The nine-stage, highly loaded compressor is designed for 12.5 pressure ratio at 27.2 kg/s (60 lbs/sec) corrected flow. The IGV and Stage 1-3 vanes are variable to control stall margin and performance at part-speed conditions. The stator schedule was modified to high-flow the compressor above 83 percent corrected speed and to provide additional stall margin in the starting range. The schedule change necessitated minor modifications to the actuation linkage, and also a flex-cable feedback was used in place of the F101 splined shaft system.

The YF101 first-stage compressor blades have leading and trailing edges "cropped" at the tip. The QCSEE utilized the full-span PV airfoil mounted on the PFRT dovetail. The mechanical rotor speed limit was set at 14,050 rpm to ensure adequate vibratory margin.

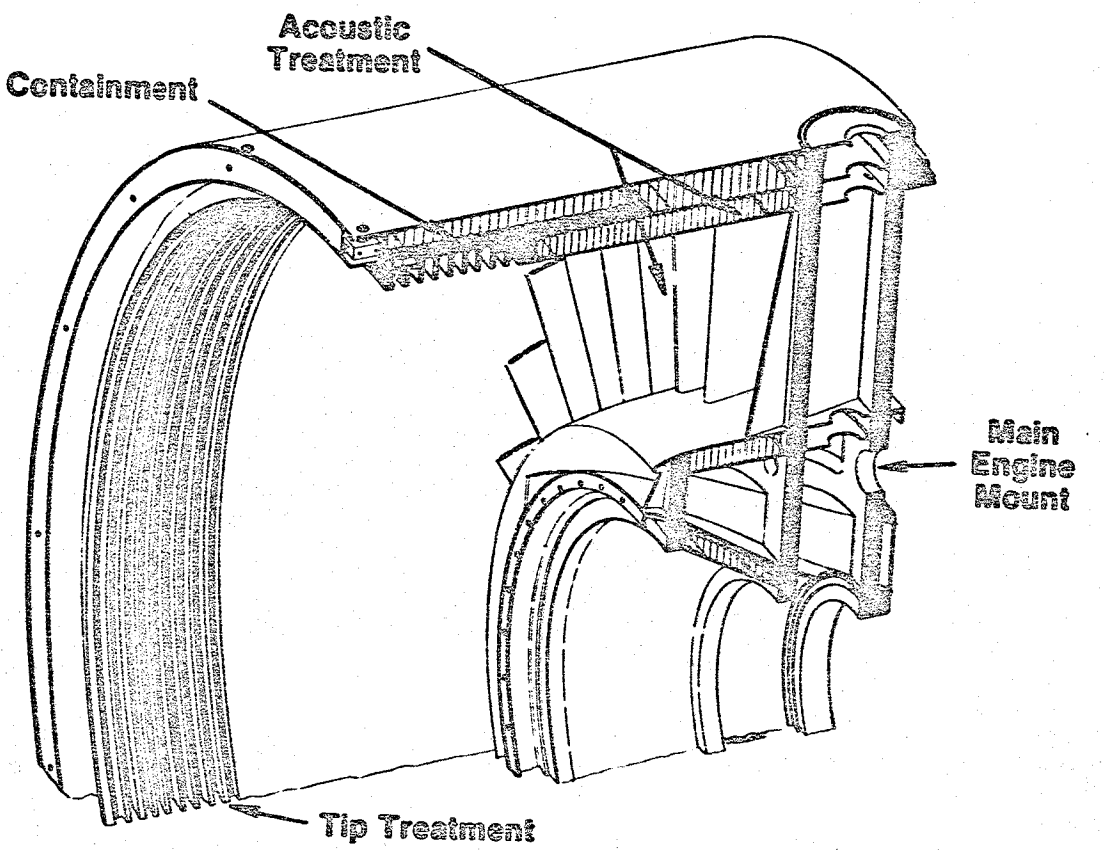

Figure 3. Composite Fan Frame.

The UTW engine used the PV central injector dome combustor to achieve lower emission levels than the PFRT design as demonstrated by rig testing. A single, manually operated ignitor was used in place of the F101 dual automatic system.

The YF101 high pressure turbine used in the QCSEE is a single-stage design utilizing very high tip speed to achieve the required level of energy extraction in a single stage. Cooling air is introduced into the rotor through an inducer located inboard of the nozzle vanes. The vanes are film/impingement cooled by CDP air. The UTW engine used F101 "warm bridge" blades having demonstrated high temperature and cyclic life advantages over the PFRT design. The blades were frequency screened to ensure that the two-stripe vibratory mode is resonant with vane passage frequency well above the operating range. HPT shrouds were of the improved PV design.

The low pressure turbine of the UTW engine was identical to the YF101 two-stage, tip shrouded design except that the PV second-stage blade was used. This blade is slightly decambered to reduce the exit swirl resulting from increased energy extraction. The turbine frame vane/struts were extended 2.54 cm (1 inch) forward to accept the greater turbine exit swirl. The frame was also modified to provide engine mounts not required in the long duct F101.

The HPT diaphragm area was increased to provide 5 percent larger flow function, and the LPT area reduced to provide 5 percent smaller flow function than in the F101. These changes, required for cycle matching, were accomplished by rotating the vanes slightly in the bands before brazing.

In order to locate the ignitor plug in the pylon region and eliminate a space problem under the core cowl, the aft end of the engine was rotated 120° clockwise with respect to the compressor. The F101 infrared pyrometer was eliminated, since the digital control provided the capability to instantaneously calculate T_{41} based on measured P_{S3}, T_{T3}, and W_f.

Because of the reduction gear system in the LP power train, the fan rotor thrust could not be balanced against the LPT rotor thrust. A balance piston was therefore added to the rear of the LPT rotor. CDP air was used to balance the turbine rotor thrust. Fan rotor thrust was carried by a high-capacity ball bearing in the fan frame.

3.5 DIGITAL CONTROL

The digital electronic manipulates variables in response to commands representing those which would be received from an aircraft propulsion system. The system includes an F101 hydromechanical control through which the digital control maintains primary control of fuel flow. The fuel-operated servomechanisms in the hydromechanical control serve primarily as back-up fuel controlling elements and limits, although they are the primary controlling elements for the core compressor stator actuators. Fan blade

pitch angle and fan exhaust nozzle area are both controlled by the digital control, which furnishes electrical signals to electrohydraulic servovalves.

The commands to the digital control are introduced through the control room elements consisting of an interconnect unit, operator panel, and engineering panel. They provide means for the engine operator to introduce commands, to switch between available operating modes, to adjust various control constants, and to monitor control and engine data. In addition to these digital commands from the control room, the system also receives a mechanical input in the form of a power lever angle (PLA) transmitted to the hydromechanical control. This serves as an input to the backup governor and operates a positive fuel shutoff valve in the control.

The following control and engine variables are sensed by the control system:

- Core speed
- Low pressure turbine speed
- Core inlet temperature
- Core stator position
- Compressor discharge temperature
- Metering valve position
- Engine inlet static pressure
- Fan inlet temperature
- Free-stream total pressure
- Fan pitch angle
- Fan nozzle position
- Compressor discharge pressure
- Power lever angle
- Power demand

The control has several manual and automatic modes of operation. In the manual mode, the operator commands fuel flow, blade angle, and exhaust nozzle area. In the fully automatic mode, the operator commands percent rated thrust; the digital control varies fuel flow to hold engine pressure ratio (as a thrust parameter), varies fan blade angle to hold fan speed, and varies exhaust nozzle area to hold inlet Mach number. In all modes, the control provides accel and decel limits, overspeed, and overtemperature limits.

3.6 FAN NOZZLE

The fan exhaust nozzle (which acts as an inlet during reverse operation) consists of four composite flaps. These flaps are driven in a closed loop system to provide a fully modulating exhaust nozzle. Six hydraulic actuators, three in each rear cowling half, are arranged circumferentially to power the flaps. Flow control is by an electrohydraulic servovalve. Synchronization in each cowl half is provided by the common center mounted actuator in each half and by structural rigidity of the flap nozzle flanges. Cross-synchronization between right and left halves is provided by a rotary shaft coupling between two opposite actuators.

3.7 CORE NOZZLE

The core nozzle is a fixed area nozzle with a separate but interchangeable outer cowl bolted to the aft cone which can be trimmed for nozzle area adjustment. A radial service strut is located at the bottom centerline of the core exhaust nozzle to provide aerodynamic fairing over the oil inlet, oil drain, seal drain, and balance piston air lines that pass through the core nozzle to the sump. The strut is designed so that the strut and service lines need not be disassembled to remove the centerbody or outer duct. Both the outer nozzle and centerbody have been fabricated in both hardwall and acoustically treated configurations.

3.8 ACCESSORY DRIVE SYSTEM

Engine accessory power is extracted from the core engine shaft through right angle bevel gearing (two F101 inlet gearboxes). The power is transmitted through radial drive shafting to a top-mounted accessory gearbox and to a scavenge pump mounted in the core cavity area on the bottom vertical centerline. Mounted on, and driven by, the accessory gearbox are the fuel pump and control, lubrication supply pump, hydraulic pump, control alternator, and starter drive pad. The radial drive shaft between the internal bevel gear and the accessory gearbox has a central support bearing to eliminate shaft critical speed problems. The shaft between the internal bevel gear and the bottom mounted scavenge pump does not require a central support bearing because of its short overall length.

3.9 INLET

Testing of the UTW engine required two inlet configurations. The NASA Quiet Engine "C" bellmouth inlet was utilized for aerodynamic and baseline acoustic testing. This inlet is mechanically decoupled from the engine to prevent overload of the composite fan frame flange due to excessive motion/vibration. An air seal is provided by an open-cell foam, Scott-Felt, bonded to one-half of the flange and pressed against the other. An acoustic seal is provided by lead foil in a vinyl cover. The second inlet tested is a graphite/

epoxy composite structure of flight contour. This inlet is directly mounted from the fan frame by 16 rotary latches. The inlet features an elevated throat Mach number (0.79) and integral acoustic treatment to suppress forward radiated fan noise.

3.10 FAN COWLING

The fan bypass duct is a graphite/epoxy composite structure consisting of two semicircular doors that include integral acoustic treatment. Core cowl access is accommodated by the hinged door construction of the outer ducting. The outer fan doors are attached to the pylon carry-through member by two heavy duty, piano-type hinges located at the top edge of the door assemblies. All fan cowl loads are carried by the fan frame.

3.11 ACOUSTIC SPLITTER

The aft duct acoustic splitter is a fabricated component consisting of aluminum sheet metal skins, machined rings, and honeycomb core resulting in a double-sandwich construction. The leading and trailing edge close-outs are machined aluminum rings. The assembly consists of two semicircular strutures supported from the fan duct doors by six stainless steel airfoil-shaped struts. Silicon seals have been applied to the ends of the splitter halves to dampen potential vibratory movement during engine testing. The splitter is designed to be removable. Separate filler pieces which duplicate the strut feet can be inserted in the fan door during engine operation without the splitter.

3.12 CORE COWL

The UTW core cowl is a composite structure made of graphite in a high temperature PMR matrix. It has a forward interface (Marman type joint) with the fan frame, and a rear interfacing slip joint with the core nozzle. Access to the compressor and turbine is provided by hinged-door construction. The core doors and skirt system are temporarily supported by the pylon through a set of pins when opened. The core cowl employs shop air for cooling. This air is ducted around the engine and released inside the core cowl. It exhausts upward through the pylon and to the fan stream,

3.13 ENGINE MOUNTS

Normal engine thrust and other operating loads are carried through the main engine mounts to the test stand. Thrust, vertical, and side loads are reacted at the front mount; vertical, side, and torque loads are taken by a three-link arrangement at the rear mount plane on the outer shell of the turbine frame.

3.14 HYDRAULIC SUPPLY SYSTEM

The hydraulic supply system provides hydraulic power to the fan nozzle (A18) actuators and the fan blade actuation system. A pressure compensated hydraulic piston pump is driven by the accessory gearbox and provides varying flow output at constant pressure to servovalves which are part of the fan duct nozzle and variable-pitch systems. Pump output flow is determined by the demand from the servovalves, varying from zero at holding condition to maximum during the engine thrust reversal transient. The hydraulic system receives and uses the same oil as the engine lubrication system. Once the hydraulic system is filled, however, it functions vary nearly as an independent closed system. A 10-micron filter provides contaminant protection at the servovalve inlet.

3.15 FUEL SYSTEM

The UTW fuel delivery system is composed of F101 engine main fuel system components. The system includes the hydromechanical control (metering section), main fuel pump, and fuel filter.

3.16 IGNITION SYSTEM

The ignition system consists of an ignition exciter box, ignition lead, and spark igniter located in the pylon. These components are of CFM56 design. The system will permit continuous sparking with a stored exciter energy of 14.5 to 16.0 joules for a delivered nominal spark energy of two joules at a nominal rate of two sparks/second. The ignition system is powered by a facility supply which provides 115-volt, 400-Hz power through permanent facility wiring to the engine-mounted ignition box. A momentary contact pushbutton on the Engine Control Module (ECM) is used to turn on the ignition system. The pushbutton legend (labeled "ON") is illuminated while the pushbutton is held in the depressed position and goes off when the pushbutton is released.

3.17 STARTING SYSTEM

An air turbine starter and control valve are mounted on the accessory gearbox. The facility system provides a regulated flow of filtered air to the engine starter for engine motoring operations. Controls are located on the ECM in the control room. The system has been designed to deliver up to 2.26 kg/s (5 lbs/sec) of shop air at 41.4 N/cm^2 (60 psig).

In the normal mode of operation, the air-start system can be operated only when the engine speed is below the minimum engagement speed set on the starter protection module, and when the main facility fuel valve is open. An emergency mode of operation bypasses the engine speed and fuel valve interlocks and permits the cell operator to motor the engine in any emergency,

such as to blow out an internal fire or to motor the engine after a flameout until it has cooled sufficiently for a safe shutdown.

3.18 SLIPRING

A 100-point, no-leak, minislipring was used to transmit blade and ring gear strain signals. Leadout and cooling lines were routed through a slip-ring service strut mounted in the inlet. The strut also acts as an anti-rotational device for the slipring.

3.19 SLAVE LUBRICATION PACKAGE

The QCSEE slave lube system is an off-engine-mounted package that conditions and stores the MIL-L-23699 lube oil. Flexible hoses are used to connect the package to the engine components. All fluid connections to the package are located on a common bulkhead on the base of the package. Electrical connections for oil level and coolng water flow measurements are made directly to connectors on the measuring devices. A leak-tight drip pan with a drain connection is provided in the base of the package.

Principal components of the QCSEE slave lube package are the main oil tank, scavenge oil filter, water-oil heat exchangers, water filter, water flowmeter, and water flow control valve. The package contains a single 0.151 m^3 (40 gal.) oil tank and two oil/water coolers rated at 528,000 J/s (30,000 Btu/min) each.

Hot, aerated scavenge return oil is pumped to the package by the engine-mounted scavenge pump. The scavenge oil first flows through the scavenge oil filter where particles, 10 micron and larger, are filtered out of the oil. If the retention capacity of the filter element is exceeded, a bypass valve opens at 34.5 N/cm^2 (50 psid ± 5 psi) to maintain lube flow. Before the bypass condition is reached, however, a "Lube Scavenge Hi ΔP" warning is given to the test operator.

Bypass indication is also provided on the filter. At 34.5 N/cm^2 ± 3.5 N/cm^2 (40 psid ± 5 psi), a red button "pops up" and becomes visible in the sight-glass atop the filter, thus providing visual indication at the slave lube package that the filter is about to bypass or is bypassing depending on the actual pressure drop across the filter. The red button will remain in the "up" position until the sight-glass is removed and the button is manually depressed. Pressure taps are provided upstream and downstream of the scavenge oil filter to monitor the pressure drop across the filter.

The hot, aerated, and filtered oil then passes through the water-oil-heat exchangers where it is cooled to 333 K (140° F) by controlling the water flow through the heat exchangers.

From the heat exchangers, oil is routed to the scavenge return port on the main oil tank. On entering the main oil tank, the oil is deaerated by flowing through the vortex generator located in the tank inlet. Clean, cooled, and deaerated lube oil is drawn through a discharge line as required to supply oil to the engine-mounted lube pump.

4.0 DESCRIPTION OF TEST FACILITY

The QCSEE UTW engine was tested at General Electric's Peebles, Ohio remote test site (Figure 4). Engine installation was at Site IV, Pad D, aeroacoustic test facility. This test facility is located 80 miles due east of the General Electric, Evendale, Ohio Plant and is readily accessible by road or air.

The facility provides for fuel, cooling water, facility and instrument air, fire protection, and thrust measurement systems. An "off engine" lube system was designed and constructed for the QCSEE Program.

Fuel is stored at a remote fuel farm (Figure 5) and is pumped through underground lines to the test pad where it passes through a 10-micron filter before going to the engine. During engine test, the fuel stopcock is operated from the facility control room. JP-5 fuel was used on the QCSEE UTW test.

Water cooling is pumped from a reservoir located on the test facility grounds. The water is filtered prior to entering the test pad manifold. Cooling water was used in the "off engine" lube system heat exchanger and was remotely controlled from the Pad D control console. Water flow was measured by use of a turbine flowmeter and was displayed and recorded during engine test. Adjustments to the water flow were required during engine test to maintain a constant oil temperature in the lube system supply. Water flow could be varied between 0 and 0.568 m^3 (0 and 150 gallons) per minute.

The facility air supply is a regulated and filtered system. Facility air was used for the air-start system, under cowl cooling, and aft sump cooling. Each of these systems was individually controlled and remotely operated from the control console during engine test. Instrument air is a dried air system used on the electropneumatic valve controllers, digital control, and slipring system.

The facility has both water sprinkler and inert gas fire protection systems. Sprinkler heads are located in the facility structure while the inert gas system is connected for use through the engine air-cooling system. Both systems can be operated from the test pad or the control room. In addition to these systems, dry chemical fire extinguishers are located at the pad for use by Peebles test personnel who have been instructed in their use.

Engine thrust was measured using a three-bridge 444,800 N (100,000 lb) load cell. The thrust system was calibrated for forward and reverse thrust testing.

The "off engine" lubrication system provided the lube oil conditioning and oil storage facilities required for engine operation. The system incorporated the same modifications that were successfully used in the initial UTW and OTW test programs. These modifications included increased lube tank capacity, oil tank heating, a slave scavenge pump for the accessory gearbox,

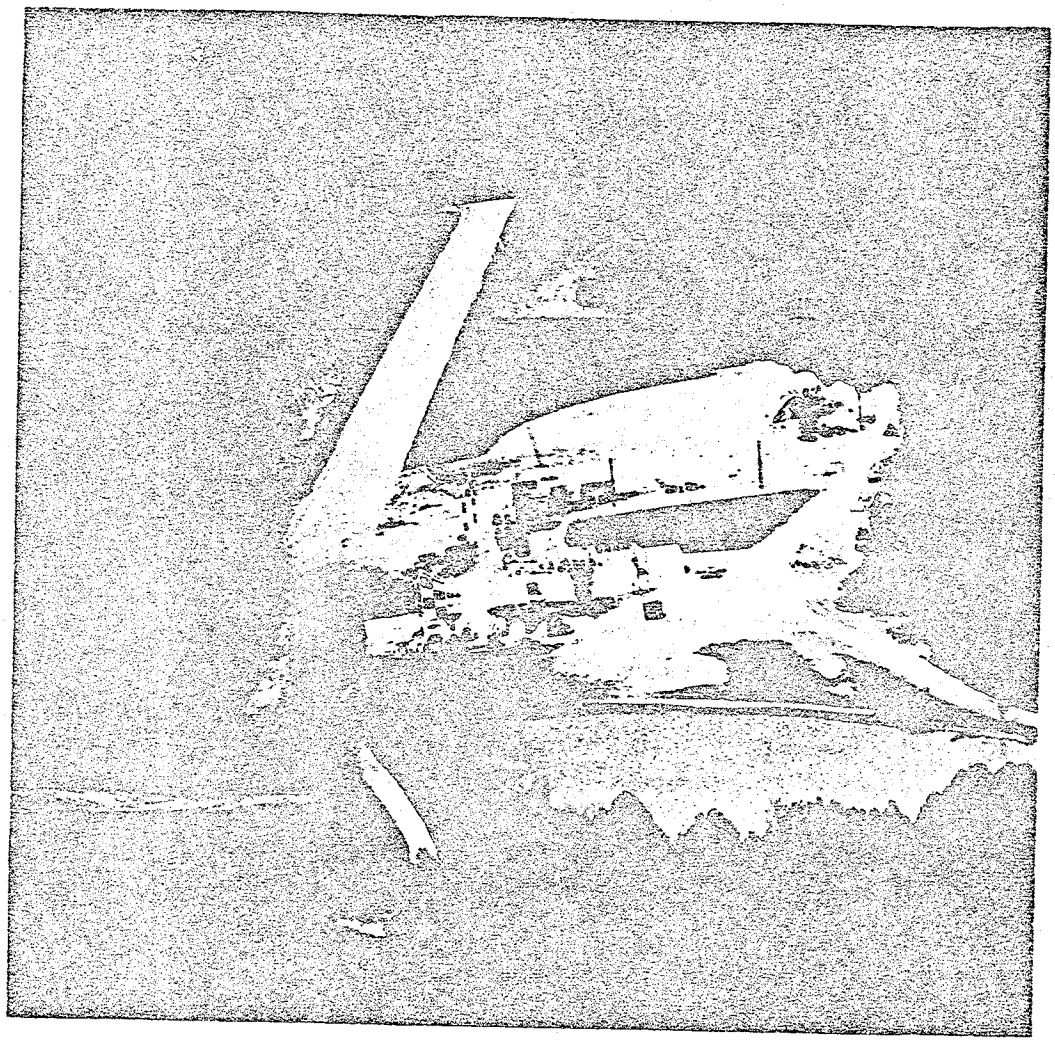

Figure 4. Peebles, Ohio Test Site IV.

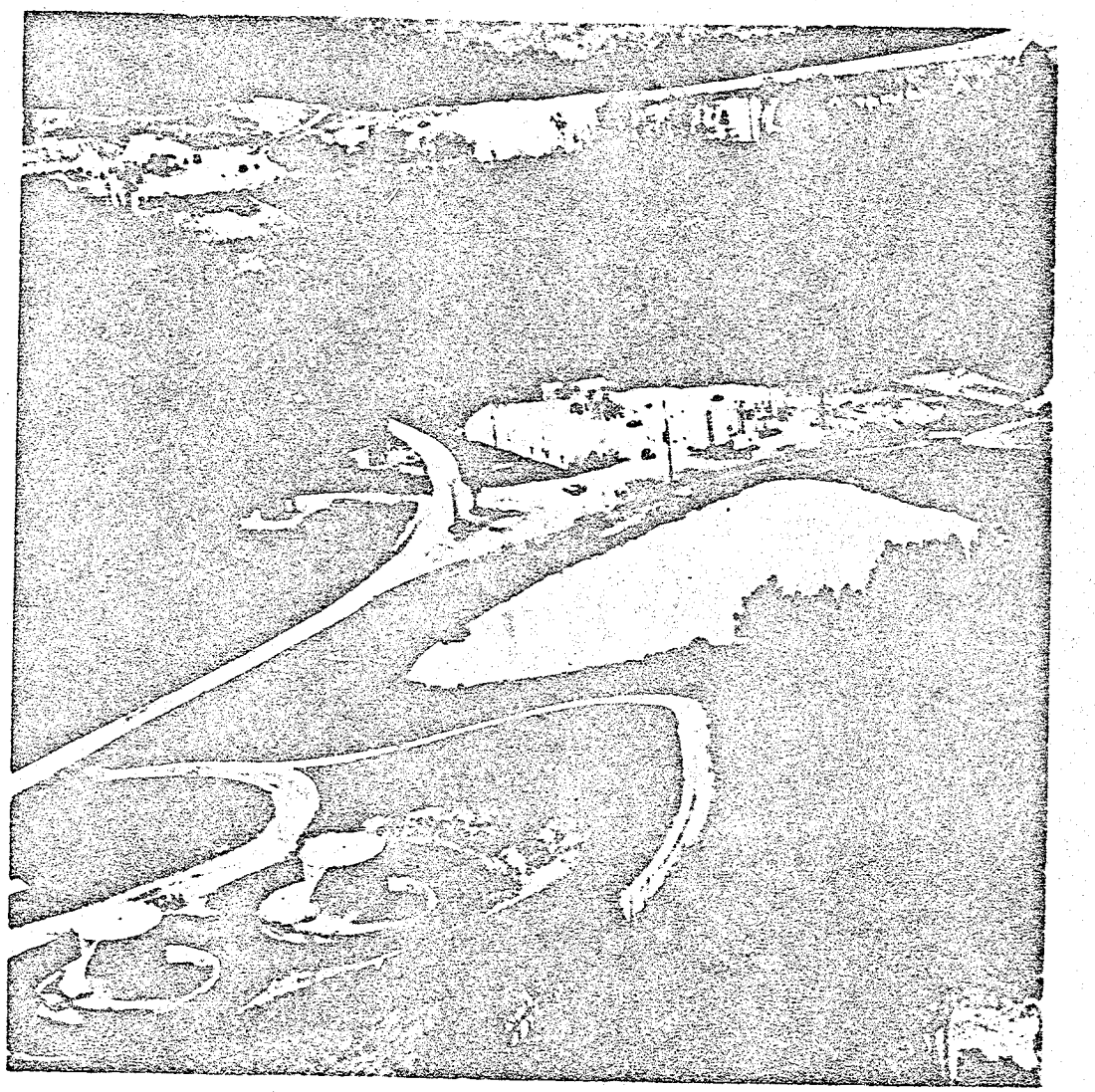

Figure 5. Peebles, Ohio Fuel Farm.

and an additional heat exchanger. During the test program, the water supply lines were insulated to eliminate the freezing problem encountered during testing in the winter months. The lube system is defined in the following drawings:

Assembly	4013180-700
Schematic	4013180-853
Engine Connections	4013180-865
Lube Tank	4013187-581
Heat Exchanger Addition	4013187-639

With the modified off-engine system, the storage capacity was 0.166 m^3 (44 gal.) with tank level readout set for between 0.083 and 0.166 m^3 (22 and 44 gal.). The system was regulated to deliver up to 0.003 m^3/s (50 gpm) of cooled, filtered, and deaerated oil to the engine lube pump at temperatures between 538 K (140° F) and 416 K (160° F). The slave scavenge pump for the accessory gearbox prevented the overtemperature problem by eliminating the flooding condition in the accessory gearbox encountered during initial engine testing of the first build, 507-001/1.

The test pad was equipped to handle the following instrumentation connections:

- 200 temperature sensors, including reference thermocouples
- 184 pressure sensors (air type) including eight vents
- 200 analog circuits (two wire-shielded pairs)
- 60 safety monitoring circuits to engine control console
- 6 traversing probe actuator circuits

Instrumentation was connected in accordance with the Test Request and Test Request changes. Recording equipment was located at the test facility control room and also at Evendale's Instrumentation Data Center. Reference the Test Request for recorder and control room setup.

A minislipring system was used for connection of fan rotor and ring gear instrumentation. The slipring coolant console was located in the facility overhead and monitored in the control room during engine testing. Reference drawings 4013181-988 and 4013180-279 for this system.

The facility is equipped with far-field microphones and stands with provisions for near-field microphones with the use of portable stands.

5.0 TEST INSTRUMENTATION

Because of the many new features incorporated in the initial testing of the UTW propulsion system, an abnormally large number of steady-state and transient pieces of instrumentation were employed. This instrumentation fell into the following general categories.

1. Operational Safety Instrumentation

   This information was displayed on the control console and either logged manually for each steady-state data point or recorded automatically by the Automatic Data Handling (ADH) System. Several types of control console displays were employed, including panel meters, digital indicators, warning lights, and two Metrascope units. This instrumentation is listed in Tables I through IV.

2. Dynamic Instrumentation

   This information primarily included strain gages and accelerometers. Data were displayed on oscilloscopes and Schlumberger Analyzers and were continuously recorded on three magnetic tape recorders. This instrumentation is listed in Tables V, VI, and VII.

3. Transient and Control Parameters

   These parameters were continuously recorded on three Sanborn recorders. The parameters are listed in Table VIII.

4. Digital Control Data

   The digital control was designed to communicate to and from the control room with an Interconnect Unit and two control panels, an Operator's Panel on the control console, and an Engineering Panel adjacent to the console.

   The Operator's Panel, in addition to the power demand lever, incorporated digital displays of critical engine parameters as listed in Table IX.

   The Engineering Panel contained control potentiometers for manual inputs to the digital control and a digital display to read out any of 44 parameters in binary code.

   These parameters were also printed out on paper tape on command during each data reading.

Table I. Safety Instrumentation.

Item Numbers	Description	Press.	Temp.	Strain Gage	Accel	Other
006341-006344	Fan Flap Link Gages			4		
006345-006347	Fan Flap Strain Gages			3		
006399	Fan Flap Vib				1	
006901	Fan Cowl Accel				1	
011001, 2	No. 3 Bearing Temp.		2			
011003, 4	Forward Sump Cavity	2				
011005	Aft. No. 3 Bearing Support	1				
011006	HPT 1/Rev.					(1) 1/Rev.
011901, 2	No. 3 Bearing Vib.			2		
031001	Radial Drive Shaft Bearing		1			
032001	AGB Vent	1				
032901, 2	AGB Vib				2	
033001-033006	Reduction Gear Bearing		6			
033007	Reduction Gear Oil Supply	1				
033008	Red. Gear Prox. Probe					Prox. Probe
033901, 2	Reduction Gear Vib				2	
070001	VSV, Stator Pot					(1) VSV
070901, 2	Compressor Aft Flng. Vib				2	
124002, 3	Plane 3 Probes	1	1			
231901	Exh. Cone Vib				1	
323001, 2	Fuel Manifold Press.	2				
323003, 4	Fuel Temperature		2			
323005	Fuel Inlet Press.	1				
323006, 7	Fuel Flow					(2) Flowmeters
323008	Fuel Manifold Temp.		1			
402001, 2	Lube Pump Disch. Press.	2				
404001, 2	Lube Scav. Disch. Press.	2				
404003, 4	Lube Scav. Disch. Temp.		2			
404005	Lube Scav. Filter Delta Press.	1				
404008, 9	Lube Supply Temp.		2			

Table I. Safety Instrumentation. (Concluded)

Item Numbers	Description	Press.	Temp.	Strain Gage	Accel	Other
404010	HX Water Flow					(1) Flowmeter
404011, 12	HX Water Temp.		2			
404013	Oil Level					Oil Level Sensor
404014	Slave Lube Tank	1				
405001	Hyd. Pump Disch. Press.	1				
417001	Lube Supply Filter Delta Press.	1				
650001, 2	Digital Control Temp.		2			
811001, 2	No. 1B Bearing Temp.		2			
811003, 4	Fan Rotor Cav. Press.	2				
811005	No. 1 Seal Air Press.	1				
811901, 2	No. 1 Bearing Support Vib				2	
812001, 2	No. 1R Bearing Temp.		2			
813001, 2	No. 2 Bearing Temp.		2			
813901, 2	No. 2 Bearing Support Vib				2	
830801-830811	Fan Blade Straw Gages		12			
835801-835812	Fan OGV Strain Gages		18			
840801-840811	Fan Frame Strain Gages		11			
840901, 2	Fan Frame Vib				2	
845001-845008	Core Cowl Skin Temp.		8			
845013-845024	Under Cowl Cavity Temp.		12			
911001, 2	No. 5 Bearing Temp.		2			
911003	No. 5 Bearing Support Temp.		1			
911004-911009	Aft Sump Cav.	4	2			
911010, 11	No. 6 Seal Air Cav. Temp.		2			
911012	No. 6 Seal Fwd Cav. Temp.		1			
911013	No. 6 Seal Fwd Cav. Press.	1				
911014	No. 6 Seal Support Temp.		1			
911015	No. 6 Seal Delta Press.	1				
911016, 17	Bal. Cav. Press.	2				
911019, 19	Bal. Cav. Temp.		2			
911020-911025	Aft Sump Air Temp.		6			
911901, 2	No. 5 Bearing Support Vib				2	

Table II. Control Console.

The following parameters were continuously displayed in engineering units on the control console.

Item	Parameter	Full Data Point
402001	Lube Pump Discharge Pressure	Log-ADH
404001	Scavenge Pump Discharge Pressure	Log-ADH
405001	Hydraulic Pump Discharge Pressure	Log
911016	Balance Cavity Pressure	Log
000009	Starter Air (Starts Only) Pressure	Log
033007	Reduction Gear Oil Supply Pressure	Log
811005	No. 1 Seal Air Supply Pressure	Log
032001	AGB Vent Pressure	Log
404014	Lube Tank Pressure	Log-ADH
323005	Fuel Pump Inlet Pressure	Log
000008	Ps3C Pressure	Log
000007	False Ps3C Pressure	Log
---	Slipring Pressurization	---
011003	Forward Sump Pressure	ADH
---	Instrument Air	---
911015	No. 6 Seal/Air Sump ΔP	Log-ADH
417001	Lube Supply Filter ΔP	Log
404005	Lube Scavenge Filter ΔP	Log
830000	Fan Speed	Log-ADH
230044	T5 Panel Meter	Log
050000	Core Speed	Log-ADH
404013	Lube Level	Log
323006	Main Fuel Flow	Log-ADH SNBRN
323007/ 404010	Verification Fuel Flow/Water Flow	Log-ADH-SNBRN/Log
230044	T5 Digital	Log
000006	Throttle Position	Log
070001	VSV Position	Log-ADH
000001	Thrust	Log-ADH

Table III. Control Console Panel Vibration Display.

Vibration Metrascope (20 Channel)		
Fan and LPT Tracking Filters (12 Indications of Vibration)	Item	Full Data Point
Fan Frame Horizontal	840902	Log 2
Fan Frame Vertical	840901	Log 2
No. 1 Bearing Support Vertical	811901	Log 2
Reduction Gear Vertical	033901	Log 2
Accessory Gearbox Horizontal	032902	Log 2
No. 5 Bearing Support Vertical	911901	Log 2
Core Bypass Filter (6 Indications of Vibration)		
No. 5 Bearing Support Vertical	911901	Log
Accessory Gearbox Horizontal	032902	Log
Reduction Gear Vertical	033901	Log
Fan Frame Vertical	840901	Log
No. 3 Bearing Support Horizontal	011902	Log
Compressor Aft Flange Horizontal	070902	Log

The above parameters were continuously displayed on the control console immediately adjacent to the engine operator. Readout was directly in mils displacement. In addition, all of the above accelerometers are included in those continuously recorded on Tape Recorder A. Note that each of the "Fan and LPT Tracking Filter" items are displayed twice; i.e., filtered for fan and LPT frequencies.

Table IV. Control Console Panel Temperature Display.

QCSEE - UTW
Temperature Metrascope

Channel	Item No.	Parameter	Channel	Item No.	Parameter
01	845 015	Under Cowl Cav.	26	033 004	Red. Gear Bearing
02	845 017	Under Cowl Cav.	27	022 005	Red. Gear Bearing
03	845 019	Under Cowl Cav.	28	033 006	Red. Gear Bearing
04	845 021	Under Cowl Cav.	29	813 001	No. 2 Bearing
05	845 023	Under Cowl Cav.	30	813 002	No. 2 Bearing
06	845 023	Under Cowl Cav.	31	011 001	No. 3 Bearing
07	845 024	Under Cowl Cav.	32	011 002	No. 3 Bearing
08	845 001	Under Cowl Skin	33	911 001	No. 5 Bearing
09	845 003	Under Cowl Skin	34	911 002	No. 5 Bearing
10	845 007	Under Cowl Skin	35	323 003	Fuel In
11	845 025	Under Cowl Skin	36	323 008	Fuel Manifold
12	845 026	Under Cowl Skin	37	404 003	Scavenge Disch.
13	845 027	Under Cowl Skin	28	032 004	Aux Scavenge
14	845 030	Under Cowl Skin	39	404 009	Lube In
15	845 032	Under Cowl Skin	40	911 006	Bal. Exhaust
16	845 033	Under Cowl Skin	41	911 018	Bal. Cavity
17	845 034	Under Cowl Skin	42	911 020	No. 5 Fwd Brg Spt
18	031 001	Midspan Bearing	43	911 021	No. 5 Fwd Brg Spt
19	812 001	No. 1R Bearing	44	911 022	No. 5 Aft Brg Spt
20	812 002	No. 1R Bearing	45	911 008	No. 6 Seal Air Supply
21	811 001	No. 1B Bearing	46	830 004	No. 6 Seal Spt
22	811 002	No. 1B Bearing	47	830 004	Slipring Bearing
23	033 001	Red. Gear Bearing	48	032 002	AGB Skin
24	033 002	Red. Gear Bearing	49	404 011	Heat X H_2O In
25	033 003	Red. Gear Bearing	50	404 012	Heat X H_2O Out

The above parameters were continuously displayed on the control console immediately adjacent to the engine operator. Readout was directly in ° F. In addition to the continuous display, all of the above parameters were recorded on ADH each time a full data reading was taken.

Table V. Tape Recorder A - Vibration.

All of the following were continuously recorded as well as displayed on the scopes.

Item	Parameter	Channel
830 007	Time Code	01
840 901	S/R Accel	02
840 902	Fan Frame (V)	03
840 902	Fan Frame (H)	04
811 901	#1 Brg (V)	05
811 902	#1 Brg (H)	06
813 901	#2 Brg (V)	07
813 902	#2 Brg (H)	08
011 901	#3 Brg (V)	09
011 902	#3 Brg (H)	10
033 901	Reduction Gear (V)	11
033 902	Reduction Gear (H)	12
070 901	C/S Aft Flange (V)	13
070 902	C/S Aft Flange (H)	14
911 901	#5 Brg (V)	15
911 902	#5 Brg (H)	16
231 901	Exhaust Cone	17
032 901	Acc. Gearbox (A)	18
032 902	Acc. Gearbox (H)	19
650 901	Digital Control	20
033 008	Proximity Probe	21
066 901	Fan Cowl	22
006 399	Fan Flap	23
055 901	Inlet Accel	24
	Core Speed	25
	LPT Speed	26
	Voice	27
		28

Table VI. Tape Recorder B - Fan Blades, OGV, Flap Link Dynamic Strain Gages.

Item	Parameter	Channel
	Time Code	01
830 801	Fan Blade Dynamic	02
830 802	Fan Blade Dynamic	03
830 803	Fan Blade Dynamic	04
830 804	Fan Blade Dynamic	05
830 805	Fan Blade Dynamic	06
830 806	Fan Blade Dynamic	07
830 807	Fan Blade Dynamic	08
830 808	Fan Blade Dynamic	09
830 810	Fan Blade Dynamic	10
830 811	Fan Blade Dynamic	11
830 813	Fan Blade Dynamic	12
830 814	Fan Blade Dynamic	13
830 816	Fan Blade Dynamic	14
830 817	Fan Blade Dynamic	15
835 801	Fan OGV Dynamic	16
835 802	Fan OGV Dynamic	17
835 803	Fan OGV Dynamic	18
835 804	Fan OGV Dynamic	19
835 805	Fan OGV Dynamic	20
835 807	Fan OGV Dynamic	21
835 809	Fan OGV Dynamic	22
006 342	Flap Link Dynamic	23
006 344	Flap Link Dynamic	24
	Fan Speed	25
	Core Speed	26
	LPT Sped	27
	Voice	28

Table VII. Tape Recorder C - Rakes, Frame, Fan Cowl, Flap Link Strain Gages.

Item	Parameter	Channel
	Time Code	01
800 801	Rake Strain Gage (Inlet)	02
800 803	Rake Strain Gage (Inlet)	03
800 805	Rake Strain Gage (Inlet)	04
800 807	Rake Strain Gage (Inlet)	05
800 809	Rake Strain Gage (Boundary Layer)	06
800 811	Rake Strain Gage (Strut)	07
800 812	Rake Strain Gage (Strut)	08
800 813	Rake Strain Gage (Strut)	09
800 817	Rake Strain Gage (Plane 25)	10
800 821	Rake Strain Gage (Plane 25)	11
	XPT Plane 25	12
	LVDT	13
006 341	Flap Link Strain Gage	14
006 343	Flap Link Strain Gage	15
006 345	Fan Cowl Skin Strain Gage	16
006 346	Fan Cowl Skin Strain Gage	17
006 347	Fan Cowl Skin Strain Gage	18
840 802	Fan Frame Strain Gage	19
840 803	Fan Frame Strain Gage	20
840 805	Fan Frame Strain Gage	21
840 808	Fan Frame Strain Gage	22
840 814	Fan Frame Strain Gage	23
840 816	Fan Frame Strain Gage	24
	Fan Speed	25
	Core Speed	26
	LPT Speed	27
	Voice	28

Table VIII. Sanborn Recorders.

Channel	Parameter	Unit	Range
Sanborn Recorder A			
1	A18 Rod End	PSIG	0-3000
2	A18 Head End	PSIG	0-3000
3	Fan Blade Static Strain	μ-in./in.	0-3000
4	Fan Blade Temperature	° F	0-250
5	Fan Blade Static Strain	μ-in./in.	0-3000
6	Fan Blade Temperature	° F	0-250
7	Fan Speed	RPM	0-4000
8	LVDT (Blade Angle)	+12° to -115°	0-10VDC
Sanborn Recorder B			
1	Fan Blade Static Strain	μ-in./in.	0-3000
2	Fan Blade Temperature	° F	0-250
3	Fan Blade Static Strain	μ-in./in.	0-3000
4	Fan Blade Temperature	° F	0-250
5	Fan Speed	RPM	0-4000
6	LVDT (Blade Angle)	Deg	0-10VDC
7	Core Speed	RPM	0-15.5K
8	---		
Sanborn Recorder C			
1	Fan Speed	RPM	
2	LVDT #1	+15° to -115°	0-10VDC
3	LVDT #2	+15° to -115°	0-10VDC
4	Hyd Open	PSIG	0-3500
5	Hyd Closed	PSIG	0-3500
6	PLA	Deg	0-100
7			
8			

Table IX. Digital Control.

Operator Panel on Control Console

The following parameters were continuously displayed in engineering units on the Digital Control Operator Panel on the control console directly in front of the engine operator.

Fan Speed	Fan Exhaust Nozzle Area	Thrust Parameter
Core Speed	Fan Pitch Angle	T41C
Power Demand	Inlet Mach Number	T41C

Engineering Panel (Adjacent to Control Console)

The Digital Control Engineering Panel includes a selectable digital display for any one of the variables listed below. Any one of the 44 may be read out, when selected, in a binary code. The operator of the engineering panel used equations for each of the parameters to convert them from binary code to engineering units. Each of the following was recorded by the engineering panel operator whenever an ADH reading is taken.

Thumb Wheel Switch Position	Parameter	Thumb Wheel Switch Position	Parameter
00	A18 TMC	24	MVP
01	βF TMC	25	βF1
02	WF TMC	26	β F2
03	WF	27	βF Demand (Auto Mode)
04	A18	28	A18 Demand (Auto Mode)
05	βF	29	T3
06	FMP	30	VSV Reset TMC
07	T41C	31	Mode Word
08	ΔP/P	32	Hydraulic Pump Disch. Press.
09	PS3/PTO	33	WF Temperature
10	Power Demand	34	βF Rate
11	PLA	35	EGT
12	N1	36	Engine Oil Inlet Temperature
13	N2	37	Scavenge Oil Temp.
14	VSV	38	Engine Oil Inlet Pressure
15	WF MC1	39	Scavenge Oil Press.
16	βF MC1	40	T25
17	A18 MC1	41	P5
18	F.I.	42	Gearbox Innerrace
19	T12	43	Bearing Temperature
20	PTO	44	Horizontal Vibration
21	P14-PTO		Vertical Vibration
22	PTO-PS11		
23	PS3		

5. Performance Instrumentation

Internal engine pressures and temperatures from rakes, static taps, and probes were recorded automatically for each data point by the ADH System. These parameters are listed in Table X.

6. Follow-on Test Console Configuration

The computerized site IV-D control console used for the follow-on testing consisted of four CRT displays. The two center CRT's displayed safety and vibration parameters. The left-hand CRT was capable of displaying as many as 23 separate pages each with 10 engine parameters listed. The console automatically monitored all parameters programmed into it and flagged those parameters which went over limit. The fourth CRT was used to display over-limit engine parameters. A list of the items programmed into the control console is shown in Table XI.

The ADH system provided direct telephone communication of data recorded at the Peebles, Ohio Test Site to the central computer in the Instrumentation Data Room (IDR) at Evendale, Ohio. The data were processed, stored, and a short list of averaged and corrected parameters was printed out on the "Quick Look" monitor in the Site IV control room as an aid in tracking the engine operating conditions. The "Quick Look" parameters are listed in Table XII.

The general layout of the control room showing locations of the various displays and control panels is shown in Figure 6.

Table X. Engine Instrumentation Hookup Aeroinstrumentation.

Item Numbers	Description	Press.	Temp.	Other
	Bellmouth Inlet			
005201-005240	(4) Inlet Rakes	20	20	
005254-005260	(1) Boundary Layer Rake	7		
005301-316	Wall Statics			
	Fan Bypass			
840001-840023	Bypass Duct Statics	23		
840024-840031	Plane 25 Statics	8		
840032-840036	Splitter Lip Statics	5		
840037-840042	Compressor Inlet Statics	6		
840043-840046	Plane 15 Statics	4		
840201-840230	(6) Compressor Inlet Rakes	30		
840231-840235	(6) Compressor Inlet Rakes		5	
840246-840250	(6) Compressor Inlet Rakes		5	
840256-840260	(6) Compressor Inlet Rakes		5	
840107-840109	(6) Compressor Inlet Rakes			(3) Dyn. Press.
	Fan OGV			
835001-835005	Island Statics	5		
835007-835008	Vane, Manifolds	2		
835010-835014	Vane, Manifolds	5		
835101-835106	Vane Probes	6	0	
	Bypass Duct			
006001-006006	Plane 15 Statics	6		
006007-006014	Wall Statics	12		
006041-006048	(3) Cobra Probes	3	3	
006361-006395	Fan Flap Statics	35		
	Exhaust Nozzle			
230001-230040	LPT Discharge Rakes	20	20	
230041-230045	Service Strut		5	
230046-230049	Wall Statics	4		

Table XI. QCSEE UTW Console Display (Site IV-D).

Parameter	Item No.	Range	Limit				
			Lo-Lo	Lo	Hi	Hi-Hi	Priority
Safety Display							
Thrust	000001	88960 N (20,000 lbs)	---	---	None	---	---
Fan Speed	830000	--- 3500 rpm	---	---	---	3400	3
EGT	230044	1089 K (1500° F)	---	---	None	---	---
Main Fuel Flow	323006	159 kg/hr (350 pph)	---	---	---	145 (320)	6
Reduction Gear Oil Supply Pressure	033007	34.5 N/cm^2 (50 psig)	21.4 (31)	0.019 (5)	---	34.5 (50)	6/6
Oil Level	404013	0.095 m^3 (25 gal.)	0.008 (2)	---	---	---	6/6
Lube Pump Discharge Pressure	402001	69 N/cm^2 (100 psig)	---	---	---	69 (100)	3
Lube Supply Temperature	404009	344 K (160° F)	---	---	328 (130)	333 (140)	5/2
VSV Stage 1	070001	--- ---	---	---	None	---	---
Vibration Display							
Digital Control/Fan Filtered	650901	0.025 cm (10 mils)	---	---	0.007 (3)	0.018 (7)	4/3
Fan Frame Vert/Fan	840901	0.025 cm (10 mils)	---	---	0.007 (3)	0.018 (7)	4/3
No. 1 Bearing Vert/Fan	811901	0.025 cm (10 mils)	---	---	0.007 (3)	0.018 (7)	4/3
Reduction Gear Vert/Fan	033901	0.025 cm (10 mils)	---	---	0.007 (3)	0.018 (7)	4/3
Accessory Gearbox Anal/Fan	032901	0.025 cm (10 mils)	---	---	0.007 (3)	0.018 (7)	4/3
No. 5 Bearing Vert/LPT Filtered	911901	0.025 cm (10 mils)	---	---	0.007 (3)	0.013 (5)	4/3
No. 5 Bearing Vert/Core Filtered	911901	0.025 cm (10 mils)	---	---	0.005 (2)	0.008 (3)	4/3
No. 3 Bearing Vert/Core	011901	0.025 cm (10 mils)	---	---	0.005 (2)	0.008 (3)	4/3
Reduction Gear Vert/Core	033901	0.025 cm (10 mils)	---	---	0.005 (2)	0.008 (3)	4/3
Compr Aft Flange Horz/Core	070901	0.025 cm (10 mils)	---	---	0.005 (2)	0.008 (3)	4/3
Page 1 - Start							
Starter Air Press.	000009	69 N/cm^2 (100 psig)	---	---	---	58.6 (85)	5
Hydraulic Pump Disch. Press.	405001	2758 N/cm^2 (4000 psig)	---	---	---	2482 (3600)	6
Core Speed	050000	--- 1400 rpm	---	---	---	--- 14050	3
Fan Speed	830000	--- 3500 rpm	---	---	---	--- 3400	3
Lube Scavenge Disch. Press.	404001	69 N/cm^2 (100 psig)	---	---	---	69 (100)	3
Instrument Air Press.	---	69 N/cm^2 (100 psig)	---	---	None	None	---
PS3C	124003	206.9 N/cm^2 (300 psig)	---	---	None	None	---
Fuel In Press.	323005	69 N/cm^2 (100 psig)	---	---	---	51.7 (75)	6
Fuel Flow Verification	323007	159 kg/hr (350 pph)	---	---	---	145 (320)	6
Reading Number	---	--- ---	---	---	None	---	---
Page 2 - Run							
Lube Supply Filter ΔP	417001	20.7 N/cm^2 (30 psid)	---	---	---	17.2 (25)	6
Scavenge Filter ΔP	404005	13.8 N/cm^2 (20 psid)	---	---	---	10.3 (15)	6
No. 6 Seal/Aft Sump ΔP	911015	13.8 N/cm^2 (20 psid)	---	---	---	6.9 (10)	6
Hydraulic Pump Discharge Press.	405001	2758 N/cm^2 (4000 psig)	---	---	---	2482 (3600)	6
Water Flow	404010	0.38 m^3/min (100 gpm)	---	---	None	---	---

Table XI. QCSEE UTW Console Display (Site IV-D). (Continued)

Parameter	Item No.	Range	Limit				
			Lo-Lo	Lo	Hi	Hi-Hi	Priority
Page 2 - Run (Continued)							
PS3C	124003	206.9 N/cm^2 (300 psig)	---	---	None	---	---
Undercowl Air Temperature	845023	811 K (1000° F)	---	---	---	644 (700)	5
Core Cowl Skin Temperature	845033	478 K (400° F)	---	---	439 (330)	450 (350)	5/2
Reduction Gear Bearing Temperature	033003	478 K (400° F)	---	---	408 (275)	417 (290)	6/3
Reading Number	---	---	---	---	None	---	---
Page 3 - Pressures							
Forward Sump Pressure	011003	13.8 N/cm^2 (20 psia)	6.9 (10)	---	---	10.3 (15)	6/6
Lube Tank Pressure	404014	13.8 N/cm^2 (20 psig)	---	---	---	10.3 (15)	6
Accessory Gearbox Vert Pressure	032001	6.9 N/cm^2 (10 psig)	---	---	---	5.5 (8)	6
No. 1 Seal Air Pressure	811005	34.5 N/cm^2 (50 psig)	---	---	---	20.7 (30)	6
No. 3 Bearing Aft Cav Pressure	011005	6.9 N/cm^2 (10 psig)	---	---	None	---	---
No. 6 Seal Air Supply Pressure	911010	34.5 N/cm^2 (50 psia)	---	---	---	24.1 (35)	6
Balance Cavity Pressure	911016	206.9 N/cm^2 (300 psia)	---	---	---	172.4 (250)	6
Scav. Pump Disch. Pressure	404001	69 N/cm^2 (100 psia)	---	---	---	69 (100)	6
Reading Number	---	---	---	---	None	---	---
Page 4 - Bearing Temperatures							
No. 1R Bearing Temperature	812001	478 K (400° F)	---	---	428 (310)	439 (330)	6/3
No. 1R Bearing Temperature	812002	478 K (400° F)	---	---	428 (310)	439 (330)	6/3
No. 1B Bearing Temperature	811001	478 K (400° F)	---	---	428 (310)	439 (330)	6/3
No. 1B Bearing Temperature	811002	478 K (400° F)	---	---	428 (310)	439 (330)	6/3
Reduction Gear Bearing Temperature	033001	478 K (400° F)	---	---	408 (275)	417 (290)	6/3
Reduction Gear Bearing Temperature	033002	478 K (400° F)	---	---	408 (275)	417 (290)	6/3
Reduction Gear Bearing Temperature	033004	478 K (400° F)	---	---	408 (275)	417 (290)	6/3
Reduction Gear Bearing Temperature	033005	478 K (400° F)	---	---	408 (275)	417 (290)	6/3
Reduction Gear Bearing Temperature	033006	478 K (400° F)	---	---	408 (275)	417 (290)	6/3
Reading Number	---	---	---	---	None	---	---
Page 5 - Bearing Temperatures							
No. 2 Bearing Temperature	813001	533 K (500° F)	---	---	428 (310)	439 (330)	6/3
No. 2 Bearing Temperature	813002	533 K (500° F)	---	---	428 (310)	439 (330)	6/3
No. 3 Bearing Temperature	011001	533 K (500° F)	---	---	428 (310)	439 (330)	6/3
No. 3 Bearing Temperature	011002	533 K (500° F)	---	---	428 (310)	439 (330)	6/3
No. 5 Bearing Temperature	911001	533 K (500° F)	---	---	439 (330)	450 (350)	6/3
No. 5 Bearing Temperature	911002	533 K (500° F)	---	---	439 (330)	450 (350)	6/3
Midspan Bearing	031001	533 K (500° F)	---	---	439 (330)	400 (260)	6
Slipring Bearing	830003	394 K (250° F)	---	---	---	367 (200)	3

Table XI. QCSEE UTW Console Display (Site IV-D). (Continued)

Parameter	Item No.	Range	Limit				
			Lo-Lo	Lo	Hi	Hi-Hi	Priority
Page 5 - Bearing Temperatures (Continued)							
Slipring Bearing	830004 394	(250° F)	---	---	---	367 (200)	3
Reading Number	--- ---	---	---	---	None	---	
Page 6 - Lube Temperatures							
Scavenge Disch. Temperature	404003	533 K (500° F)	---	---	---	433 (320)	6
Aux. Scav. Disch. Temperature	032004	533 K (500° F)	---	---	None	---	---
Bal. Exh. Cavity Temperature	911006	978 K (1300° F)	---	---	---	922 (1200)	6
Bal. Cavity Temperature	911018	978 K (1300° F)	---	---	---	922 (1200)	6
No. 5 Bearing Fwd Support Temp	911020	533 K (500° F)	---	---	---	522 (480)	6
No. 6 Seal Air Supply Temperature	911008	811 K (1000° F)	---	---	---	589 (600)	6
No. 6 Seal Support Air Temperature	911012	533 K (500° F)	---	---	---	422 (300)	6
No. 5 Bearing Aft Support Temperature	911022	533 K (500° F)	---	---	None	---	---
Fuel Manifold Temperature	323008	533 K (500° F)	---	---	None	---	---
Reading Number	---	--- ---	---	---	None	---	---
Page 7 - Undercowl Air Temperature							
Fwd. Undercowl Cavity Temperature	845015	533 K (500° F)	---	---	---	450 (350)	5
Fwd. Undercowl Cavity Temperature	845017	533 K (500° F)	---	---	---	450 (350)	5
Fwd. Undercowl Cavity Temperature	845019	533 K (500° F)	---	---	---	450 (350)	5
Fwd. Undercowl Cavity Temperature	845020	533 K (500° F)	---	---	---	450 (350)	5
Aft Undercowl Cavity Temperature	845021	811 K (1000° F)	---	---	---	644 (700)	5
Aft Undercowl Cavity Temperature	845022	811 K (1000° F)	---	---	---	644 (700)	5
Aft Undercowl Cavity Temperature	845023	811 K (1000° F)	---	---	---	644 (700)	5
Aft Undercowl Cavity Temperature	845024	811 K (1000° F)	---	---	---	644 (700)	5
Reading Number	---	--- ---	---	---	None	---	---
Page 8 - Core Cowl Skin Temperature							
Core Cowl Skin Temperature	845001	533 K (500° F)	---	---	439 (330)	450 (350)	5/2
Core Cowl Skin Temperature	845003	533 K (500° F)	---	---	439 (330)	450 (350)	5/2
Core Cowl Skin Temperature	845007	533 K (500° F)	---	---	439 (330)	450 (350)	5/2
Core Cowl Skin Temperature	845025	533 K (500° F)	---	---	439 (330)	450 (350)	5/2
Core Cowl Skin Temperature	845026	533 K (500° F)	---	---	439 (330)	450 (350)	5/2
Core Cowl Skin Temperature	845027	533 K (500° F)	---	---	439 (330)	450 (350)	5/2
Core Cowl Skin Temperature	845030	533 K (500° F)	---	---	439 (330)	450 (350)	5/2
Core Cowl Skin Temperature	845032	533 K (500° F)	---	---	439 (330)	450 (350)	5/2
Core Cowl Skin Temperature	845034	533 K (500° F)	---	---	439 (330)	450 (350)	5/2
Reading Number	---	533 K (500° F)	---	---	None	450 (350)	5/2

Table XI. QCSEE UTW Console Display (Site IV-D). (Concluded)

Parameter	Item No.	Range	Limit				
			Lo-Lo	Lo	Hi	Hi-Hi	Priority
Page 9 - Vibration							
No. 5 Bearing Vert/Fan Filtered	911901	0.025 cm (10 mils)			0.008 (3)	0.018 (7)	4/3
Fan Frame Horz/LPT	840902	0.025 cm (10 mils)	---	---	0.008 (3)	0.013 (5)	4/3
Fan Frame Vert/LPT	840901	0.025 cm (10 mils)	---	---	0.008 (3)	0.013 (5)	4/3
No. 1 Bearing Vert/LPT	811901	0.025 cm (10 mils)	---	---	0.008 (3)	0.013 (5)	4/3
Reduction Gear Vert/LPT	033901	0.025 cm (10 mils)	---	---	0.008 (3)	0.013 (5)	4/3
Accessory Gearbox Axial/LPT	032901	0.025 cm (10 mils)	---	---	0.008 (3)	0.013 (5)	4/3
Accessory Gearbox Horz/LPT	032902	0.025 cm (10 mils)	---	---	0.008 (3)	0.013 (5)	4/3
Accessory Gearbox Axial/Core	032901	0.025 cm (10 mils)	---	---	0.008 (3)	0.013 (5)	4/3
Fan Frame Vert/Core	840901	0.025 cm (10 mils)	---	---	0.005 (2)	0.008 (3)	4/3
Reading Number	---		---	---	0.005 (2) None	0.008 (3) ---	4/3 ---

*Priority	CRT Display Command
1	Shutdown
2	Return to idle
3	Backoff
4	Hold
5	Adjust air, H_2), N_2. . .
6	Monitor
7	Edit System

Table XII. Quick-Look Parameters.

Typewritten output available in the control room from the ADH system for each full data point taken.

Item	Parameter	Units
XNL	Physical fan speed	rmp
XNH	Physical HP compressor speed	rpm
T2AP	Fan inlet temperature	° F
A18	Bypass nozzle throat area	$in.^2$
Pitch	Fan blade angle	degrees
PCNLR	Percent corrected fan speed	percent
PCNHR	Percent corrected core speed	percent
WFM	Main fuel flow	pph
FAN TORQ	Fan torque, calculated	ft/lb
E2AD15	Bypass duct inlet efficiency	---
W2AR	Corrected fan-face total flow	pps
XM11	Inlet throat Mach number	---
W25R	Corrected core inlet airflow	pps
P3/P25	HP compressor pressure ratio	pps
P15MW/2A	Fan bypass pressure ratio	---
E25D3	HP compressor adiabatic efficiency	---
P21MW/2A	Fan hub pressure ratio	---
T41X	HPTR inlet total temperature (T5, energy balance)	° R
T41XK	HPTR inlet total temperature (T5 energy balance corrected)	° R
FNR	Corrected thrust	lb
SFCR	Corrected sfc	lb/hr/lb
T41C	HPTR inlet total temperature (T3, P3, Wf digital control)	° R
E2AD21	Fan hub adiabatic efficiency	---
T55	Exhaust gas temperature	° F

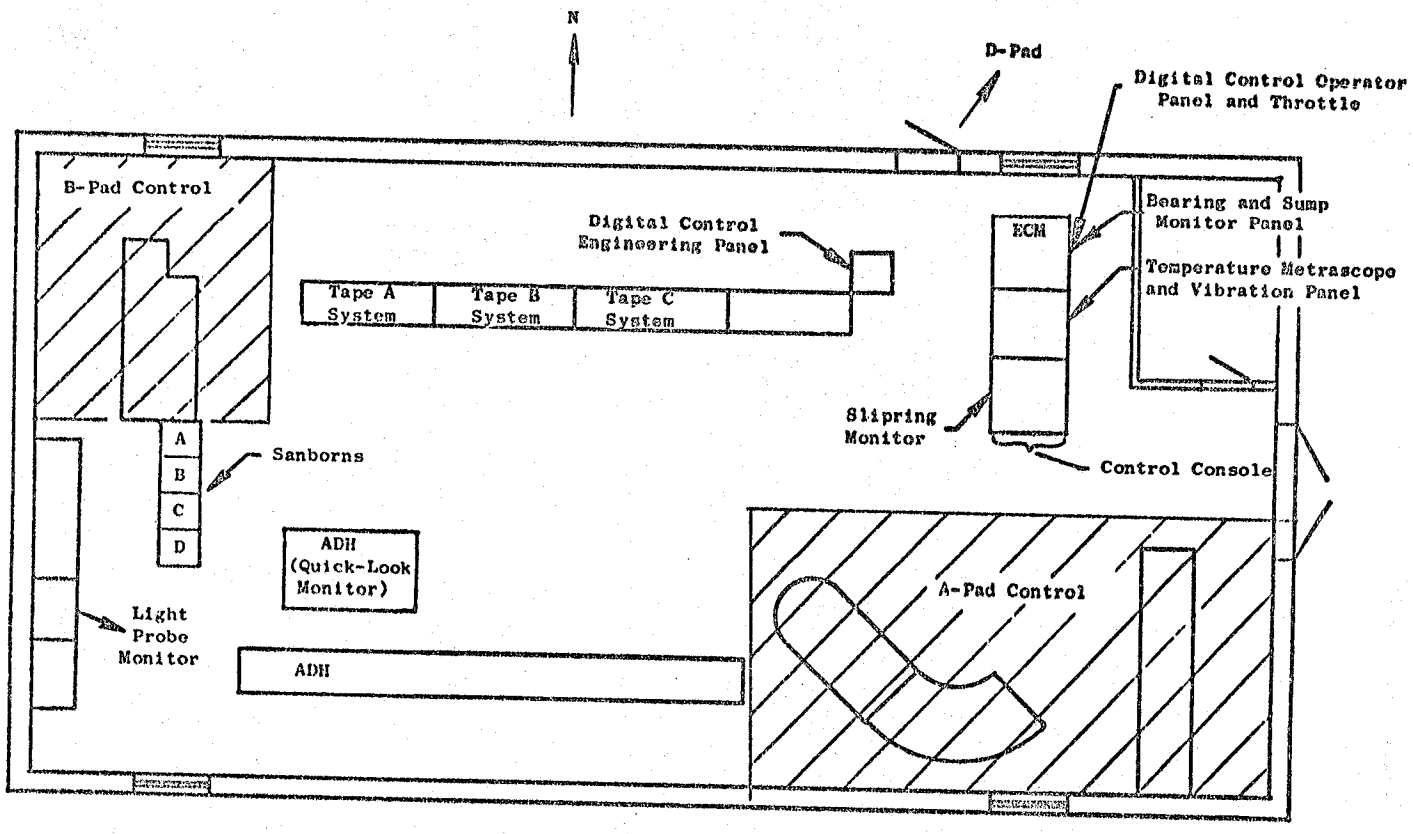

Figure 6. QCSEE OTW Mechanical Checkout Control Room Layout, Peebles Site IV.

6.0 HISTORY OF TEST

The QCSEE UTW engine, 507-001/2, was reassembled using the General Electric fan pitch actuator system. The engine was delivered to Peebles Test Operation on 7/25/77. Engine installation began on the test stand at Site IV, Pad D. The composite fan duct and core cowling were fitted to the engine after it was installed on the test stand. The hardwall core nozzle and bellmouth inlet were installed (Figure 7). The slave lubrication system was serviced with Royal 899 oil and the two oil level indicators were calibrated.

The thrust measuring system was calibrated in both the forward and reverse thrust modes. The load cell used was a 444,800 N (100,000 lb) cell with a three-bridge circuit. Bridge B did not calibrate properly and was not used for data reduction but was recorded for reference.

A helium leak check was performed on the fan frame on 8/1/77. Three small leaks were detected and sealed at points where instrumentation penetrated the fan frame. No other leak sources were found.

The variable stator vanes, Stage 1 and Stage 3 position potentiometers, fan rotor beta angle, and fan nozzle area were calibrated. Stage 1 potentiometer was set from -1°42' open to +45°23' closed; Stage 3 was set from -0°44' open to +37°28' closed. Fan beta angles were calibrated between -116°5' open and +11°45' closed. Fan nozzle maximum open area was 2.69 m^2 (4167 $in.^2$). A mechanical stop was installed to limit the minimum closed nozzle area to 1.36 m^2 (2110 $in.^2$). The core nozzle area was fixed at 0.361 m^2 (560 $in.^2$).

Instrumentation was connected per Test Request and Test Request Changes. Four inlet rakes, one inlet boundary layer rake, three cobra traverse probes in the fan bypass duct, and four LPT discharge rakes were installed. The slipring system was installed to monitor fan blade stresses. The recording equipment used for the test is listed below:

Item	Serial Number
Digital	60953
Sanborn A	4951
Sanborn B	4953
Sanborn C	4952
Tape Recorder A	2092
Tape Recorder B	2087
Tape Recorder C	4920

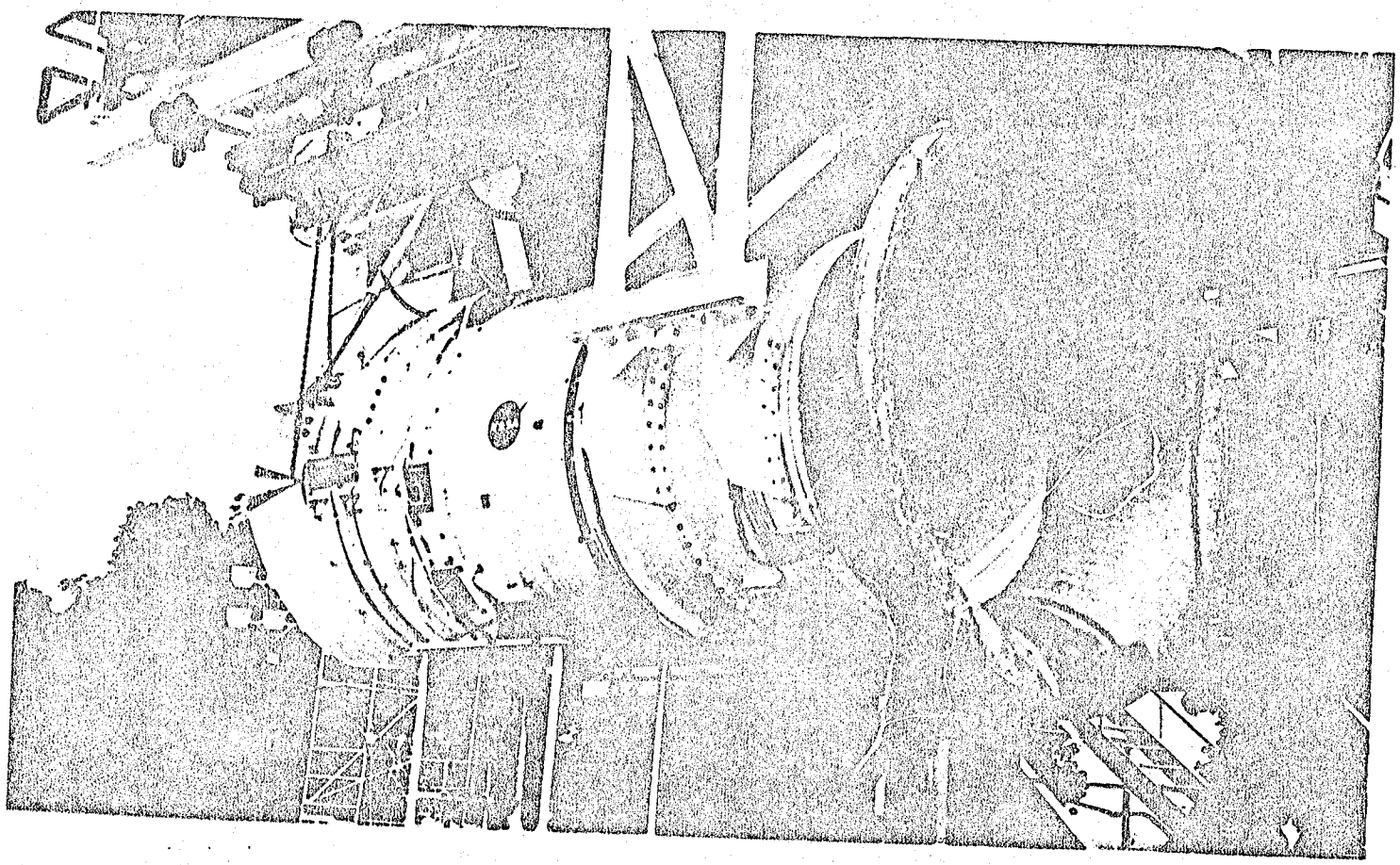

Figure 7. Initial UTW Test Configuration.

On August 31, 1977, engine installation and the engine and facility prerun checklists were completed. Initial dry motoring of the engine was discontinued after water was discovered in the starter air line. The problem was traced to a faulty automatic facility water dump valve, and was corrected. A second dry motor was attempted, but fuel vapors were seen exiting from the core nozzle. Several diagnostic motorings traced the problem to the hydro-mechanical control failing to shut off the fuel flow. The control was removed and a subsequent bench test revealed the cause to be a misindexed throttle shaft. The shaft was reindexed, and the hydromechanical control reinstalled on the engine. A successful dry and wet motor was performed and the engine prepared for its first fire-to-idle attempt.

On September 8, 1977, the engine was successfully fired-to-idle for the first time. The fan nozzle area was varied from 1.61 m^2 (2500 $in.^2$) to 1.68 m^2 (2600 $in.^2$); fan beta angle was varied from +3° to +5°; and fan idle speed varied from 1750 to 1965 rpm. The functioning of the fan speed control mode was also checked. Vibration activity in the front end of the engine was running one to two mils higher than on the first engine build, but was still within limits. No lubrication system or digital control problems were encountered. The engine was shutdown after 36 minutes of total running time until the remaining engine monitors arrived.

The following is a history of the test between 9/8/77 and 5/1/78.

Run:	No. 1 - Mechanical Checkout
Date:	9/9/77
Run Time:	1 hour 36 minutes
Total Engine Run Time:	2 hours 12 minutes
ADH Readings:	No. 11 through 13

Prior to this run, several instrumentation faults discovered on the previous day's run were corrected. The first three starts were uneventful. The engine could not be accelerated above 1900 fan rpm due to high overall fan one/rev vibration levels, with the slipring showing 16 mils double amplitude. Field balance weights were added to the spinner after each run.

After Start No. 4 of this test, vibration levels at idle were acceptable, with the slipring showing only three mils. Fan, core, and LPT levels were also low. During an accel to 80 percent fan speed, the slipring accelerometer reached 20 mils at 2550 fan rpm. The engine was immediately decelerated to idle where all vibration levels returned to their previous amounts. Several field balance readings were taken and the engine shutdown to change balance weights. While inspecting the spinner during this shutdown, it was discovered that the slipring was loose. The slipring was removed and returned to the Evendale plant for teardown, inspection, and reassembly. This concluded Run No. 1.

During the test, the digital control performed well, holding fan speed within ± 2 rpm, fan nozzle area within ± 0.001 m^2 (± 2 $in.^2$), and fan pitch angle within ± 0.1°. While at 1800 fan rpm, the fan pitch was varied

from +5° to -5° with no apparent change in vibration levels or significant hysteresis in setting fan pitch angle. ADH readings were taken at 0° fan pitch when setting angles from both open and closed directions. The engine was acceled and deceled on fan speed control. Fan nozzle area was 1.61 m^2 (2500 $in.^2$) throughout the test.

Reduction gear oil supply pressure was higher than on the previous build. There was no appreciable oil consumption during the test. Fan blade stresses appeared to be as susceptible to crosswinds as the original set on the first build. All other stresses and engine temperature were well behaved.

Run:	No. 2 - Mechanical Checkout
Date:	9/14/78
Run Time:	2 hours 56 minutes
Total Engine Run Time:	4 hours 26 minutes
ADH Readings:	No. 14 through 19

Prior to this test, the slipring was disassembled, inspected, rebuilt, and reinstalled on the engine. Instrumentation faults discovered during Run No. 1 were corrected. The purpose of this test was to evaluate the vibration characteristics of the engine.

The test began with Engine Start No. 8. High vibration levels were indicated on the slipring as the engine approached 80 percent fan speed (2740 rpm). Four field balance runs were made in an attempt to reduce this slipring vibration activity. The vibration level was fan one/rev in origin and slowly increased with increasing fan speed. All remaining engine vibration levels and operating parameters were well behaved.

Further testing was terminated pending inspection of the slipring and spinner.

Run:	No. 3 - Mechanical Checkout
Date:	9/27/77 and 9/23/77
Run Time:	4 hours 26 minutes
Total Engine Run Time:	8 hours 52 minutes
ADH Readings:	No. 20 through 22

Actions taken prior to this run were:

- Removed inlet rakes for better access to spinner
- Inspected slipring and spinner for runout and flatness
- Removed slipring and returned it to Evendale for bench testing
- Rechecked the calibration on all of the engine's accelerometers

- Removed core nozzle and added oil leakage holes to the under side of the turbine frame to minimize the possibility of an aft sump fire. The nozzle was then reinstalled.

- Installed a drain tube to the No. 6 seal drain line.

While in Evendale, a tangential accelerometer was added to the slipring housing, and the system balanced while on the bench test rig. The slipring was returned and installed on the engine 9/21/77. The slipring housing was realigned and dowel pinned to the spinner to reduce runout below the level of the previous engine run. The inlet rakes were then reinstalled.

The purpose of this test was to establish an acceptable field balance of the engine. In all, ten balance runs were made. As before, vibration levels at idle were acceptable, but the slipring accelerometer indicated high levels as fan speed was increased. Fan blade angle was set at +5° and fan nozzle area was 1.61 m^2 (2500 $in.^2$) throughout the test. Changes in balance weights were made after each run, with no significant reduction in slipring vibration. An oil leak at the hydraulic depressurization valve which was discovered mid-way through the test was corrected and testing was resumed. Further field balance running was suspended when another oil leak was detected at the hydraulic servo package. All other engine parameters remained normal throughout this run. Maximum speeds obtained were 2508 rpm fan and 12,000 rpm core.

Run:	No. 4 - Mechanical Checkout
Date:	9/27/77 through 9/29/77
Run Time:	19 hours 50 minutes
Total Engine Run Time:	28 hours 42 minutes
ADH Readings:	No. 23 through 67

Prior to this run, two additional accelerometers were added to the fan frame, and the hydraulic servo block was repaired and reinstalled. A dry motor was performed with no leaks evident.

Nine diagnostic field balance runs were made, commencing with Engine Start No. 22. The runs, primarily at speeds between 1800 and 2600 fan rpm, totaled approximately 5 hours and 25 minutes of running time. During this time, oil consumption was running about 0.004 to 0.008 m^3 (1 to 2 gallons) per hour. The ninth run was stopped due to low oil level in the facility hydraulic throttle system. The indicator was replaced and mechanical checkout resumed with Engine Start No. 31. Finally, an acceptable balance was made and the normal test plan was resumed.

During the test, fan speed was varied between 1800 and 3240 rpm and fan nozzle area from 1.36 m^2 (2110 $in.^2$) to 1.87 m^2 (2900 $in.^2$). Fan blade angles were varied between +9° closed to -7° open at 90 percent (3078 rpm) and 96.5 percent (3130 rpm) fan speed with no problems. Both the fan pitch and fan nozzle area actuation systems performed smoothly. All bearing and lubrication system parameters remained normal during the test, although oil consumption continued at about 0.0076 m^3 (2 gallons) per hour. The lube tank was serviced with 0.0456 m^3 (12 gallons) of Royal 899 oil during the test.

In order to complete the test, two intermediate field balances were required on the fan rotor due to vibration characteristic changes. High vibration levels at low speeds required that the fan idle speed be adjusted to 1800 rpm. High fan blade stresses, in the range of the two per rev/first flex crossover, necessitated rapid accels from 2000 to 2500 rpm fan speed at all times. Wind conditions were moderately low and steady during testing, and no further blade stress problems were encountered. Core cowl skin temperatures did not exceed 366 K (200° F).

In all, 44 full data points were taken, including traversing of the three fan bypass duct cobra probes. This test concluded mechanical checkout.

Run:	No. 5 - Baseline Acoustic Test
Date:	10/5/77 through 10/7/77
Run Time:	15 hours 43 minutes
Total Engine Run Time:	35 hours 33 minutes
ADH Readings:	No. 68 through 107

Prior to this test, the following actions were taken:

- Removed slipring, slipring strut, and fan inlet rakes
- The fan and core cowl doors were cleaned and the acoustic treatment on each taped
- Removed LPT discharge rakes
- Replaced heat exchanger water flowmeter
- Serviced lube tank with Royal 899 to give an indicated level of 0.0757 m^3 (20 gallons)
- Set up instrumentation to record near-field, far-field, and wall dynamic pressure acoustic data

Zero and facility sound readings were taken and the test began with Engine Start No. 38. A total of 10 acoustic data points were taken before rain forced an engine shutdown. Running time was 1 hour and 8 minutes. Engine vibration characteristics were well within limits up to 3000 rpm fan speed reached.

Testing resumed 10/6/77 when the weather improved and the rain ceased. Twelve acoustic data points were taken before the winds increased in velocity and changed direction to blow directly up the engine's tail pipe. This direction proved to cause maximum fan blade stresses, and eventually forced a shutdown to avoid exceeding blade stress limits after approximately one hour of testing. Post shutdown inspections revealed nearly 15 percent of the core cowl tape missing and incipient separation of a portion of the fan cowl tape. The lube system was serviced with 0.0076 m^3 (2 gallons) of Royal 899, and the missing cowling tape replaced.

Testing was resumed 10/7/77 with Engine Start No. 40. While setting 3116 rpm fan speed, there was a sudden loss of fuel in pressure resulting in an immediate shutdown from that speed. A faulty air regulator was repaired and the test resumed with Engine Start No. 41. The sudden shutdown apparently caused a shift in the fan rotor balance as indicated by high vibration levels at speeds which had previously shown no activity. Three field balance runs were made before vibration levels returned to acceptable limits. The remainder of the baseline acoustic test was completed without incident.

A total of 41 acoustic far-field data points were recorded with a maximum fan speed of 3161 rpm (97 percent) being reached. Fan nozzle area was varied from 1.36 m^2 (2110 $in.^2$) to 1.87 m^2 (2900 $in.^2$) and fan blade angle between +5° closed to -5° open. Post shutdown inspection revealed that 15 to 20 percent of the core cowl tape was again missing. Approximately 0.038 m^3 (10 gallons) of oil was consumed during the 15-hour test. Other than the high blade stresses which occurred with engine tailwinds, and the fan rotor balance shift, all engine parameters were well behaved.

Run:	No. 6 - Composite Nacelle Performance Test
Date:	11/2/77 and 11/3/77
Run Time:	8 hours 4 minutes
Total Engine Run Time:	43 hours 37 minutes
ADH Readings:	No. 108 through 134

Actions taken prior to this run are listed below:

- Removed bellmouth inlet and inlet adapter
- Removed tape from fan and core cowl
- Removed hardwall core nozzle and installed acoustically treated nozzle
- Reworked core cowl to relieve interference with the core nozzle
- Replaced a cracked flange on the balance piston line
- The composite inlet was installed to the engine and a flowpath mismatch (inlet to fan frame) was discovered. The inlet was removed and returned to Evendale for machining and rebonding to correct the problem.
- The General Electric variable pitch actuator was removed, disassembled, and reassembled using a thinner shim to eliminate backlash and balance shifts while running.
- The acoustic splitter was fitted to the composite fan doors and installed
- A portion of the core door blanket was removed and additional cooling manifolds added. This was to help cool the core cowl skin during reverse testing.

- The variable pitch actuator with its thinner shim was installed in the engine and a fan blade recalibration was completed.
- The fan blades were frequency scanned with no problems noted
- A helium leak check of the fan frame was attempted in hopes of finding the source of the high oil consumption. Equipment failure with the helium checking device prevented completion of the test
- The remachined inlet returned, and was installed on the engine. (See Figure 1 for inlet installation photograph.)
- Installed four inlet rakes, one inlet boundary layer rake, T2 sensor, and three cobra probes in the fan bypass duct
- The engine was borescoped with nothing unusual recorded
- Removed the two accelerometers mounted on the fan frame for the last run and installed them on the inlet
- Installed five additional skin thermocouples to each core door in the aft under cowl cavity area
- Installed slipring and slipring strut
- Reprogrammed recording equipment for performance testing
- Installed inlet support bands around composite inlet

An air motor was performed to check for fuel and hydraulic leaks with none recorded. The first start was terminated after 15 minutes to correct an instrumentation fault in Reading PS3. The second run was stopped after 25 minutes due to high fan blade stresses caused by increasing wind speeds. The weather improved and the test resumed with Engine Start No. 47. Three field balance runs were made; at their completion, the engine vibration characteristics were as low as in any previous run. No further balance shift was noted during the remainder of the test.

Speed range tested varied from 1800 to 3180 rpm (97 percent) fan speed with fan nozzle areas between 1.36 m^3 (2110 $in.^2$) and 1.87 m^2 (2900 $in.^2$). Fan blade angles were varied between -8° open to +9° closed. While running steady state at 90 percent (2970 fan rpm, 13,526 core rpm), -7.6° fan blade angle and 1.6 m^2 (2500 $in.^2$) fan nozzle area, there was a sudden loss of core speed signal, hydraulic and fuel pump discharge pressure. The engine was immediately shutdown and a post shutdown investigation revealed the following.

- No visible external signs of distress except for nonstructural damage to the skin of the fan frame's 12:00 strut, apparently from radial drive shaft failure
- No damage to the inlet or core discharge
- Borescope inspection of the compressor and combustor revealed no damage

- Slight accumulation of metal particles on the scavenge magnetic plug
- No accumulations were noted on the lubrication system filter screens
- The output end of the radial drive shaft turned by hand, indicating it was no longer coupled to the core

The accessory gearbox was removed and the severed radial drive shaft was removed. The shaft was returned to Evendale for inspection and analysis.

Oil consumption during the test was about 0.0038 m^3 (1 gallon) per hour. The reshimming of the fan actuator appeared to have successfully eliminated the fan roter balance shift problem. Blade stress limits were exceeded five times due to sudden gusts of wind at which point the engine speed was reduced to a safe point. This concluded Run No. 6.

Run:	No. 7 - Flight Inlet Stress/Engine Pressure Ratio/Inlet Mach Number Control Mode Checks
Date:	12/3/77
Run Time:	7 hours 16 minutes
Total Engine Run Time:	50 hours 53 minutes
ADH Readings:	No. 135 through 167

Actions taken prior to this run are listed below:

- Inspections of the accessory gearbox were made to determine amount of misalignment between the shaft and gearbox
- The accessory gearbox was disassembled and the bevel gear which mates with the drive shaft was thoroughly inspected
- Radial drive shaft midspan bearing was borescoped with no damage noted
- Repaired the damaged fan frame pylon
- Modifications were made to the spare radial drive shaft and a new sleeve tube was manufactured
- A helium leak check of the fan frame was made and a small leak at the 2:00 strut was isolated and corrected
- The new sleeve, radial drive shaft, and reassembled accessory gearbox were installed on the engine using new alignment procedures and tooling. Final alignment checks were recorded
- Reinstalled engine piping in accessory area

On 12/2/77, dry and wet motoring checks were successfully carried out. The next day, the engine was run at idle for 30 minutes with no leaks or discrepancies noted. Four ADH readings were taken while at idle. The engine was then preped to run the continuation of the inlet stress check.

On 12/7/78, the weather improved and the engine was fired-to-idle but had to be shutdown minutes later due to lack of cooling water to the oil heat exchanger. Investigation proved that the main facility water supply lines had frozen due to the extremely cold ambient temperature. All efforts to thaw the ice failed and the run was cancelled until additional heating equipment could be installed.

A scheduled run for 12/13/77 was aborted when the prestart checks revealed that the slave lube oil/water heat exchangers had ruptured, apparently from the same circumstances that had allowed the facility water lines to freeze. The two heat exchangers were removed and returned to the vendor for repair. Due to the long estimated repair time, five to six weeks, the OTW heat exchangers at NASA-Lewis were shipped to Peebles and installed. The lube syatem was drained of all contaminated oil and the system flushed with new oil. All lines were reinstalled and the lube tank serviced with 0.053 m^3 (14 gallons) of Royal 899.

Continuation of the flight inlet stress check began 12/16/77 with Engine Start No. 54. In all, 25 full data points were recorded, bracketing the planned takeoff region for acoustic testing. Fan blade angles were varied from -10° open to +9° closed, fan nozzle area between 1.87 m^2 (2900 $in.^2$) and 1.36 m^2 (2110 $in.^2$). Maximum fan speed was 3137 rpm (97 percent). The stress check was completed and adjustments were made on the engineering panel to run the pressure ratio control mode test. This was successful with fan speeds being set from idle to 97 percent, nozzle area from 1.48 m^2 (2300 $in.^2$) to 1.87 m^2 (2900 $in.^2$), and fan blade angles between +5° closed and -5° open. The inlet Mach number control test was also performed successfully over the range of Mach numbers between 0.874 and 0.744, holding Mach number with 0.002 of the selected valve.

Actual test corduct went very smoothly, with minimum difficulties. The pretest fan frame leak repairs appeared to have been effective in controlling overall oil consumption, which averaged 0.001 m^3 (0.33 gallon) per hour during the final 6.5 hours of testing. Engine vibration levels were consistent with previous runs. Sensitivities noted were higher vibration levels with smaller nozzle area and more open (negative) blade angles. All other engine parameters were well behaved.

Post shutdown inspections revealed that the concave surface skin had blown off one of the fan frame struts at approximately the 8:00 position. The skin separated at the strut nose joint and partially delaminated as the skin peeled away. No other damage was noted. This concluded Run No. 7.

Run:	No. 8 - Fully Suppressed Acoustic Test
Date:	1/3/78 through 1/4/78
Run Time:	5 hours 45 minutes
Total Engine Run Time:	56 hours 38 minutes
ADH Readings:	No. 168 through 196

Prior to this test, the following activity was completed:

- Added heat tapes to the heat exchangers

- Removed slipring, inlet rakes, and boundary layer rake. Installed all blankoff pads
- Repaired damage fan frame strut skin
- Installed acoustic probes and wall dynamic pressures. Set up recording equipment for acoustic test
- Serviced lube tank to indicate 0.076 m^3 (20 gallons) of Royal 899
- The leading edges of all fan frame struts were covered with fiberglass patches to prevent any repeats of the skins blowing off. New urethane tape was placed over the patches.
- During the fan frame repair, one of the fan blades received a nick on its surface. The blade was repaired.
- A leak was discovered in the lube supply line, and the line replaced.

Snow and high winds prevented engine testing for the remainder of the year. On 1/3/78, the weather improved and the fully suppressed acoustic test began with Engine Start No. 56. Fifteen far-field acoustic data points were taken, including nine at approach conditions and four along the takeoff operating line, before high and gusting winds terminated the run. The control system Recovery Mode was satisfactorily checked out for both the full manual and Mach number modes. Oil consumption was 0.011 m^3 (3 gallons) for the ~6-hour test. All vibration and engine safety parameters remained satisfactory.

The post shutdown inspection revealed minor damage to the fan doors, fan blade tips, and fan frame tip treatment cathedrals. These damaged areas were repaired. High winds and extremely heavy snow accumulation prevented any further testing for the next 8 weeks.

Run:	No. 9 - Fully Suppressed Acoustic Test
Date:	3/10/78
Run Time:	2 hours 23 minutes
Total Engine Run Time:	59 hours 1 minute
ADH Readings:	197 through 200

The following events occurred prior to the test on March 10, 1978.

- Three acoustic microphone stands were damaged by high winds and repaired.
- Repaired defective acoustic probe actuator
- On 2/2/78, several dry motors were made to determine the cause of fan pitch closure, upon engine shutdown, and correlation between blade pitch readings between ADH and the control panel. The Elgar

"off engine" power supply as connected to the digital control during the air motors to keep the control in regulation during coastdown. As long as the control remained in regulation, the blade pitch did not close. Blade pitch readings between ADH and the control panel agreed within 0.2° on the five angles checked

- A fractured water facility water valve was discovered and repaired. The fracture evidently was caused by freezing water
- On 2/15/78, the engine was air motored to lubricate internal parts
- 2/27/78, the winds subsided enabling some acoustic probe data to be taken. ADH readings 192 through 195 were recorded before the winds increased again, forcing the engine to shutdown to remain within the allowable blade stress envelope. Run time was 1 hour and 8 minutes. Several dynamic pressure sensors in the acoustic traverse probes were damaged and the probes returned to Evendale for repair. Fan frame vibration levels were significantly higher than in previous runs. All other engine parameters were normal
- The thrust measuring system was checked out. Bridge A on the load cell was out; Bridge B drifted 400 N (90 lbs); and Bridge C was reading accurately
- The acoustic fan OGV and core discharge traverse probes were re-installed
- On 3/9/78, two starts were aborted due to loss of starter air pressure during a momentary lull in the weather. By the time additional air compressors were hooked up, bad weather had set in again

Finally, on 3/10/78, the weather was greatly improved and the fully suppressed acoustic test began with Engine Start No. 59. A small facility fuel leak was discovered and corrected. Acoustic traverse probe data were taken at two approach thrust 56,500 N (12,700 lb) conditions.

While at 97 percent fan speed (3096 rpm) at a fan nozzle area of 1.87 m^2 (2900 $in.^2$), the indicated fan pitch angle readout changed from +2.9° closed to -137° open over a time span of 8 seconds. All other engine parameters, core speed, Mach number, T5 and vibration levels, remained constant. Since no cause could be detected for this sudden angle change, the engine was immediately shutdown. All vibration levels remained normal during the decel. Preliminary inspection revealed no visible damage and the fan blade pitch was +2° closed as compared to the commanded position of +3° closed. The Elgar "off engine" power supply was connected and the LVDT readout appeared to be working normally, but still indicating -137°.

On 3/11/78, the fan actuator was removed from the engine revealing that the differential assembly had failed and was heavily damaged. It was removed

from the actuator and returned to Evendale for inspection. The engine was secured, concluding Run No. 9.

Run:	No. 10 - Fixed Pitch Mechanical Checkout - -5° Blade Angle
Date:	3/31/78
Run Time:	1 hour 56 minutes
Total Engine Run Time:	60 hours 57 minutes
ADH Readings:	No. 202 through 206

The differential and no-back were disassembled and the differential hardware deemed not reusable. A new differential was ordered; but due to the long procurement time, hardware was designed and fabricated to allow testing of the engine with fixed pitch. The engine's forward sump was inspected, cleaned and lubricated. Tooth pattern checks on the reduction gear star showed no unusual patterns.

Electrical modifications were made to the digital control; consisting of "jumpering" the LVDT and fan pitch servo leads, which was necessary for fixed pitch testing. Hydraulic lines running from the fan pitch servo block to the forward sump were disconnected and capped. The no-back system was reassembled and installed in the engine along with the fixed pitch hardware, fan actuator package, and slipring. The lube tank was serviced with 0.026 m^3 (7 gallons) of Royal 899, and the engine preped to run. The fan blade angle was fixed at -5°27' open. After motoring, the fan blade angle measured at -5°19'.

On 4/3/78, the weather cleared and the test began with Engine Start No. 60. Only one shutdown to change balance weights was required. Testing included adjusting nozzle areas from 1.42 m^2 (2200 $in.^2$) to 1.87 m^2 (2900 $in.^2$). Blade stresses were evaluated up to 98.6 percent fan speed (3200 rpm). Maximum thrust obtained was 81,087 N (18,230 lbs) at 3100 fan rpm, 1.42 m^2 (2200 $in.^2$) fan nozzle area and an inlet Mach number of 0.82.

No control or vibration problems were encountered after the field balance. Postrun measurement confirmed that the fan blade pitch did not change during running. Approximately 0.0076 m^3 (2 gallons) of oil was consumed during the 2-hour run. This concluded Run No. 10 and the engine was readied for fixed pitch acoustic testing.

Run:	No. 11 - Fixed Pitch Fully Suppressed Acoustic Test
Date:	4/3/78
Run Time:	2 hours 50 minutes
Total Engine Run Time:	63 hours 47 minutes
ADH Readings:	No. 208 through 225

Prior to this run, the slipring was removed and the spinner cap installed. The core exhaust acoustic traverse probe and far-field sound microphones were set up. The fan blade angle remained fixed at -5°19' open.

Four field balance runs were required to rebalance the fan rotor prior to running the acoustic test, with the apparent cause for the balance shift being the removal of the slipring. Sixteen acoustic data points were recorded at 2500, 3040 (92 percent), 3140 (95 percent), and 3187 (98 percent) rpm fan speed at fan nozzle areas of 1.42 m^2 (2200 $in.^2$), 1.48 m^2 (2300 $in.^2$), 1.52 m^2 (2360 $in.^2$), 1.55 m^2 (2400 $in.^2$), 1.58 m^2 (2450 $in.^2$), and 1.61 m^2 (2500 $in.^2$); providing a good matrix of data near takeoff thrust. Maximum thrust achieved was 77,400 N (17,400 lbs) at 3140 fan rpm and 1.48 m^2 (2300 $in.^2$) fan nozzle area. Maximum speed obtained was 3187 fan rpm which was dictated by a T41C limit of 1444 K (2600° R). The test was terminated prematurely when wind speeds increased beyond the allowable envelope set by fan blade stresses. No probe traverse data were taken.

Engine operation was smooth throughout the test with no appreciable consumption of oil. This concluded Run No. 11, as the engine was readied for reverse thrust mechanical checkout.

Run:	No. 12 - -95° Blade Angle Reverse Performance Test
Date:	4/6/78
Run Time:	1 hour 22 minutes
Total Engine Run Time:	65 hours 9 minutes
ADH Readings:	No. 226 through 236

Prior to this test, the following actions were taken:

- Removed all acoustic traverse probes
- Installed four inlet rakes and one boundary layer rake facing aft
- Installed three cobra traverse probes in the fan bypass duct facing aft
- Removed fins from boattail
- Removed acoustic splitter and installed blankoff pads
- Installed an additional accelerometer on the lower left fan nozzle flap
- Set up recording equipment for reverse thrust testing per Test Request
- Removed the spinner and actuator cover and adjusted fan blades to a measured angle of -95° open. Reinstalled cover, spinner, slipring, and slipring strut
- Serviced lube tank with Royal 899 to indicate 0.068 m^3 (18 gallons)

A dry motor was performed and the fan nozzle flaps actuated between 2.45 m^2 (3800 $in.^2$) and 2.61 m^2 (4050 $in.^2$). Some slight vibration was observed in the upper two flaps during the motor. The engine was then run at idle for 15 minutes with the nozzle flaps full open, indicating 2.64 m^2 (4100 $in.^2$) nozzle area. Nothing unusual was recorded during the idle check or in the post shutdown inspection that followed.

The reverse thrust performance test began with engine start No. 70. The nozzle area was adjusted to 2.64 m^2 (4100 $in.^2$) and idle fan speed to 1800 rpm. Indicated reverse thrust was -11,920 N (-2,680 lbs) at idle. ADH and traverse probe data were recorded at 1900 rpm fan speed. A slow accel to 2485 fan rpm was made where the T5 limit of 1033 K (1400° F) was reached. The engine could not be stabilized at this point due to high fan blade stresses, and was backed off to idle. Maximum reverse thrust was -20,038 N (-4505 lbs) while at the 2485 rpm. High under cowl cavity temperatures resulting from the decel to idle required the engine to be shutdown for cooling.

After a period of cooling, the engine was again started, and acceled to 2200 rpm fan speed, the highest speed at which fan blade stresses would allow prolonged running. ADH and traverse probe data were recorded. Another quick accel to 2460 fan rpm was made before reaching the T5 limit, but high blade stresses forced an immediate reduction back to 2000 rpm. High undercowl cavity temperatures were encountered again, 548 K (527° F), forcing engine shutdown. This concluded -95° reverse thrust performance testing.

Engine vibrations were slightly higher during reverse testing. Fan blade stresses approached 200 percent of scope limits while operating at the T5 limit. Post shutdown inspection revealed nothing unusual.

Run:	No. 13 - -95° Blade Angle Reverse Acoustic Test
Date:	4/7/78
Run Time:	36 minutes
Total Engine Run Time:	65 hours 47 minutes
ADH Readings:	No. 237 through 246

The boundary layer rake and four inlet rakes were removed. The acoustic splitter was installed and the oil tank serviced with Royal 899 oil to indicate 0.068 m^3 (18 gallons). The recording equipment was set up for acoustic far-field data.

The engine was fired-to-idle with Engine Start No. 72. Acoustic far-field data and full ADH points were recorded at 1800, 1900, 2000, 2100, and 2200 rpm fan speed. A slow accel and decel from 2000 to 2400 rpm was made with maximum recorded thrust being -19,170 N (-4310 lbs). Nozzle area for the entire test was a full open 2.64 m^2 (4100 $in.^2$). The engine was decelled to idle to cool before shutdown but high reduction gear vibrations necessitated an immediate shutdown. A 2-minute air motor was made to cool the engine down shortly afterwards. A post-shutdown inspection was made with no discrepancies noted.

Run:	No. 14 - -8° Blade Angle Fully Suppressed Stress Check
Date:	4/8/78
Run Time:	1 hour 1 minute
Total Engine Run Time:	66 hours 48 minutes
ADH Readings:	None

The purpose of this test was to stress map the fan blade performance over the engine operating range at a -8° blade angle. The spinner and fan pitch actuation cover were removed, and the blade pitch changed to -7°52' open.

The test began with Engine Start No. 73. Vibration levels on the fan rotor were high at idle and the engine was shutdown to change balance weights. The second start showed reduced vibration levels enabling completion of the test. The engine was acceled slowly from idle to 2000 fan rpm, then rapidly through the fan blade two/rev critical, to 2500 rpm and slowly acceled again until the T41C limit was reached (2951 fan rpm). The stress sweeps included nozzle areas of 1.48 m^2 (2300 $in.^2$), 1.52 m^2 (2360 $in.^2$), 1.58 m^2 (2450 $in.^2$), and 1.87 m^2 (2900 $in.^2$). Panel readings were recorded at each point. Both the fan blade stress and vibration survey were acceptable for further running under the same prevailing wind conditions. No engine related problems were encountered. The engine was then preped for acoustic testing.

Run:	No. 15 - -8° Blade Angle Fully Suppressed Acoustic Test
Date:	4/15/78
Run Time:	1 hour 38 minutes
Total Engine Run Time:	68 hours 26 minutes
ADH Readings:	251 through 263

The slipring was removed and the engine preped to run; however, high prevailing wind conditions prevented testing for one week. On 4/15/78, wind conditions improved and testing began with Engine Start No. 76. Engine vibration levels were low and no field balance was required. ADH and far-field data points were recorded at 80, 89, 91 percent and maximum speed limited by T41C (2578, 2797, 2928, and 3100 fan rpm) at 1.53 m^2 (2360 $in.^2$), 1.48 m^2 (2300 $in.^2$), 1.54 m^2 (2400 $in.^2$), and 1.58 m^2 (2450 $in.^2$) fan nozzle areas.

High winds forced an engine shutdown midway through the test. An inlet inspection revealed part of the blade platform had lifted on fan blade No. 13. The damaged area was sprayed with a sealer to prevent further lifting. The remainder of the test passed without incident. Post shutdown inspections revealed no other damage.

Run:	No. 16 - -3.5° Blade Angle Fully Suppressed Acoustic Test
Date:	4/16/78
Run Time:	2 hours 9 minutes
Total Engine Run Time:	70 hours 35 minutes
ADH Readings:	No. 264 through 284

Prior to this test, the spinner and fan actuator covers were removed and the fan blades adjusted to -3°20' open. The cover and spinner were then reinstalled. ADH and acoustic far-field data points were recorded at 91, 95, and 97 percent (2939, 3068, and 3100 fan rpm) for nozzle areas of 1.87 m^2 (2900 $in.^2$), 1.64 m^2 (2550 $in.^2$), 1.58 m^2 (2450 $in.^2$), 1.55 m^2 (2400 $in.^2$), and 1.48 m^2 (2300 $in.^2$). Additional speed points of 80 and 87 percent (2585 and 2810 fan rpm) were recorded for 1.52 m^2 (2360 $in.^2$) fan nozzle area. Gusting wind conditions forced four shutdowns during the test in order to stay within the wind speed envelope for blade stresses. Steadily rising wind velocity finally terminated the last two planned data points. This concluded Run No. 16.

Run:	No. 17 - -100° Blade Angle Reverse Acoustic Test
Date:	4/21/78
Run Time:	30 minutes
Total Engine Run Time:	71 hours 5 minutes
ADH Readings:	No. 284 through 286

The spinner and fan actuator cover were removed and the fan blade angle set at -100° open. The cover, spinner, and slipring were installed and the engine preped to run. High wind conditions exceeding the blade stress wind envelope limits delayed testing for several days. On 4/21/78, the winds died down and the test began with Engine Start No. 82. ADH and sound readings were taken at idle 1800 fan rpm with the nozzle area at full open 2.64 m^2 (4100 $in.^2$). Engine vibration levels were low; however, the fan nozzle area readout on the operator's panel was changing by as much as 0.04 m^2 (60 $in.^2$). A slow accel to maximum allowable fan speed was stopped when high fan blade stresses were encountered at 2300 rpm.

The fan nozzle area was reduced to 2.51 m^2 (3900 $in.^2$) with the same variation noted. A second slow accel to maximum fan speed was aborted, again due to high blade stresses. A rapid accel from idle to 2645 rpm was then successfully performed and the engine stabilized as ADH and sound readings were taken.

A visual inspection of the fan nozzle flaps was made at this time, and it was discovered that the top left-hand flap was vibrating approximately 2.54 cm (1 inch) at the tip. The other upper flap was vibrating at a smaller amplitude and the bottom two flaps showed no signs of movement. Since the upper flaps were not instrumented, an evaluation of the vibration mode could not be made. The engine was immediately brought back to idle, allowed to cool for 5 minutes and shutdown. A post shutdown inspection revealed no damage to the nozzle flaps. Further reverse testing was canceled pending further investigation of the flap vibration.

Run:	No. 18 - Variable Pitch Functional Checkout
Date:	4/27/78
Run Time:	1 hour 29 minutes
Total Engine Run Time:	72 hours 34 minutes
ADH Readings:	No. 288 through 294

The purpose of this test was to checkout the operation of the rebuilt Variable-Pitch Mechanism. The slipring, spinner, fan actuator, and fixed-pitch hardware were removed and the new differential assembly installed. The hydraulic motor was installed, the hydraulic lines reconnected, and a hydraulic cart used to pressure check the system at 1034 N/cm^2, 1500 psia. No leaks were discovered; however, as the hydraulic pressure reached approximately 827 N/cm^2 (1200 psia) with the fan nozzle flaps full open and against the mechanical stops, the upper left flap began vibrating in the same mode as observed during the last reverse thrust test with a peak displacement at the tip of approximately 2.03 cm (0.8 in.). The upper right flap was vibrating at a smaller rate of about 0.64 cm (0.25 in.) while the lower two flaps appeared to remain stationary. A snapping sound was emitted from the top left nozzle actuator and was assumed to be the sound of the actuator port valve opening and closing. The nozzle flap vibration ceased as the hydraulic pressure was reduced below 827 N/cm^2 (1200 psia). All further actuations were made with the hydraulic pressure at this level or lower.

The fan actuator was reinstalled and the digital control electronic systems were restored for variable-pitch operation. Using the hydraulic cart, the blades were actuated from +17°10' closed to -112°14' open which was the full mechanical travel available. The Elgar "off engine" power supply was connected to the digital control and the blades actuated from +9.7° closed to -112°41' open using the full range of the fan blade pitch pot on the operator's panel. The fan blades were then calibrated over this same range using the operator's panel blade angle readout and an inclinometer to measure blade angles. The hydraulic cart was removed and original engine piping restored. The spinner, slipring, and slipring strut were installed and the engine preped to run. All recording instrumentation was set up for a vibration, stress, and mechanical performance survey.

The Elgar power supply was removed and the engine air motored to 3800 core rpm for 3 minutes. The fan nozzle was adjusted to 1.61 m^2 (2500 in.^{2}) and blade angle adjusted from +3.5° to +8° then back to +5° closed. After motoring, the blade angles were measured to have fully closed to +9.5°. The Elgar power supply was again connected to the digital control to prevent the blades from closing down during shutdown, and the engine motored to 3800 rpm for 3 minutes. Blade angle was adjusted to +5° closed and measured after coast down to be +4°50'. The engine was motored for 5 minutes while the fan nozzle area was set at 2.61 m^2 (4050 in.^{2}) and the fan blades actuated to -100° open. Upon coast down, the measured blade angle was -99°40'. A final air motor was performed and the blades actuated to +5° closed and nozzle area set at 1.61 m^2 (2500 in.^{2}). The inclinometer measured blade angle on shutdown was +4°50'. The Elgar was removed and the core exhaust acoustic probe installed. One far-field microphone was also set up.

The test began with Engine Start No. 83. An idle leak check was performed with no problems indicated. Two changes in balance weights were required to reduce slipring vibration to previous test levels. Fan blades were closed to +8° where fan speed stabilized at 2100 rpm. Two attempts were made to open the blade angle to -5° but high fan rotor vibrations prevented operating at angles more open than 0°. The fan blades were set to +5°, and

the engine acceled to 2600 rpm. Again, the blades were closed to +8° with no problems; high vibration levels prevented opening blades beyond +1°. The engine was acceled to 3000 rpm fan speed and the blades closed to +8° and opened to 0° where high vibration levels again occurred.

Six ADH readings were taken during the test. Digital control readings were taken at +8°, +5°, and 0° blade angles while at idle, 2600, and 3000 rpm fan speed. Fan nozzle area remained 1.61 m^2 (2500 $in.^2$) for these points. Acoustic core probe and far-field data were recorded at idle, 2600 and 3000 fan rpm with the blade angle set at +3.3° closed and 1.87 m^2 (2900 $in.^2$) fan nozzle area. Other than high fan rotor vibration levels at open blade angles, the engine operated as smoothly as in previous variable pitch tests. Maximum indicated thrust was approximately 54,700 N (12,300 lbs) at 3000 fan rpm and 0° blade angle.

An extensive post shutdown inspection revealed nothing but normal engine wear. No appreciable amount of oil was consumed during the test. All oil and hydraulic system filters and screens were removed and inspected with nothing unusual found. This completed the testing for this installation of the QCSEE UTW engine. The engine was removed from the test stand and all engine hardware packed for storage awaiting test stand availability for further follow-on acoustic testing.

Prior to the follow-on acoustic testing, the following pre-installation activity took place:

- A frequency scan and ultrasonic inspection of the composite fan blades found nothing unusual.
- A helium leak check of the fan frame found only one leak from an instrumentation leadout tube at 4 o'clock.
- Installed six wall static pressure taps on the inner flowpath of the composite inlet at stations 106.61 and 122.76.
- Repaired cathedral tip treatment on the fan frame in several areas.
- Visually inspected fan flaps and composite nacelle for faults with nothing unusual recorded.
- Began programming of the new Site IV-D control console for QCSEE usage.
- The thrust measuring system was calibrated in the forward mode up to 88,960 N (20,000 lbs). The load cell used was a 444,800 N (100,000 lbs) cell with a three-bridge circuit.
- Performed a zyglo inspection of the fan spinner. The spinner was approved for further testing.

Engine installation on the Site IV-D test stand began 6/27/78. The hardwall core nozzle and centerbody bellmouth inlet and the composite fan and

core cowling were installed. The slave lubrication system was cleaned and serviced with Royal 899 oil. The oil level sensor was calibrated at this time.

The variable stator vanes, Stage 1 and Stage 3, fan blade angle and fan nozzle area were calibrated with the entire electronic network, Sanborn Recorders Digital Control, and the Data Modernization System (DMS) and control console programmed. Blade angles were calibrated between +9.1° closed and -9.3° open. The fan nozzle actuator required rerigging to place the actuator against its stops in the fully closed position. Nozzle area was calibrated between 1.36 m^2 (2108 $in.^2$) and 1.87 m^2 (2909 $in.^2$) as measured. The fan blade angle and fan nozzle area measured curves were programmed into the DMS and control console programs. These values differed slightly from the indicated A18 and blade angle as seen on the operator's panel. Blade angles were always set using the control console angle. Fan nozzle area deviation between the console and operator's panel was so small that the latter indication was used when setting A18 for operator ease. The core nozzle remained fixed at 0.361 m^2 (560 $in.^2$).

Instrumentation was connected per the Test Request and Test Request Changes. Only safety, control, and basic aeroperformance instrumentation were terminated. Six wall dynamic pressures and the fan OGV acoustic traverse probe were installed. The slipring system was not used during the entire follow-on test sequence. The acoustic treatment on the fan doors, fan nozzle flaps, core doors, and fan frame OGV's were taped for the first baseline acoustic test.

On 7/3/78, engine installation and the facility prerun checklists were completed. The initial dry and wet motors were performed with some minor rerigging of the throttle required to achieve the correct stopcock position. A small hydraulic leak around an instrumentation fitting was corrected. The first attempt to fire-to-idle was aborted due to a loss of core speed at 4400 rpm. The problem was traced to an errant setting on the starter protection module; and was corrected by raising the starter cut-off speed to 7900 core rpm.

Two successful starts were then made; but in each case an immediate shutdown was required. The first shutdown was made after the lube pump discharge pressure failed to rise to an acceptable level. A misprogrammed pressure transducer was found to be the cause and was corrected. The second shutdown was made after the control console CRT failed to display safety parameters while running at idle. Two dry motors were made to troubleshoot the control console problem.

On 7/14/78, three attempts to fire-to-idle, to further troubleshoot the control console problem, were made; and in each case, were aborted due to insufficient starter air pressure. A defective facility air valve was isolated as the problem. The engine was then fired-to-idle by manually opening the starter air valve. The engine was shutdown after 2 minutes of running at idle and a booster on the starter air valve was replaced. A subsequent dry motor showed the starter air valve to be functioning correctly again. The T3 sensor going to the digital control was found to be

damaged and was replaced at this time. Total engine time after this test was 10 minutes.

On 7/15/78, the engine was fired-to-idle to check out the console and DMS programs. A small accel from 1800 to 1900 fan rpm was made. The blade angle and nozzle area remained +5° closed and 1.61 m^2 (2500 $in.^2$) respectively throughout the 24-minute idle run. Several engine logs and DMS readings were taken. All engine operating parameters appeared the same as in Run No. 18 of the last test. A portion of the tape on the core cowl had lifted during the run and was repaired. Work began on setting up the far-field microphones in preparation for the first acoustic test. Total engine run time was 34 minutes and engine logs 1 through 9 and DMS readings 1 through 11 had been recorded. The following is a history of the test between 7/15/78 and 7/21/78.

Run:	No. 19 - Unsuppressed Acoustic Test (Conf. 1B)
Date:	7/15/78 through 7/16/78
Run Time:	7 hours 22 minutes
Follow-on Test Run Time:	7 hours 56 minutes
Total Engine Run Time:	80 hours 30 minutes
DMS Readings:	No. 12 through 42
Engine Logs:	No. 14 through 72

Prior to this test, the fan nozzle and core exhaust acoustic probes were installed. The first part of this run was devoted to achieving an acceptable balance for the range of blade angles to be tested, 8° open to +9° closed. The test began with Engine Start No. 4; however, a misprogramming of the engine vibration sensors was detected and the engine was shutdown to effect repairs. The test resumed with Engine Start No. 5. The engine was accelerated in steps up to 3000 fan rpm with blade angle set at +5° closed, and A18 at 1.61 m^2 (2500 $in.^2$) with no significantly high vibration levels noted. The engine was decelerated to 2800 fan rpm and the blade angle opened to 0° where high fan filtered vibrations were encountered. The engine was shutdown and a field balance weight added at Position 11. The engine was fired-to-idle and accelerated in steps up to 3100 rpm, where the blade angle was adjusted from +5° closed to -5° open. While the vibration levels were improved, they were still too high for prolonged running. The engine was shutdown and the amount of balance weight at Position 11 was decreased.

The next attempt to fire-to-idle was aborted when the engine failed to light 15 seconds after fuel was supplied. The test resumed with Start No. 7. The engine was accelerated to 3100 rpm, the nozzle area adjusted to 1.48 m^2 (2300 $in.^2$), and the blade angle varied between +9° closed and -8° open with very little vibrational activity. The nozzle was then opened to 1.61 m^2 (2500 $in.^2$) and the blades varied between +9° and -8° again with only slight vibrational activity. The engine was then shutdown to correct some acoustic instrumentation faults before proceeding with acoustic testing. Test run time was 4 hours 3 minutes. During the shutdown, 0.0076 m^3 (2 gallons) of Royal 899 oil was added to the lube tank.

The acoustic test began with Engine Start No. 8. The fan OGV, fan nozzle, and core exhaust acoustic probes were traversed at maximum fan speed (3100 rpm) at blade angles of +4.3° and -5°, at nozzle areas of 1.65 m^2 (2550 $in.^2$) and

1.52 m^2 (2360 $in.^2$), respectively. The engine was shutdown and the traverse probe stands removed in preparation for far-field testing.

Far-field acoustic testing began with Start No. 9. This portion of test ran very smoothly with only one shutdown to check a high core cowl skin temperature indication required. Fourteen far-field sound readings were taken at blade angles varying between +1.8° and -8°, nozzle areas between 1.52 m^2 (2360 $in.^2$) and 1.87 m^2 (2900 $in.^2$) at idle, 80, 85, 90, and 92.5 percent and 3100 rpm fan speed. The acoustic array portion of the test was deleted when several of the array microphones could not be properly calibrated due to moisture in the system.

The engine performed well throughout the test with no lube system, hydraulic system, or digital control problems recorded. The midspan bearing ran at its limit of 544 K (260° F) during extended running at maximum fan speed due to the fact that the heat exchanger could only cool the supply oil to 327 K (140° F) at this speed. 0.023 m^3 (6 gallons) of oil was consumed during the test. Sound Readings No. 145 through 162 were recorded. This completed the fully unsuppressed acoustic test.

Run:	No. 20 - Acoustic Baseline Test (Configuration 2)
Date:	7/16/78 through 7/17/78
Run Time:	10 hours 38 minutes
Follow-on Test Run Time:	18 hours 34 minutes
Total Engine Run Time:	91 hours 08 minutes
DMS Readings:	No. 43 through 104
Engine Logs:	No. 73 through 141

Prior to this test, the tape was removed from the fan frame OGV's and damaged areas of tape repaired on the fan and core cowling acoustic treatment. The test began with Engine Start No. 11. Twenty-three far-field acoustic points were set and recorded before high winds forced a shutdown after 2 hours and 33 minutes of run time. Blade angles had been varied between -3.3° and -5.0° at nozzle areas of 1.52, 1.58, and 161 m^2 (2360, 2450, and 2500 $in.^2$) at speeds from 2600 to 3100 rpm. During this shutdown, the acoustic array was prepared.

The winds subsided and the test resumed with Start No. 12. Array data were recorded at 94.6 percent fan speed at +4.3 and -5° blade angle and at 1.52 and 1.65 m^2 (2360 and 2550 $in.^2$) nozzle areas, respectively. High winds forced another shutdown eliminated the last two aiming angles of the latter array point. The array was removed from the sound field and far-field acoustic testing began with Start No. 13 when favorable wind conditions returned.

With the fan nozzle area set at 1.52 m^2 (2360 $in.^2$) and at 94.6 percent fan corrected fan speed (3085 rpm), far-field points were recorded at +5°, 0°, -2°, -4°, -6°, -7°, and -8° blade angles. With the blade angle remaining at -8° open, speed points of 92.5, 90, 85, and 80 percent corrected fan speed, respectively were set. While setting these 11 acoustic points, there was no variation in the engine vibrational chartacteristics. While at 80 percent fan speed, the nozzle was adjusted to 1.87 m^2 (2900 $in.^2$) and the blade angle set to +3.3°. An acceleration to 91.9 percent speed was aborted when the No. 1

bearing and fan frame horizontal accelerometers reached 4 mils double amplitude at approximately 2950 fan rpm. The blade angle was set to +5°, the nozzle area to 1.61 m^2 (2500 $in.^2$) and another acceleration attempted; but again, high vibrational activity forced a backoff to 2500 rpm. Two more attempts to accelerate the engine to max speed were made with -3° and -8° blade angles with similar results. Vibration levels were safe at 2500 fan rpm but would steadily increase with increasing fan speed until the 4 mil double amplitude fan filtered frequency limit was reached. The engine was shutdown to rebalance the fan. Total follow-on test run time was 13 hours 28 minutes.

During this shutdown, the field balance weight at position 11 was removed and the lube system serviced with 0.023 m^3 (6 gallons) of Royal 899 oil. Engine testing resumed with Start No. 14. An accel to 3100 rpm fan speed was successfully made with a +5° blade angle and 1.61 m^3 (2500 $in.^2$) nozzle area as vibrational activity returned to approximately the same levels as before the balance shift occurred. Far-field data were taken at +3.3°, +1.8°, +0.4°, and -3.3° blade angle. Another balance shift was recorded as an attempt to close the blade angle to +4.3° was made. No. 1 bearing and fan frame horizontal fan filtered accelerometers reached 4.1 mils double amplitude at 2950 rpm fan speed. The blade angle was then opened to -8° and the engine accelerated to 3100 rpm fan speed with no vibrational problems. The remaining five far-field data points were taken at this blade angle and the engine was shutdown to install the core exhaust and fan nozzle acoustic probes.

A small perforation, approximately 1.27 cm (one-half inch) in diameter, was discovered on the outer wall of the fan frame duct and repaired. The probes were installed and 0.011 m^3 (3 gallons) of Royal 899 added to the lube tank. Testing resumed with Start No. 15. Two accelerations to maximum fan speed (3100 rpm) with +4.3° and +2° blade angles were aborted due to high vibration levels. Maximum speed was finally obtained with a 0° blade angle setting and 1.87 m^2 (2900 $in.^2$) nozzle area. This blade angle was used for the approach point in taking fan nozzle, core exhaust, and fan OGV traverse probe data. Core probe data were recorded at nine speeds: the fan nozzle and OGV probes at two. Approach point was 0° blade angle, 1.65 m^2 (2550 $in.^2$) nozzle area and 56,900 N (12,800 lbs) of thrust; while takeoff was -5°, 1.52 m^2 (2360 $in.^2$), and 74,700 N (16,800 lbs), respectively. Thrust was corrected, installed thrust. This concluded configuration #2 acoustic testing.

Sound readings No. 163 through 227 were recorded during this test. Although a majority of running was at high speeds, over 3000 fan rpm, the engine performed well with the two fan rotor balance shifts being the only problem. The control console and the DMS data system were plagued with numerous difficulties, resulting in failure to obtain a DMS readings at several acoustic speed points. 0.034 m^2 (9 gallons) of oil was consumed, however, a leaking instrumentation leadout tube discovered on the fan frame during the posttest inspection was considered the cause.

Run:	No. 21 - Core Treatment Effect Accoustic Test (Configuration 3)
Date:	7/19/78
Run Time:	6 hours 52 minutes
Follow-on Test Run Time:	25 hours 26 minutes

Total Engine Run Time:	98 hours 0 minutes
DMS Readings:	No. 109 through 148
Engine Logs:	No. 142 through 179

Prior to this test, the following configuration changes were made:

- Removed the bellmouth inlet and installed the composite flight inlet.
- Installed acoustic splitter.
- Removed tape from all acoustic treatment and cleaned surfaces where adhesive remained.
- Installed acoustic traverse probes at the fan face and inlet throat.
- Resealed the leaking instrumentation leadout tube at 4 o'clock on the aft side of the fan frame.
- Installed a microphone in the pylon area to measure undercowl cooling air noise escaping through the pylon.
- Serviced lube system with 0.011 m^3 (3 gallons) of Royal 899 oil.
- Prepared far-field and acoustic array microphones for acoustic testing.
- Terminated static pressure on inlet.

The test began with Engine Start No. 16. All 22 far-field acoustic points were recorded without incident. Engine vibration levels were low at all speeds, for all blade angles (+3 to -8°) and nozzle areas 1.87 to 1.52 m^2 (2900 to 2360 $in.^2$) tested. The T41C limit of 1700 K (2600° F) was encountered at the -8°, 1.52 m^2 (2360 $in.^2$) and 3100 fan rpm condition. The engine was then shutdown to install the acoustic array. The postrun inspection revealed material lifting slightly from the instrumented core inlet OGV at approximately 12 o'clock. The material was an adhesive-epoxy used to blend in the flowpath over the vane mounted sensors. Repair was delayed until completion of the array test.

Two-thirds of the array data was acquired before increasing wind speeds forced a shutdown to stay within the blade stress limit envelope. The winds did not subside until late that night. During this time, the core inlet OGV instrumentation was repaired and the fan and core exhaust acoustic probes installed. The fan face probe's strain gages were inoperative, prohibiting the probe from being traversed.

No fan rotor balance shifts occurred during this test. In fact, engine vibration levels were lower than at any time during the entire test program. The repair of the leaking instrumentation leadout tube, prior to this test, successfully controlled oil consumption.

No lube system or control problems were encountered, although due to the high ambient temperature, 301 K (82° F), the T41C limit was approached at high speeds and closed nozzle areas. The repairs made to the OGV instrumentation remained intact during the probe run. Acoustic Readings No. 226 through 274 were recorded during this test.

Run:	No. 22 - Splitter Effect Acoustic Test (Configuration 4)
Date:	7/20/78 through 7/21/78
Run Time:	8 hours 4 minutes
Follow-on Test Run Time:	33 hours 30 minutes
Total Engine Run Time:	106 hours 4 minutes
DAS Readings:	No. 151 through 175
Engine Logs:	No. 180 through 238

Prior to this test, the following configuration changes were made:

- Removed acoustic splitter and installed blankoff pads.
- Removed the hardwall core nozzle and centerbody and installed the acoustically treated nozzle and centerbody.
- Removed core exhaust and fan duct discharge acoustic probe stands.
- Repaired strain gages on the fan face acoustic probe.
- Programed Sanborn Recorders for control transient testing to immediately follow this acoustic test.

Testing began with Engine Start No. 19. Eight far-field data points were recorded before high wind speeds forced an engine shutdown after 1 hour and 29 minutes. The winds subsided an hour later and testing resumed. Nine more far-field and one traverse probe speed points were recorded before high winds forced another shutdown. During this shutdown, the core exhaust and fan discharge acoustic traverse probe stands were installed. The wind speed dropped, and the test resumed with Start No. 21. Four core probe data points were recorded when the exhaust probe's dynamic pressure sensors began malfunctioning, eliminating any further traversing of this probe. The fan face, fan OGV, and fan exhaust probes were traversed at takeoff and approach power settings completing the planned acoustic test program. Total follow-on test run time was 30 hours, 4 minutes at this point. Sound readings No. 275 through 298 had been taken. The control room recording equipment was not prepared for transient control testing.

With the engine at idle, 1800 fan rpm, the engineering panel potentiometers were adjusted to the following values shown in Table XIII.

Table XIII. Automatic Control Mode Test.

Function	Value
A18 rate	0.774 m^2/sec (1200 $in.^2$/sec.)
A18 roof	1.71 m^2 (2652 $in.^2$)
A18 max	1.87 m^2 (2900 $in.^2$)
A18 min	1.42 m^2 (2200 $in.^2$)
WF auto gain	Nominal
BF servo gain	Nominal
Max EPR	11.6
BF rate	85°/sec
BF floor	+5.0°
Manual BF gain	Nominal
XM11	0.835*
N1 Schedule	2900**

* Indicated XM11 - Actual XM11 = 0.79
**2789 rpm, Physical on 267 K (20° F) day

Note that blade angles are always set from the closed position while nozzle areas are set from the open position. Unless otherwise noted, an engine log was recorded at each point beginning with Engine Log No. 206. The nozzle was opened to 1.87 m^2 (2900 $in.^2$) and blade pitch adjusted to +8° closed where fan speed stabilized at 1964 rpm. As the auto forward mode was activated, the fan increased to 2100 rpm while the core remained at 10,935. Since the fan was now operating in a critical blade stress range, the core idle speed was adjusted to 10,760 rpm, slowing the fan to 1974 rpm. The control was then switched from auto forward to full manual and back to the auto forward mode, during which fan speed dropped to 1948 and went back to 1970 rpm.

Using Power Demand Pot No. 1 (PDP1) successive accelerations to 80, 85, 90, 95, and 100 percent power demand were made without difficulty. While at 100 percent, the A18 roof was adjusted to 1.82 m^2 (2817 $in.^2$), fan speed limit raised to 3050, and Engine Log No. 215 recorded. The A18 roof was readjusted back to 1.72 m^2 (2670 $in.^2$), the engine pressure ratio (EPR) pot setting on the engineering panel increased to 600, and Log No. 217 recorded. Inlet Mach number was increased from 0.785 to 0.792 on the engineering panel with the only change being a slight increase in nozzle area as shown in Engine Log No. 218. A deceleration from 100 to 90 percent then an acceleration back to 100 percent power demand was performed without incident concluding the steady-state portion of the controls test. The EPR pot setting was returned to 250 in preparation for transient testing. Table XIV lists the parameters at each of the steady-state points recorded.

Table XIV. Steady-State Speed Points.

Engine Log	Power Demand, %	Core Speed	Fan Speed	Blade Angle	A18 ($in.^2$)	Corrected Thrust (lbs)
206	idle	10935	1964	+8.1	2900	3869
207	idle	10935	2100	+8.1	2900	3775
208	idle	10760	1974	+8.8	2900	3350
209	80	12289	2862	+3.3	2900	10169
210	85	12446	3007	+2.4	2900	10941
211	90	12675	2990	-1.6	2900	12495
212	95	12765	2983	-2.1	2728	13239
213	100	12866	2970	-2.8	2463	13950
214	100	12871	2970	-2.5	2817	13636
215	100	12871	3031	-2.0	2817	13576
217	100	13321	3037	-7.2	2430	16640
218	100	13332	3031	-7.2	2468	16362
219	90	13070	3049	-4.5	2900	14733
220	100	13342	3044	-7.8	2476	16402

Using PDP1, a decleration to 60 percent corrected thrust, 43,770 N (9840 lbs), was made and log 221 recorded. Power Demand Pot No. 3 (PDP2) was then adjusted to the same setting as PDP1 and the control switched from PDP1 to PDP2. The engine accelerated slightly and PDP2 was adjusted to set 60 percent thrust again. Control was switched back to PDP1 and log 224 recorded. An acceleration to 65 percent thrust, 47,415 N (10,660 lbs), using PDP1 was performed. A transient from 65 to 60 percent and another back to 65 percent power demand was made by switching the control from PDP1 to PDP2 and back to PDP1 without incident as engine logs 225 through 227 were recorded. The engine was accelerated to 80 percent thrust 58,357 N (13,120 lbs) using PDP1 and PDP2 adjusted to the same pot setting. The control was switched to PDP2 and Log 228 recorded. Switching back to PDP1, an acceleration to 85 percent thrust, 62,000 N (13,940 lbs) was performed and engine log 229 taken. A transient from 85 to 80 and back to 85 percent thrust was then successfully performed.

Using the engineering panel, the engine was set to 100 percent thrust, 72,950 N (16,400 lbs), and then back to 95 percent, 69,300 N (15,580 lbs). PDP2 was adjusted to the same value as PDP1, the control switched to PDP2, and engine log 230 recorded. Switching back to PDP1, the engine was accelerated to 100 percent thrust. A transient from 100 to 95 percent thrust and back to 100 percent was made without incident by switching control from PDP1 to PDP2 and back to PDP1, completing the small transient portion of the test. The EPR pot setting was adjusted to 250 and the engine decelerated to idle with a core speed of 10,700 rpm and fan speed of 1756 rpm. The control was

switched to the full manual mode, but was immediately returned to auto forward when fan speed dropped to 1364 rpm. The fan pitch floor was adjusted to +8° closed on the engineering panel to prevent a recurrence of the event and the full manual mode again selected. Using PDP1, 45 percent power demand was set. The nozzle area and blade angle were adjusted to 100 percent thrust settings, 1.59 m^2 (2470 $in.^2$) and -7.2°, respectively. An acceleration to 2500 fan rpm was aborted when the control console failed to display speeds and fuel flows. The blades were adjusted to +5° and the engine shutdown to effect repairs on the console. Total engine run time was 32 hours, 22 minutes.

The console was repaired and testing resumed with Start No. 22. Wind conditions were becoming unfavorable for prolonged running, so testing began with the long transients. Nozzle area and fan blade angle were set at 1.87 m^2 (2900 $in.^2$) and +8.4. The auto forward mode was selected and the blade angle floor pot adjusted to -3°. An acceleration to 62 percent thrust, 45,227 N (10,168 lbs), was performed using PDP1 and Engine Log 232 recorded. PDP2 was then adjusted to the 62 percent thrust setting and the control switched from PDP1 to PDP2 and back to PDP1 again without incident. An acceleration to 70 percent corrected thrust, 51,060 N (11,480 lbs) was performed followed by Engine Log 233. Wind speeds in excess of the blade stress limit envelope forced a return to idle speeds. During a momentary wind lull, the engine was accelerated back to 70 percent thrust, and a transient to 62 percent and back to 70 percent thrust was performed without mishap. An attempted acceleration to 80 percent thrust was aborted when fan speed increased to 3150 rpm. The engine pressure ratio was reduced twice: once to achieve a fan speed of 3050 and once for 3030 rpm, but in each case fan speed would increase to 3100 rpm as 80 percent thrust was approached. The fan speed schedule was then adjusted to achieve a fan speed of 3000 and finally 2900 rpm. The blade angle auto gain was also adjusted upward at this time.

Another attempted acceleration to 80 percent thrust was thwarted when the power demand pot ran out of travel. Finally, by adjusting the EPR, 80 percent thrust, 58,360 N (13,120 lbs), was obtained and engine Log No. 234 recorded. A transient from 80 to 62 and back to 80 percent corrected thrust was then performed with no faults evident. 85 percent thrust, 62,000 N (13,940 lbs) was then set by again adjusting engine pressure ratio and Log No. 235 recorded. A transient from 85 to 62 and back to 85 percent corrected thrust was completed without apparent incident. However, inspections of high speed Sanborn traces revealed that the engine had overshot the fan speed limit of 3100 rpm, peaking at approximately 3200. No further transient accelerations were made. Engine pressure ratio was adjusted to achieve 90 percent corrected thrust, 65,530 N (14,733 lbs), and a transient deceleration to 62 percent successfully performed. A normal deceleration to idle was made where the blade pitch pot on the engineering panel was reset to nominal and the control switched to full manual. Nozzle area was set at 1.61 m^2 (2500 $in.^2$) and blade pitch at +5° closed, respectively, while Engineering consulted on the fan speed overshoot problem. High wind speeds forced an engine shutdown due to fan blade stress limits. During this shutdown, the decision was

made not to continue with further transient testing at this time. This completed the planned follow-on test program. Table XV lists the steady-state parameters at each of the transient points tested.

Table XV. Steady-State Parameters.

Engine Log	Thrust, %	Core Speed, RPM	Fan Speed, RPM	Pitch Angle, degrees	AIS		Corrected Thrust	
					m^2	($in.^2$)	N	(lb)
221	60	12215	2815	+3.4	1.8710	(2900)	43457	(9770)
224	60	12257	2818	+3.5	1.8710	(2900)	44347	(9970)
225	65	12450	2972	+3.5	1.8710	(2900)	47780	(10742)
226	60	12236	2782	+3.4	1.8710	(2900)	42118	(9469)
227	65	12401	2972	+3.4	1.8710	(2900)	47149	(10600)
228	80	12774	3033	-1.2	1.7219	(2669)	58384	(13126)
229	85	12855	3046	-1.5	1.5890	(2463)	6185[illegible]	(13906)
230	95	13194	3043	-6.2	1.7419	(2700)	68086	(15307)
231	idle	11730	1786	-7.2	1.5948	(2472)	—	—
232	62	12373	2856	+3.3	1.8710	(2900)	45681	(10270)
233	70	12579	3086	+3.0	1.8710	(2900)	51339	(11542)
234	80	12881	2912	-1.9	1.5884	(2462)	59203	(13310)
235	85	12947	2887	-2.9	1.5884	(2462)	61534	(13834)
236	90	13084	2911	-5.3	1.5890	(2463)	64892	(14589)

An extensive post shutdown inspection revealed nothing unusual. No appreciable amount of oil was observed on the engine or test facility. All hydraulic and oil system filters and screens were removed, inspected, and cleaned with nothing unusual found. The composite cowling, flaps, and blades showed no unusual wear or damage of any kind. A borescope inspection of compressor, combustor, and HP turbine revealed no damage. A frequency scan of the fan blades found no significant changes. This completed the testing program for the QCSEE UTW engine.

7.0 PROPULSION SYSTEM PERFORMANCE

7.1 PERFORMANCE COMPARISON

Performance testing on the UTW experimental engine was near completion on Build 1 when the exhaust nozzle support ring failure occurred. When testing was resumed on the second build following repairs, the performance goals were limited to verification of previous Build 1 measurements and completion of reverse mode testing. Instrumentation to measure component performance was not as extensive as that of Build 1 because of the limited goals. In addition, the composite nacelle components incorporated in Build 2 did not have provision for as much instrumentation as the boilerplate parts used on Build 1.

The second build demonstrated overall performance comparable to that of Build 1. There was an improvement in specific fuel consumption at takeoff thrust. At 97 percent fan speed, the sfc from test measurements was lower than that previously estimated from Build 1 data.

Maximum reverse mode thrust achieved was 27 percent, compared to the goal of 35 percent. Engine stress and temperature limits restricted operation at higher reverse thrust.

7.2 FAN PITCH ANGLE

All UTW Build 1 readings were taken with fan rotor pitch angle set by actuation toward the closed (+) direction. This was necessary because of actuation system torque limitations. On Build 2, with the ball spline actuation system installed, the same procedure was used for initial testing in which the bellmouth was used, with the exception of a few hysterisis points. Following installation of the flight-type inlet, the pitch setting procedure was changed so that all readings (again, excepting hysterisis points) were taken with pitch set by actuation in the open (-) direction. This change was made because it was felt that actuation against the blade air loads might improve the consistency of blade positioning.

Comparison of the test data shows that actual fan rotor pitch angle was different between the engine builds for the same indicated pitch angle. The difference in pitch angle between two builds is shown in Figure 8. (See Plotting Symbols in Table XVI.) The trends in Figure 8 also show that when pitch angle was set by actuation in the closed (+) direction, Build 2 was approximately 1.6° more closed than Build 1 at an indicated +5°, and 2.7° more closed than Build 1 at +5°. When pitch was set in the open (-) direction, there was an additional difference of approximately 1.4° further closed from the Build 1 position, due to actuation system hysterisis.

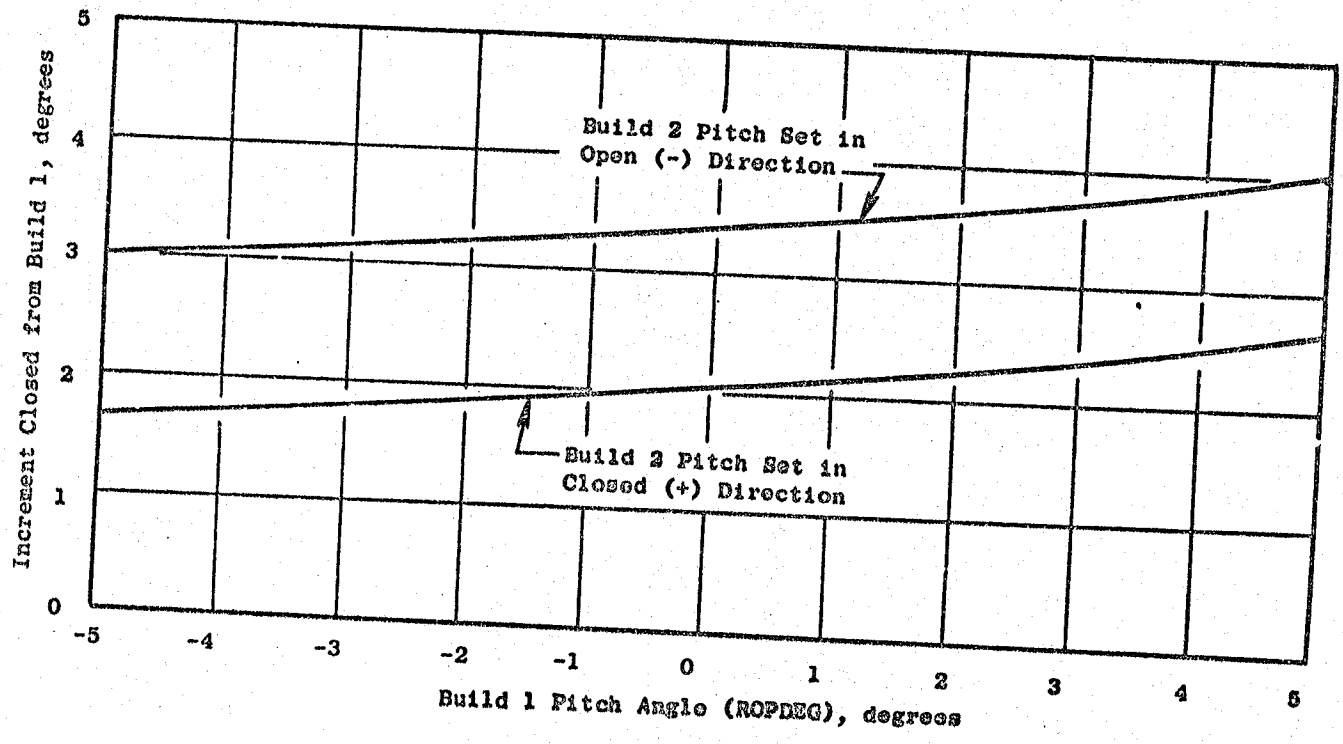

Figure 8. Pitch Angle Comparison Between Build 1 and Build 2.

Table XVI. Plotting Symbols.

Indicated Bypass Exhaust Nozzle Area (A18)	
	2100 In.^{2}
	2250
	2300
	2350
	2400
	2500
	2650
	2900
	3100

Forward Mode Fan Pitch Angle (ROPDEG) Bellmouth	
	9°
	5°
	0°
	-5°
	-7°
	-8°
	-10°

Reverse Mode Fan Pitch Angle (ROPDEG)		
Performance Reading		Acoustic Reading
	-105°	
	-100°	
	- 95°	

The shift in pitch angle between the two builds may be indicative of a basic calibration repeatability/accuracy problem. It may be noted that there also appeared to be a shift between the first and second runs on Build 2. The second run, which was for follow-on acoustic testing after repair of the pitch actuation system, appeared to have pitch angles about 1.4° closed from the preceding Build 2 data.

7.3 THRUST VERSUS AIRFLOW

Thrust-airflow characteristics for the test readings taken with the bellmouth mounted are shown in Figure 9. For bypass stream exhaust nozzle areas (A18) of 1.35, 1.61, and 1.87 m^2 (2100, 2500, and 2900 $in.^2$), the data may be directly compared to Build 1 results. For an A18 of 1.48 m^2 (2300 $in.^2$), there were no directly comparable Build 1 data, so the trend for 1.52 m^2 (2350 $in.^2$) A18 on Build 1 is included instead. The data presented in Figure 9 show that the thrust-airflow trends for Build 2 are consistent with Build 1 results.

7.4 FUEL FLOW VERSUS AIRFLOW

Fuel flow versus airflow for the bellmouth runs is presented in Figure 10. The trends for Build 2 match those of Build 1, allowing for the data scatter normally present in fuel flow.

7.5 UNINSTALLED SPECIFIC FUEL CONSUMPTION

The sfc objective for the UTW is 0.00934 g/sN (0.33 lb/hr/lb) at 81.4 kN (18,300 lbs) thrust, uninstalled on a standard day, 288.15 K (518.67° R). Nominal takeoff airflow is 405.5 kg (894 lbs/sec) at a corrected fan speed (PCNLR) for 94.5 percent. During Build 2 testing, there were no additional data obtained at takeoff thrust and 94.5 PCNLR. However, there were data at 97 PCNLR which included takeoff thrust level. These data show an improvement in sfc at takeoff thrust over previous projected Build 1 trends, which had been extrapolated from data at lower speeds.

SFC trends are presented in Figure 11. The Build 1 trends shown in Figure 11 correspond to Build 2 indicated values. They are extrapolated to 97 PCNLR based on the extensive fan mapping data, and allow for the pitch angle shift noted between the two engine builds. At takeoff thrust, the sfc on Build 2 is about 0.00925 g/sN (0.327 lb/hr/lb) at -5° indicated pitch angle, set toward closed. (This corresponds to -3.37° on Build 1, which probably represents the actual angle.) The airflow at this condition was about 1 percent higher than the nominal value. The data for indicated 0° on Build 2 (+2.10°, Build 1) correspond well. At -5°, there is less consistency between the data for the two builds.

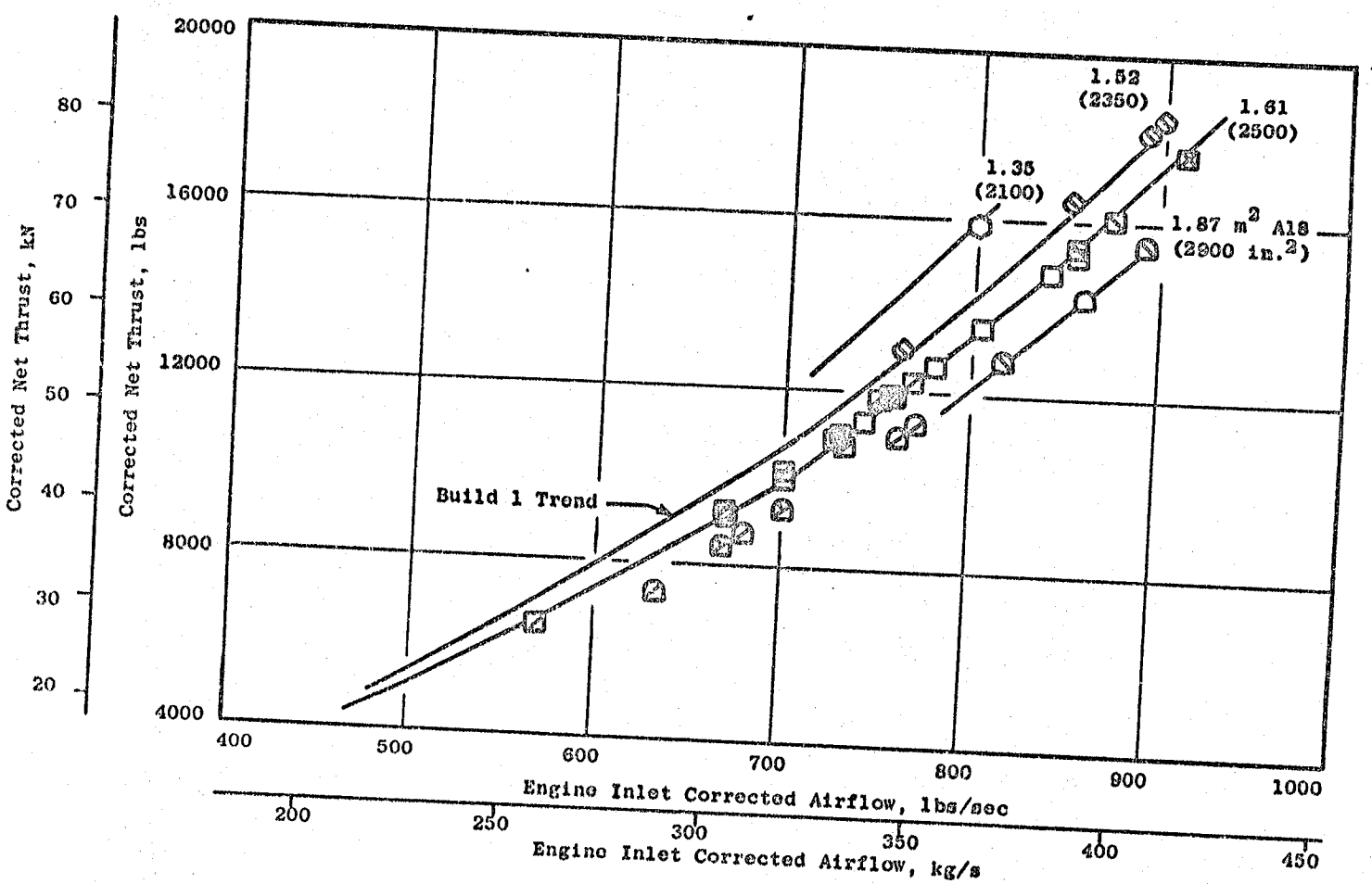

Figure 9. Thrust Versus Airflow with Bellmouth.

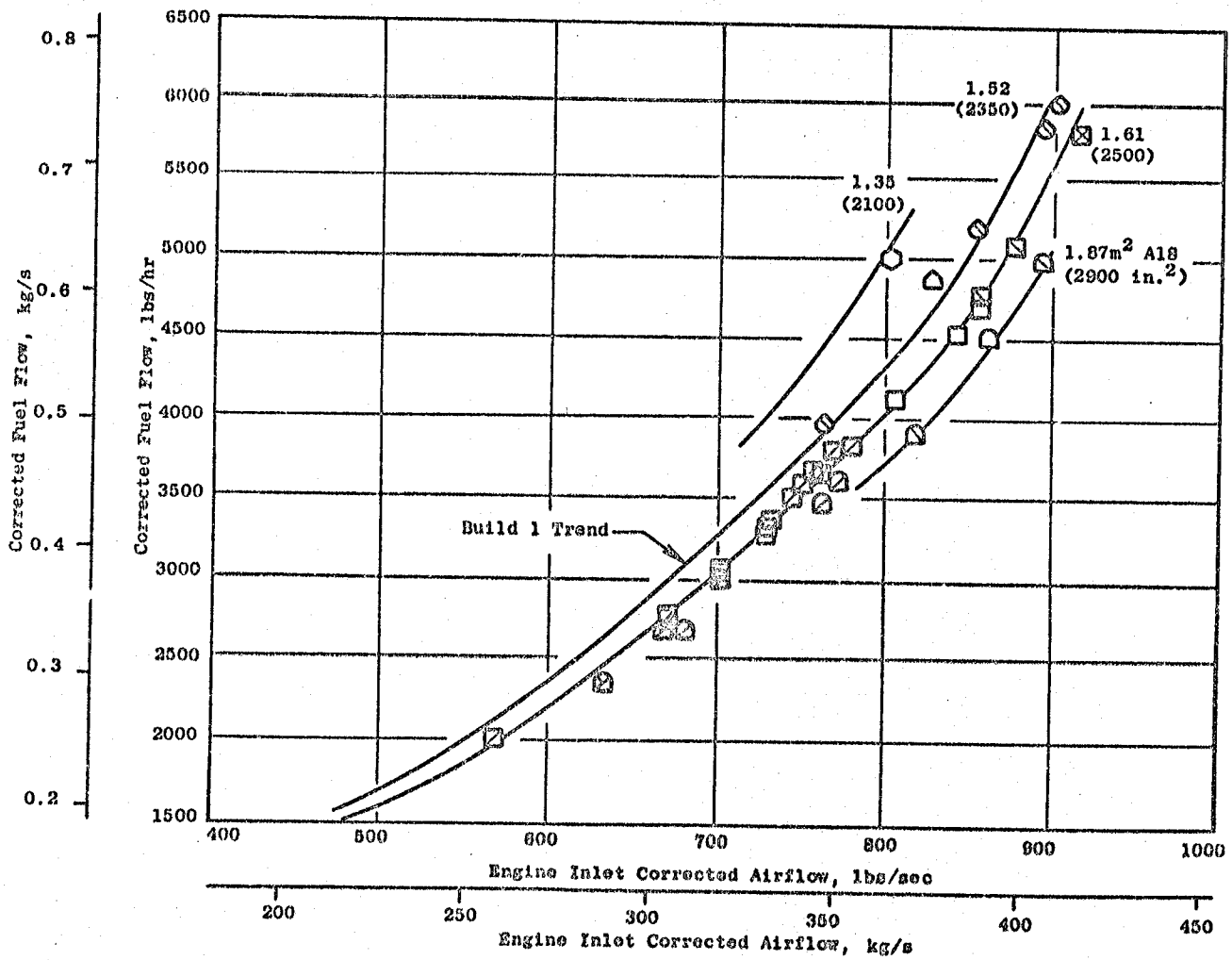

Figure 10. Fuel Flow Versus Airflow with Bellmouth.

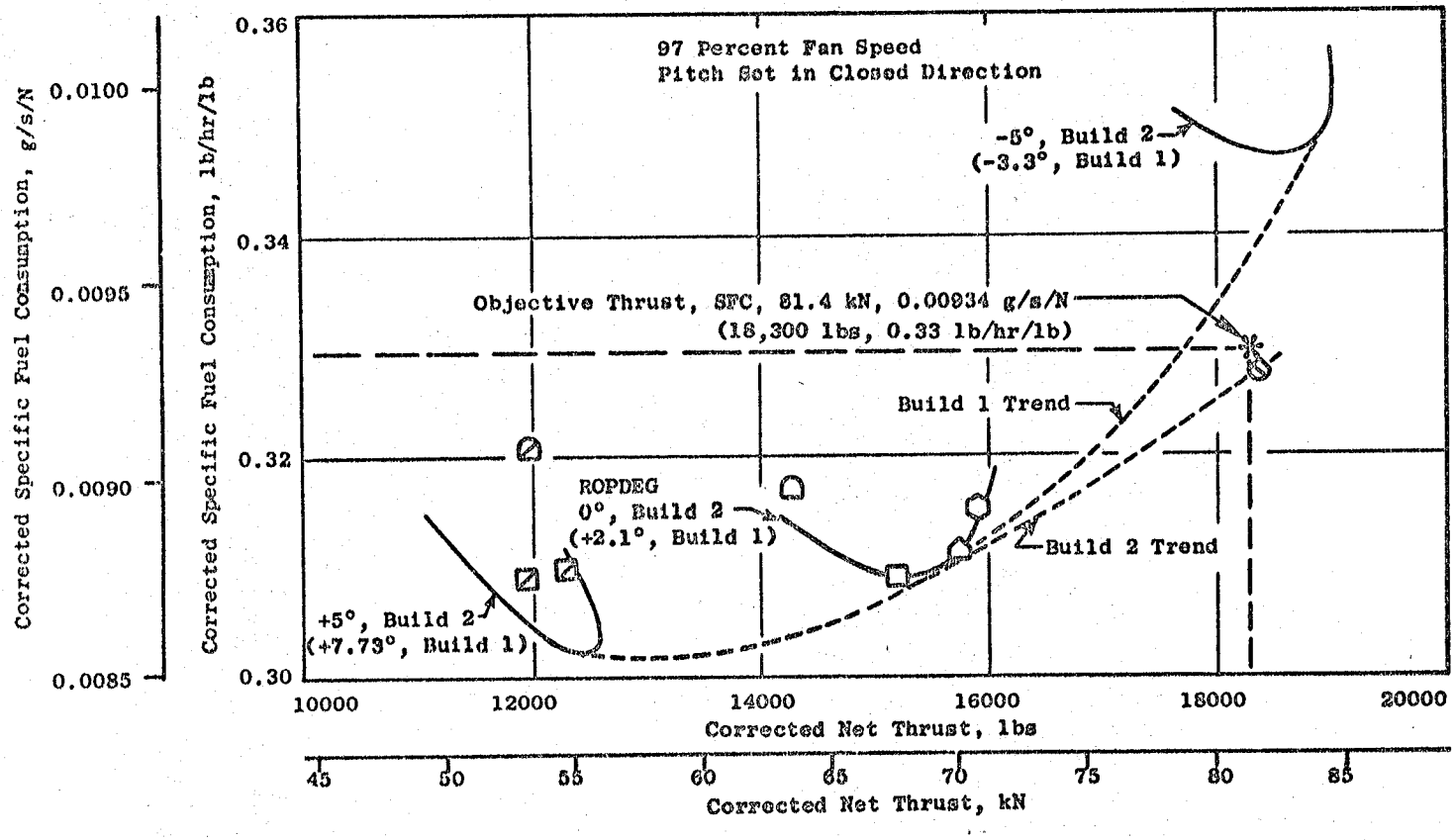

Figure 11. Specific Fuel Consumption Versus Thrust, Uninstalled.

7.6 REVERSE MODE PERFORMANCE

Reverse mode performance testing on Build 2 was done with the fan pitch angle set at -95°. At the time this test was conducted, the actuation system components were being repaired so the blades were positioned by means of the pitch lock adaptor. Since there was some uncertainty during the Build 1 tests as to possible effects of the splitter on reverse mode fan performance, it was removed for Build 2 reverse mode performance testing. The splitter was re-installed for later follow-on acoustic tests so it was possible to assess its effect on overall performance.

The maximum reverse thrust level achieved on Build 2 was -21.1 kN (-4748 lbs), or 27 percent of forward mode installed thrust at takeoff. Although the potential for higher thrust is within engine speed limitations, either blade stresses or LP turbine discharge temperature became limiting when higher levels were attempted.

Reverse mode thrust trends versus fan speed for Build 2 are shown in Figure 12. Also shown in Figure 12 are data from Build 1 and some of the Build 2 acoustic readings. These data are not necessarily directly comparable as noted below:

- The Build 1 data were taken with the splitter installed and the original rotor pitch actuation system.
- The Build 2 performance readings are without the splitter, utilizing the pitch lock adaptor.

At -95° pitch angle, the effect of the splitter on thrust may be noted by comparing the Build 2 performance and acoustic data in Figure 12. At 55 PCNLR, the splitter introduces a loss of 1112 N (250 lbs); at 67 PCNLR, the splitter loss increase to 1334 N (300 lbs). The difference in trend between Build 1 and Build 2 readings at -100° pitch angle may be due to differences in actual blade angle because of the different blade positioning mechanisms.

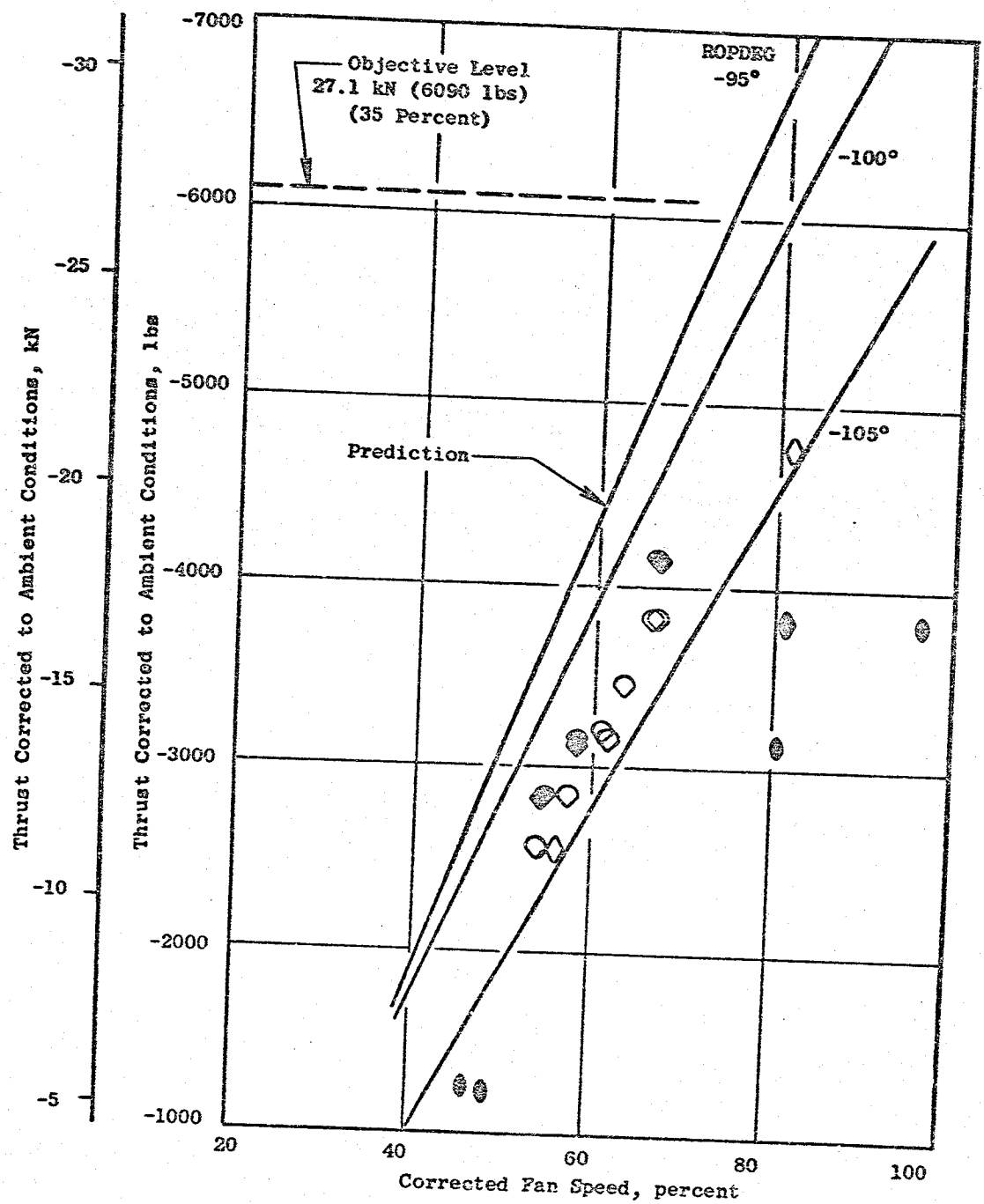

Figure 12. Thrust Versus Fan Speed, Reverse Mode.

8.0 UTW FAN AERODYNAMIC PERFORMANCE

8.1 FORWARD MODE PERFORMANCE

The performance characteristics of the Build 2 fan were similar to those of the Build 1 fan in both forward and reverse modes of operation. A discussion of the Build 1 fan performance and its comparison with the 20-inch diameter scale-model fan simulator tests is given in Reference 1. Although the Build 2 fan did not have sufficient instrumentation for a thorough evaluation of forward mode performance, the available data indicated that the fan flow-pumping capacity and pressure rise at blade pitch settings of -5°, 0°, and +5° were essentially the same for both builds after adjusting for the shift in pitch indication as described in Section 7.0. Build 2 reverse mode performance data were obtained with a configuration somewhat different from that of Build 1, and the comparisons are discussed in the following section.

8.2 REVERSE MODE PERFORMANCE

Build 2 reverse mode aerodynamic performance testing was performed with a single configuration. The fan blades were set at -95° from nominal pitch, and the acoustic splitter in the aft fan duct was removed. Some overall engine performance data were obtained in Build 2 with the splitter installed, but no fan performance data were obtained for this configuration since the fan duct could not be traversed with the splitter in place. Build 1 testing had been performed at blade pitch settings of -105° and -100°, with the acoustic splitter in place. The scale-model fan, described in Reference 3, was tested at all three pitch settings without the acoustic splitter, but at speeds higher than those achieved with the Build 2 fan. There were significant geometric differences between the scale-model fan and the UTW engine fan. The fan aft duct, or "exlet", had a bellmouth-shaped entrance in the simulator, but this entrance in the engine fan consisted of discrete tabs with large gaps in between. The fan rotor hub flowpath and platform geometry of the scale model was smoother and had smaller gaps than the engine fan. Also, the inlet throat of the simulator contained large instrumentation rakes which reduced the physical area by approximately 5 percent, whereas the inlet throat in the engine was relatively unobstructed.

As observed with the Build 1 fan, the reverse thrust produced by the Build 2 fan was significantly lower than that predicted by the scale-model fan when operated at the same speed and pitch setting. However, the effect of removing the acoustic splitter in Build 2 showed a noticeable improvement in the measured thrust. In both builds, the fan produced about 70 percent of the predicted reverse thrust with the splitter installed, but the Build 2 fan thrust increased to 80 percent of the predicted value at the same speed and blade pitch angle when the acoustic splitter was removed (Figure 12). Lack of sufficient instrumentation prevented an evaluation of how much the exlet losses

were reduced when the splitter was removed and, thus, how much effect on thrust might be expected from this change. It could not be determined if removing the splitter had any effect upon the fan's basic pumping characteristics.

Figure 13 presents the engine data from both builds compared to the scale model's reverse mode performance. Pressure ratio shown in Figure 13 was calculated using the atmoshperic engine inlet value and data from the fixed rakes located immediately downstream of the rotor blades in the engine inlet duct. Fan overall pressure rise was significantly lower in the engine than expected from the simulator tests, by an amount sufficient to be consistent with the lower-than-expected reverse thrust. Since the inlet pressure was taken as atmospheric for the data in Figure 13, higher losses in the engine exlet duct would have contributed to the apparent low fan pressure rise. Some cobra probe traverse measurements in the aft duct taken during Build 1 indicated that the exlet recovery (expressed as the ratio of total pressures from Plane 15 to atmospheric) was 1 to 2 percent lower than was measured in the simulator tests, and the recovery could well have been even lower than the traverses indicated. Another possible explanation for the apparent low fan pressure rise is that the rotor hub geometry differences noted earlier, or a difference in the amount of flow entering the core engine inlet duct, might have reduced the amount of separated flow present near the centerline of the engine's inlet duct during reverse thrust operation. A reduction in the size of this dead-water region would have increased the effective discharge area of the fan and lowered its operating line. Finally, the relatively unobstructed inlet throat in the engine, compared to that in the scale model with roughly 5 percent rake blockage, contributed to the lower fan operating line, although this effect is only enough to explain about 25 percent of the discrepancy. While insufficient data were recorded in engine Builds 1 and 2 to resolve this question, it is a subject that deserves further testing and analysis since it directly affects the ability to predict fan performance during reverse mode operation.

Figure 14 compares the flow-passing capability of the engine with that of the scale model. At a given pitch angle and speed, the engine fan pumped slightly less flow than the simulator, on the order of 5 percent, although this percentage is probably within the accuracy of the engine flow measurement in reverse-mode operation. The flow again is corrected by the atmospheric pressure at engine inlet, not the fan inlet pressure. The difference in true rotor inlet corrected flow thus would have been less than shown in Figure 14 if flow induction losses were higher in the engine than in the simulator.

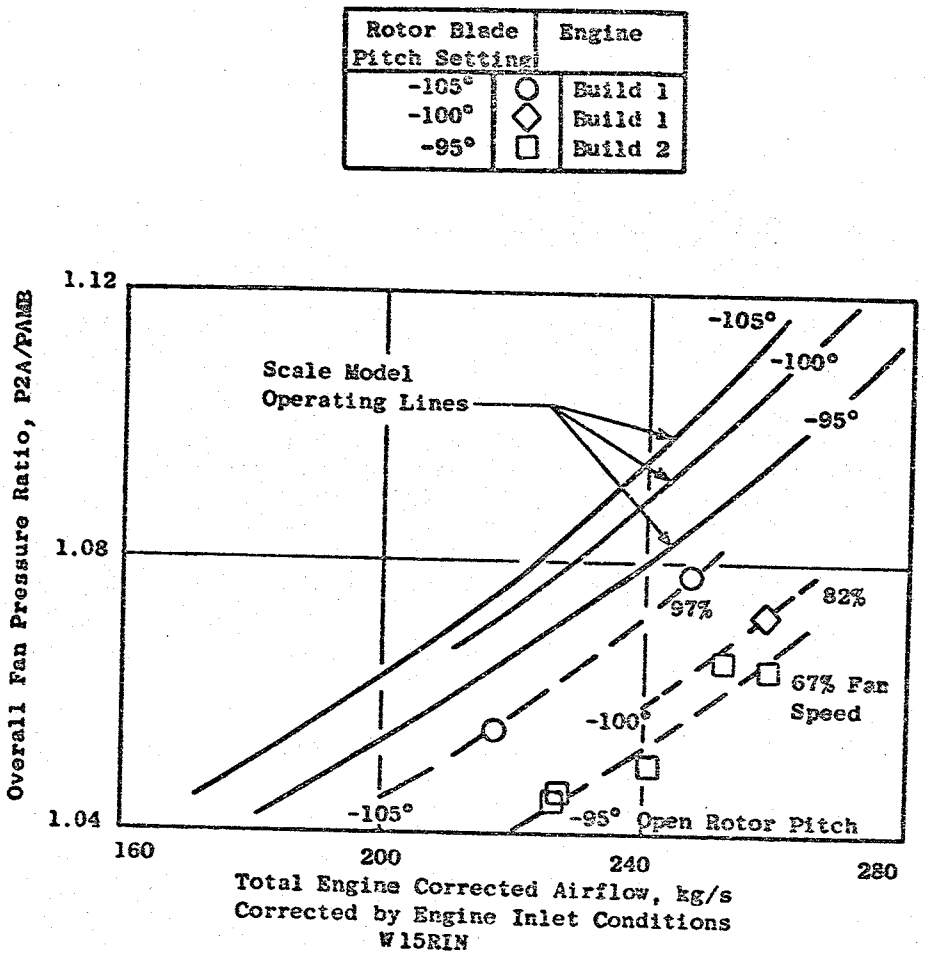

Figure 13. UTW Engine Fan Reverse Performance.

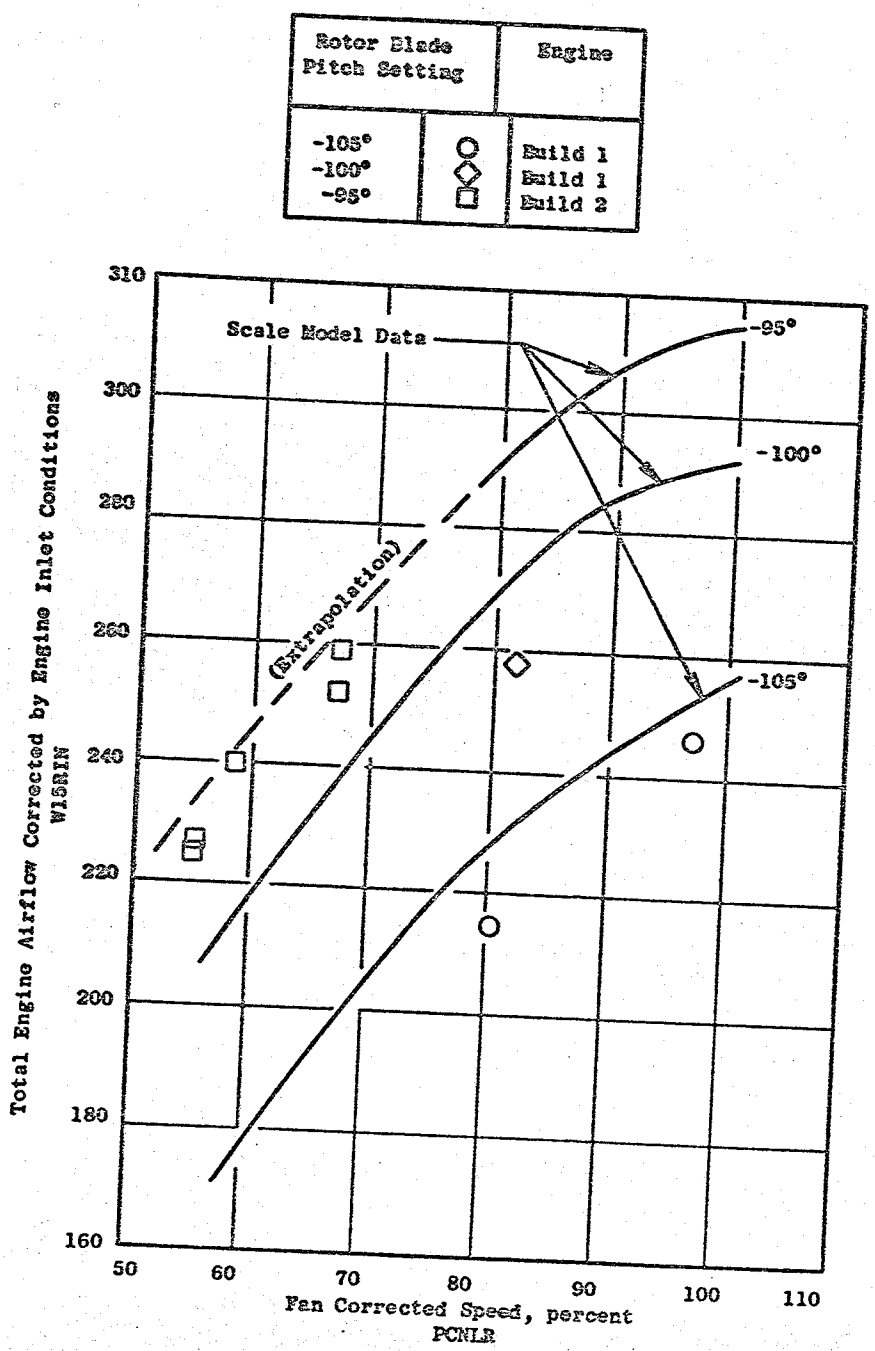

Figure 14. UTW Engine Flow Versus Fan Speed.

9.0 SYSTEM DYNAMICS

The overall vibration response characteristics of the QCSEE UTW engine (Build 2) were found to be within acceptable limits for normal engine operation. Fifteen vibration sensors were used to evaluate the engine response.

The synchronous vibration levels for both the LP and HP rotor activities were again very low throughout the operating ranges. Levels were still generally less than 0.00254 cm (1 mil) double amplitude (DA) indicating well balanced LP and HP rotor systems.

The fan synchronous vibration levels were comparable to the Build 1 configuration levels. The maximum steady-state value observed for the various pickups on the last day of testing at the Peebles Facility (7/21/78) are shown in Table XVII. The typical one/rev fan synchronous vibration levels were more like those shown in Table XVIII.

While the fan vibration levels for Build 2 testing were generally low, the highest levels were observed in November 1977 during fan blade pitch angle and fan nozzle area excursions. These data are reported as follows:

Test: QCSEE UTW Composite Inlet

Engine No: 507/001/2

Test Date: 11/3/77

Excursions: Change of fan blade pitch angle from -5° to -10° and change of fan nozzle area from 1.87 m^2 (2900 $in.^2$) to 1.39 m^2 (2150 $in.^2$).

Data Analysis: An examination of the reduced vibration data included a gradual increase in vibration levels across the board for both of these excursions. The increase was more significant when the nozzle area was reduced. A backoff was called when the nozzle area was 1.39 m^2 (2150 $in.^2$) because of high slipring vibrations.

Table XIX shows the fan synchronous vibration levels at nozzle area values of 1.87 m^2 (2900 $in.^2$) and 1.39 m^2 (2150 $in.^2$). The slipring radial vibration pickup indicated an increase from 10 to 21 mils-DA. The blade angle for this excursion was -8° and the fan speed was 2976 rpm.

Table XVII. Maximum Fan Synchronous Vibration Response for QCSEE UTW Engine (Build 2) Accelerometers.

Vibration Sensor	Fan Speed (rpm)	Maximum Response cm (mils) DA
Fan Cowl	2958	0.0064 (2.5)
Fan Frame - V	2958	0.0091 (3.6)
Fan Frame - H	3100	0.0025 (1.0)
No. 1 Brg - V	3104	0.0064 (2.5)
No. 1 Brg - H	3104	0.0097 (3.8)
No. 2 Brg - H	1974	0.0097 (3.8)
No. 3 Brg - V	3104	0.0043 (1.7)
No. 5 Brg - V	2815	0.0081 (3.2)
No. 5 Brg - H	2625	0.0056 (2.2)
Red. Gear - H	3104	0.0097 (3.8)
Comp. Stator - H	2808	0.0066 (2.6)
Exhaust Cone	2815	0.0066 (2.6)
Acc. Gearbox - A	3104	0.0023 (0.9)
Acc. Gearbox - H	2800	0.0091 (3.6)
Digital Control	2800	0.0097 (3.8)

Test Date: July 21, 1978

Table XVIII. Typical Steady-State Fan Synchronous Vibration Response for QCSEE UTW Engine (Build 2) Accelerometer.

	Steady-State Fan Speed RPM						
Vibration Sensor	1605 cm (mils)-DA	1800 cm (mils)-DA	2505 cm (mils)-DA	2650 cm (mils)-DA	2815 cm (mils)-DA	2980 cm (mils)-DA	3083 cm (mils)-DA
Fan Cowl	0.0005 (0.2)	0.0003 (0.1)	0.0013 (0.5)	0.0030 (1.2)	0.0030 (1.2)	0.0028 (1.1)	0.0013 (0.5)
Fan Frame - V	0.0008 (0.3)	0.0008 (0.3)	0.0013 (0.5)	0.0041 (1.6)	0.0046 (1.8)	0.0053 (2.1)	0.0033 (1.3)
Fan Frame - H	0.0003 (0.1)	0.0003 (0.1)	0.0005 (0.2)	0.0010 (0.4)	0.0013 (0.5)	0.0013 (0.5)	0.0008 (0.3)
No. 1 Brg - V	0.0020 (0.8)	0.0015 (0.6)	0.0005 (0.2)	0.0023 (0.9)	0.0058 (2.3)	0.0033 (1.3)	0.0023 (0.9)
No. 1 Brg - H	0.0023 (0.9)	0.0023 (0.9)	0.0023 (0.9)	0.0023 (0.9)	0.0033 (1.3)	0.0035 (1.4)	0.0033 (1.3)
No. 2 Brg - H	0.0033 (1.3)	0.0023 (0.9)	0.0008 (0.3)	0.0041 (1.6)	0.0051 (2.0)	0.0043 (1.7)	0.0013 (0.5)
No. 3 Brg - V	0.0008 (0.3)	0.0005 (0.2)	0.0010 (0.4)	0.0023 (0.9)	0.0028 (1.1)	0.0028 (1.1)	0.0018 (0.7)
No. 5 Brg - V	0.0003 (0.1)	0.0003 (0.1)	0.0005 (0.2)	0.0030 (1.2)	0.0081 (3.2)	0.0053 (2.1)	0.0028 (1.1)
No. 5 Brg - H	0.0015 (0.6)	0.0028 (1.1)	0.0013 (0.5)	0.0023 (0.9)	0.0023 (0.9)	0.0003 (0.1)	0.0003 (0.1)
Red. Gear - H	0.0023 (0.9)	0.0018 (0.7)	0.0033 (1.3)	0.0051 (2.0)	0.0070 (2.8)	0.0023 (0.9)	0.0013 (0.5)
Comp Stator - H	0.0005 (0.2)	0.0003 (0.1)	0.0013 (0.5)	0.0036 (1.4)	0.0053 (2.1)	0.0048 (1.9)	0.0025 (1.0)
Exhaust Cone	0.0013 (0.5)	0.0015 (0.6)	0.0030 (1.2)	0.0036 (1.4)	0.0065 (2.6)	0.0046 (1.8)	0.0025 (1.0)
Acc Gearbox - A	0.0003 (0.1)	0.0003 (0.1)	0.0003 (0.1)	0.0003 (0.1)	0.0003 (0.1)	0.0003 (0.1)	0.0003 (0.1)
Acc Gearbox - H	0.0005 (0.2)	0.0008 (0.3)	0.0015 (0.6)	0.0048 (1.9)	0.0065 (2.6)	0.0068 (2.7)	0.0035 (1.4)
Digital Control	0.0003 (0.1)	0.0005 (0.2)	0.0008 (0.3)	0.0008 (0.3)	0.0008 (0.3)	0.0005 (0.2)	0.0005 (0.2)

Table XIX. Fan Synchronous Vibration Levels for Nozzle Area Excursion for the QCSEE UTW Engine (Build 2) - Composite Inlet Test.

(Fan Blade Pitch Angle = -8°)
(Fan Speed = 2976 rpm)

Vibration Sensor	A = 1.87 m^2 (2900 $in.^2$) cm (mils)-DA	A = 1.39 m^2 (2150 $in.^2$) cm (mils)-DA
Slip Ring Radial	0.0254 (10.0)	0.0533 (21.0)
Fan Frame Vert	0.0043 (1.7)	0.0102 (4.0)
Digital Control	0.0025 (1.0)	0.0075 (3.0)
No. 1 Brg Vert	0.0005 (0.2)	0.0008 (0.3)
No. 1 Brg Horiz	0.0025 (1.0)	0.0056 (2.2)
Slip Ring Tang	0.0038 (1.5)	0.0071 (2.8)
No. 2 Brg Horiz	0.0013 (0.5)	0.0025 (1.0)
No. 3 Brg Vert	0.0020 (0.8)	0.0051 (2.0)
No. 3 Brg Horiz	0.0025 (1.0)	0.0051 (2.0)
Reduction Gear Vert	0.0076 (3.0)	0.0127 (5.0)
Reduction Gear Horiz	0.0025 (1.0)	0.0038 (1.5)
Comp Case Aft Flange H	0.0038 (1.5)	0.0051 (2.0)
No. 5 Brg Vert	0.0038 (1.5)	0.0089 (3.5)
Acces. Gearbox - Axial	0.0020 (0.8)	0.0056 (2.2)
Acces. Gearbox Vert	0.0038 (1.5)	0.0089 (3.5)
Fan Frame Horiz	0.0025 (1.0)	0.0041 (1.6)
Fan Cowl	0.0025 (1.0)	0.0051 (2.0)
Comp Inlet - Vert	0.0038 (0.5)	0.0064 (2.5)
Comp Inlet - Horiz	0.0013 (0.5)	0.0025 (1.0)

Table XX shows the vibration levels at blade angles of -5° and -10°. The nozzle area was 1.87 m^2 (2900 $in.^2$) for the excursion from -5° to -10° at a fan speed of 2981 rpm.

To summarize, vibration levels observed were sensitive to a change in the fan blade angle or a change in the fan nozzle area. Further, a combination of a closed blade angle (-8° to -10°) and a low nozzle area, 1.39 m^2 (2150 $in.^2$), exhibited vibration levels which exceeded the established limits for the slipring vibration pickup. The other pickups remained within the established limits.

For subsequent testing, the combination of blade angle and nozzle area conditions which produced high levels of vibration were avoided.

Table XX. Fan Synchronous Vibration Levels for Fan Blade Pitch Angle Excursion for the QCSEE UTW Engine (Build 2) - Composite Inlet Test.

(Fan Nozzle Area = 2900 in.^{2})
(Fan Speed = 2981 rpm)

Description	Blade Angle B = -5° cm	(mils)-DA	B = -10° cm	(mils)-DA
Slip Ring Radial	0.0330	(13.0)	0.0406	(16.0)
Fan Frame Vert	0.0043	(1.7)	0.0056	(2.2)
Digital Control	0.0020	(0.8)	0.0043	(1.7)
No. 1 Brg Vert	0.0010	(0.4)	0.0015	(0.6)
No. 1 Brg Horiz	0.0023	(0.9)	0.0025	(1.0)
Slip Ring Tang	0.0033	(1.3)	0.0038	(1.5)
No. 2 Brg Horiz	0.0025	(1.0)	0.0036	(1.4)
No. 3 Brg Vert	0.0020	(0.8)	0.0025	(1.0)
No. 3 Brg Horiz	0.0036	(1.4)	0.0046	(1.8)
Reduction Gear Vert	0.0076	(3.0)	0.0089	(3.5)
Reduction Gear Horiz	0.0051	(2.0)	0.0064	(2.5)
Comp Case Aft Flange Horiz	0.0036	(1.4)	0.0178	(1.7)
No. 5 Brg Vert	0.0051	(2.0)	0.0071	(2.8)
No. 5 Brg Horiz	0.0008	(0.3)	0.0008	(0.3)
Access. Gearbox - Axial	0.0020	(0.8)	0.0025	(1.0)
Access. Gearbox - Vert	0.0036	(1.4)	0.0038	(1.5)
Fan Frame Horiz	0.0038	(1.5)	0.0046	(1.8)
Fan Cowl	0.0036	(1.4)	0.0048	(1.9)
Comp Inlet - Vert	0.0038	(1.5)	0.0064	(2.5)
Comp Inlet - Horiz	0.0025	(1.0)	0.0025	(1.0)

10.0 COMPOSITE FAN BLADES

10.1 BLADE DESCRIPTION

The blades incorporated in the UTW fan rotor are of variable-pitch design that offer full reverse thrust capability. The design includes 18 composite fan blades fabricated from a hybrid combination of Kevlar 49, AS graphite, boron, and S-glass fibers in a PR288 epoxy resin matrix. The blades incorporate a metal leading edge to provide foreign object damage (FOD) and erosion protection. Solidity of the blade airfoil is 0.95 at the OD and 0.98 at the ID, permitting rotation of the blades into the reverse thrust mode of operation through both the flat-pitch and stall-pitch directions. A spherical casing radius and a spherical blade tip provide close blade tip clearances throughout the range of blade pitch angle settings. Each blade is attached by a dovetail to a rotor trunnion at the blade root. The trunnions are retained in the disk by ball bearings. Retainer straps, attached to the trunnion, lock the blade in an axial position and resist trunnion opening deflections under blade centrifugal loading.

Design requirements for the UTW composite fan blade were established to provide realistic long-life operation of a flight engine. Design details are provided in Reference 4. Results of bench and whirligig testing showing that the blades have satisfactory margins for the structural and aeromechanical requirements of the engine are provided in Reference 5.

The finished composite fan blade is shown in Figure 15. It consists of a molded composite blade, a molded composite platform, and a metal outsert on the dovetail. The blade is made up of a solid composite airfoil and a straight bell-shaped composite dovetail. The blade has a reduced leading edge thickness to allow a final coating of wire mesh/nickel plate for leading edge protection within the final aerodynamic contour. The dovetail is undercut at the leading and trailing edges to permit better transitioning of the cambered airfoil section into the straight dovetail to match the rotor trunnion configuration.

The blade is made up of 0.25-mm (0.010-inch) plies of Kevlar 49, AS graphite, boron, and S-glass fibers impregnated with PR288 epoxy resin. The S-glass plies are placed near the surface in the lower region of the blade to provide high tensile strength and high strain-to-failure characteristics for flexural loading. Boron and graphite torsional stiffening plies in the airfoil region of the blade are oriented at $\pm 45°$ to provide the shear modulus required for a high first-torsional frequency. The boron plies are placed toward the outer surface and graphite in the inner regions. Plies of Kevlar 49 are interspersed throughout the blade with the majority of them being oriented with their fibers in the longitudinal direction of the blade. Several Kevlar 49 plies in the tip region of the blade are oriented at 90° to the longitudinal axis to provide chordwise strength and stiffness to the blade. All airfoil plies extend continuously down into the dovetail and are interspersed with insert plies which act to fill out the enlarged dovetail cross section.

C-2

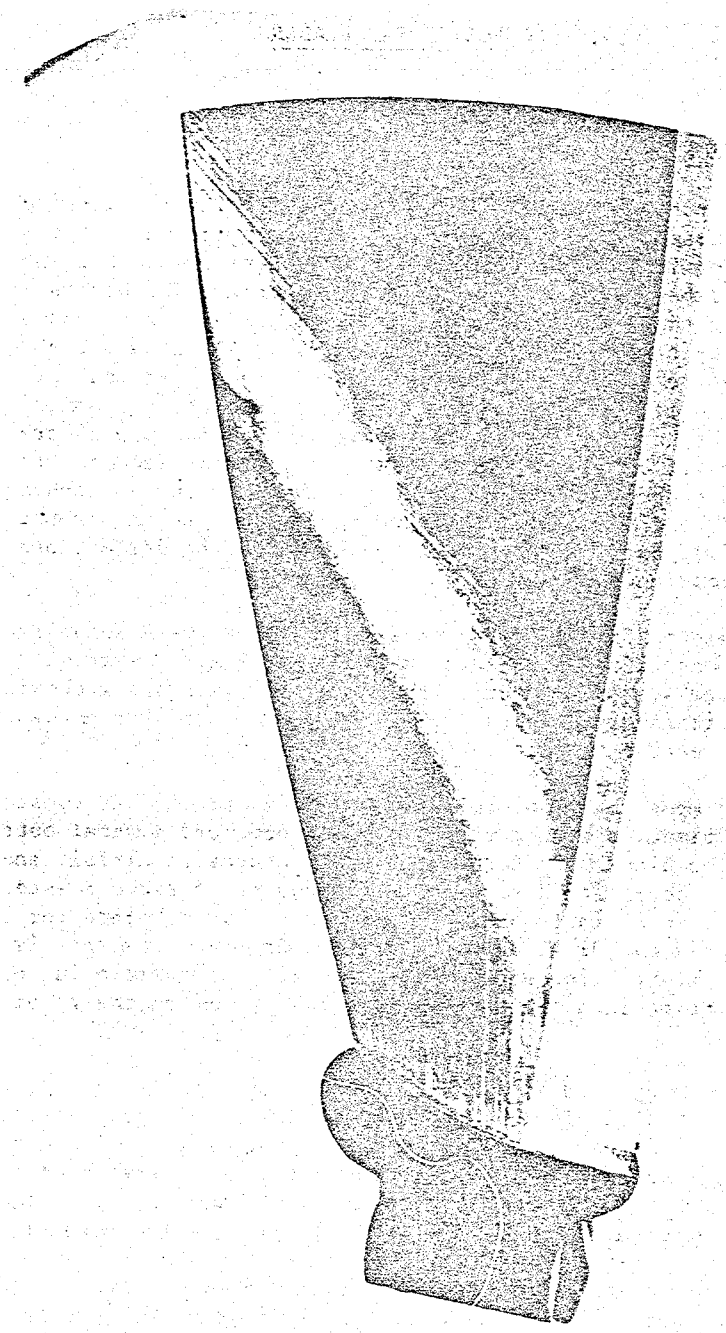

Figure 15. QCSEE UTW Composite Blade with Platform (C76011062).

The composite platform is a tapered beam, cantilevered from the blade root, and consists of a honeycomb core stabilized by upper and lower graphite/epoxy face sheets. The platform is molded and bonded in place on the blade forming a one-piece structure. Structural plies extend around the blade root leading and trailing edge undercuts, entrapping the platform beneath the airfoil overhangs. The platform construction is shown in Figure 16, and the overall blade dimensions and configuration are shown in Figure 17.

10.2 PRETEST PREDICTIONS

The blade stress vibratory characteristics were determined from a three-dimensional finite-element analysis, blade bench testing and single-blade spin testing. Figure 18 is a map of calculated radial steady-state stresses for the concave and convex blade faces, and Figures 19, 20, and 21 show calculated relative radial stresses over the blade for the first three vibratory modes. The maps of relative radial stresses under vibratory conditions show the changes in stress locations for the different vibratory modes. Blade bench and whirligig test data agreed closely with these predictions.

Blade vibratory strengths were determined from specimen and QCSEE blade tests and are shown on the fatigue S-N curve (Figure 22), and the fatigue stress-range diagram (Figure 23). The fatigue S-N curve shows the maximum blade stress for various members of flexural cycles that will cause the blade to initiate delamination and cause loss of blade frequency. The upper curve gives the minimum strength of the composite material based on flat specimen, axial-axial fatigue testing. The allowable blade fatigue strength was based on the material minimum-strength curve and blade high-cycle-fatigue test data. It includes allowance for three standard deviations of strength property variation. The lower curve defines the stress limits for engine testing and was determined using various factors which are discussed under "scope limits." The fatigue stress-range diagram shows the allowable radial alternating stress as a function of the blade mean stress. The allowable stress levels for this curve were selected as the point on the S-N curve for allowable blade stress where no loss in frequency would occur after 1,000,000 flexural cycles with allowance for three standard deviations of material property variation. Measured strains in the blade radial (spanwise) direction along with a material modulus of elasticity of 6.9×10^6 N/cm^2 (10×10^6 psi), were used to calculate all stresses and strengths. This approach provided a consistent basis for setting scope limits, gage monitoring, and comparing stresses during the various phases of blade testing. Blade "instability" or "limit cycle variation" was a primary consideration in the blade design. Detailed discussion of this is covered in Reference 4.

Critical speeds of the coupled blade/trunnion/disk system were calculated and plotted in the form of a Campbell diagram. The predicted criticals are discussed and compared to engine test data in a subsequent paragraph.

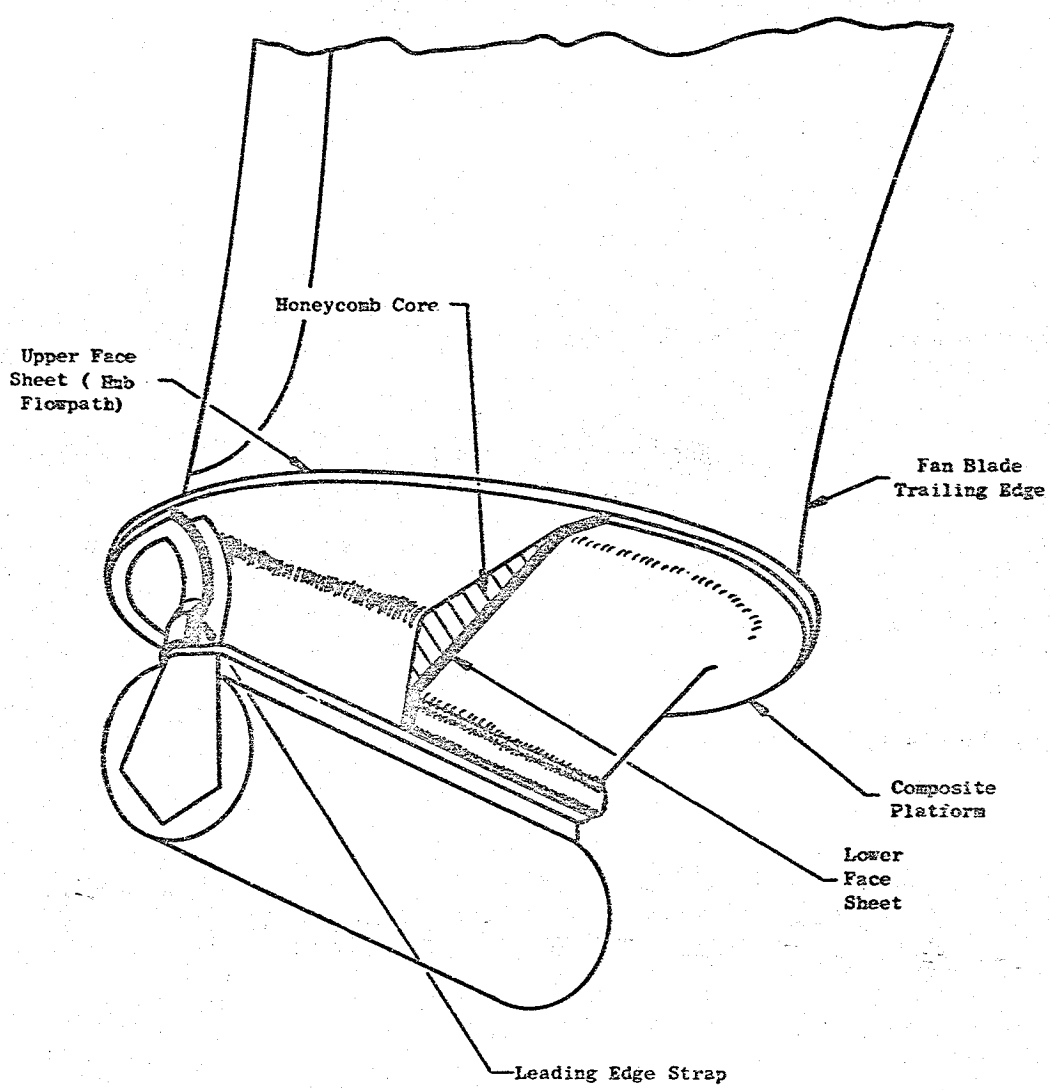

Figure 16. Platform Construction.

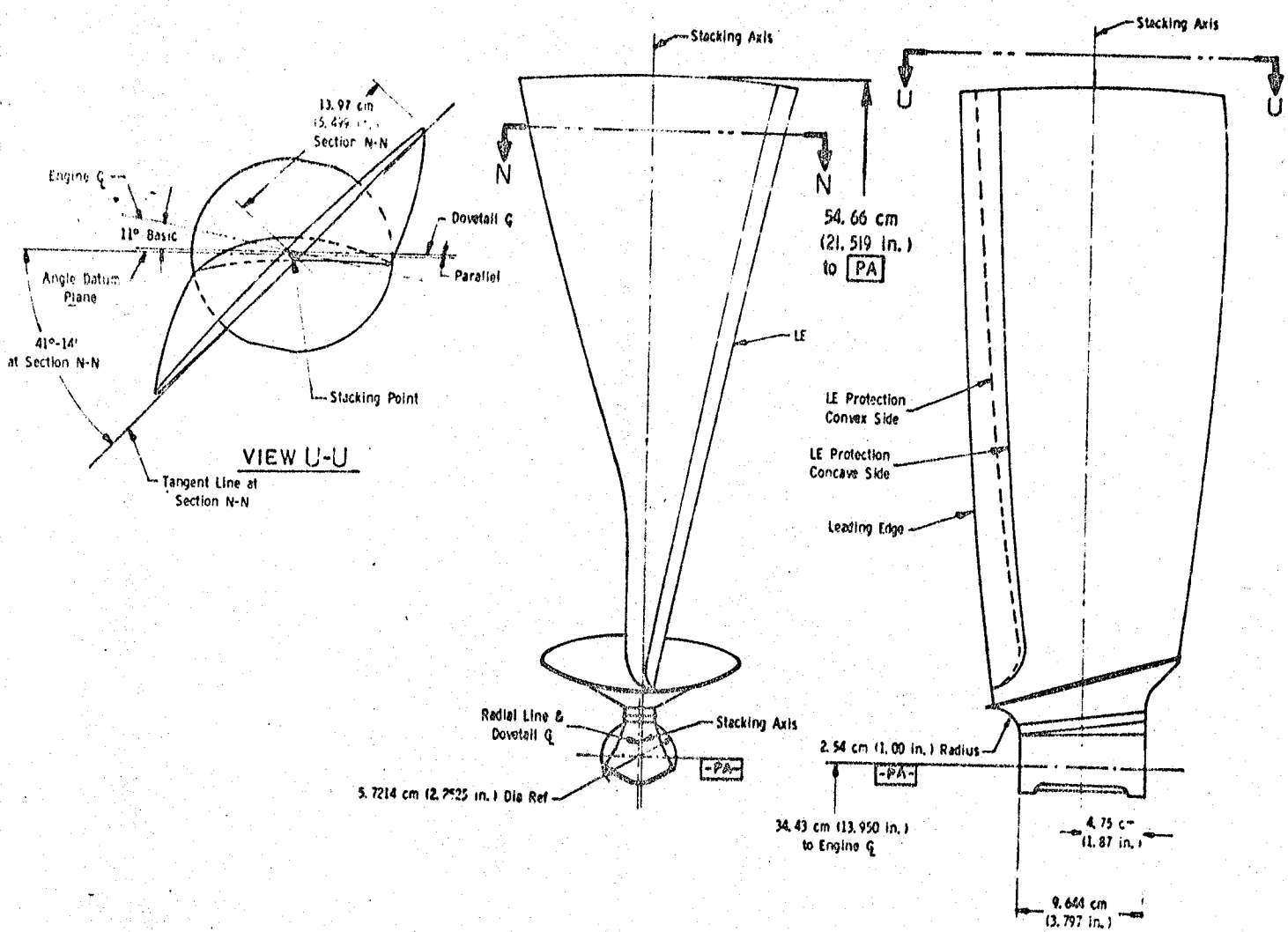

Figure 17. Composite Blade Configuration.

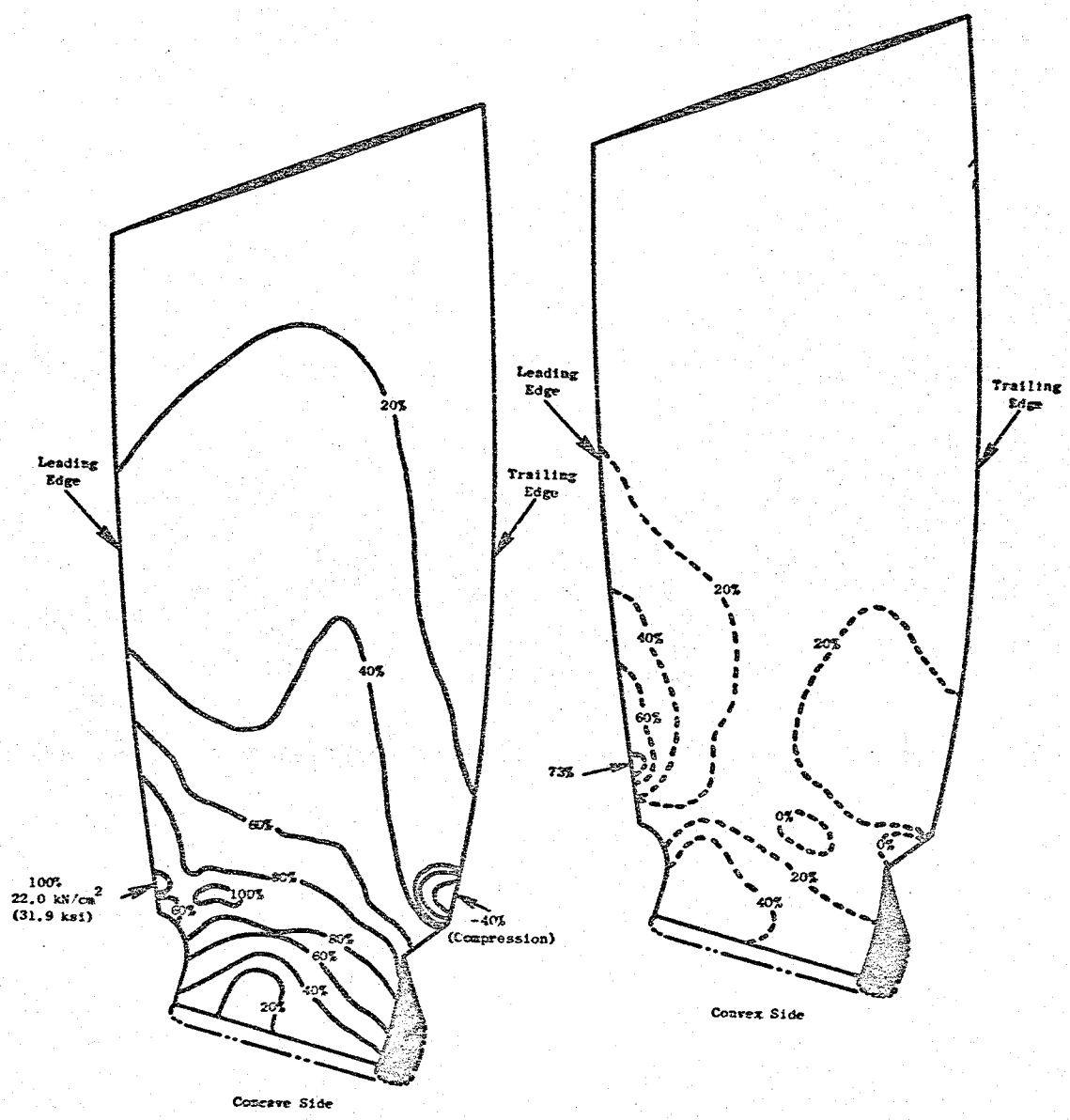

Figure 18. Calculated Blade Radial Stress.

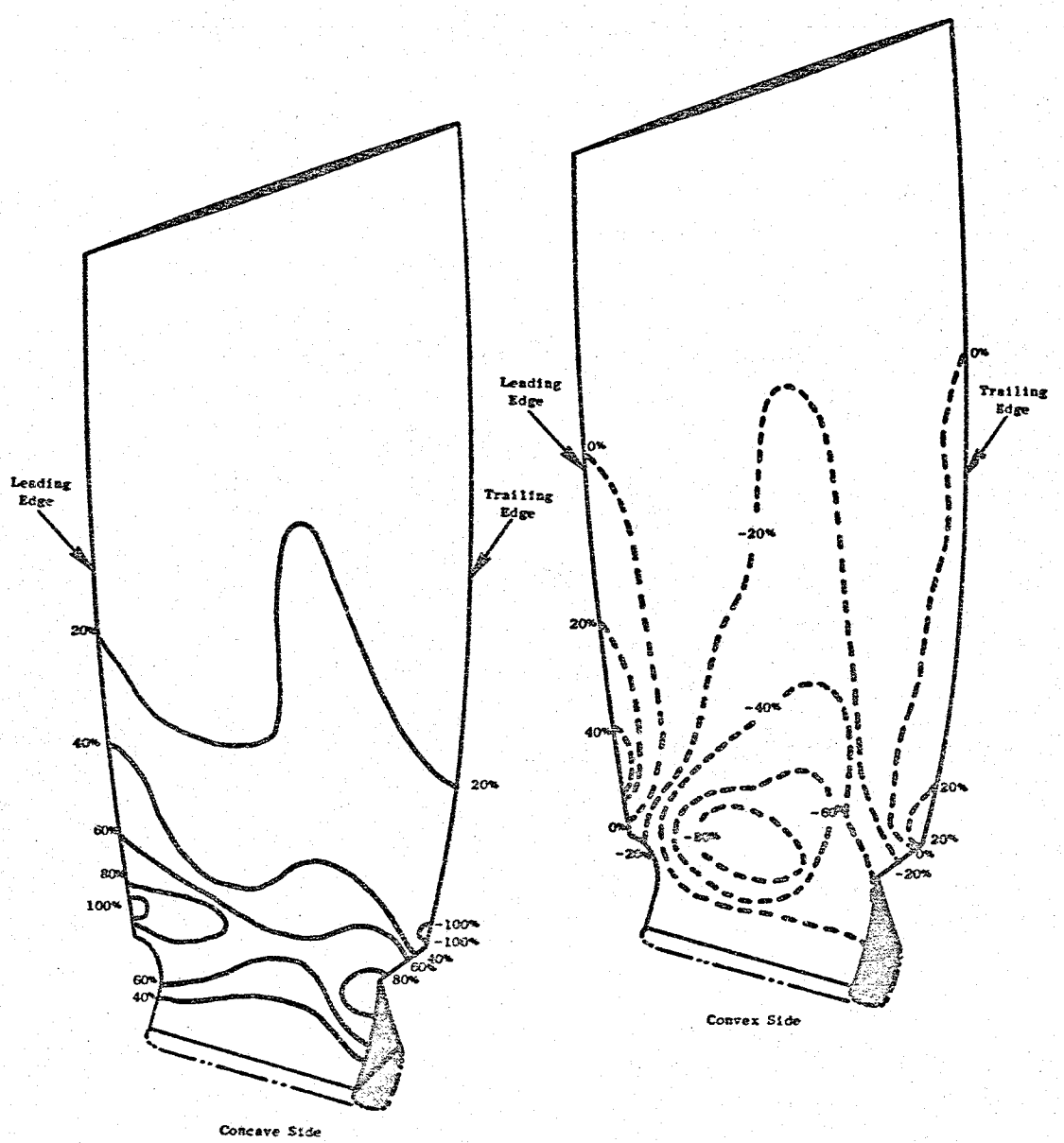

Figure 19. Calculated Blade Relative Radial Stresses for First Flexural Modes.

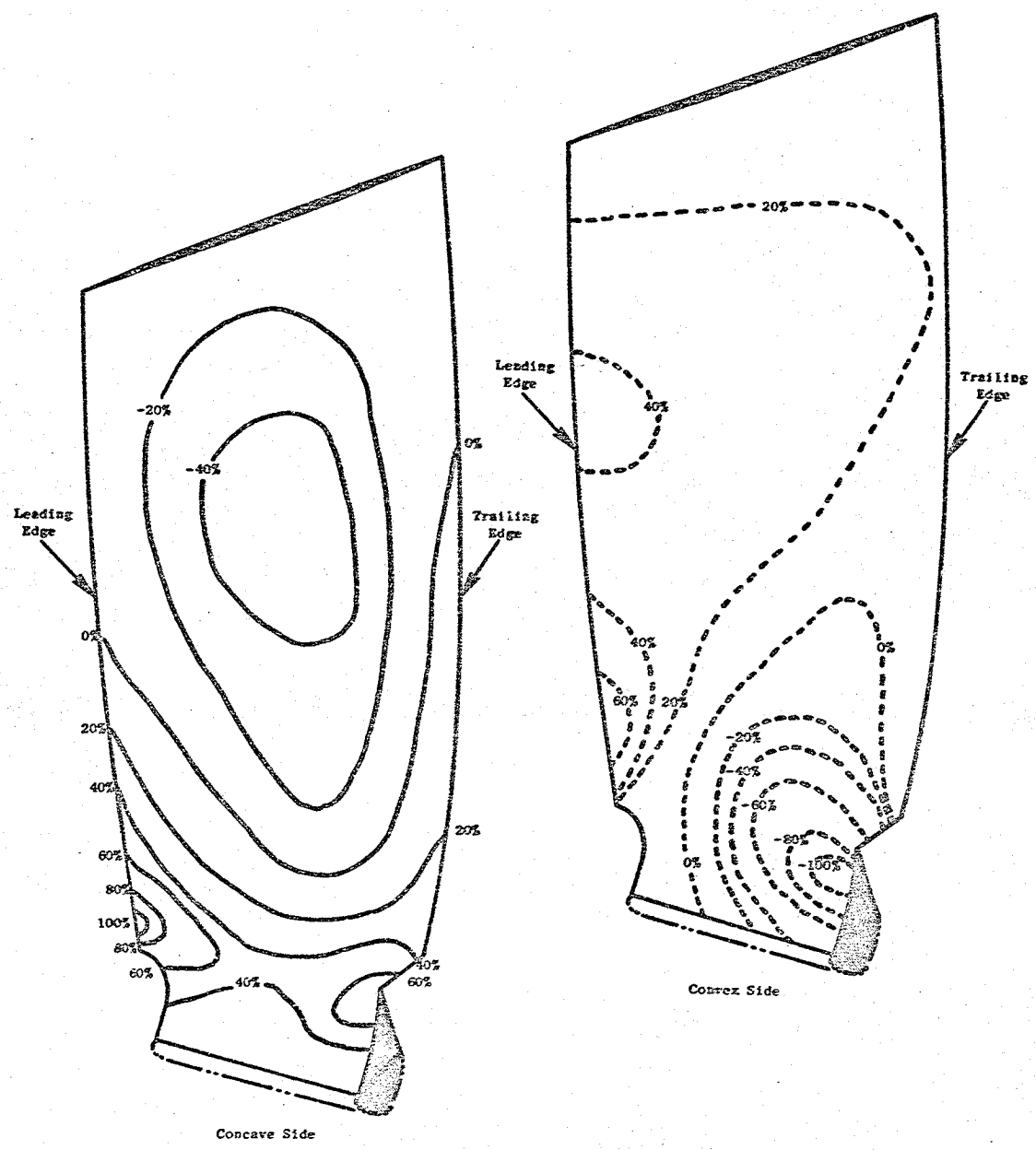

Figure 20. Calculated Blade Relative Radial Stresses for Second Flexural Modes.

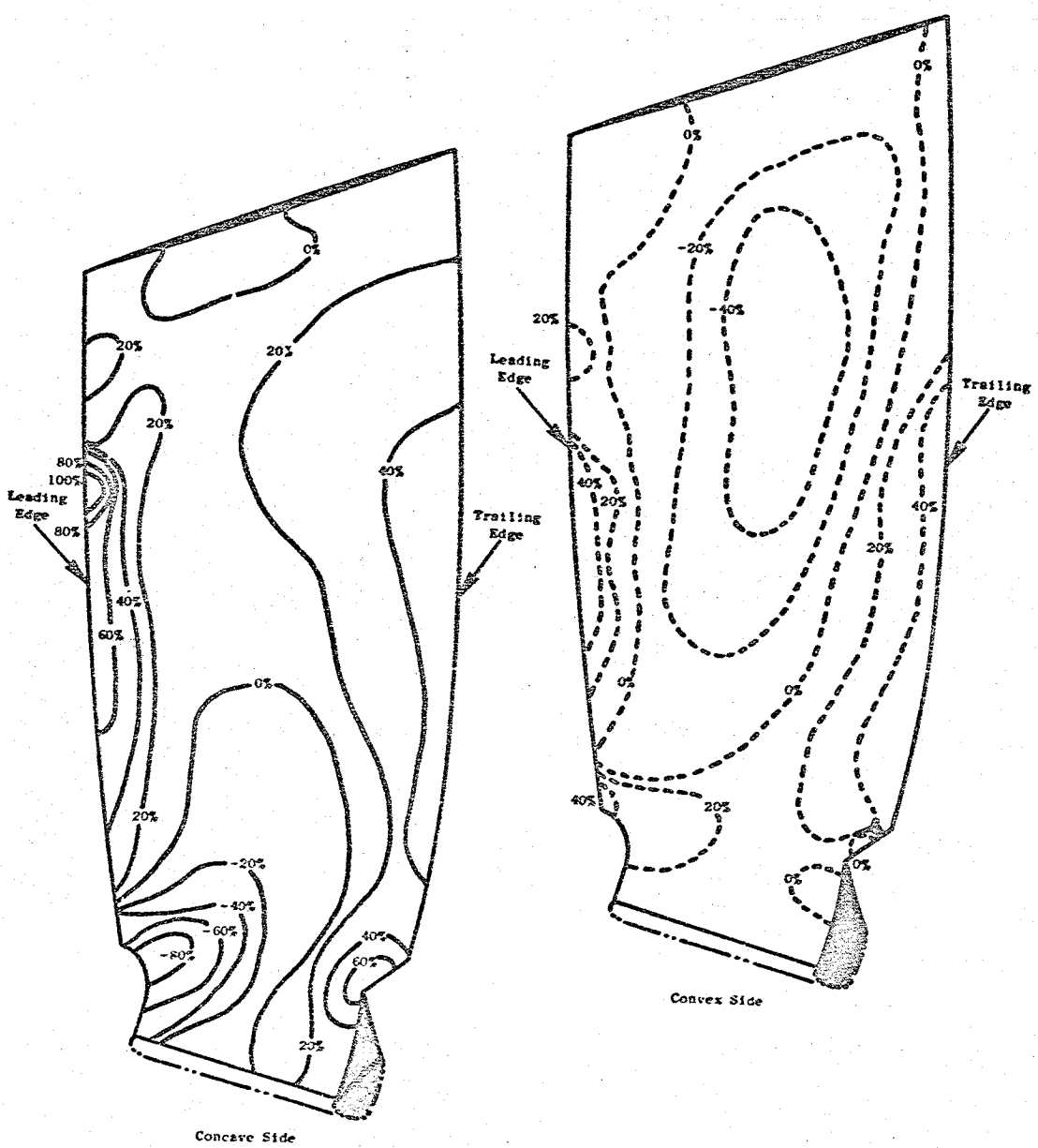

Figure 21. Calculated Blade Relative Radial Stresses for First Torsional Modes.

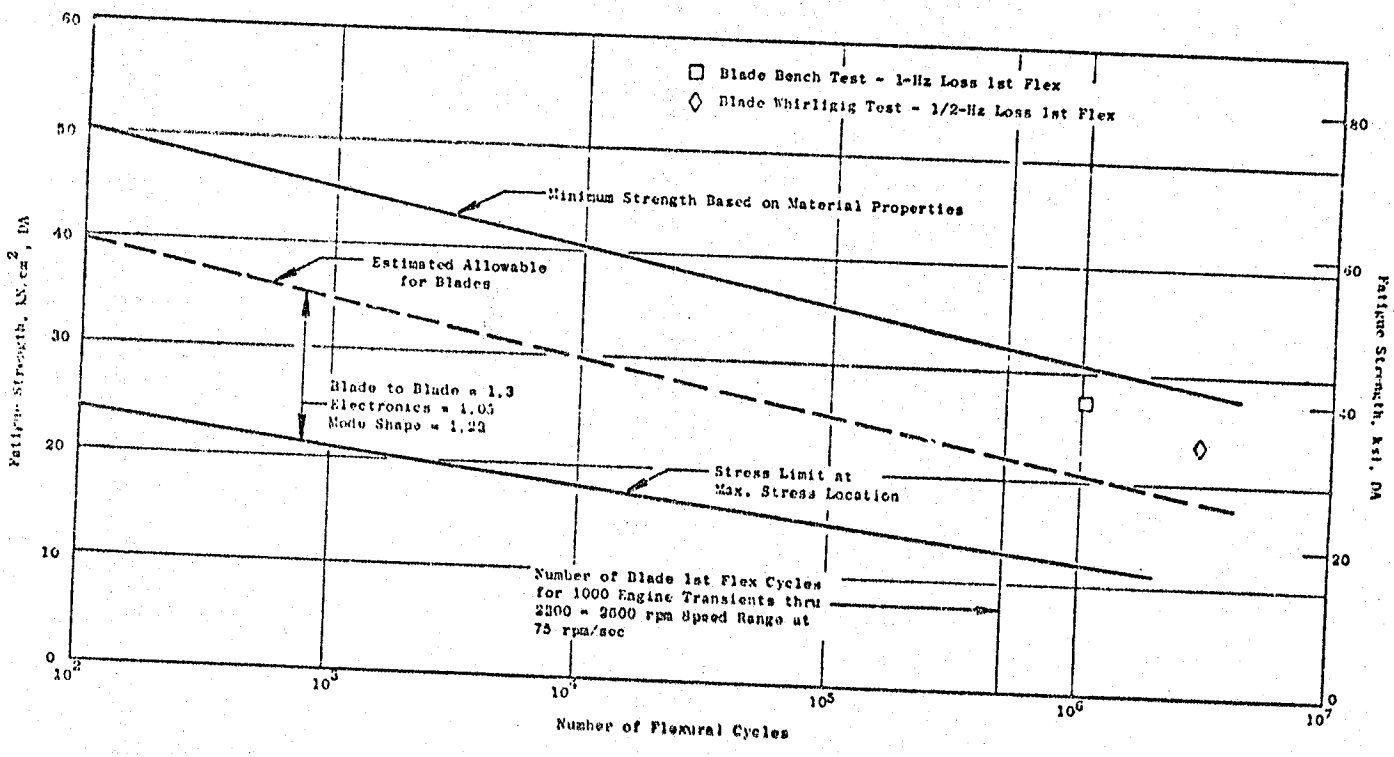

Figure 22. Fatigue S-N Curve for QCSEE Blade.

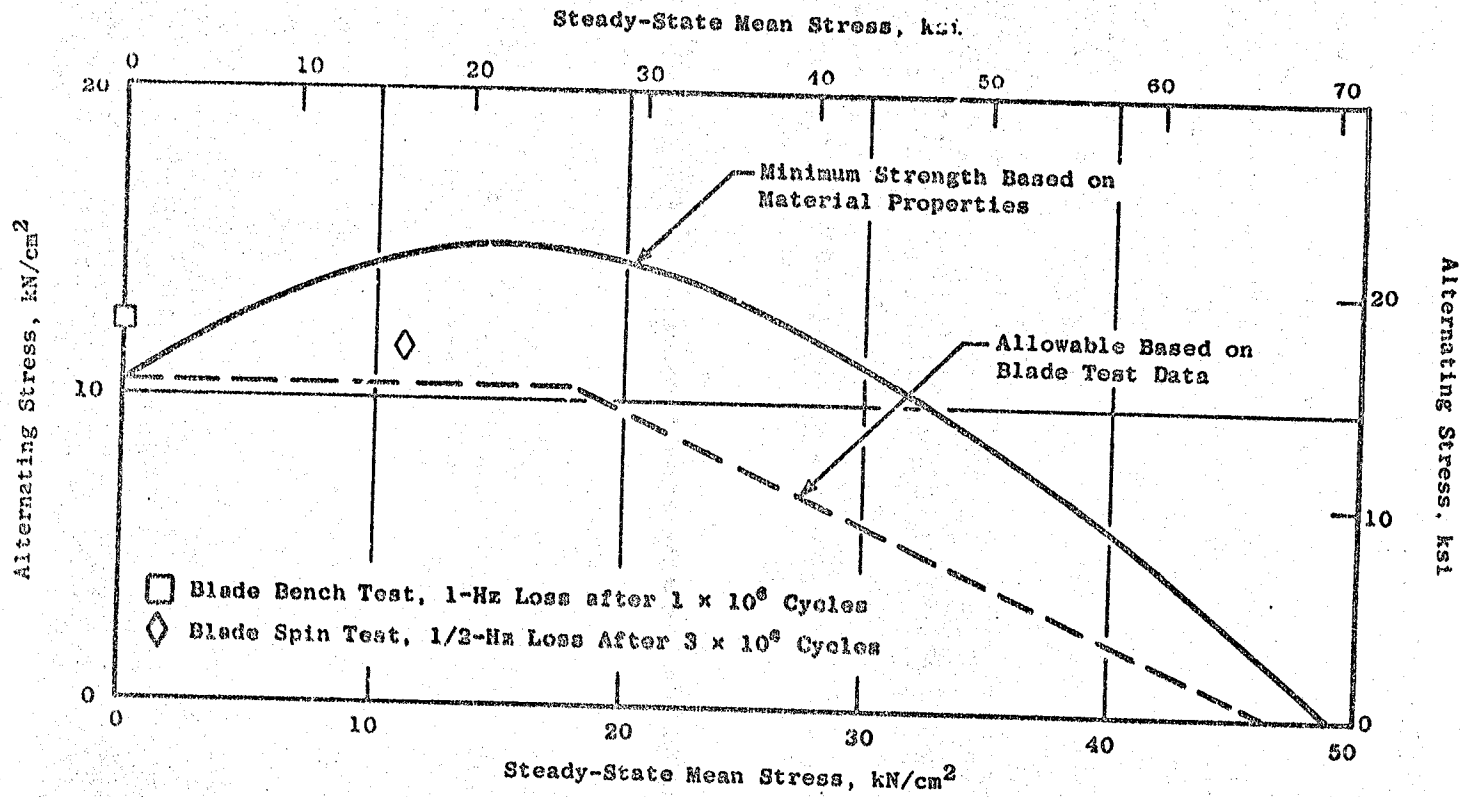

Figure 23. Allowable Stress-Range Diagram - Blade Radial Stress

10.3 BLADE INSTRUMENTATION AND SCOPE LIMITS

Six of the fan blades were instrumented with 13 dynamic strain gages located on the blades as shown in Figure 24. The 13 dynamic strain gages were located at four different locations on the blades to provide a balance between having commonality of gages, having gages at different strain levels for gage-life considerations, having gages responsive to the different vibratory modes, and providing verification of the vibratory stress distributions on the blades during engine test. The vibratory stress patterns for the blade vibratory modes were determined by finite-element analysis and by laboratory tests. The blade strain gage locations were selected so that at least one of the locations would be responsive to blade vibration in each of the five lower blade modes.

"Scope limits" or vibratory stress limits for these gages were calculated for each of the lower-blade modes. These limits normally represent the maximum vibratory stress at which the blade may be allowed to continuously vibrate without initiating a fatigue failure at some location on the blade. This point where the fatigue crack would be initiated is referred to as the "critical location" and is different for each vibratory mode. In the QCSEE composite blades, the fatigue failure mode would be an internal delamination which would result in a drop in blade natural frequency rather than the usual fatigue crack observed in metal blades.

The critical location and the fatigue strength normally depend upon both the steady-state and vibratory stresses; since the blade steady-state stress pattern increases roughly with the speed squared, the scope limits normally would be calculated as a function of fan speed. However, over the range of steady-state stresses anticipated for the QCSEE blade, the composite material fatigue strength is insensitive to the level of steady-state stress (i.e., is constant). The scope limits, therefore, can be considered independent of fan speed over the operating range of this engine.

Another complication encountered in calculating scope limits for an adjustable-pitch fan is that the steady-state stress pattern is also a function of the blade pitch angle. This is because the aerodynamic blade loading and the twisting moment generated by the radial centrifugal field are pitch-angle dependent. The effect of these changes on the blade steady-state stress pattern is not insignificant for a fan to be tested in a pitch-angle range of approximately 180°. Technically, correct blade scope limits normally would require the calculating of a carpet-of-values as a function of both speed and pitch angle. Again, it was not necessary to take this approach since the composite-blade fatigue limit is independent of the steady-state stress patterns. The fatigue limit diagram used was the average fatigue limit curve minus three standard deviations which represents the minimum expected material properties.

With the critical point located, the allowable vibratory stress at this location available, and the vibratory stress pattern known, the scope limit for a particular airfoil strain gage may be calculated using the following equation:

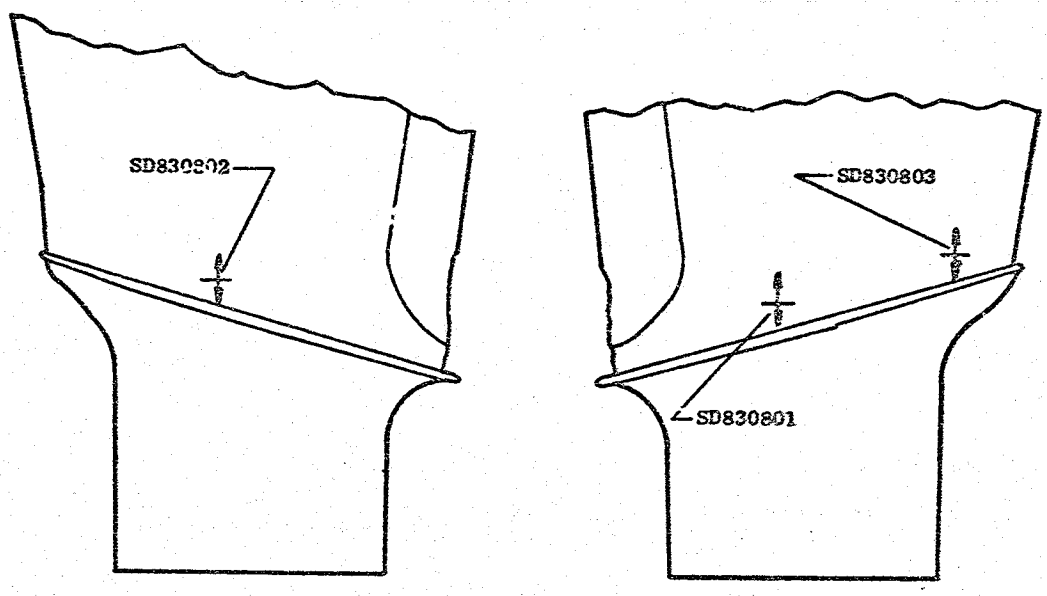

Blade S/N Q14 (Slot 5)

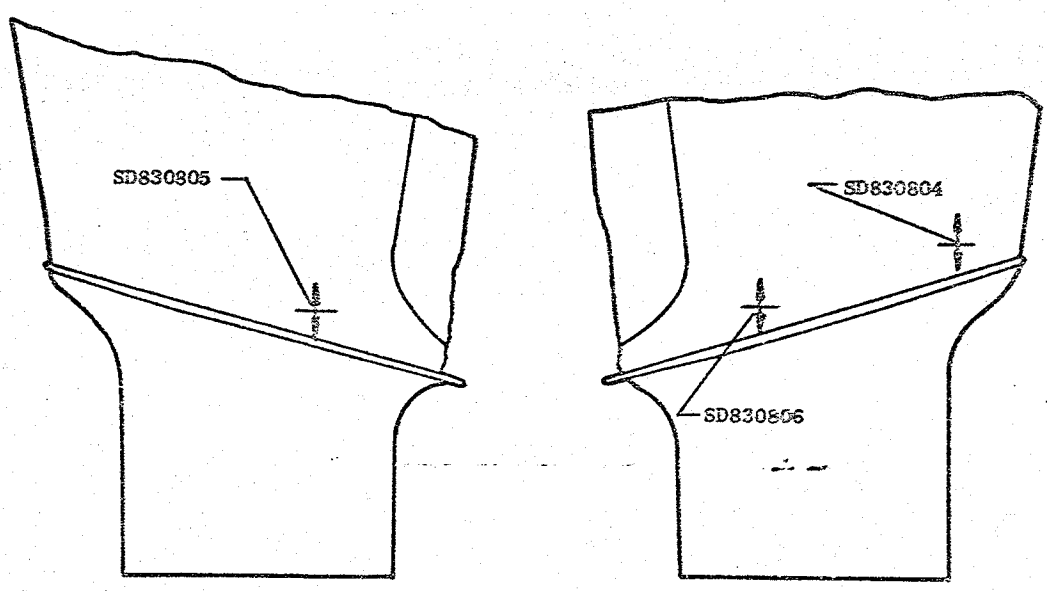

Blade S/N Q15 (Slot 6)

Convex Side

Concave Side

Figure 24(a). Locations of Fan Blade Instrumentation.

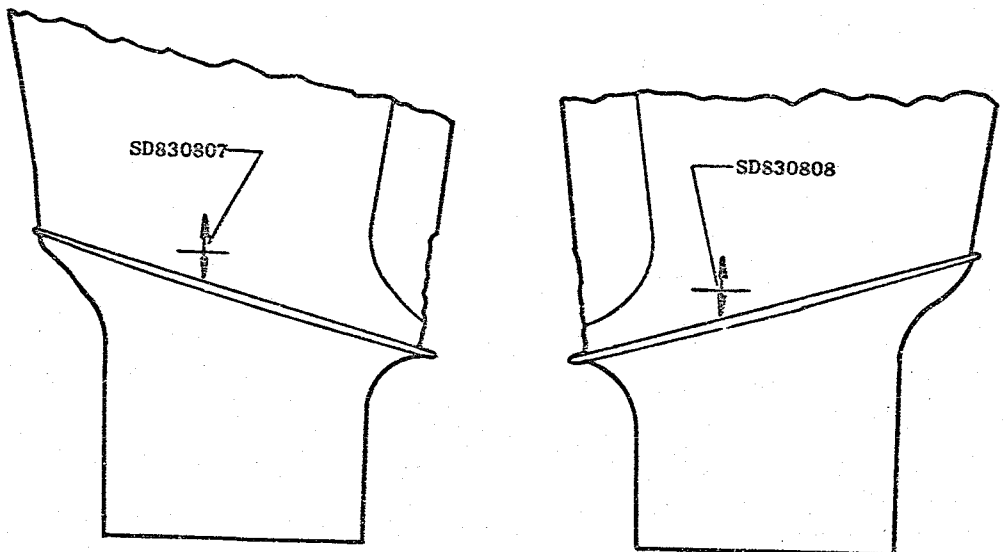

Blade S/N Q24 (Slot 7)

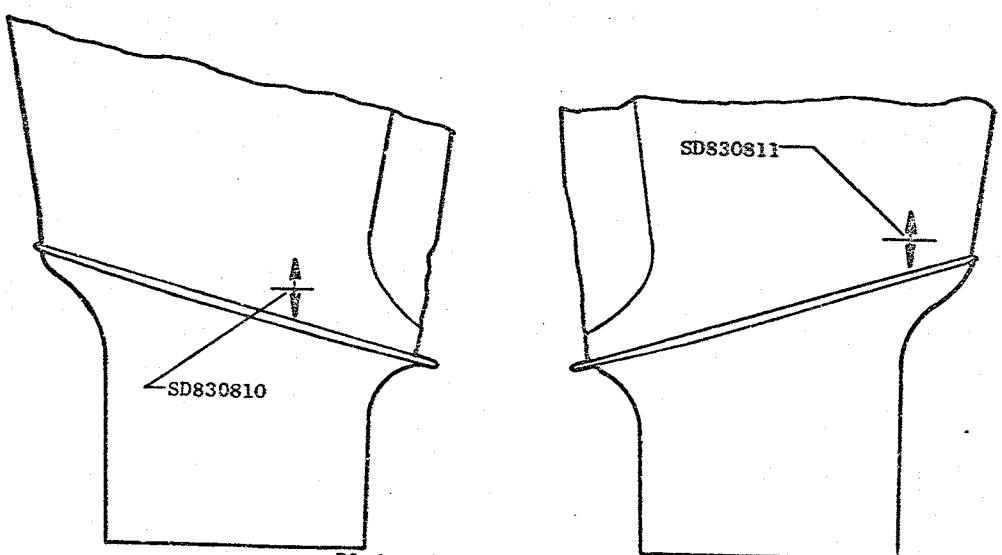

Blade S/N Q20 (Slot 14)

Convex Side

Concave Side

Figure 24(b). Locations of Fan Blade Instrumentation.

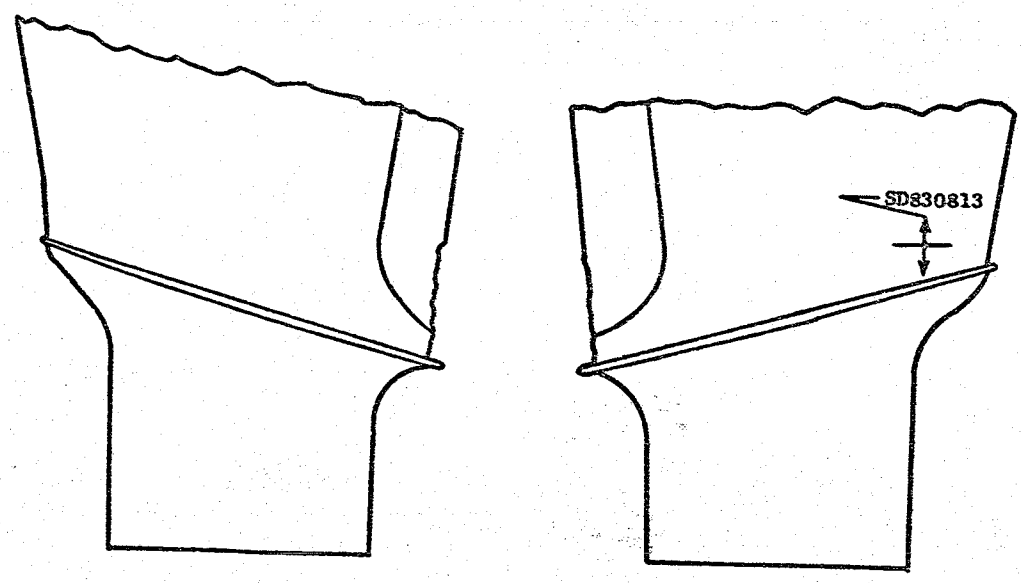

Blade S/N Q27 (Slot 15)

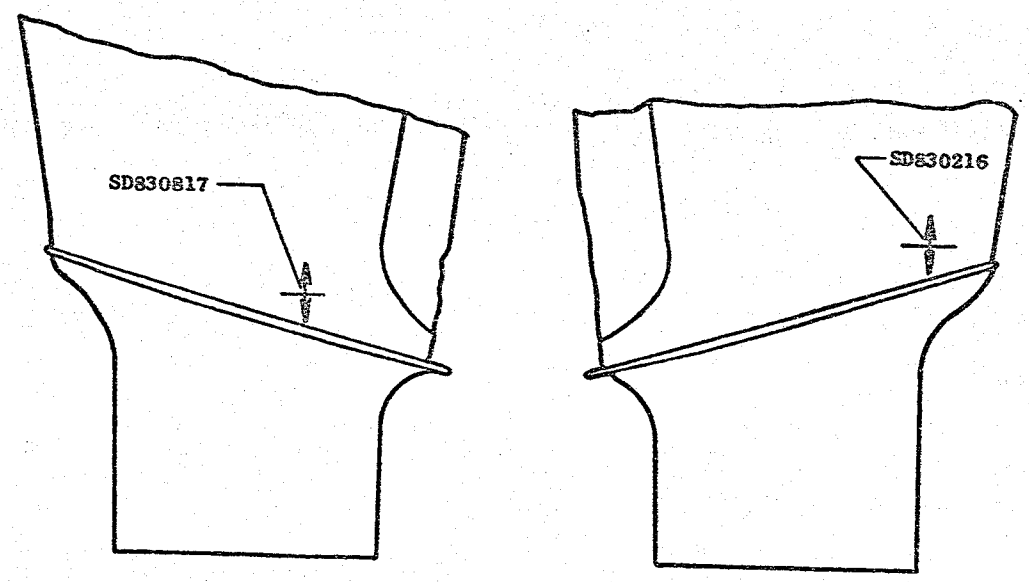

Blade S/N Q23 (Slot 16)

Convex Side

Concave Side

Figure 24(c). Locations of Fan Blade Instrumentation.

$$\text{Scope Limit} = \frac{2(\sigma \text{ gage}/\sigma \text{ critical point})\ \sigma e}{K_1 K_2 K_3}$$

where

σ_e = The single-amplitude endurance limit at the critical point on the blade in this vibratory mode as determined by the fatigue limit diagram for the blade material.

$\frac{\sigma \text{gage}}{\sigma \text{critical point}}$ = The ratio of the vibratory stress at the location of the strain gage to the vibratory stress at the critical point on the blade for the vibration mode being considered.

K_1 = A blade-to-blade vibratory response variation allowance factor (1.3 based on past metal blade experience).

K_2 = A factor for allowance for tolerance in the strain gage electronics circuit (1.05).

K_3 = An allowance for the sensitivity of the monitoring gage to slight changes in mode shape, such as might be expected due to manufacturing tolerance, 0.32 cm (1/8 in.) gage mislocation, etc. (1.22).

It is easier in practice to read a vibratory stress signal on an oscilloscope from the peak-to-peak of the wave rather than its amplitude. Scope limits, therefore, are normally calculated in this manner. This peak-to-peak or double-amplitude method of presenting scope limits is the reason behind the "two" in the numerator of the scope limit equation. The scope limits for the QCSEE fan blades are listed in Table XXI.

10.4 TEST RESULTS

The QCSEE UTW engine, 507-001/2, was tested with a slipring installed to determine the mechanical integrity of the fan during forward and reverse thrust testing and to obtain data applicable to future safe engine operation. Aeromechanical test coverage was provided for the initial tests of each configuration affecting blade dynamic response: different inlet configurations, forward and reverse thrust operation, blade pitch variations, and fan nozzle variations.

Two inlet configurations were tested during forward thrust operation, the standard bellmouth and the high throat Mach number inlet. The high throat Mach number inlet was also used for reverse thrust operation.

Engine mechanical checkout for forward thrust included performance mapping typically along three operating lines [fan nozzle areas of 14,800 cm^2

Table XXI. UTW Fan Blade Scope Limits.

kN/cm^2 (ksi) - double amplitude with
$E = 6.9 \times 10^6$ N/cm^2 (10^7 psi)

Group	Mode Zero Speed Frequency, H_Z				
	1F (62)	2F (186)	1T (292)	4th (396)	5th (613)
A*	4.0 (5.8)	5.0 (7.2)	3.2 (4.7)	3.9 (5.6)	2.8 (4.0)
B*	4.7 (6.8)	5.6 (8.1)	--- ---	2.8 (4.0)	2.6 (3.8)
C*	3.5 (5.1)	2.1 (3.0)	3.7 (5.4)	4.3 (6.3)	3.2 (4.7)
D*	5.6 (8.2)	3.3 (4.8)	--- ---	5.9 (8.6)	6.5 (9.4)

*

Group	Gage Number
A	SD830801, 806, 808, 813
B	SD830802, 807
C	SD830803, 804, 811, 816
D	SD830805, 810, 817

(2300 in.^{2}), 16,100 cm^2 (2500 in.^{2}), and 18,700 cm^2 (2900 in.^{2}) for the bellmouth inlet and 13,500 cm^2 (2100 in.^{2}), 16,100 cm^2 (2500 in.^{2}), and 18,700 cm^2 (2900 in.^{2}), for the hybrid inlet] at five speeds (65, 80, 90, 95, and 97 percent) with variations in blade pitch angles from -7° open to +9° closed for the bellmouth inlet and from -10° open to +9° closed for the hybrid inlet. Reverse thrust operation was performed with fixed pitch: the blade pitch angle was set at -95° or -100° open. A sketch of the blade position geometry is shown in Figure 25.

The predicted Campbell diagram for the UTW fan blade assembled in the trunnion and disk was determined from single blade whirligig spin tests. This is presented in Figure 26, along with the frequencies observed during engine tests and the laboratory bench test frequencies (blade only). Blade vibratory overstress condition did occur below the fan idle speed at the 3/rev and 4/rev first flexure crossovers. These conditions, however, do not present a problem from the blade mechanical standpoint in view of the rapid rate of acceleration and deceleration through these points.

The flexural frequency at the 2/rev crossover occurs above flight idle speed and below the normal operating speed for takeoff, climb, and maximum-cruise flight conditions. Therefore, the 2/rev crossover was considered a transient point in the speed range not subject to continuous steady-state operation. Blade excitation stresses at the 2/rev crossover were monitored carefully throughout engine testing.

Fan blade vibratory response throughout the engine tests consisted primarily of integral order resonances such as 2/rev, 3/rev, 6/rev, and 9/rev. The primary vibratory response was the first flexure 2/rev forced excitation. The second flexure and first torsional natural frequencies were essentially nonexistent. Above the 2/rev crossover speed range, the fan blade exhibited very low response in the first flexural mode.

The blades were free from self-excitation vibration at all conditions tested, although stall mapping was not performed with this engine.

Whenever testing was done with the slipring installed, blade vibratory stresses were continuously recorded on a 28 channel FM magnetic tape recorder and monitored on individual scopes. One of these gages was always displayed and monitored on a Schlumberger frequency spectrum analyzer. At the conclusion of the engine tests, six of the original 13 gages were still functional.

10.4.1 Forward Thrust Vibratory Response

During the initial part of the test, the engine had a bellmouth inlet installed. Subsequently, the bellmouth was replaced with the high throat Mach number inlet, and the acoustic splitter was installed in the fan exit duct. Forward thrust testing included performance mapping typically along three

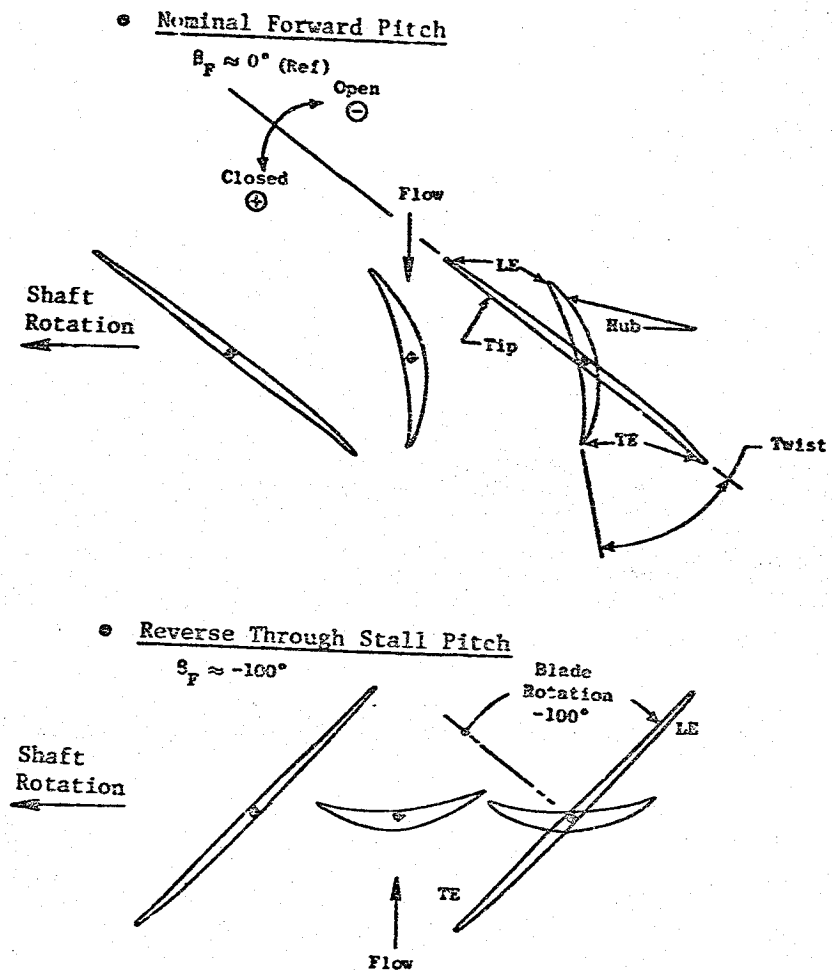

Figure 25. UTW Fan Blade Geometry at Different Blade Pitch Angle Settings.

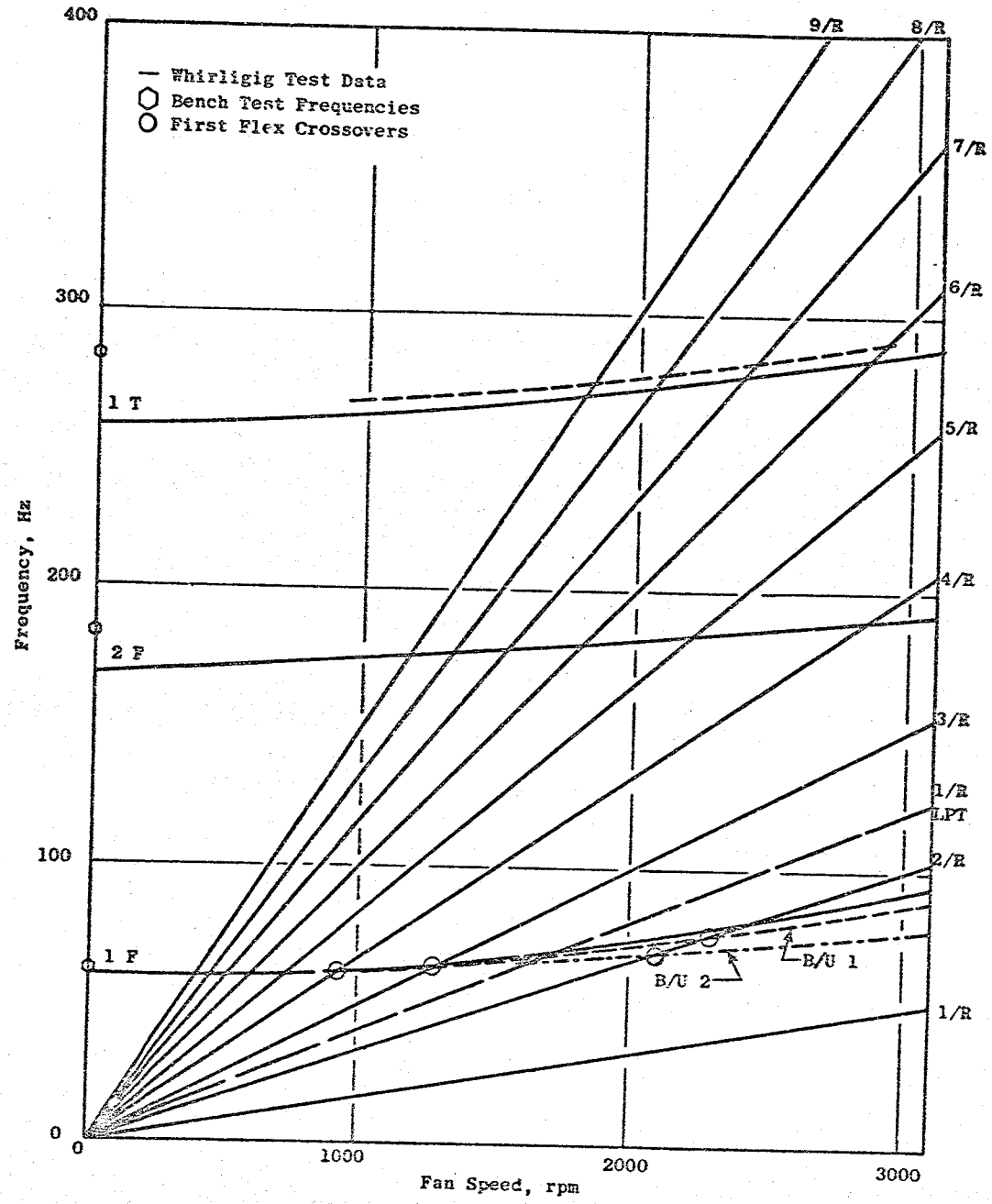

Figure 26. QCSEE UTW Campbell Diagram.

operating lines (fan nozzle areas of 14,800 cm^2 (2300 $in.^2$), 16,100 cm^2 (2500 $in.^2$), and 18,700 cm^2 (2900 $in.^2$) for the bellmouth inlet and 13,500 cm^2 (2100 $in.^2$), 16,100 cm^2 (2500 $in.^2$), and 18,700 cm^2 (2900 $in.^2$) for the high throat Mach number inlet) at five speeds (65, 80, 90, 95, and 97 percent) with variations in blade pitch angles from -7° open to +9° closed for the bellmouth inlet and from -10° to +9° closed for the high throat Mach number inlet.

The vibratory response of the blades, virtually the same for both inlets, was primarily in the first flexure mode forced by the 2/rev excitation. Vibratory responses in other modes were insignificant. Figure 27 shows a typical vibratory response for decelerating through the operating range and through the 2/rev crossover. The magnitude of the vibratory stress at the various frequencies is shown by the length of the vertical lines on the diagram. Here it can be seen that almost all of the stress (the maximum is about 150 percent of scope limits in this case) is due to the first flexure mode forced by the 2/rev excitation. During forward thrust testing, blade stresses reached about 250 percent of limits for a few cycles while accelerating and decelerating through the 2/rev crossover.

At a given fan speed, variations in nozzle area had no significant effect on the blade vibratory stresses with either the bellmouth or the high throat Mach number inlet. Also, for either inlet, blade vibratory stresses increased slightly as the blade pitch was changed from closed to open, near the nominal blade stagger -- sometimes by a factor of two, and they tended to decrease with increasing fan speed. However, for the high throat Mach number inlet configuration during a moderate accel/decel with a 13,500 cm^2 (2100 $in.^2$) nozzle area (highest throttled condition), the blade stress levels decreased with increasing fan speed; but for a 18,700 cm^2 (2900 $in.^2$) nozzle area, the blade stresses increased with increasing fan speed.

Other than the aforementioned forced resonance condition, all overstress conditions on the fan blades were due to high winds/inlet distortion. Inlet distortion/crosswinds caused blade vibratory stresses to exceed the current fatigue criteria -- reaching as high as 200 percent of limits. The blade vibratory responses are extremely sensitive to wind conditions. In general, almost any tailwind or crosswind, at any engine speed, is capable of producing an overstress condition. However, the blade vibratory response seems to be the most sensitive to tailwind (possibly with some reingestion and inlet lip separation) conditions.

As mentioned earlier for the QCSEE composite blades, the fatigue failure mode would be an internal delamination of the blade filament plies which would result in a drop in blade natural frequency rather than the usual metal blade fatigue crack. Frequencies versus speed were monitored during all phases of testing for the instrumented blades, and zero-speed (bench) frequencies were measured after each major phase of testing on all the blades. There was no detectable change in either the static frequency on any blade or the frequency at speed during test on any of the instrumented blades. If some slight internal damage (delamination) had occurred from overstress conditions, it would take approximately 1,000,000 cycles (3.5 hours) at 21 kN/cm^2 (30 ksi) DA to

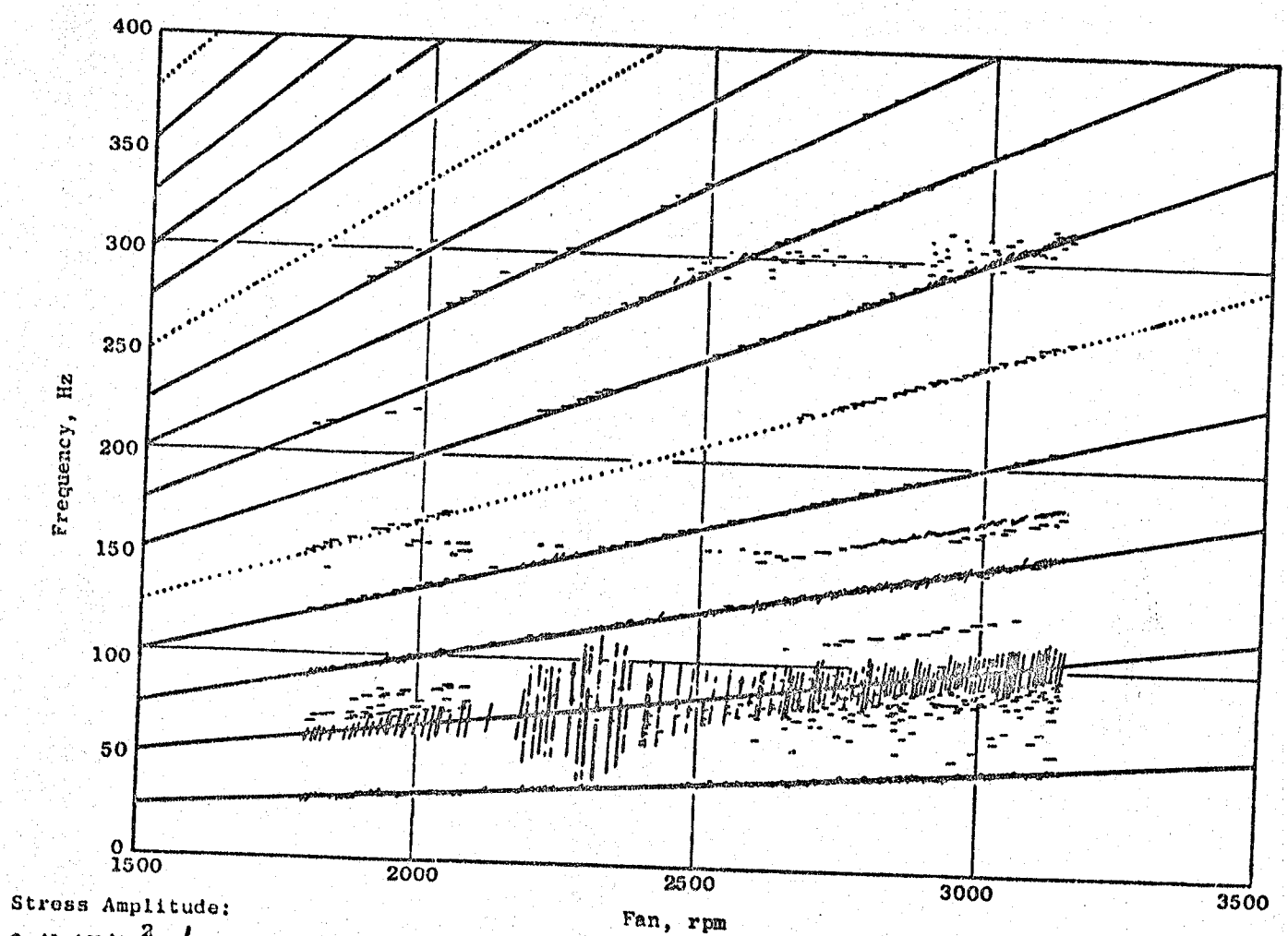

Stress Amplitude:

2.41 kN/cm^2
(3.5 kpsi)

Figure 27. QCSEE UTW 507-001/2 Campbell Diagram.

propagate the delamination to the point of losing 1.5 percent in the first flexure natural frequency. Even at this point, the blade would be structurally sound. During single-blade whirligig spin testing, a drop in frequency of 5 percent was considered to be a failure even though the blade was still structurally sound from a centrifugal load standpoint.

10.4.2 Reverse Thrust Vibratory Response

There were two reverse thrust tests with aeromechanical coverage conducted with Build 2 of this engine. The first test was done with a fixed pitch blade angle of -95° open with the high throat Mach number inlet installed and initially without the acoustic splitter in the fan duct. With the blade at this angle (Figure 25) the trailing edge becomes the leading edge and the chamber is in the right direction for reverse thrust. Run time at this blade angle was about 2 hours, with the acoustic splitter being installed after the first 90 minutes.

Set at -95° open, the blades exhibited highly modulated separated flow vibration (SFV) from idle (1800 rpm) to 2485 rpm, the highest speed attained at this blade angle due to both the T5 limit and the high blade stresses. Throughout the above speed range, the blade vibratory stresses, consisting mostly of SFV, exceeded scope limits from 180 to about 250 percent for a few cycles. It was observed that higher speeds produced more severe SFV. At -95°, the least open blade position for reverse thrust, the fan blades were operating close to stall -- hence the highly modulated SFV.

During the initial portion of this reverse thrust test, the wind was very erratic, varying from 2 to 10 mph at 0° to 360°. For the latter portion of this test (during the accels), the wind calmed to 3 to 5 mph at 130° to 150°. Wind effects on blade stress seemed to be negligible, but they were probably being masked by the high SFV. There was no apparent change in the blade first flexural frequency relative to that observed during forward thrust testing. Also, if there was any difference in the blade vibratory response depending upon whether or not the acoustic splitter was installed, it was entirely masked by the SFV.

The second reverse thrust test was done with a fixed pitch blade angle of -100° open, with the acoustic splitter installed, and with the high thrust Mach number inlet. The run time in this configuration was only 30 minutes due to excessive vibration of the upper left-hand (aft looking forward) nozzle flap.

At idle, the blades still showed a considerable amount of SFV, although not as severe as that for the -95° blade angle; however, the blade stresses were within limits. As the speed was increased to a maximum of 2600 rpm, the SFV modulation approached that of the -95° test, but the vibratory stress levels remained below 200 percent of scope limits. During this test, the wind varied from 4 to 8 mph at 250° to 290°. Again, if there were any wind effects on blade stresses, they were hidden in the SFV.

10.4.3 Effects of Inlet Distortion on Blade Stresses

There were basically two factors which produced aeromechanical concerns on this fan: the first flex response forced by 2/rev (crossover) as previously mentioned and resolved by maintaining a rapid acceleration rate through the 2100 to 2400 rpm speed range, and the sensitivity of the blades to inlet distortion caused by wind conditions.

Wind velocity and direction relative to the inlet seem to be the major contributors to overstress conditions observed on the fan blades. Limited data precludes conclusive vibratory stress response correlation with wind speed and direction, particularly for winds from the west and southwest (engine inlet centerline was at 190° from the north). As previously mentioned, any appreciable tailwind or crosswind may result in a fan blade overstress condition.

Utilizing the available data, blade stress wind limit envelopes can be constructed for different engine speeds. Figures 28, 29, 30, and 31 depict such envelopes for idle, 80, 90, and 95 to 97 percent speeds, respectively. The lack of wind data from the south, southwest, and west can be seen on the envelopes for idle and 90 percent speed (Figures 28 and 30). In addition, if all the above wind envelopes are superposed, the blade stress wind envelope for any engine speed (Figure 32) is obtained. This composite plot can be used as a limit curve when operating the engine in forward thrust without stress monitoring.

For reverse thrust, the fan was close to stall with a fixed pitch blade angle of -95° open, and very limited wind/stress data was obtained with the blade set at -100° open. However, if the data is enveloped, the blade stress wind limit envelope for reverse thrust shown in Figure 33 results.

10.5 CONCLUSIONS

10.5.1 Forward Thrust

- At constant fan speed, variations in nozzle area had no significant effect on blade vibratory stresses.
- At constant fan speed, blade vibratory stresses increased slightly as the blade pitch was changed from closed to open in the 0° to -5° range.
- With either the bellmouth or the high throat Mach number inlet, blade stress levels tended to decrease with increasing fan speed.
- With the high throat Mach number inlet during a moderate accel/decel and a 13,500 cm^2 (2100 $in.^2$) nozzle area, the blade stresses decreased with increasing fan speed; but with an 18,700 cm^2 (2900 $in.^2$) nozzle area, the blade stresses increased slightly with increasing fan speed.

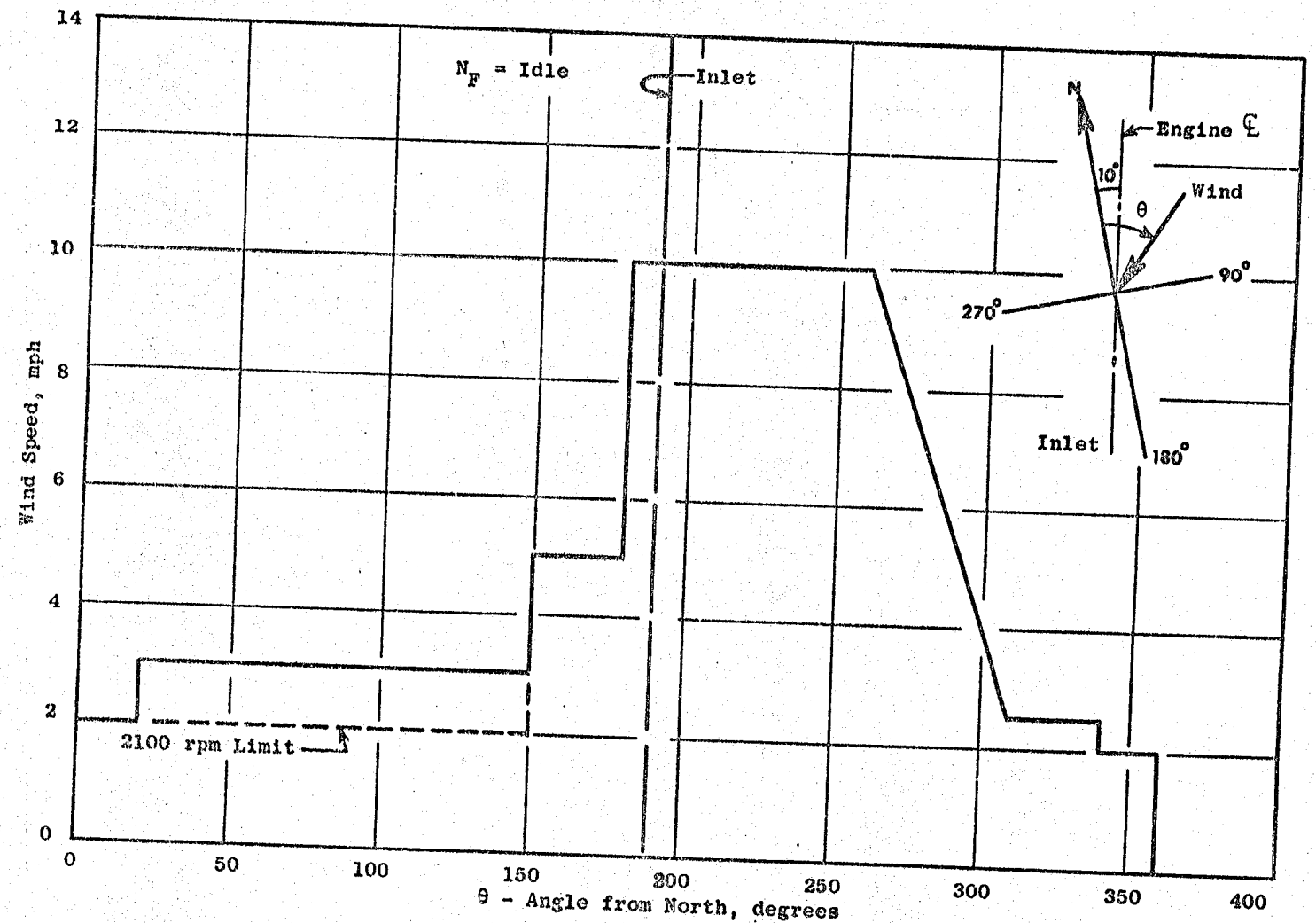

Figure 28. QCSEE UTW Blade Stress Wind Limits.

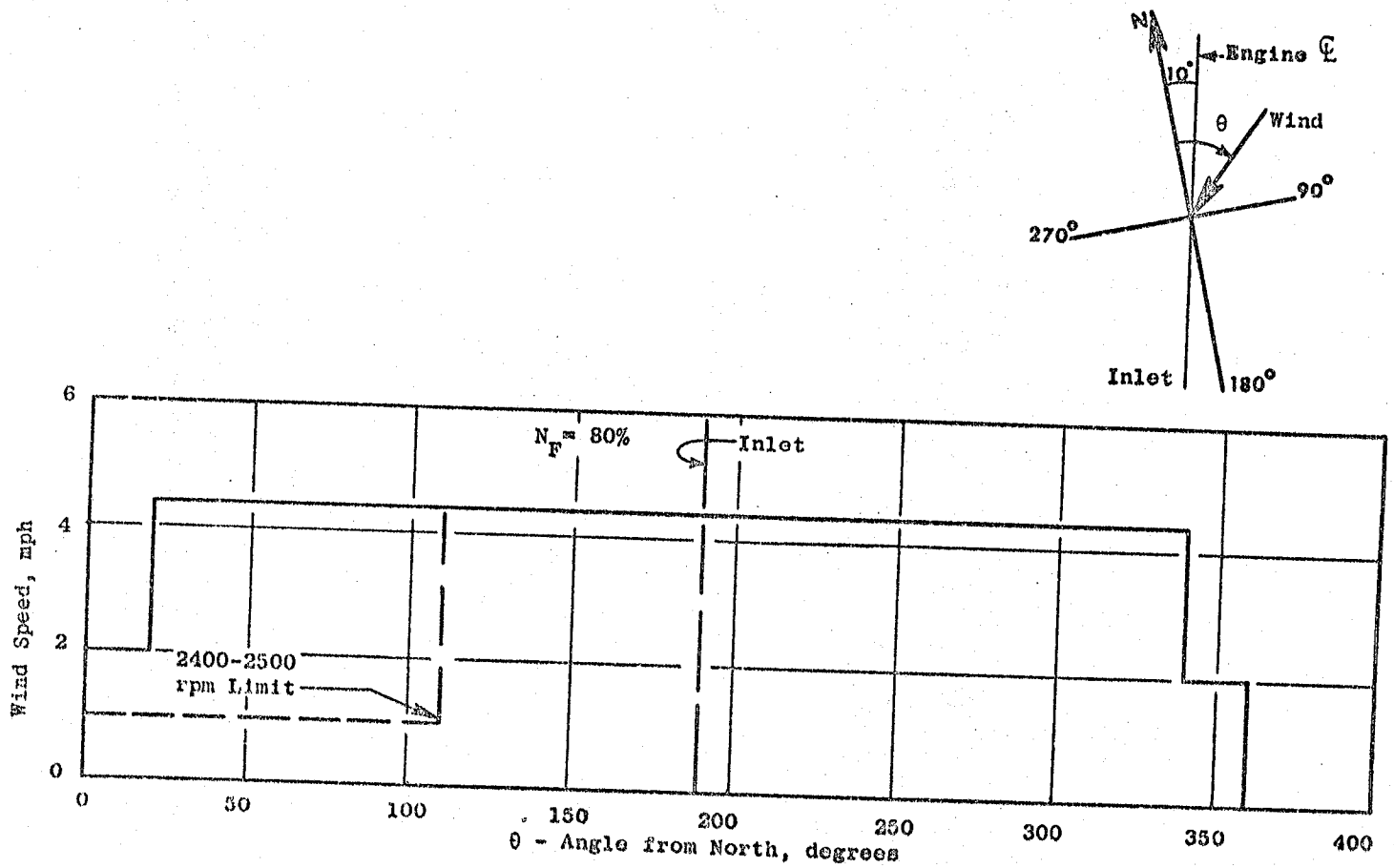

Figure 29. QCSEE UTW Wind Effects on Blade Stresses.

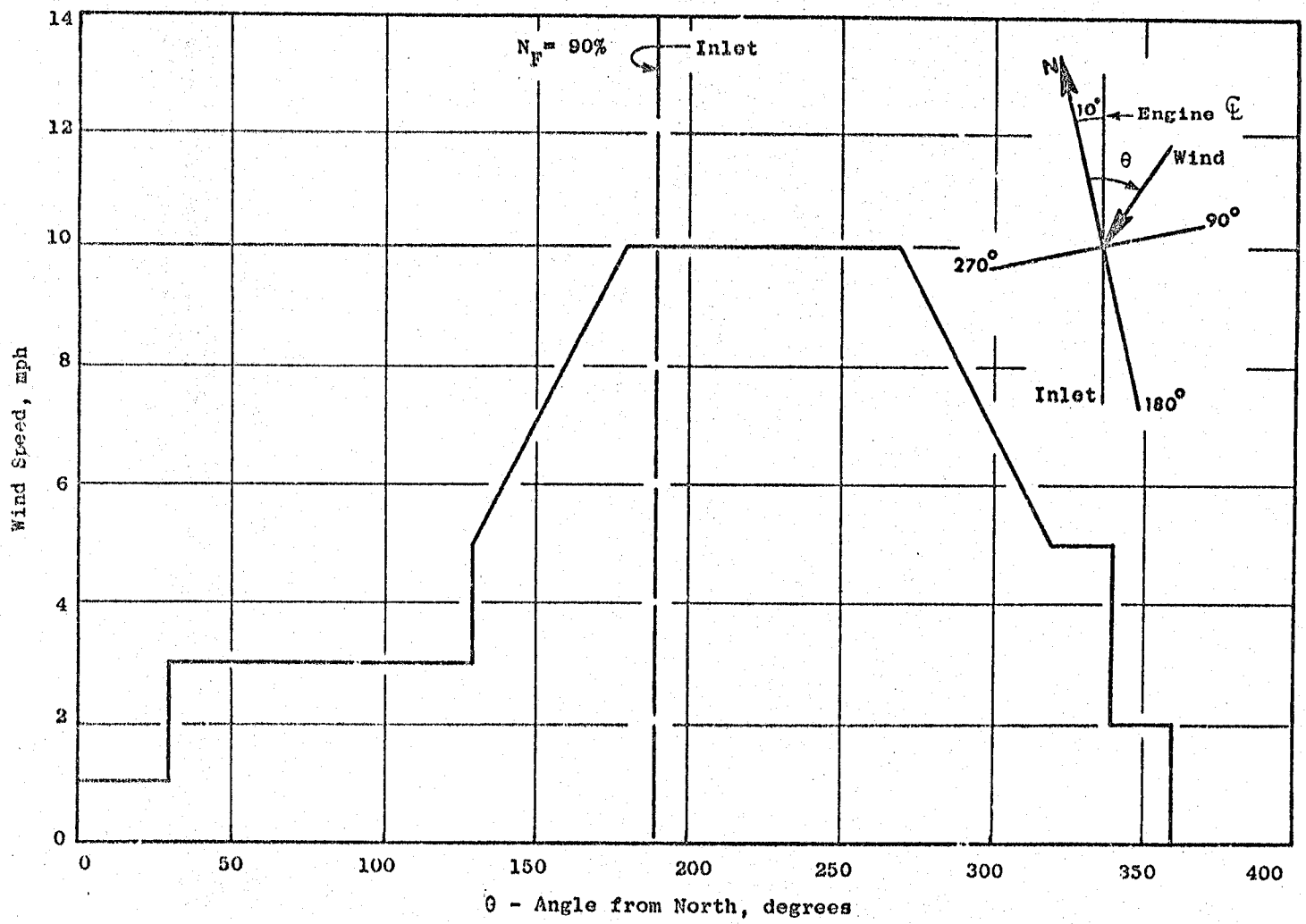

Figure 30. QCSEE UTW Blade Stress Wind Limits.

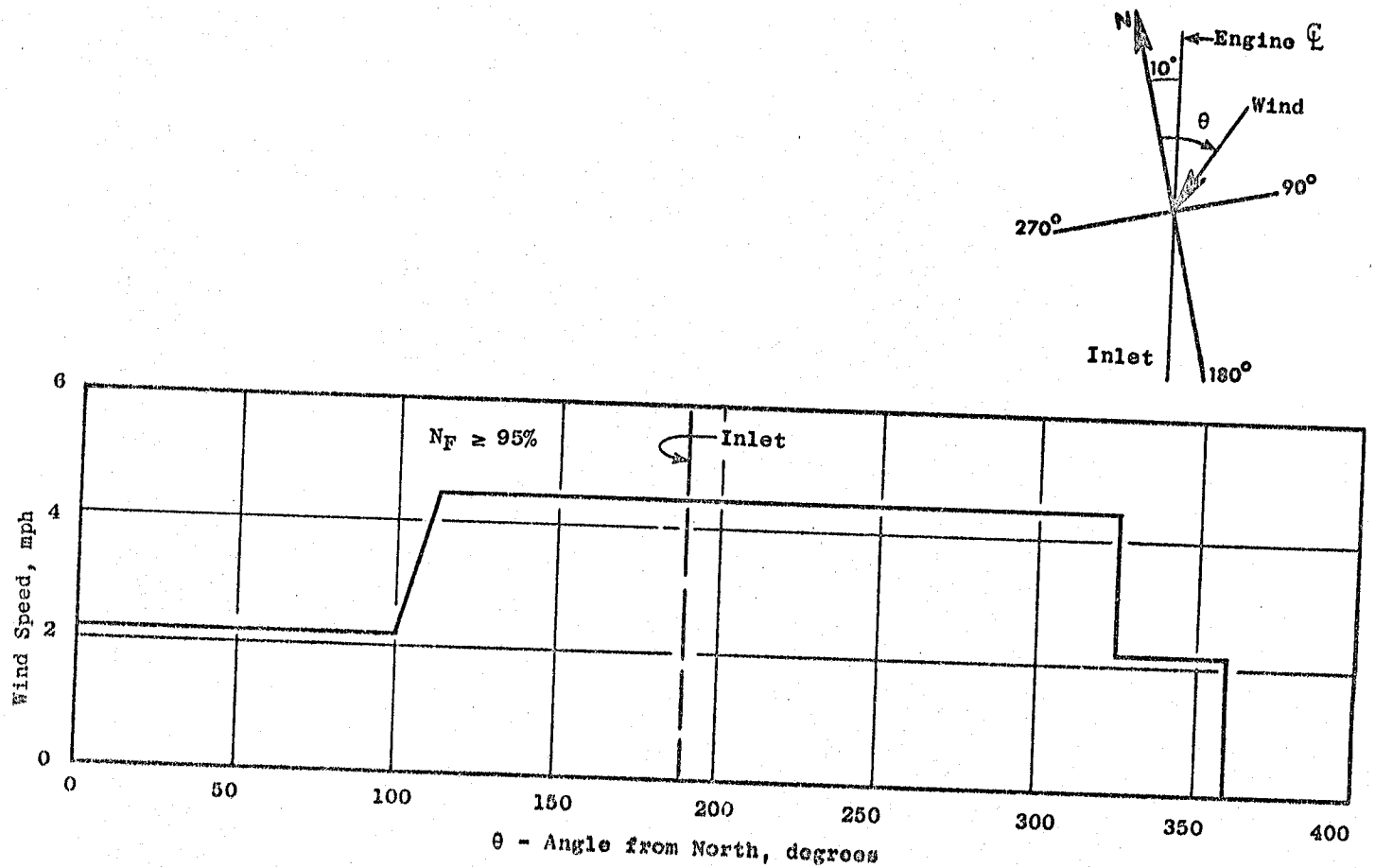

Figure 31. QCSEE UTW Wind Effects on Blade Stresses.

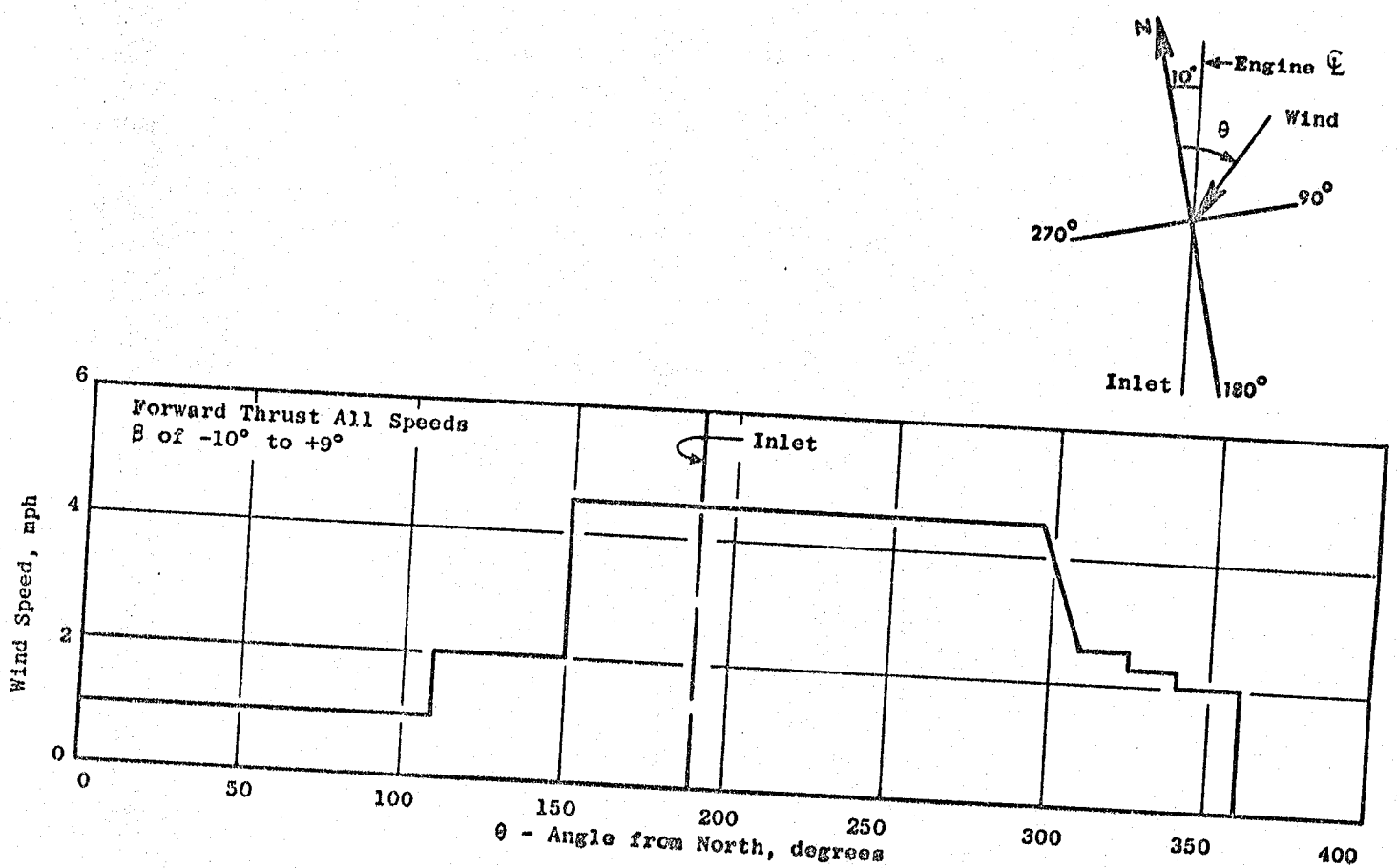

Figure 32. QCSEE UTW Wind Effects on Blade Stresses.

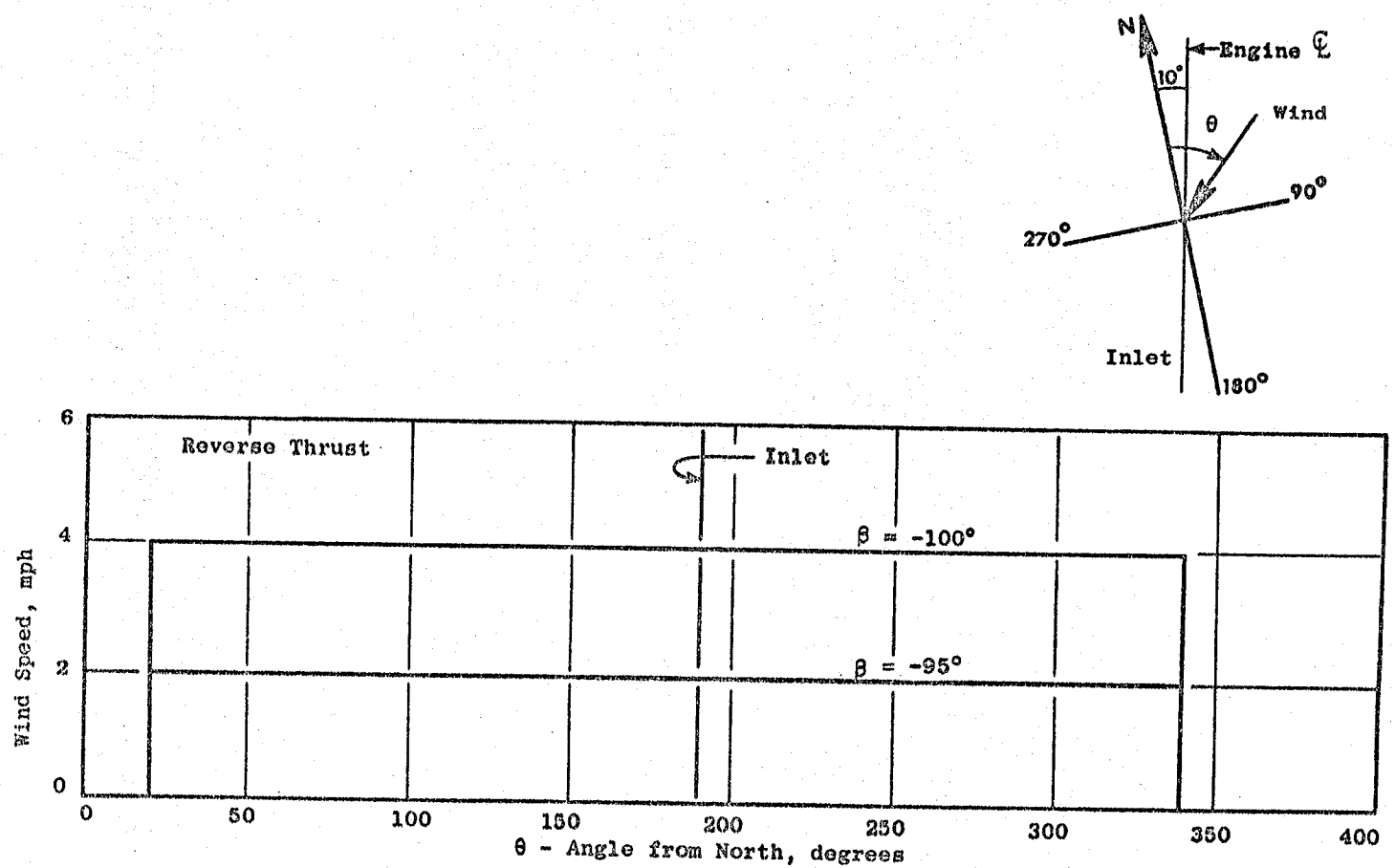

Figure 33. QCSEE UTW Wind Effects on Blade Stresses.

- Blade vibratory response is extremely sensitive to wind/inlet distortion conditions.

- Tailwinds (possibly with some reingestion or inlet lip separation) seem to be the worst wind condition.

10.5.2 Reverse Thrust

- With the blade pitch set at -95° open, overstress conditions due to highly modulated SFV were observed from idle to 2485 rpm.

- With the blade pitch set at -100° open, the SFV was less severe than that at -95°, with idle speed stress levels below scope limits. But as the speed was increased, the SFV blade stresses increased to levels above the established scope limits.

10.5.3 General

- There are conservatisms inherent in the fatigue criteria/scope limits, and it is unlikely that any blade damage has occurred thus far.

- The fan speed at which the 2/rev first flexure crossover occurred was lower for Build 2 than for Build 1 of this engine. However, the Build 2 first flexure natural frequency did not change throughout the tests reported herein.

10.5.4 Recommendations

- The blade stresses should be monitored during further engine tests.

- Reverse thrust testing with the blades open should be done at angles more open than -95°.

- The present scope limits, although conservative, should be maintained for overall engine safety.

11.0 MAIN REDUCTION GEAR

The UTW engine has a star-type epicyclic reduction gearset located in the forward engine sump to reduce the low-pressure turbine speed to fan rotor speed. The gearset is shown schematically in Figure 34. The gearset consists of a flexibly mounted sun gear, which drives six star gears, which are mounted on a fixed carrier and which drive a ring gear. The ring gear is flexibly mounted to the fan shaft. Principle design characteristics of the gears are listed in Table XXII.

During testing of the UTW engine, the main reduction gear operated without problems. As in previous testing, ring gear strain gages indicated vibratory stress well within allowable limits. Maximum bearing temperature did not exceed the 403 K (265° F) limit. Engine heat rejection data reported in Section 12.0 of this report, was 31.16 x 10^4 J/sec (17,708 Btu/sec) at takeoff speed. Although the contribution of the main reduction gear to the total heat rejection cannot be accurately determined, the gear efficiency appeared to be 1 to 2 percent below the design objective value of 99.2 percent.

The engine was not disassembled at the conclusion of testing however, the variable pitch mechanism was removed on March 11, 1978 and the main reduction gear was exposed. The gear tooth patterns indicated normal uniform wear across the tooth faces. Total engine running time on the gear at that time was 106:13 hours.

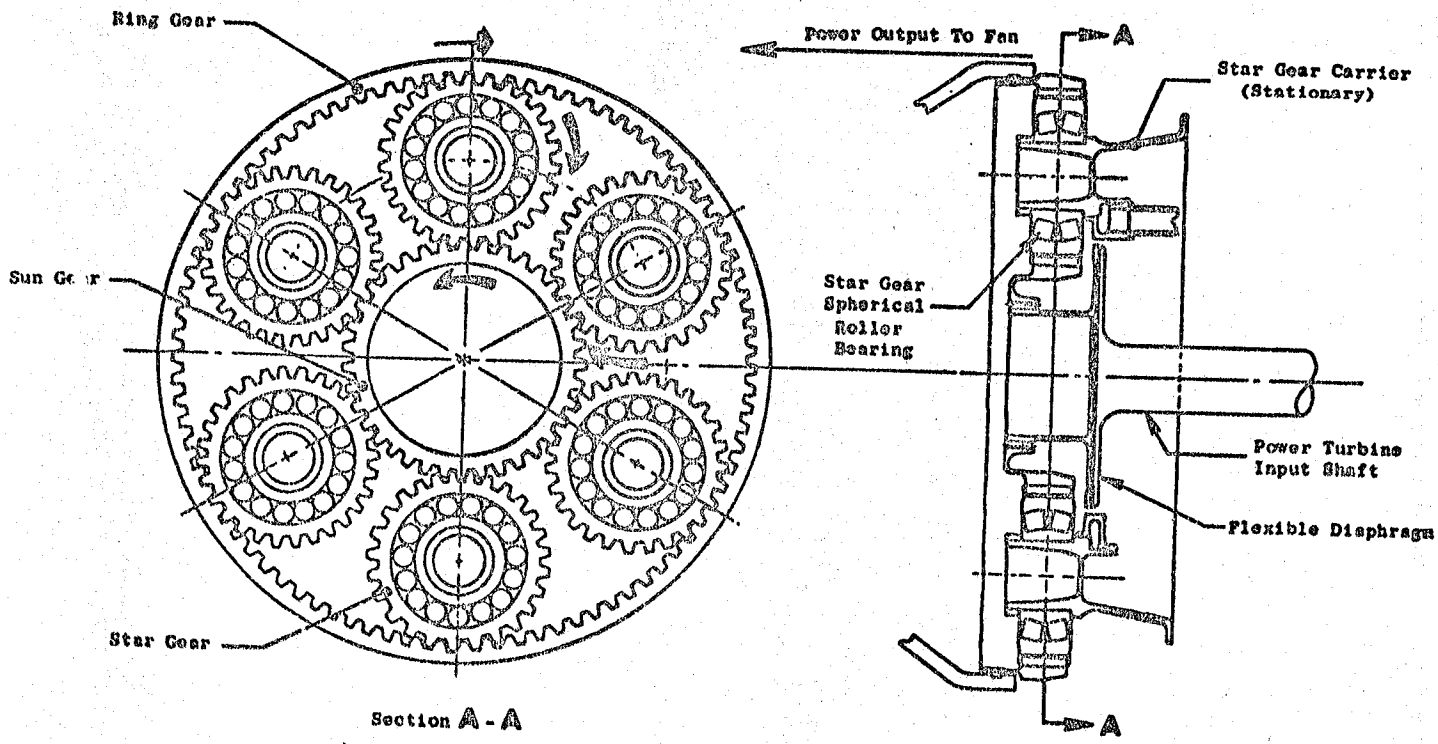

Figure 34. Main Reduction Gear Configuration.

Table XXII. UTW Reduction Gear Design Details.

[Takeoff, 306 K (90° F) Day]
(100% Power, 100% Speed)

Gear Ratio	2.465
Turbine Power	9889 kw (13,256 hp)
Turbine Speed	7747 rpm
Gear Pitch Line Velocity	97.1 m/sec (19,117 ft/min)
Star Gear Speed	10,577 rpm
Bearing Load	33,925 N (7627 lb)
Number of Stars	6
Number of Gear Teeth	
Sun Gear	71
Star Gear	52
Ring Gear	175
Hunting	Yes
Nonfactoring	Yes

12.0 LUBRICATION AND ACCESSORY DRIVE SYSTEM

12.1 SYSTEM DESCRIPTION

The UTW engine utilizes six main shaft bearings to support the rotating turbomachinery. The short construction of the concentric UTW rotors permits a two-bearing support system for each rotor. The No. 1B and 1R bearings support the fan rotor. The high pressure core rotor is supported by the No. 3 and No. 4 bearings. The No. 2 and No. 5 bearings support the low pressure turbine and power transmission shaft. Both the fan and low pressure turbine shaft are soft coupled to the engine main reduction gear to minimize induced loads on the gears. The core thrust bearing located in the engine forward sump provides more precise control of the compressor blade clearances.

Application of a main reduction gear between the fan and low pressure turbine requires that the normal axial load "tie" between fan and low pressure turbine components be severed; as a result, the No. 2 thrust bearing must react the full aft load of the turbine without any negating forward thrust from the fan. In order to reduce the bearing load to an acceptable level, a thrust balance cavity has been added to the rear sump. This cavity uses compressor discharge air to pressurize a balance piston, providing a forward compensating force on the turbine rotor. A high-load-capacity CF6 No. 1 thrust bearing is used in the design to react the fan axial loads.

A top-mounted accessory gearbox is driven from the core by an F101 internal bevel gearset and a long radial drive shaft. The length of this shaft requires a midspan bearing to provide critical speed margin. An additional F101 internal bevel gearset located in the bottom half of the engine is combined with a short radial shaft and a second bevel gearset located in the core cowl area to drive a vane-type pump that scavenges oil from both the forward and aft sumps. This pump, along with a remotely mounted pump, scavenges the top-mounted accessory gearbox.

The lubrication system is designed on the basis of current dry sump technology utilizing a circulating oil system. Internal engine and gearbox passages are used wherever possible for oil delivery and return. Venting and pressurization functions also make use of internal engine passages where possible.

12.2 INSTRUMENTATION

Each sump of the QCSEE UTW engine was instrumented as follows to ensure safe operation of the engine:

- The outer race temperature of each main shaft bearing was measured in two places.

- The sump pressures and the carbon seal ΔP were measured for each main shaft seal
- Temperature in the aft sump cavity was measured.
- The pressure and temperature were measured in the balance piston pressurization and exhaust cavities.
- The inner race temperature of each star gear bearing was measured.
- The lube pressure in the manifold supplying oil to the reduction gearing was measured.
- The lube supply and scavenge pump discharge pressures were measured.
- ΔP across the supply filter was measured.

The lube system package was instrumented to measure the following parameters:

- Oil reservoir lube level
- Oil reservoir internal pressure
- Scavenge filter ΔP
- Scavenge discharge temperature
- Lube supply temperature
- Heat exchanger ΔT on oil side
- Heat exchanger waterflow and ΔT on water side

12.3 TEST EXPERIENCE

The sump and the accessory system, with the exception of a radial shaft failure, performed well throughout the test phase of the second build of the QCSEE UTW engine.

12.3.1 Main Shaft Bearings

The test limits of 450° C (350° F) were not exceeded during any of the testing. Figures 35 through 37 show representative temperature data for these bearings as a function of engine speed.

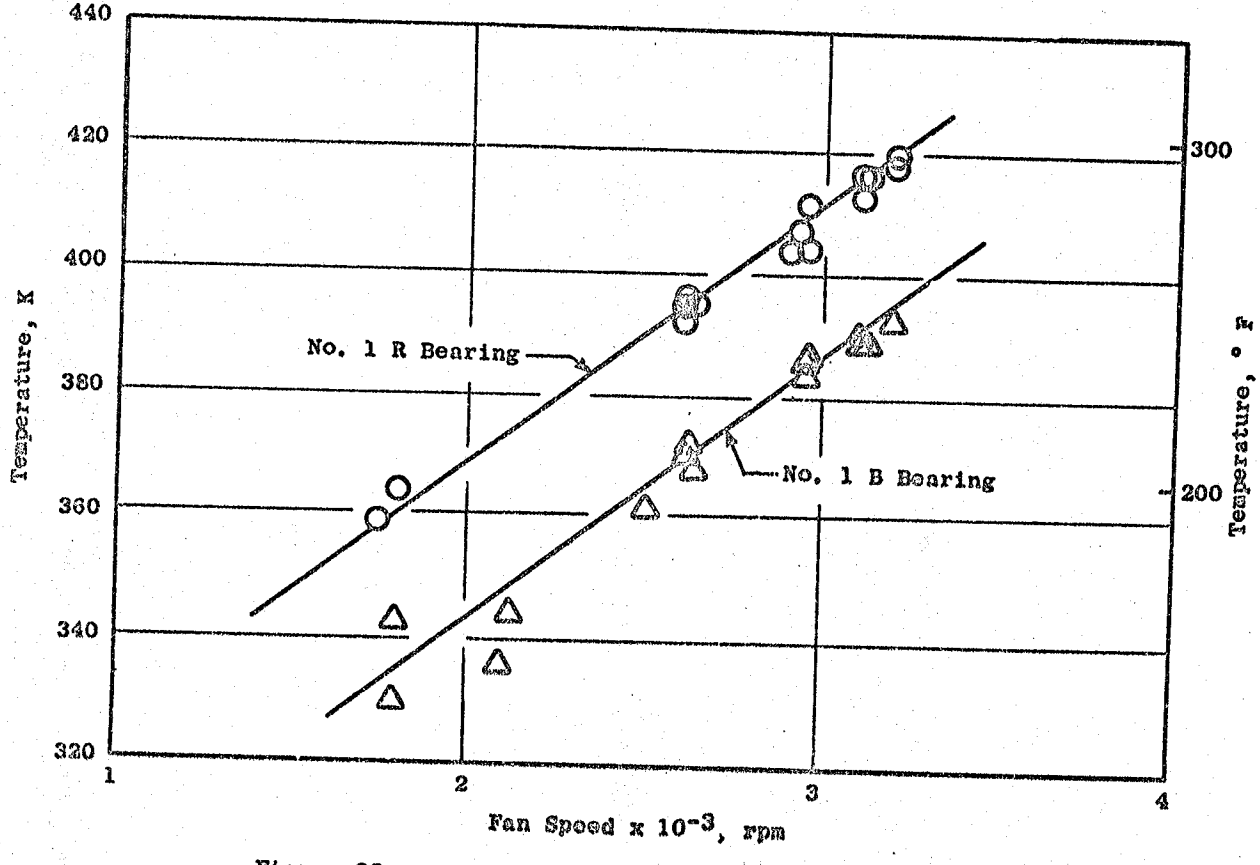

Figure 35. Outer Race Temperature Versus Fan Speed.

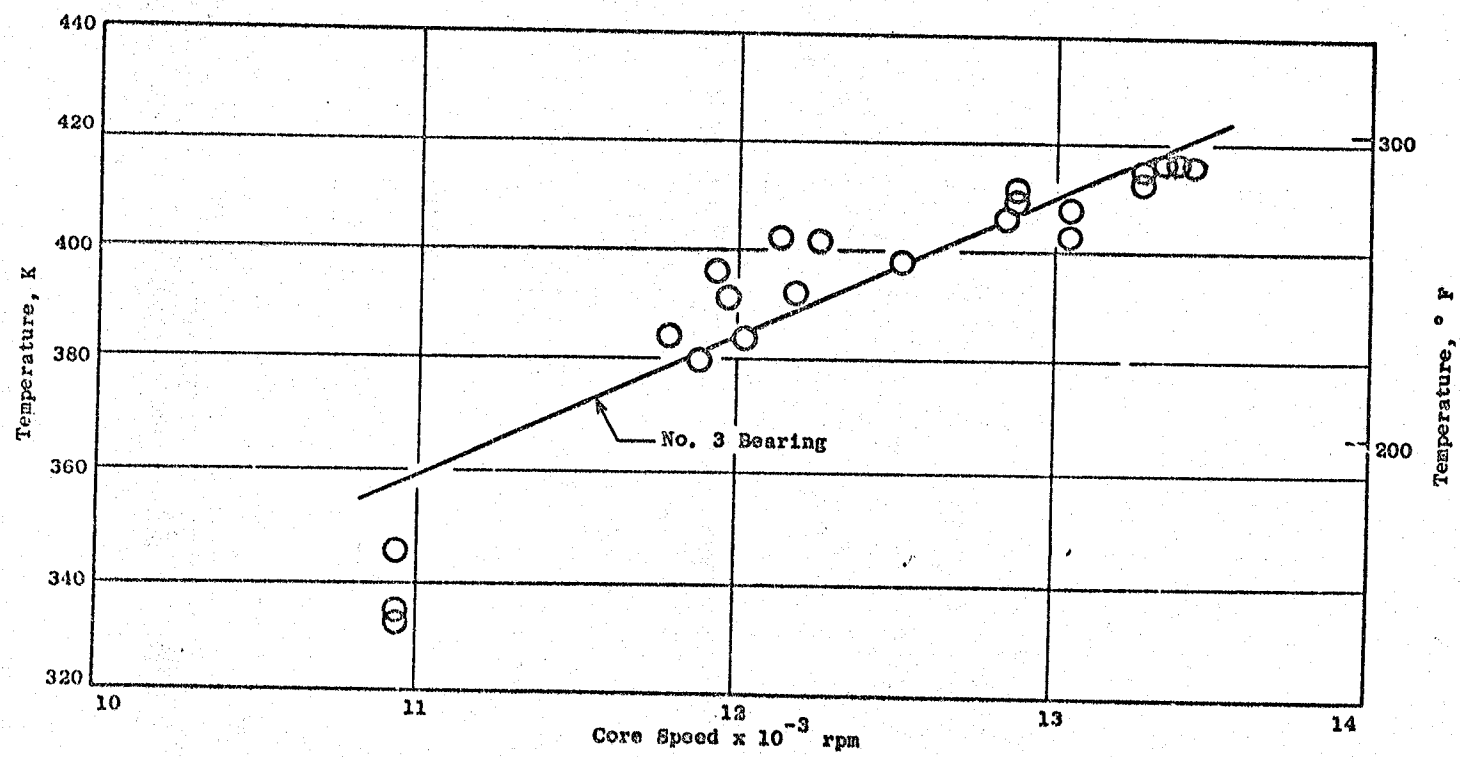

Figure 36. Outer Race Temperature Versus Core Speed.

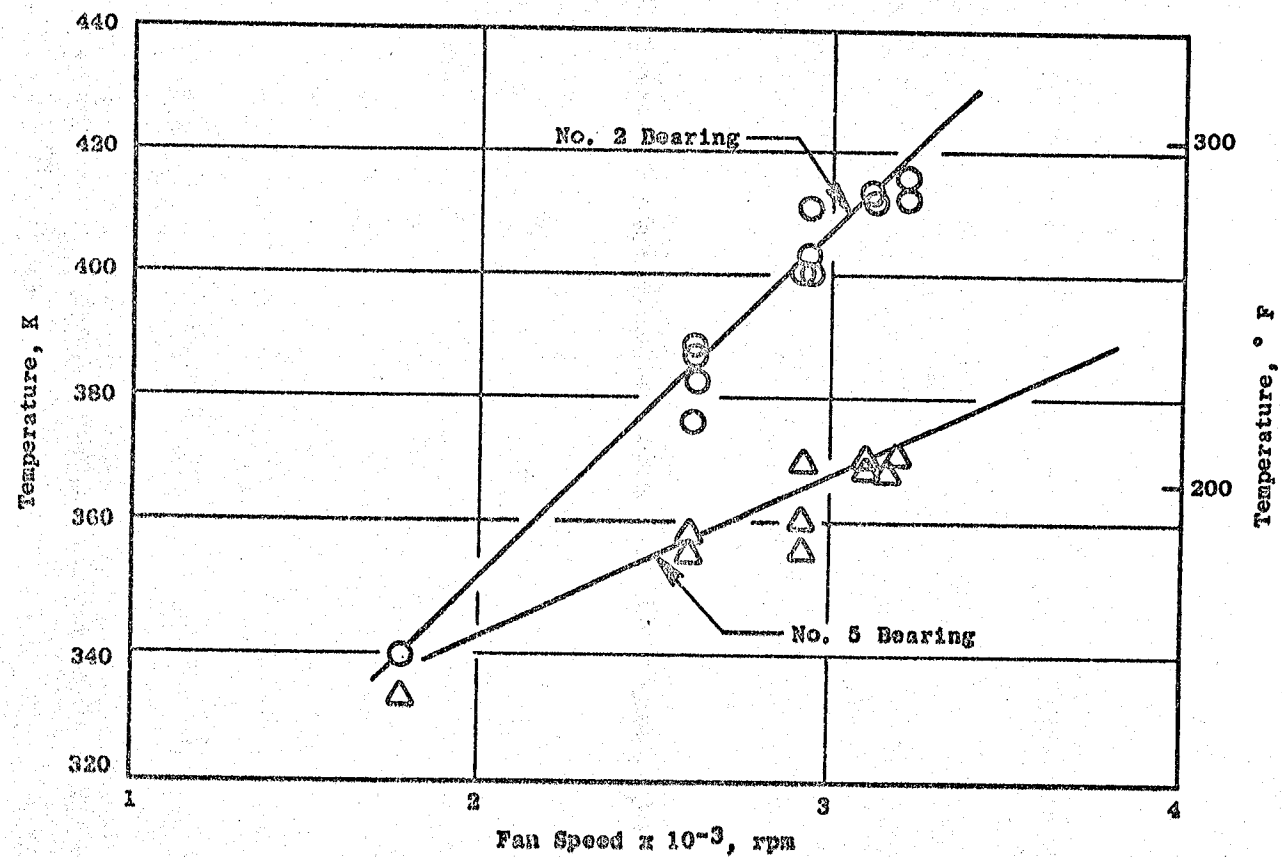

Figure 37. Outer Race Temperature Versus Fan Speed.

12.3.2 Lube Supply and Scavenge System

The lube supply and scavenge pressures as a function of core speed are shown in Figures 38 and 39. These pressures are compared to the first build data. The supply system pressures in Build 2 were higher than Build 1 for two reasons:

- Sump pressures were higher because eductor was not used. An eductor was used in Build 1 to lower sump pressures to minimize frame oil leaks.
- Cooler oil temperatures were provided in Build 2. The cooler oil, being more viscous, requires a higher pressure to flow the same network.

The scavenge pressure was higher than Build 1 because of the higher pressure drop of the two heat exchangers used versus the one used in Build 1. The scavenge pressure levels were similar to the QCSEE OTW engine which also used two heat exchangers.

12.3.3 Heat Rejection

For the second build of the QCSEE UTW engine, two LM2500 heat exchangers mounted in series were used. This is the same arrangement as the QCSEE OTW engine. Table XXIII shows a comparison of the first and second build heat rejection for the QCSEE UTW engine. Figure 40 also shows heat rejected to the heat exchangers as a function of fan speed.

12.3.4 Accessory Drive System

The second build of the QCSEE UTW engine featured an accessory gearbox (AGB) modified to the same configuration which was run on the OTW engine. The modification includes the following:

- A remote scavenge pump was used which scavenged directly from the bottom of the gearbox.
- Windage shrouds were added to the vertical bevel gear and the forward side of the horizontal bevel gear.
- Holes were drilled in the horizontal bevel gear and through a vertical partition in the gear housing to improve the internal venting of the gearbox.

At no time during the engine testing did the accessory gearbox scavenge oil temperature exceed the allowable limit of 433° C (320° F). For the majority of testing, it was below 400° C (260° F).

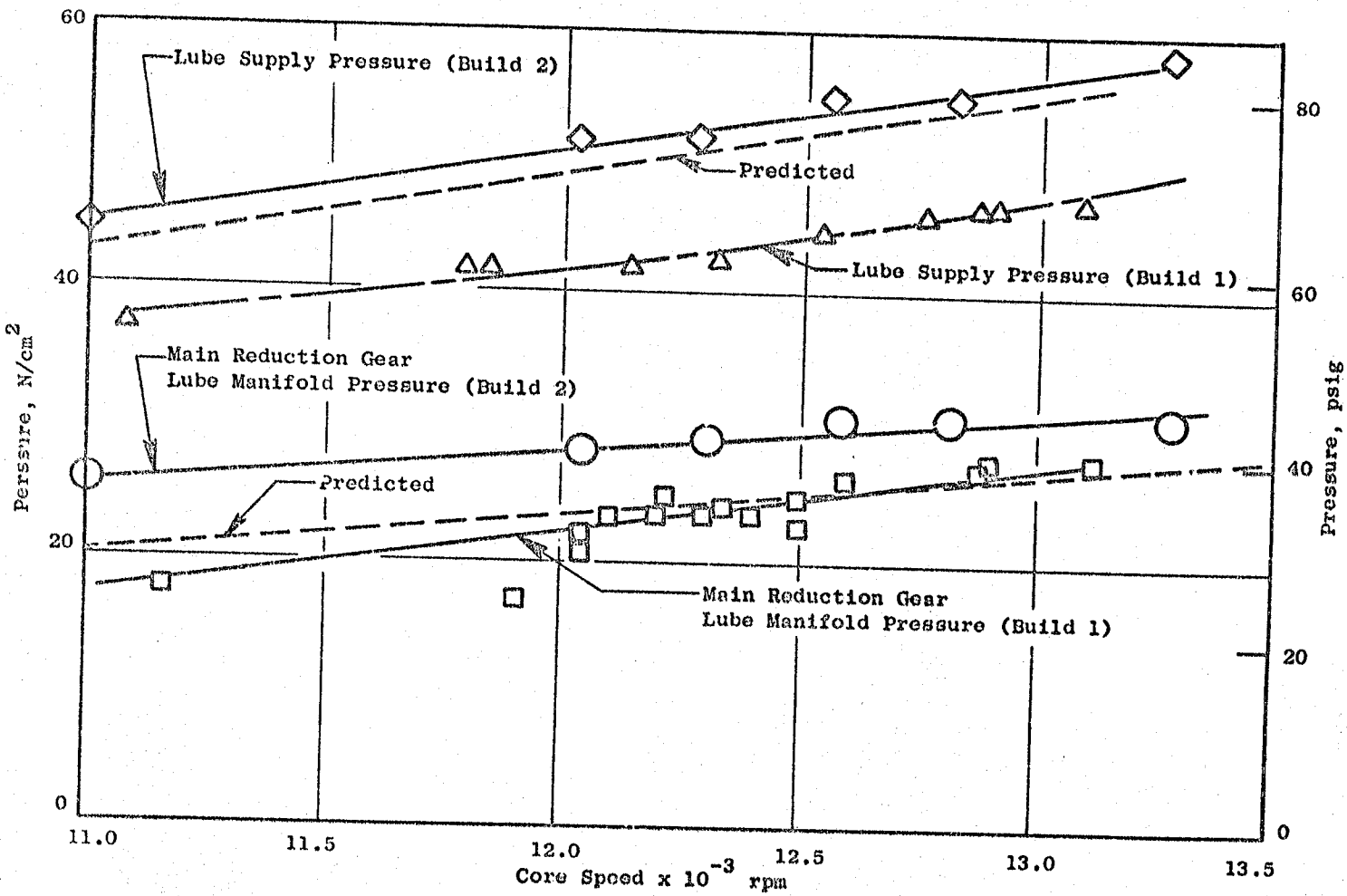

Figure 38. Lube Supply Pressure Versus Core Speed.

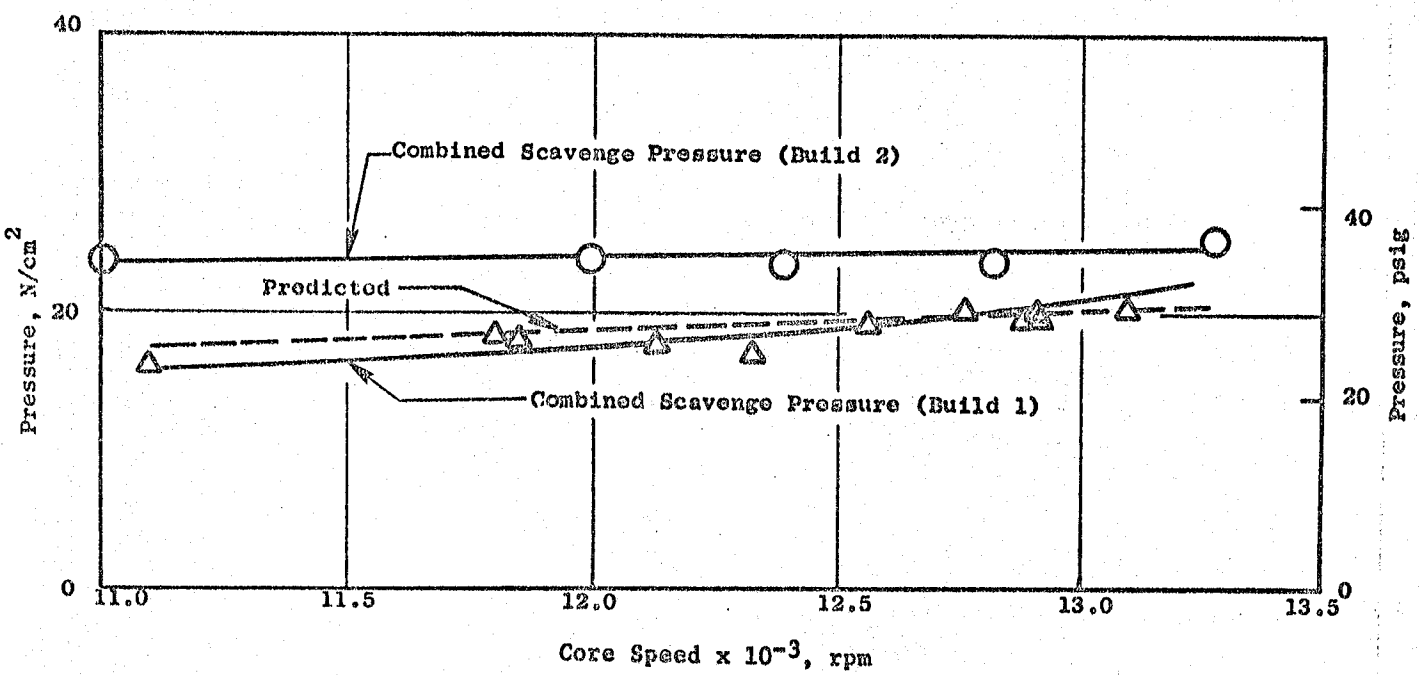

Figure 39. Lube Scavenge Pressure Versus Core Speed.

Table XXIII. Engine Heat Rejection.

	Build 1 Measured	Build 2 Measured
HPT, % rpm	80.6%	88.1%
LPT, % rpm	94.5%	98.78%
Lube Flow	2189.2 cm^3/sec (34.7 gpm)	2290.2 cm^3/sec (36.3 gpm)
Scavenge Temperature	< 393 K (< 248° F)	< 366.3 K (< 200° F)
Lube Temperature	< 331.9 K (< 138° F)	< 333 K (< 140° F)
Total Engine Heat Rejection	28.04 x 10^4 J/sec (15,933 Btu/min)	31.16 x 10^4 J/sec (17,708 Btu/min)

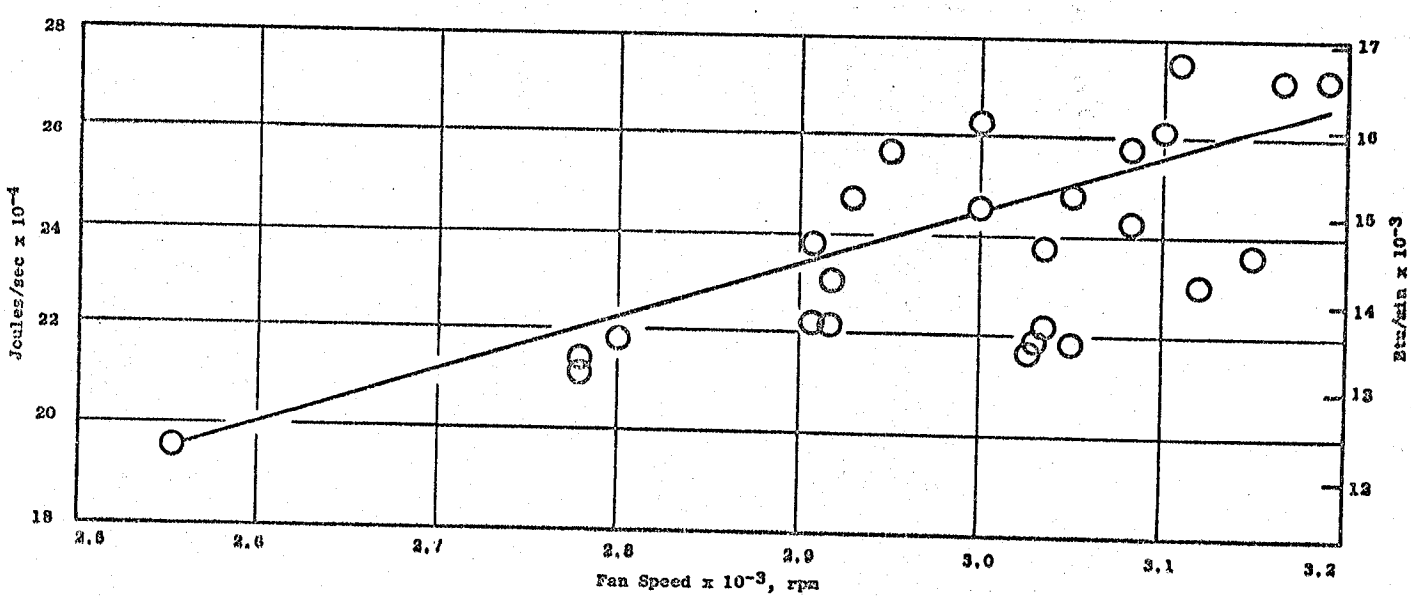

Figure 40. Engine Heat Rejection Versus Fan Speed.

12.3.4.1 Radial Shaft Failure

On November 3, 1977, the engine sustained a failure in the radial drive shaft connecting the PTO gearbox with the accessory gearbox. The failed shaft is shown in Figure 41. A visual inspection showed heavy spline wear on the loaded faces of the teeth but concentrated at the tooth ends. It was concluded that the shaft failed in fatigue which started near the root of a spline tooth, progressed axially about 5.08 mm (0.20 inch), diagonally across the spline, and then circumferentially around the shaft.

Calculated stresses in the spline are low unless the shaft is severely misaligned. Just adjacent to the failed area, two teeth are cut back to allow for a retaining pin which secures a pressed-in plug in the end of the shaft. Removing these teeth causes the adjacent teeth to carry more load in a misaligned condition. Dimensional checks on the fan frame AGB mounting cup showed the cup cocked relative to the AGB which caused shaft misalignment.

The pressed-in plug in the shaft end also increases the stresses in the area of the spline tooth root.

The following was done to reduce the spline tooth loading:

- The AGB alignment procedure was changed to ensure proper shaft alignment.
- The press fit of the shaft plug was reduced to minimize the stresses in the area of the spline roots.
- The spline teeth were cut back 12.7 mm (0.50 inch) to make all spline teeth equal length.

After installing the modified shaft, testing was completed without incidence.

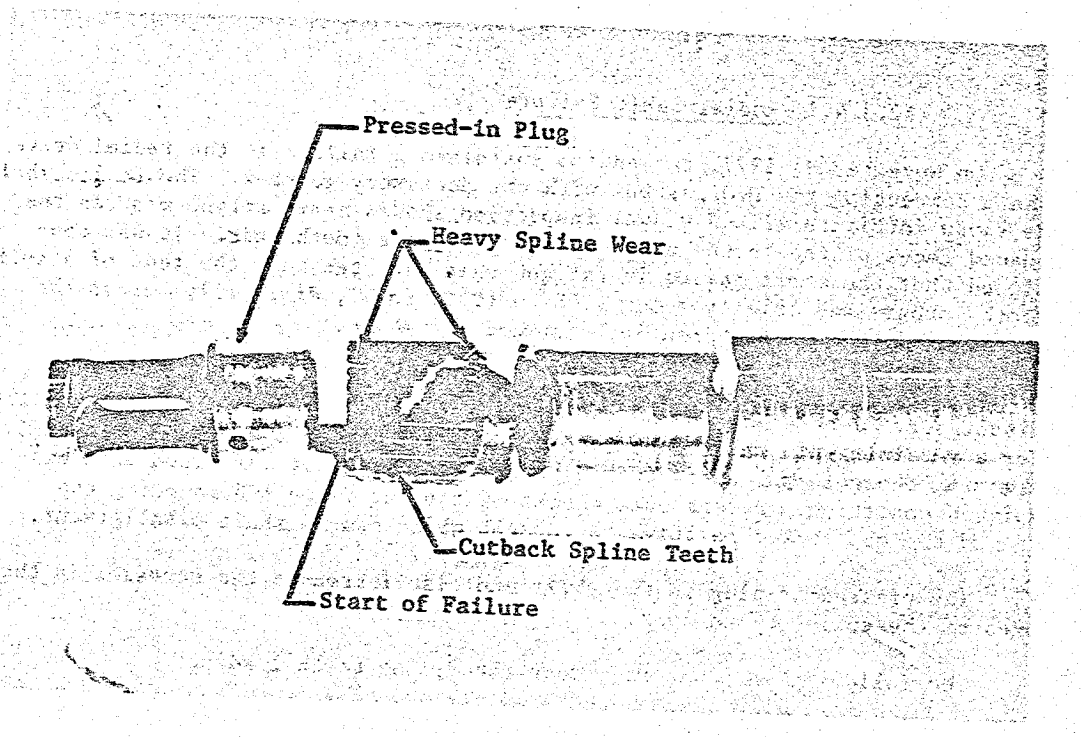

Figure 41. Radial Drive Shaft Failure.

13.0 FAN FRAME

The QCSEE integrated fan frame is a graphite/epoxy structure which incorporates the fan casing, fan bypass vanes, and core frame. It provides the primary support for the engine and is 2.00 m (78.8 inches) in diameter, 0.9525 m (37.5 inches) in length, and weighs 315.2 kg (695 lbs) at engine assembly not including the engine mounts.

During the second build of the UTW, the frame was instrumented with a total of six strain gages. Three of these were located in the engine mount area as shown in Figure 42. The other three gages were located on the fan bypass vanes as shown in Figure 43.

None of the gages in the mount area showed any significant response during engine operation. This was expected since normal operating loads are quite low compared to the five blade-out loads for which the structure was designed. The highest stress observed during engine test was only 2 percent of the ultimate strength of the material. Stresses that low cannot be detected on the engine monitor scopes.

The only frame gages showing any activity during engine operation were the working gages on the bypass vanes. All observed stresses on these vanes were low, less than 4 percent of the ultimate strength of the material at the worst case of 95 percent fan speed, an AI8 of 1.87 m^2 (2900 $in.^2$), and a blade angle of -5°. These stresses were caused by a 2/rev forced input. The stresses became less as AI8 was decreased and/or the blade angle moved from negative angles toward positive angles.

It was possible, by increasing the scope sensitivity, to detect the vane natural frequencies (first flex only) as they were excited by a fan 18/rev. These frequencies were lower than expected based on bench testing of a single vane. It is probably that the actual end fixity of the vanes is somewhat less than it was for the bench test specimen which had its ends cast in Devcon (a filled epoxy). The bench test results are shown in Figure 44 along with the natural frequency data obtained during engine running. The "open-2" expected values shown in Figure 44 were analytically extrapolated from the "closed-2" bench test data. Stresses increased momentarily as the fan speed passed through these frequencies but never exceeded 4 percent of the ultimate strength capability.

The first engine problem encountered which involved the fan frame was on 11/3/77. After 50 hours 53 minutes of engine running, the UTW engine was shutdown due to a severed radial drive shaft. Since the break in the shaft occurred at the top end near the gearbox, the remaining length of shaft was allowed to orbit within the cavity formed by the pylon airfoil panels. This orbiting punctured holes in both pylon panels at the top, midspan region. In addition to the panel damage, an unbond also occurred in the fairing "boots" that wrap around the pylon vane/casing interface. The repair was made by

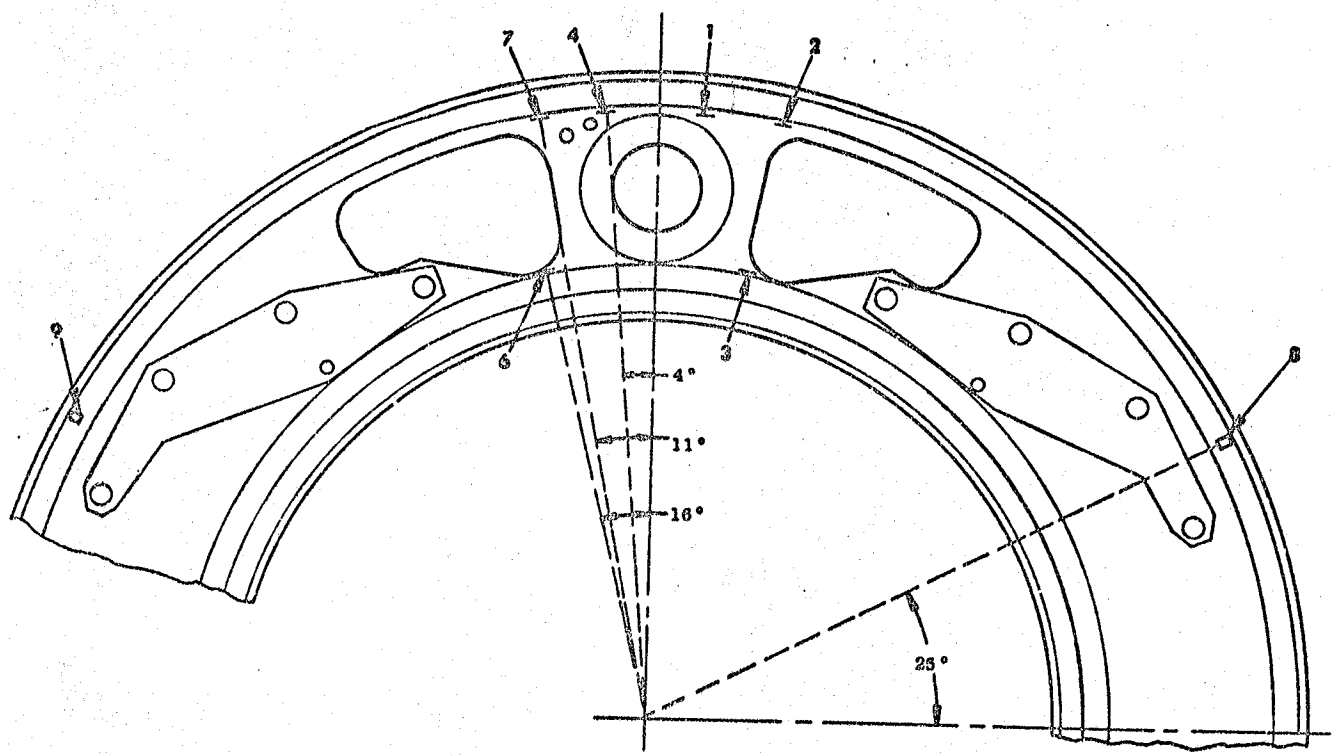

Back of Aft Wheel Splitter Ring - Mount Area

Gages are Symmetrical About Vertical Centerline

Note: Gages 8 and 9 are located on the fan flow splitter surface 10.16 cm (4 in.) forward of the vane trailing edge.

Figure 42. Strain Gage Locations for UTW Fan Frame, Mount Area.

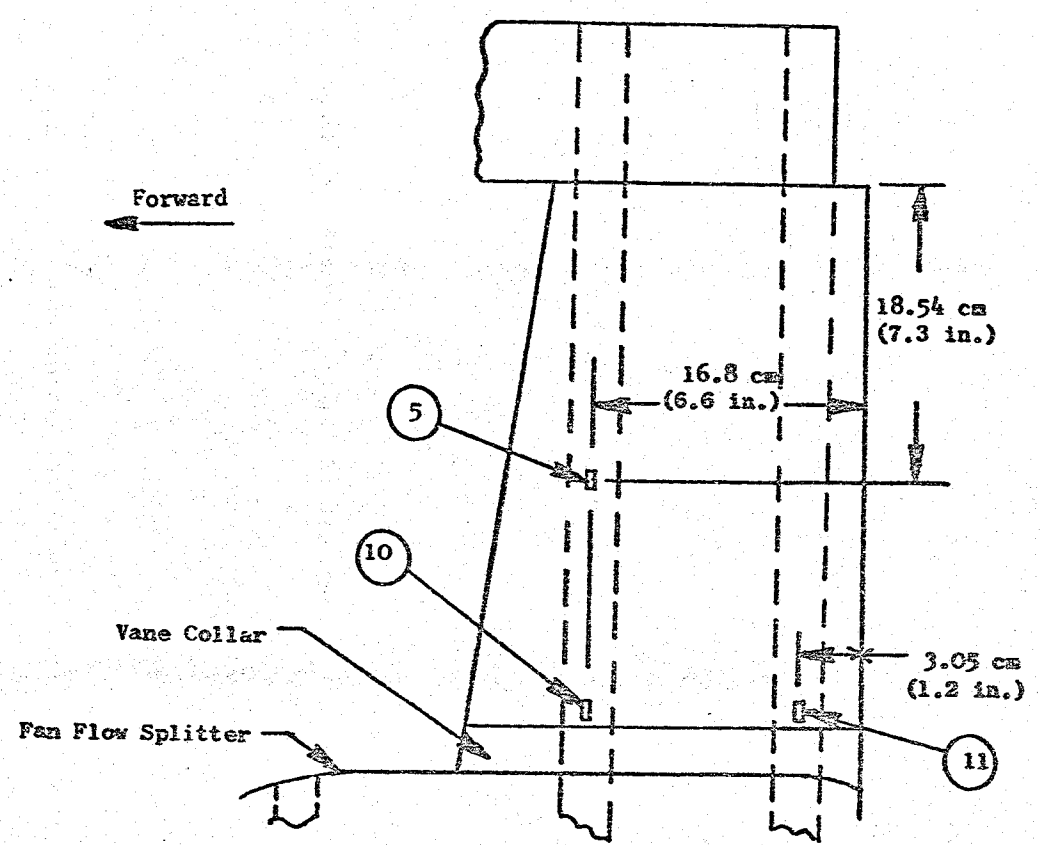

NOTES:

1. All gages are on the concave side of the vane.
2. Gage 5 is on vane 2 (clockwise, aft looking forward)
3. Gages 10 and 11 are on vane 26

Figure 43. Strain Gage Locations for UTW Fan Frame, Bypass Vanes.

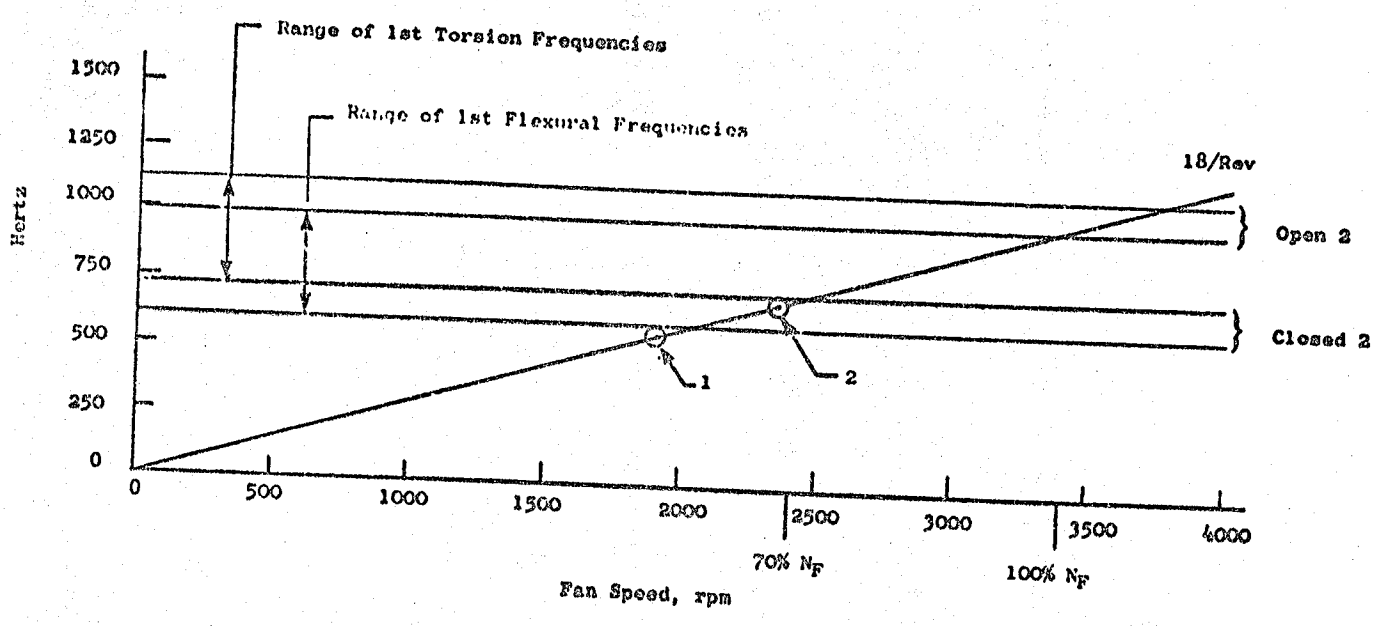

Natural Frequencies for the Closed-2 Vane Were Obtained from Bench Tests.

Natural Frequencies for the Open-2 Vanes Were Extrapolated from Closed-2 Data Analytically.

Results of Engine Tests:

1. Closed-1 Vane First Flex at N_F = 1900 RPM and 570 Hz.
2. Open-2 Vane First Flex at N_F = 2350 RPM and 704 Hz.

Figure 44. Natural Frequencies of QCSEE Bypass Vanes.

grinding away the damaged "boot" and skin only in the 5 cm (2 inches) by 7.6 cm (3 inches) damaged region, and then rebonding an overlap patch on the airfoil panel. After the patch was cured, a new section of fairing "boot" was bonded over the patched region. After curing, the patch and fairing "boot" were ground to form a smooth blend with the original components.

Although no visual damage was detected on any internal pylon hardware, the intersections of all metal-to-composite components were sealed with either Dow Corning DC 94-009 fluorosilicone rubber or Furane 9210 adhesive. After this sealing, the frame was helium-leak checked, and a sump leak was detected in the aft cavity of the 2 o'clock core strut. The cavity was cleaned with MEK and then Furane 9210 adhesive was poured into the cavity. This repair proved effective since the oil consumption dropped dramatically to approximately one quart per hour for the remaining testing.

The next repair occurred after 56 hours 38 minutes of engine running. A portion of the concave airfoil panel on the 8 o'clock bypass vane was ripped from the leading edge aft approximately 3.8 cm (1-1/2 inch). Beyond this point, the top two layers of graphite plies were peeled off the panel for approximately the entire vane. Damage near the vane hub indicated FOD ingestion. The repair was accomplished by removing the outer fairing "boot" and then grinding the entire vane panel until all damaged plies were removed. A new concave bypass vane panel was then bonded over the remaining panel and a new outer fairing bonded at the outer case region. A curved rectangular panel was bonded over the inner edge of the panel and the inner fairing "boot". All bonding was performed with Furane 9210 adhesive. Since the panel used for the repairs had no acoustic holes, the 10 cm (4 inch) by 25 cm (10 inch) acoustic region was permanently plugged. To prevent any further leading edge damage, the leading edges of all remaining bypass vanes were covered with one layer of 7.6 cm (3 inch) wide 181 style fiberglass cloth impregnated with Furane 9210 adhesive. After curing, new 10 cm (4 inch) wide urethane tape was applied over all of the bypass vane leading edges.

The final repairs were performed after 59 hours 1 minute of running. The repair required three new 15 cm (6 inch) by 2.5 cm (1 inch) fiberglass/epoxy patches to be bonded onto the forward side of the second tip-treatment cathedral. The patches were precurved and then bonded with Furane 9210 adhesive.

In summary, no structural problems or unexpected stresses were encountered during engine testing. The vane natural frequencies were somewhat lower than predicted and caused no problems. Several damaged areas were found in the frame during engine operation but these were repaired on the test stand. Damage sustained from foreign object ingestion was minor and easily repairable. Oil leakage from the frame, which had been a problem during Build 1 testing, was effectively sealed by potting the critical areas with Furane adhesive. No oil consumption was reported during the final test runs.

14.0 COMPOSITE NACELLE

Figure 45 shows the nacelle components installed on the UTW engine on the test stand.

14.1 INLET

The composite inlet is a honeycomb sandwich structure with Kevlar 49/epoxy face sheets and aluminum core. Mounting to the fan frame is provided by means of quick disconnect rotary latches. The overall length is 184.07 cm (72.47 inches) and the outside diameter is 200.15 cm (78.8 inches). A cross section through the inlet is shown in Figure 46.

Instrumentation consisted of 40 wall static pressure pickups, pressure indicators for the digital control, plus provisions for mounting a pitot static pickup, an inlet temperature sensor, six inlet/distortion rakes, a boundary layer rake, a cobra traversing probe, and four wall Kulites. Supporting provisions were also made for the slip ring strut. As static testing inlet loadings are very low, no strain gages were installed.

When the inlet was first mounted on the fan frame, it was discovered that the inner flowpath at the fan frame interface was under size by approximately 0.635 cm (0.25 inch) on the radius. This was corrected by filling the last 15.24 cm (6.0 inches) of the inlet honeycomb with microballoon filled epoxy, machining a straight taper from the existing contour to the correct exit diameter, and covering this repair with a 4 ply, 181 figerglass/epoxy lamination. This resulted in the loss of approximately 0.84 square meters (9 square feet) of acoustical suppression area.

It was also discovered that there were some unbonded areas in the inner panel axial splice joints. These were repaired by injecting room temperature curine EA 901/81 epoxy adhesive into the bondline. No further problems were encountered with the inlet during testing and posttest inspection did not uncover any indications of damage or delamination.

14.2 CORE COWL

The core cowl consists of two semicircular honeycomb sandwich doors made of fiberglass/polyimide cores faced with T300 graphite/polyimide (PMR) skins. The cowl is 181.83 cm (71.59 inches) long and the maximum outside diameter is 112.42 cm (44.26 inches). Instrumentation consisted of four static wall taps, 16 inner skin surface thermocouples, and 12 core cowl cavity air thermocouples. To assure that no overheating of the cowl would occur during static engine testing, a stainless steel foil covered Min-K insulation blanket was

Figure 45. Nacelle Components Installed on the UTW Engine.

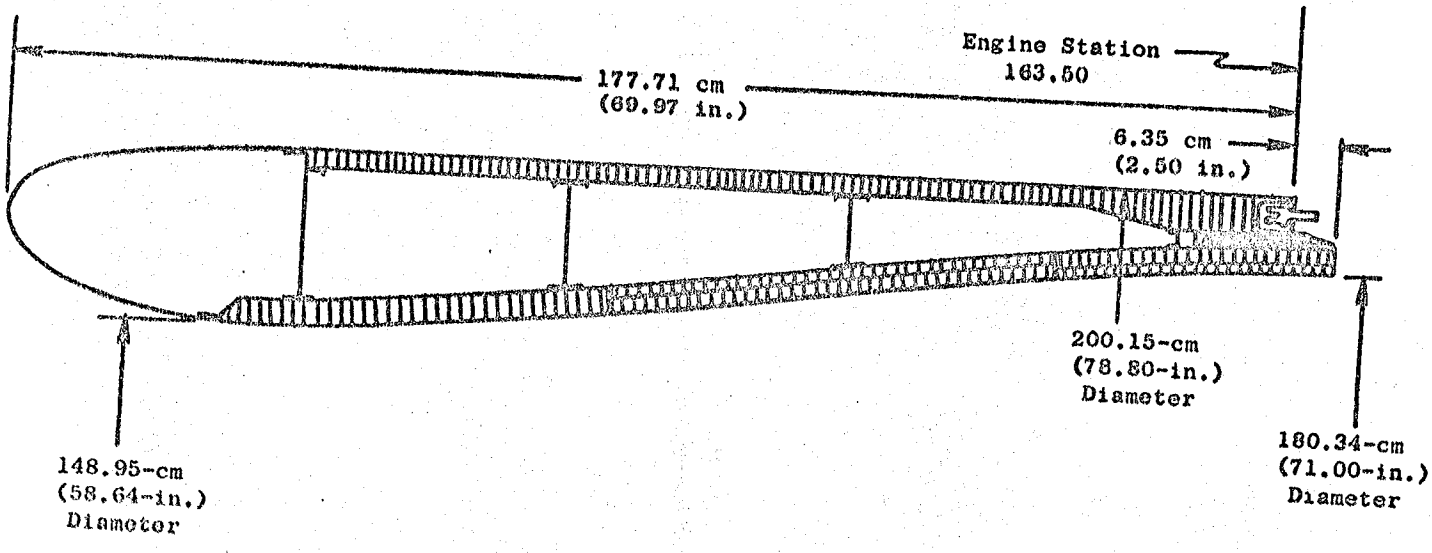

Figure 46. QCSEE Inlet Axial Cross Section.

incorporated over the last 82 cm (32.3 inches) of the inner skin surface, this blanket being held approximately 0.635 cm (0.25 inch) off the skin surface by standoff blocks. In addition to the fan cooling air, shop air was directed between the blanket and the cowl inner skin during engine testing. The cooling system operated satisfactorily with the maximum recorded temperature reading 232.2° C (450° F) on the steel aft ring which was not insulation blanket covered and 133.9° C (273° F) on the cowl inner skin. No damage or delamination was observed during test or posttest inspections. A view of the inner wall of the core cowl with the insulation blanket installed is shown in Figure 47.

14.3 FAN EXHAUST DUCT OUTER COWL

The fan exhaust duct outer cowl is composed of two semicircular honeycomb sandwich doors hinged to the pylon and latched together along the bottom centerline. The construction is a full depth aluminum honeycomb with a Kevlar/epoxy outer face sheet and a porous graphite/epoxy inner face sheet to provide acoustic treatment. Three fan nozzle actuators are mounted in cavities in each door, these actuators being covered by streamlined fiberglass/epoxy fairings. Provisions for mounting the variable fan nozzle flaps were provided in the graphite/epoxy fan duct aft ring. The fan duct is 124.3 cm (48.92 inches) long and the outside diameter is 200.2 cm (78.8 inches). Figure 48 shows a cross section through the outer cowl at an actuator installation; while Figure 49 is a view of the completed cowling prior to installation on the test stand.

The fan duct outer cowl instrumentation consisted of 12 inner flow surface static pressure taps, along with provisions for mounting four wall Kulites, one traversing total pressure/total temperature probe, two traversing dynamic pressure probes, and four strain gages which were applied to the outer skin in the vicinity of the lower left-hand nozzle flap hinge. Highest observed skin stresses during static engine testing were less than 13.79 MPa (2000 psi) versus the allowable of 314.40 MPa (45,600 psi).

During the engine installation, a large facility fuel fitting was inadvertently dropped on the right-hand cowl causing a half-moon shaped gash, approximately 6.35 cm (2.5 inches) long, through the outer skin. A section of the skin approximately 3.8 cm (1.5 inch) by 7.6 cm (3.0 inches) surrounding this area was removed and replaced with three plies of 181 fiberglass using EA 901/B1 room temperature curing adhesive. In addition, during the testing period, a delamination of the outer skin in the left-hand door consisting of an area approximately 6.4 cm (2.5 inches) by 14.0 cm (5.5 inches) and located about 25.4 cm (10 inches) from the aft end and 5.1 cm (2 inches) above the lower actuator cavity was repaired by injecting Furane 9210 adhesive into the delaminated area through a series of holes drilled in the skin. No further damage or delaminations were suffered during the balance of the testing either in the repaired area or the rest of the cowling.

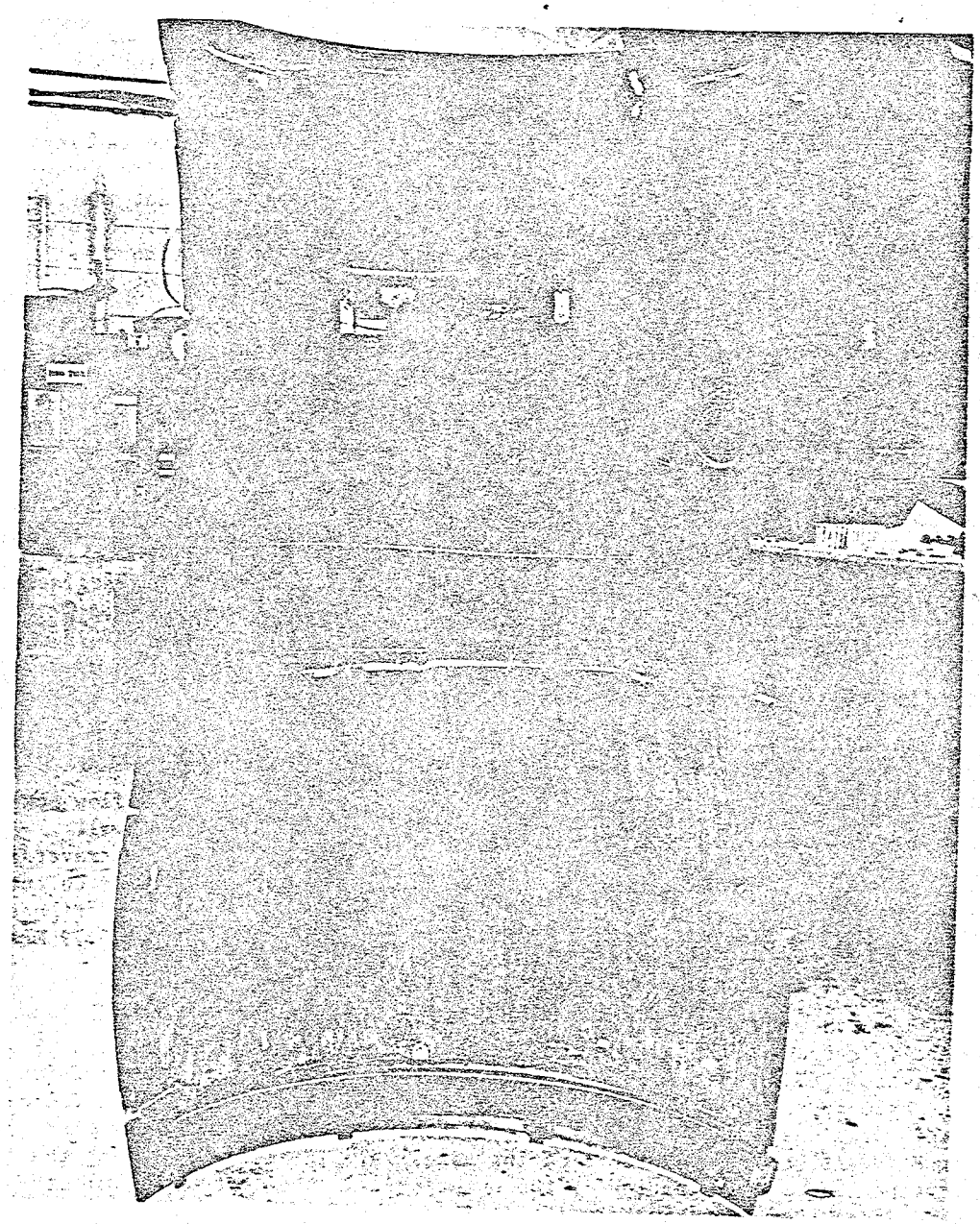

Figure 47. Core Cowl Door Inner Surface.

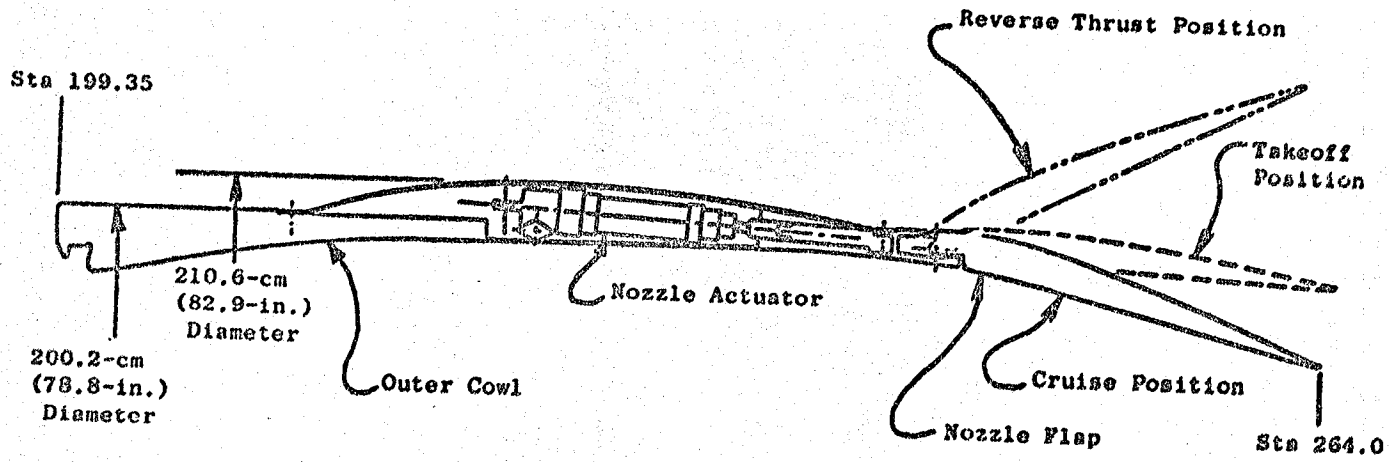

Figure 48. Outer Cowl Cross Section.

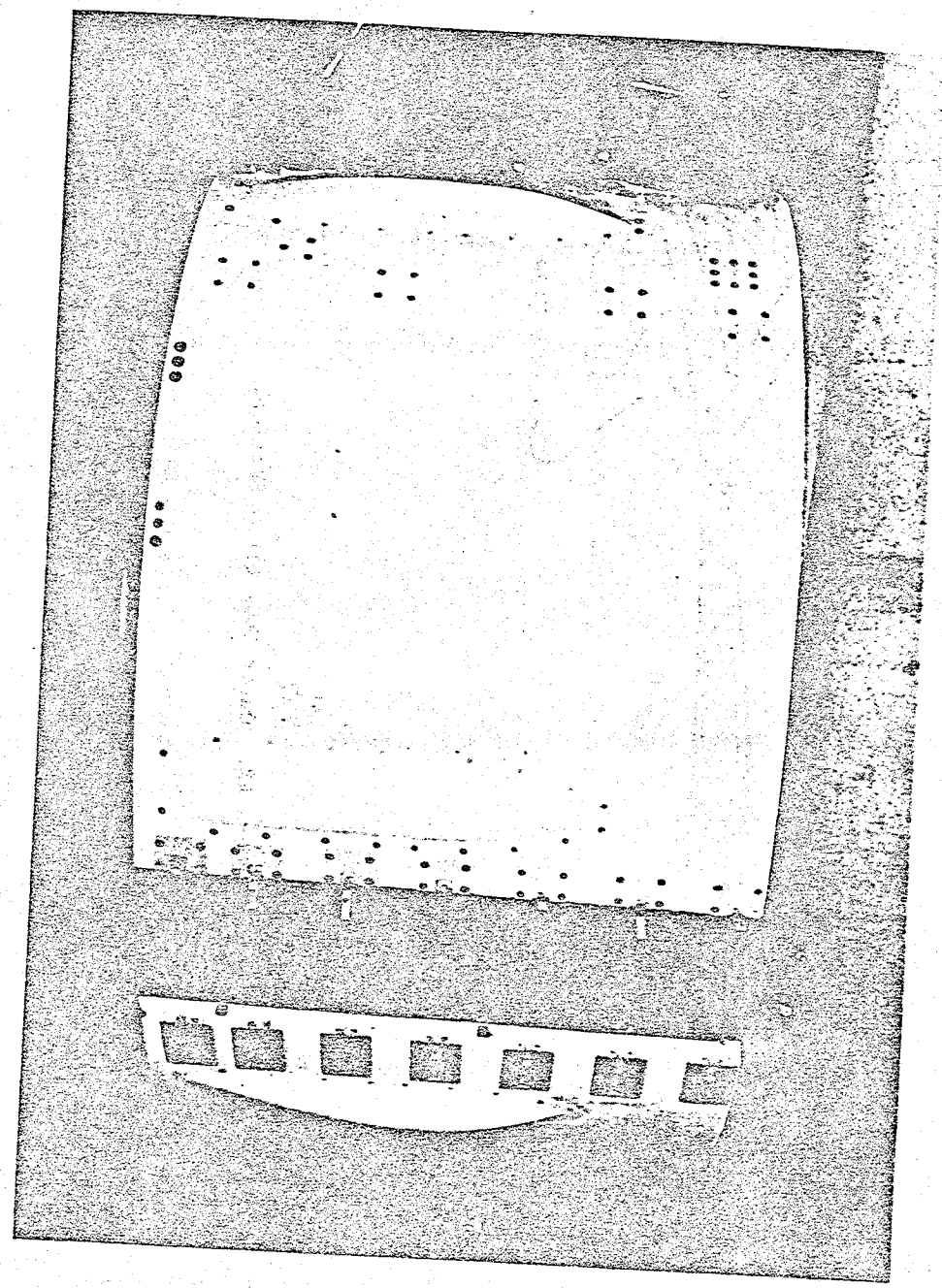

Figure 49. Core Cowl Before Installation on Test Stand.

14.4 FAN EXHAUST NOZZLE

The fan exhaust nozzle consists of four fully modulating variable flaps capable of providing various areas for forward thrust and also of flaring outwards to provide increased area for inlet flow to the variable-pitch fan in the reverse mode of operation. Each flap is 44.96 cm (17.7 inches) in axial length from its hinge centerline to its trailing edge. The upper flaps are 83.7° wide and the lower flaps are 84.5° wide. The flaps are attached to the aft ring of the fan duct by means of hinges, each flap having a pair of hinges 30.5 cm (12 inches) apart at the flap centerline along the flap forward closeout. The flaps are connected to the actuation system in the outer fan cowl by links and link clevises located outboard of each hinge. Figure 50 shows the nozzle schematically. Located along the axial edges of each flap are seal assemblies which were designed to give full sealing up to a nozzle area of 1.678 m^2 (2600 $in.^2$). From this point to the full-reverse flap position, the seals disengaged. Figure 51 shows link installation and seal positions at various nozzle openings. The flaps are of a full depth aluminum honeycomb construction with Kevlar/epoxy outer skins and perforated graphite/epoxy inner skins.

The actuation links of the lower left-hand flap were instrumented with strain gages, while the flap inself had a series of dynamic and static pressure taps and accelerometer installed.

No problems were encountered with the fan nozzle during any of the forward or reverse thrust testing. Posttest inspection did not reveal any damage or delaminations. Highest observed link stress was less than 34.47 MPa (5000 psi) versus an allowable of 289.58 MPa (42,000 psi).

During installation and checkout of the nacelle for the final acoustic testing, it was noted that the fan nozzle flaps on the right-hand door were out of phase with those on the left-hand door by approximately 0.64 cm (0.25 inch) in the radial direction. A check revealed that the actuation system on the left-hand door was not achieving full required actuator stroke indicating that the actuator stops were incorrectly rigged. Resetting the actuator stops would have entailed removal of the actuators from the installation and resetting of the stops on the bench with its attendent several days loss of testing time. As the flaps could be rerigged so that only the reverse thrust nozzle area was affected, and as no reverse thrust mode testing was planned, the flaps were rerigged to the required forward thrust areas and the actuator stops were left as is. It was also noticed during this fan nozzle calibration, that the upper left-hand flap, to which the feedback actuator is attached, oscillated in a slow, continuous rate with the amount of excursion increasing as the actuation system pressure was increased. This would explain the variations in nozzle area observed during testing. No problems were encountered during the final testing phase.

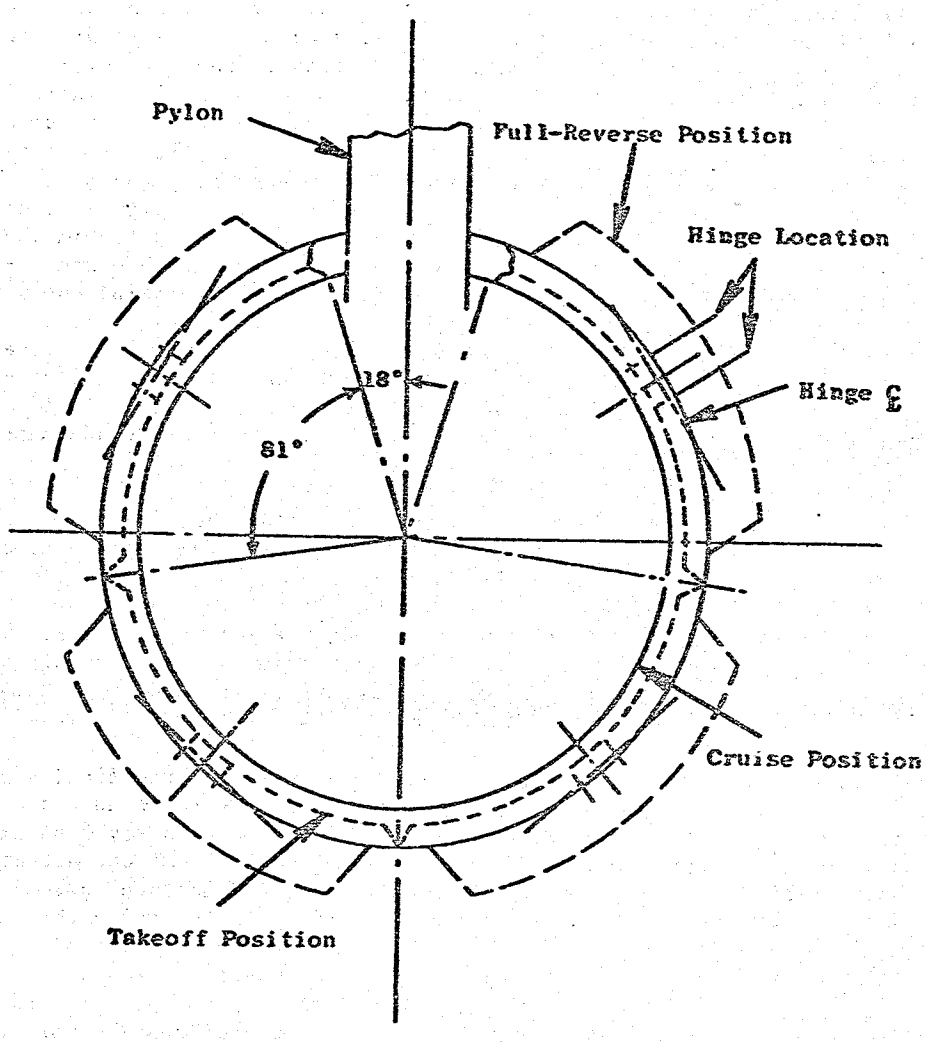

Figure 50. Flare Nozzle Flap Schematic.

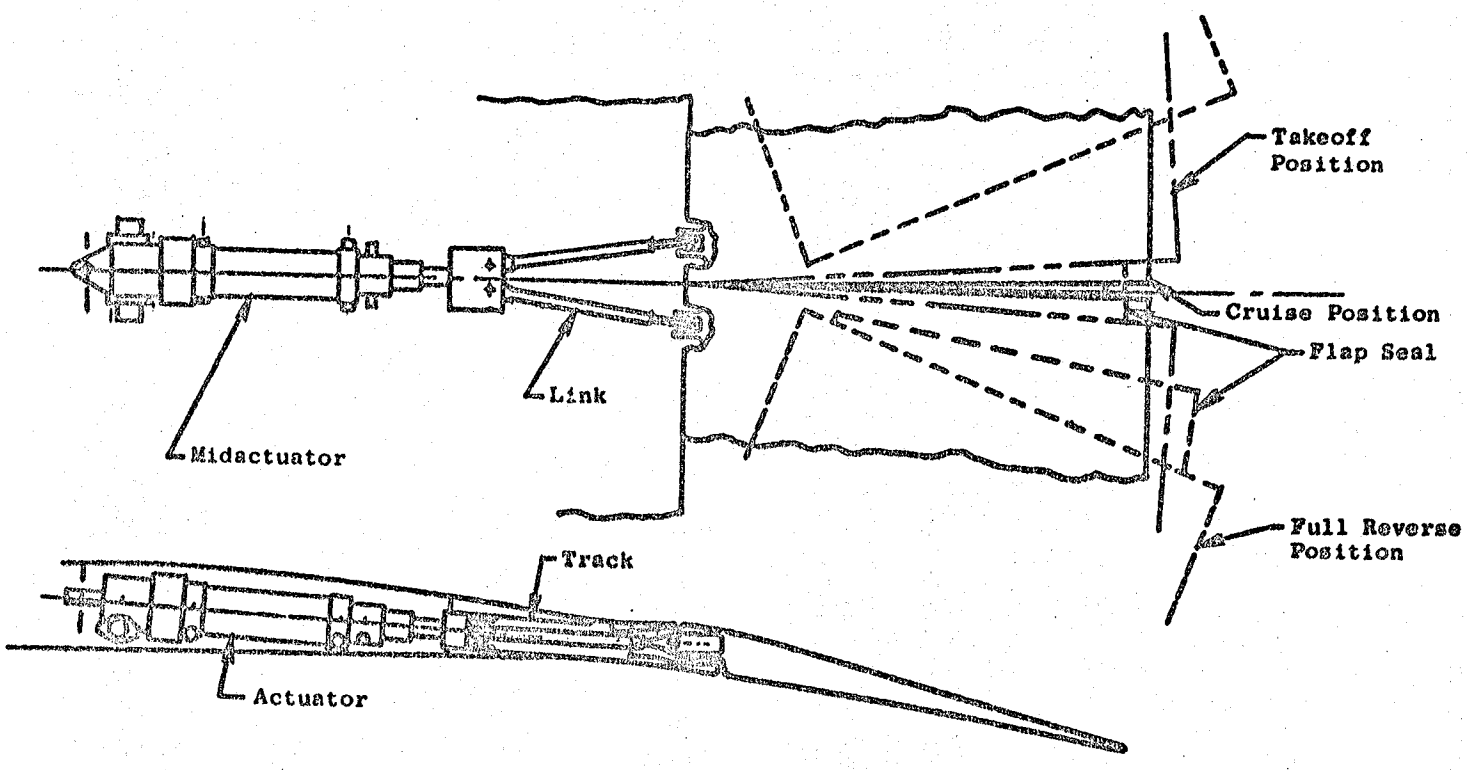

Figure 51. Variable Flap Nozzle.

15.0 DIGITAL CONTROL SYSTEM

15.1 CONTROL SYSTEM DESCRIPTION AND TEST SUMMARY

Buildup No. 2 of the UTW engine included a system which controlled four engine variables: fuel flow, compressor variable stator position, fan pitch angle, and fan nozzle area. Figure 52 is a schematic of this system.

The key QCSEE control system elements are an engine-mounted digital electronic control, designed specifically for the QCSEE, and a modified F101 hydromechanical control. The digital control provides primary control of fuel flow by controlling an electrohydraulic servovalve which serves as the primary input to the fuel metering section of the hydromechanical control. The fuel-operated servomechanisms in the hydromechanical control serve primarily as back-up controlling elements and limits, although they are the primary controlling elements for the compressor variable stator actuators.

The hydromechanical control is mounted on an F101 fuel pump which is a centrifugally boosted, positive displacement, vane pump. Pump discharge flow is delivered to the control through the mounting interface and the control returns excess fuel to the vane element inlet through a similar channel.

The fuel system includes an eductor to evacuate interstage seal cavities with fuel-handling components and thus reduce the possibility of external fuel leakage.

Fan pitch angle and fan exhaust nozzle area are both controlled solely by the digital electronic control which furnishes electrical signals to electrohydraulic servovalves in the servovalve assembly. These servovalves directed hydraulic fluid to the hydraulic motor which positions the fan pitch mechanism and to the six hydraulic rams which position the variable fan exhaust nozzle in response to the signals from the digital control.

The hydraulic system which supplies the pitch and nozzle servovalve assembly consists of an engine-driven, variable displacement, constant pressure piston pump, a filter, and the servovalves. The system is essentially a closed circuit with only a small fluid interchange with the engine lubrication system for cooling and to transiently account for differential actuation areas.

In order to achieve operational flexibility, the input commands to the digital electronic control are introduced through the control room elements shown on Figure 53. The interconnect unit, operator panel, and engineering panel are actually peripheral elements of the digital control. They provide the means for the engine operators to introduce commands, switch between available operating modes, adjust various control constants, and monitor control and engine data. The transmission of data in both directions between the control room and the digital control is done by means of multiplexed

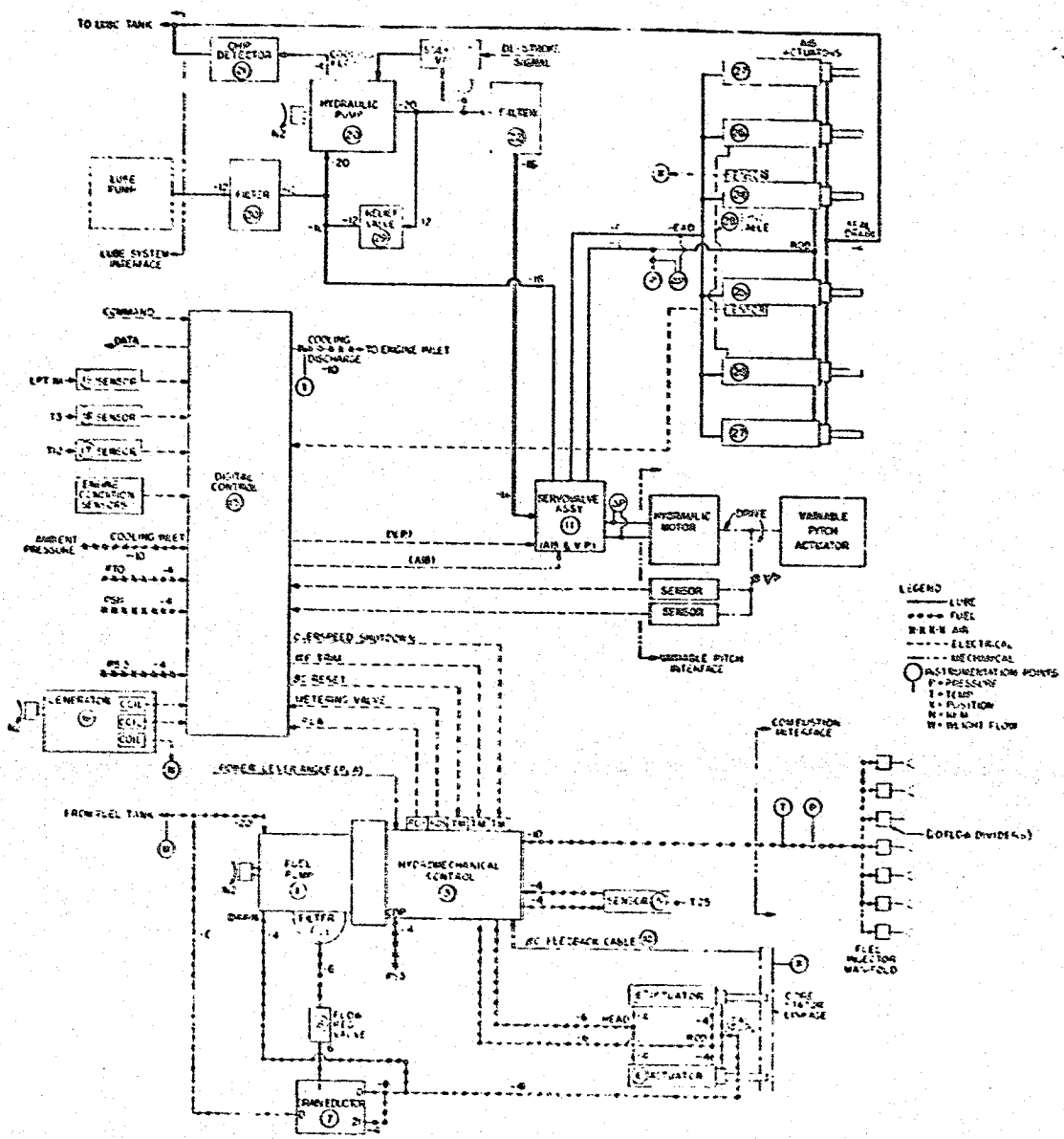

Figure 52. System Interconnection Schematic.

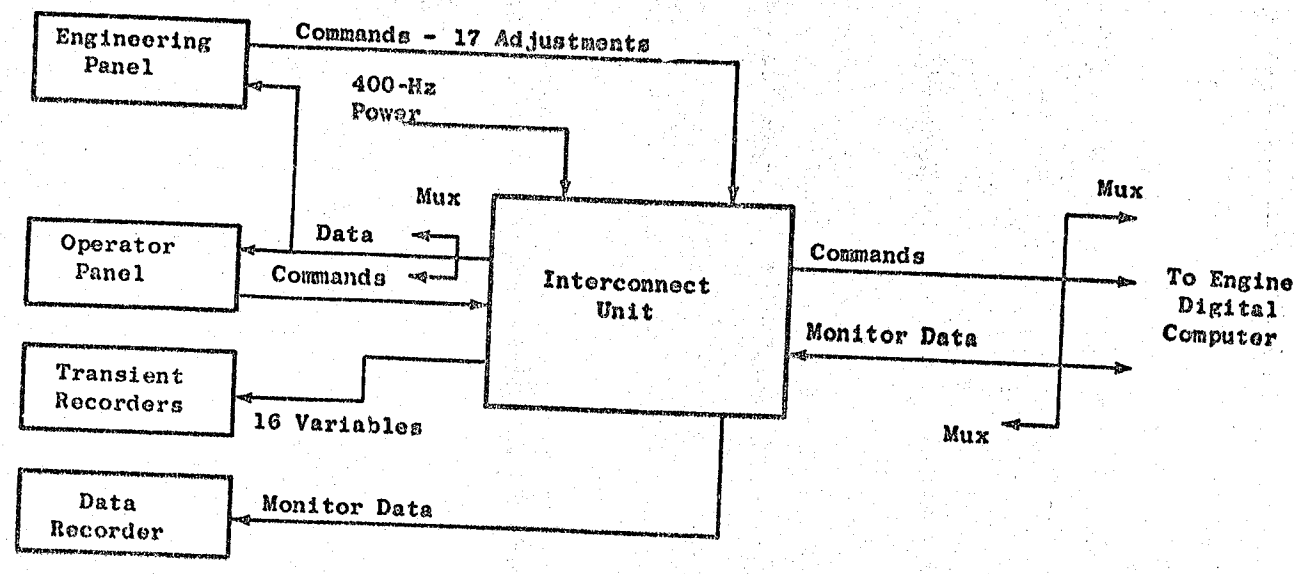

Figure 53. Control Room Elements of QCSEE Digital Control.

digital electronic signals. This data cable was approximately 274 meters (900 feet) long in the QCSEE installation in the Peebles test facility.

In addition to digital commands from the control room, the system also receives a mechanical input in the form of a power lever angle (PLA) transmitted to the hydromechanical control. This serves as an input to the back-up governor and operates a positive fuel shutoff valve in the control.

The QCSEE control system has several different modes of operation, a manual mode designed to accommodate experimental mapping of engine characteristics, an automatic mode providing integrated operation of engine variables, and several partially automatic modes which allow a continuous and orderly approach to fully automatic operation. A majority of engine testing was done in the manual control mode but satisfactory operation was demonstrated and data were accumulted in the automatic pressure ratio control mode, the automatic inlet Mach number control mode, and the fully automatic control mode. These are discussed below along with other aspects of control system operation during testing.

15.2 CONTROL DURING ENGINE STARTS

Engine starts were generally satisfactory throughout the test program with the hydromechanical control scheduling fuel flow and compressor stators to bring the engine smoothly to idle speed without stall or overtemperature. A typical start is shown on the data traces of Figure 54. As the traces indicate, fan pitch is closed and the fan nozzle is open during the start until the core-engine-driven control alternator develops sufficient voltage to produce proper digital control operation. This occurs at approximately 20 percent speed, 2900 rpm, as indicated by the initiation of digital control data signals such as PS3/PTO on the trace. This off-schedule pitch angle and nozzle area at the low end of the start region caused no operational problems.

15.3 MANUAL FAN SPEED CONTROL

Much of the testing was done in the full manual mode. In this mode, the control system modulates fuel flow to set fan speed in accordance with a potentiometer lever on the operator control panel in the control room except as limited by fuel schedule, temperature, overspeed, or minimum idle speed limits. With the fan speed lever, it was possible to set fan speed at the exact level desired and the control maintained that speed within ±5 rpm regardless of the fan pitch or nozzle area. Figure 55 shows engine data plotted on the manual fan speed schedule.

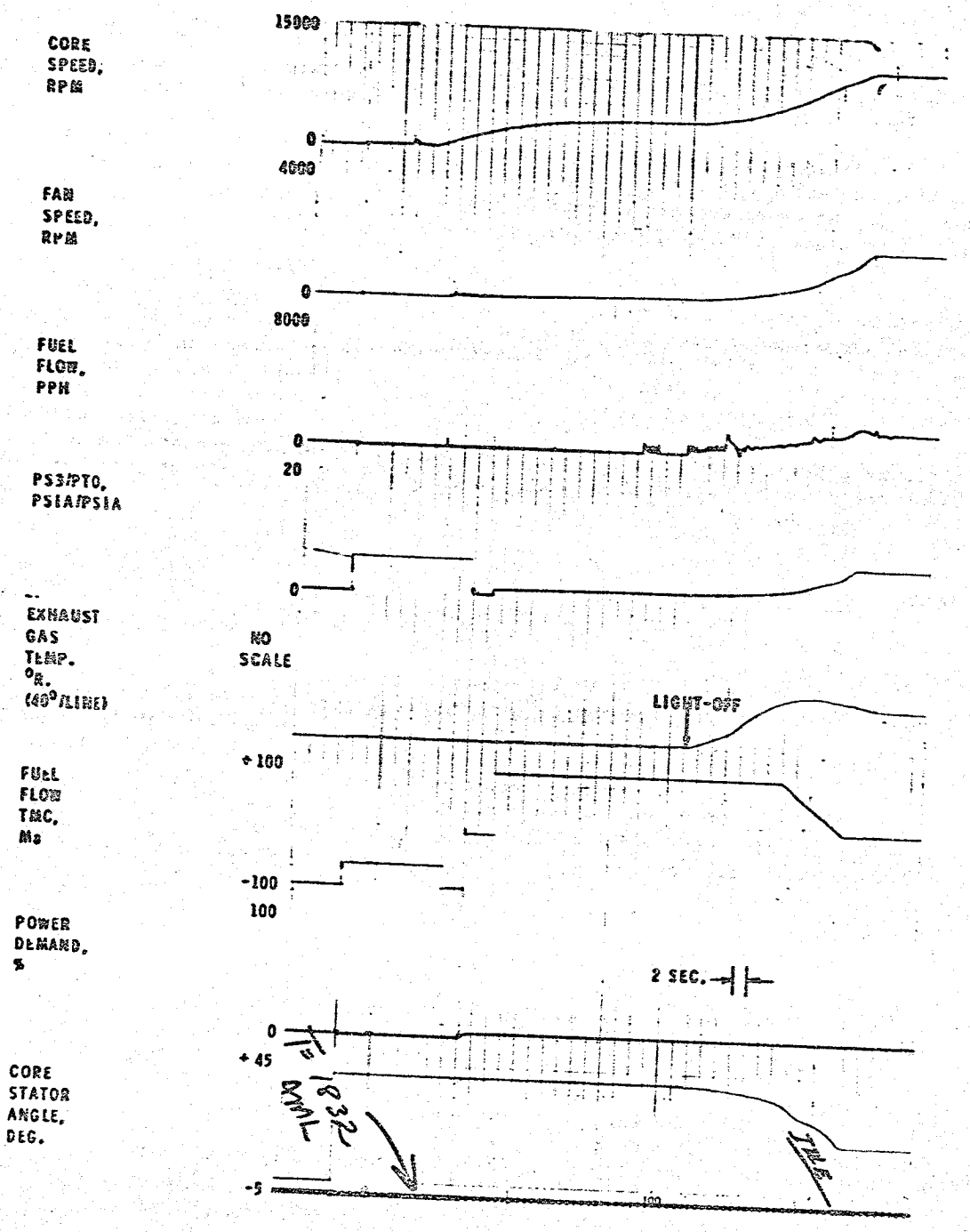

Figure 54(a). Typical Start.

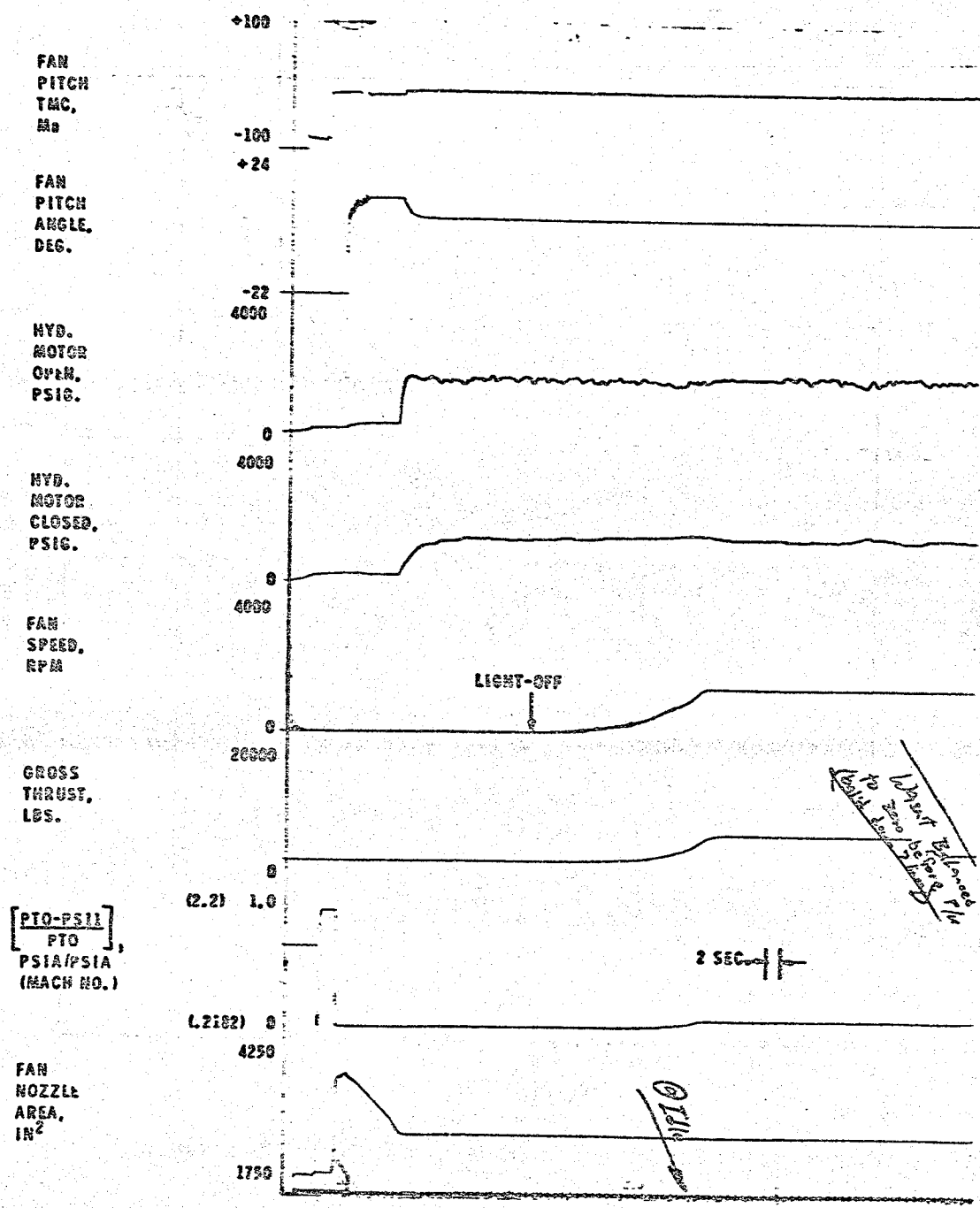

Figure 54(b). Typical Start.

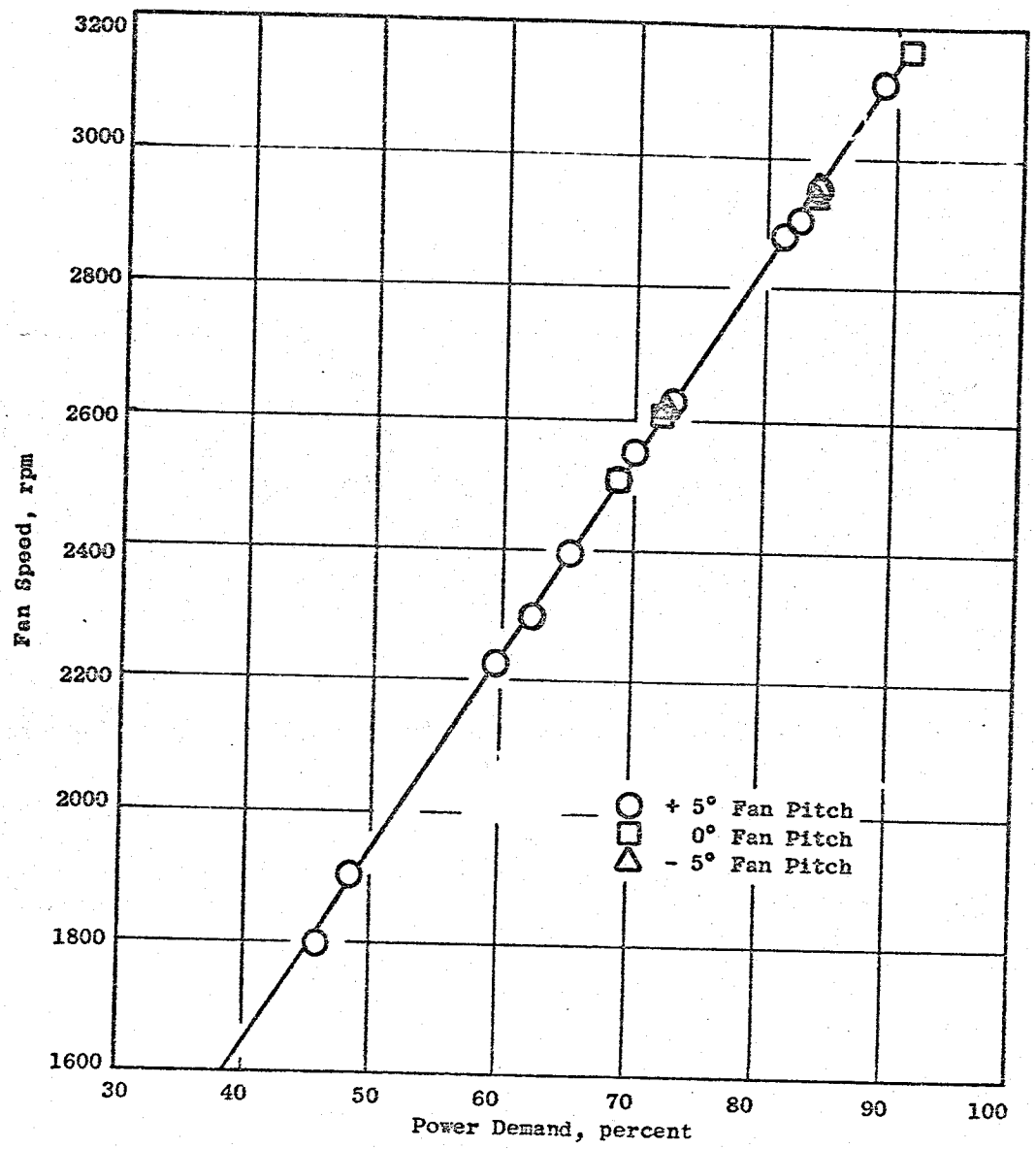

Figure 55. Fan Speed Versus Power Demand, QCSEE UTW 507-001/2.

15.4 MANUAL FAN PITCH CONTROL

In the manual control mode, fan pitch is positioned by the digital control in response to a rotary potentiometer on the operator control panel. With this control loop, it was possible to set fan pitch to any desired setting with a resolution of 0.1° and the pitch remained within 0.4° of this setting as engine speed and nozzle area were varied over a wide range. Stability of this control loop also proved to be excellent. Figure 58(b) is a data trace showing a fan pitch change using the manual control potentiometer.

Data from engine testing with fan pitch manually controlled revealed hysteresis in the pitch acutation mechanism. Figure 56 shows data from a run in which fan pitch was moved in increments in both directions between +10° and -10° at two different fan speeds with the fan nozzle constant. At any particular thrust level, if corrected fan speed, nozzle area, and ambient conditions are constant, then actual fan pitch must also be constant. Thus the spread in indicated pitch (measured at the input to the actuation mechanism) at constant thrust and corrected speed on Figure 56 indicates hysteresis in the actuation mechanism between the position transducers and the fan blades. To compensate for this, pitch settings were approached from the closed direction and calibration data were taken in the same way. The source of the hysteresis has not been identified.

15.5 MANUAL FAN NOZZLE CONTROL

Manual control of the fan nozzle on the UTW engine is accomplished in the same manner as manual fan pitch control in that fan nozzle area is positioned by the digital control in response to a rotary potentiometer on the operator control panel.

This potentiometer signal was converted to a digital signal and transmitted to the engine digital control. During engine test, this control loop proved to be accurate and stable with the nozzle in the forward thrust region; but near the reverse position (divergent flaps), some instability was encountered. Figure 59(b) shows a manual nozzle area change in the forward thrust region. The change is smooth and operation before and after the change was stable. It was possible to set the nozzle with a resolution of 6 sq cm (1 $in.^2$) and it would remain within 26 sq cm (4 $in.^2$) of that setting as speed and pitch were varied over a wide range.

During engine operation in the reverse thrust configuration, with the nozzle under manual control, nozzle oscillations were encountered. Typically the peak-to-peak mangitude of the oscillations was ±480 sq cm (± 75 $in.^2$) and the frequency approximately 8.3 Hertz. The reason for this oscillation at the reverse position has not been identified. One possible factor is the reverse flow of air past the flaps but this cannot be the sole cause of the problem because an intermittent, small oscillation at the full open position

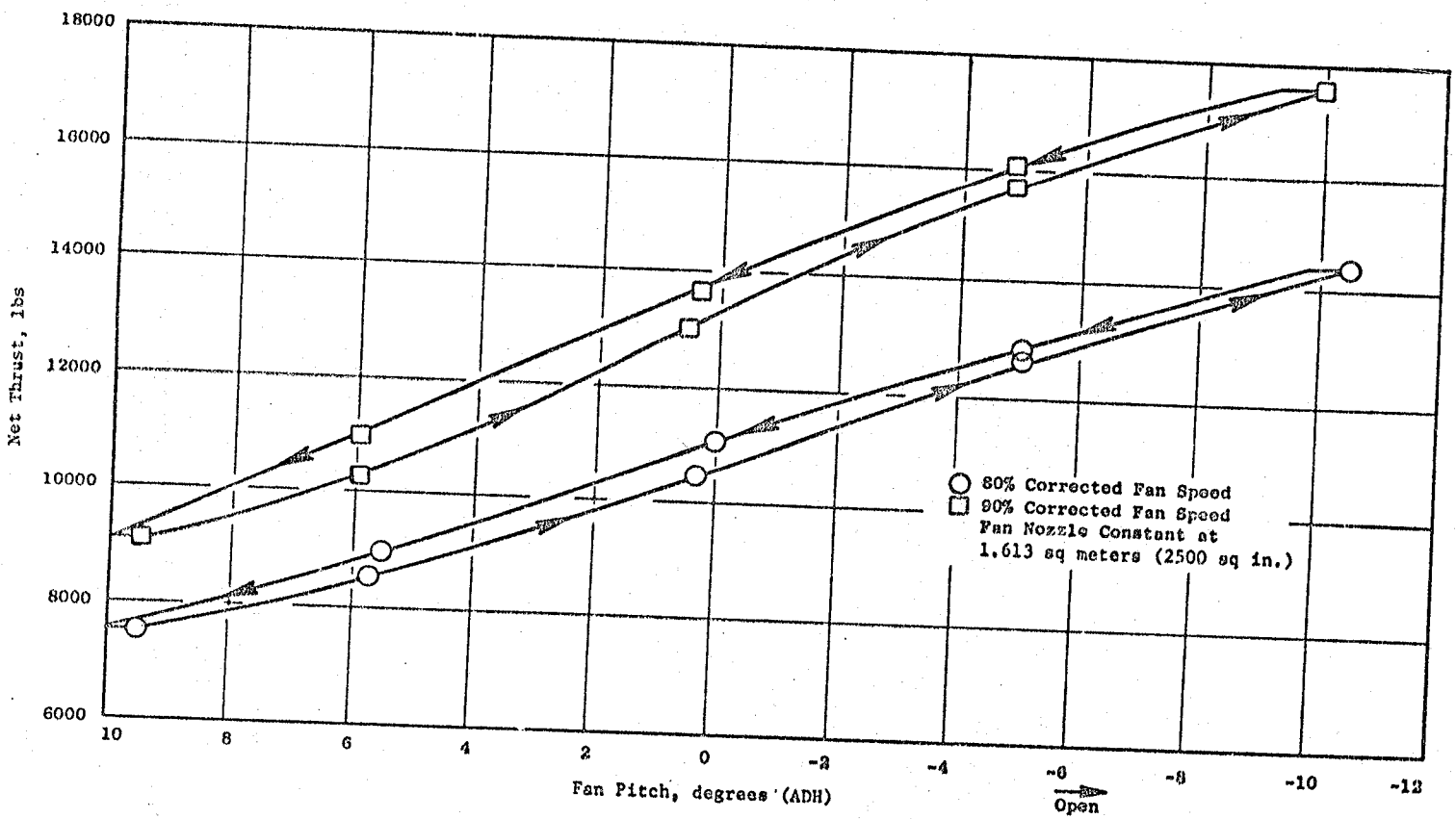

Figure 56. Fan Pitch Hysteresis Check, QCSEE UTW 507-001/2.

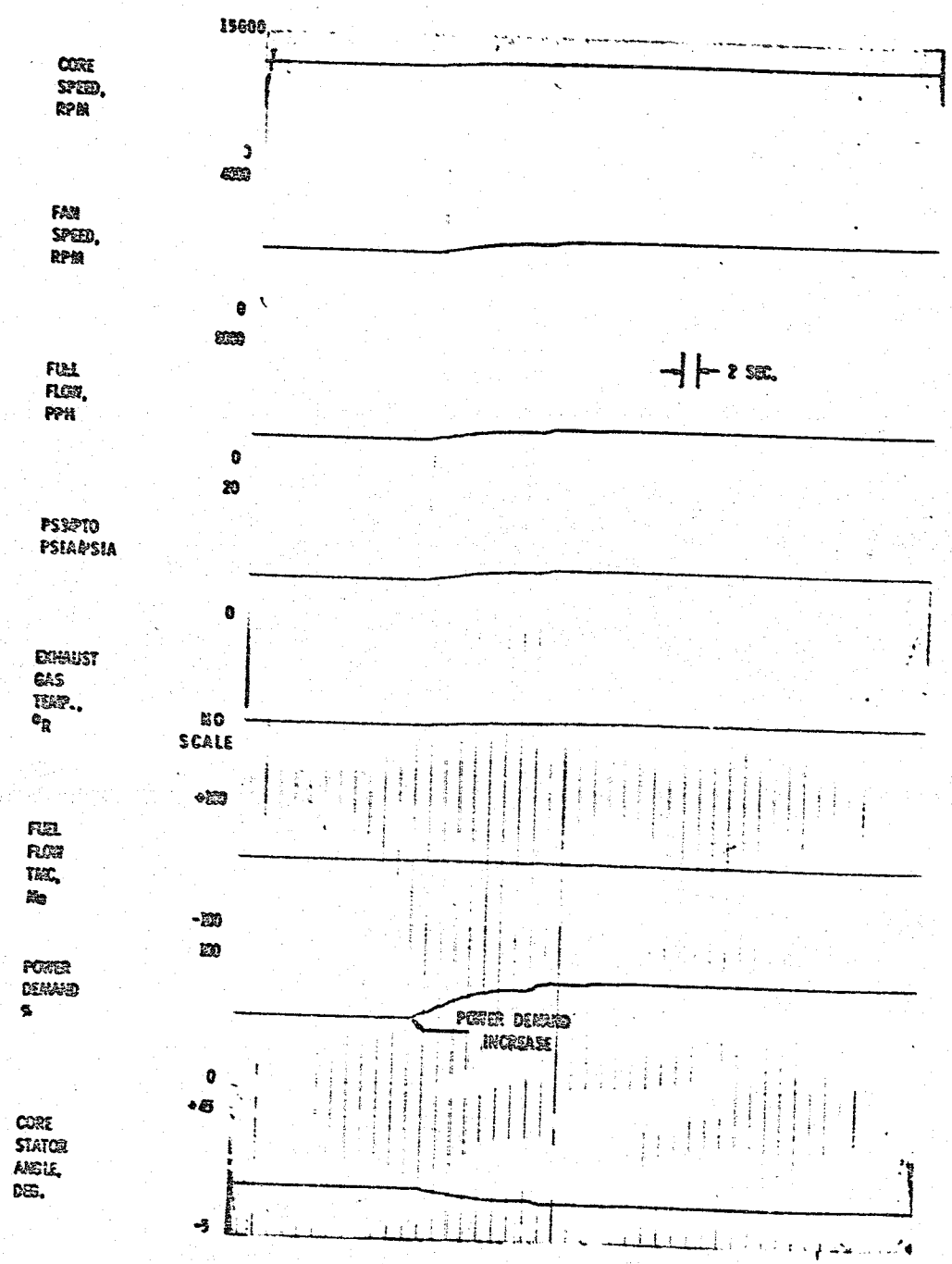

Figure 57(a). Pressure Ratio Control Mode, Power Demand Change.

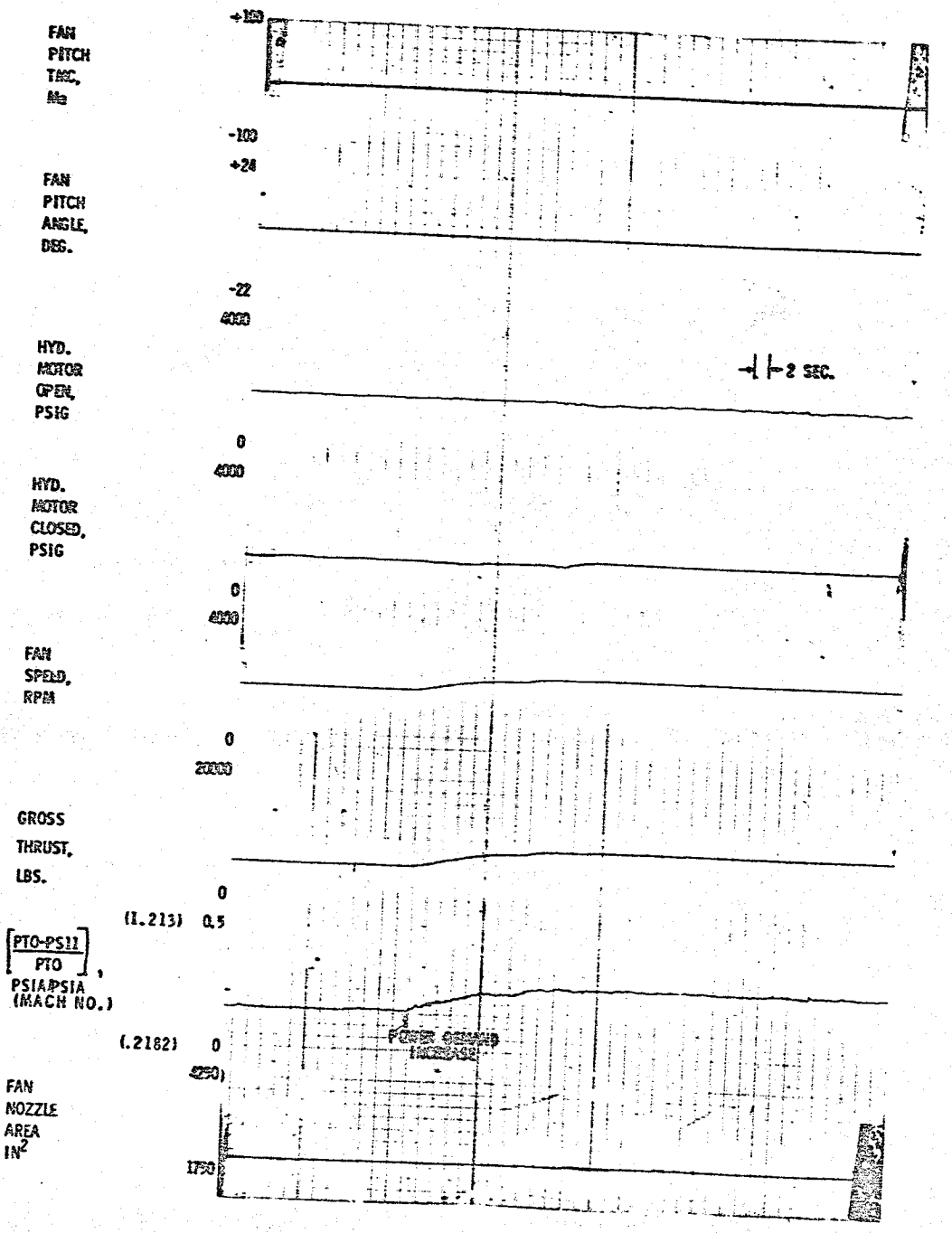

Figure 57(b). Pressure Ratio Control Mode, Power Demand Change.

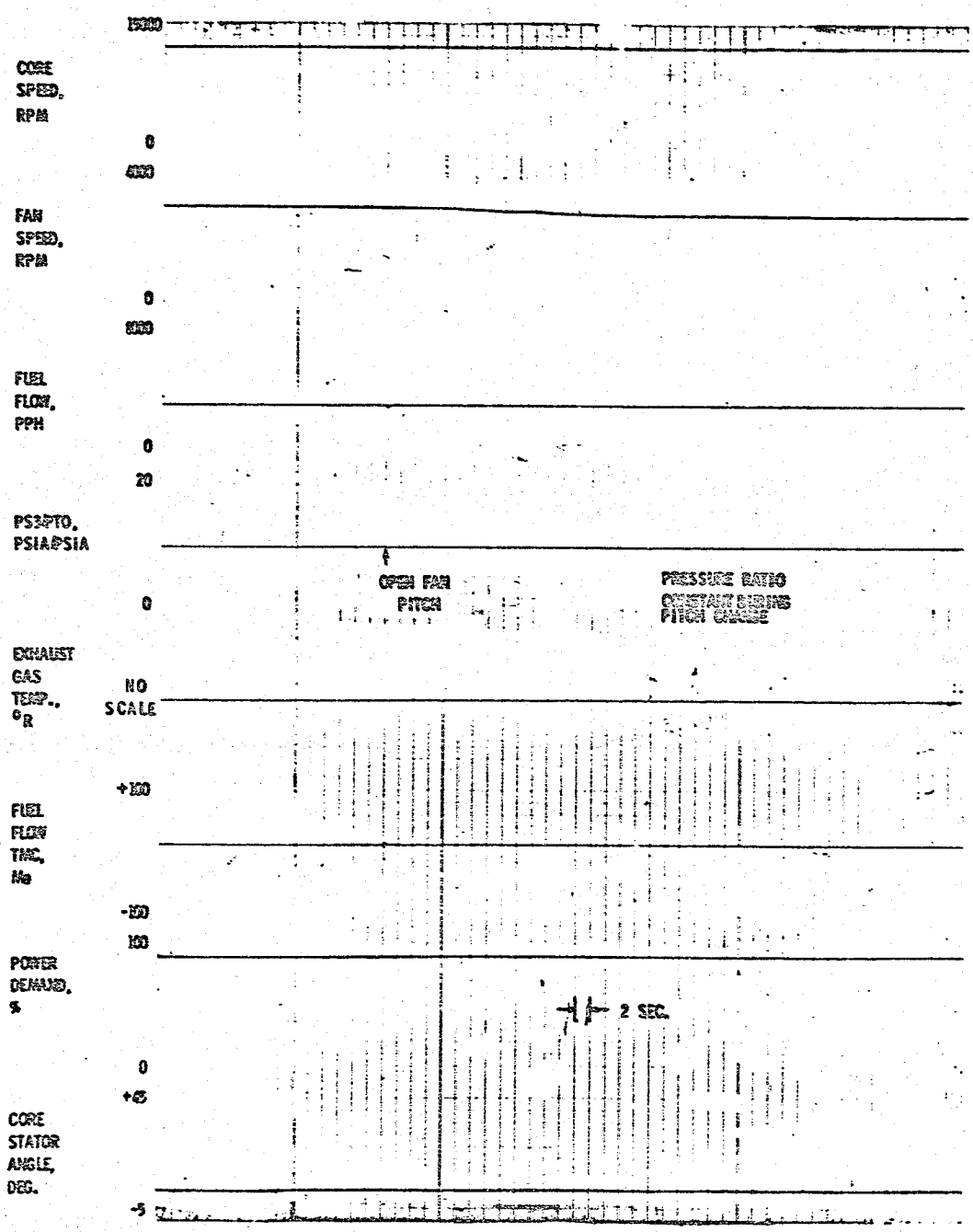

Figure 58(a). Pressure Ratio Control Mode, Fan Pitch Angle Change.

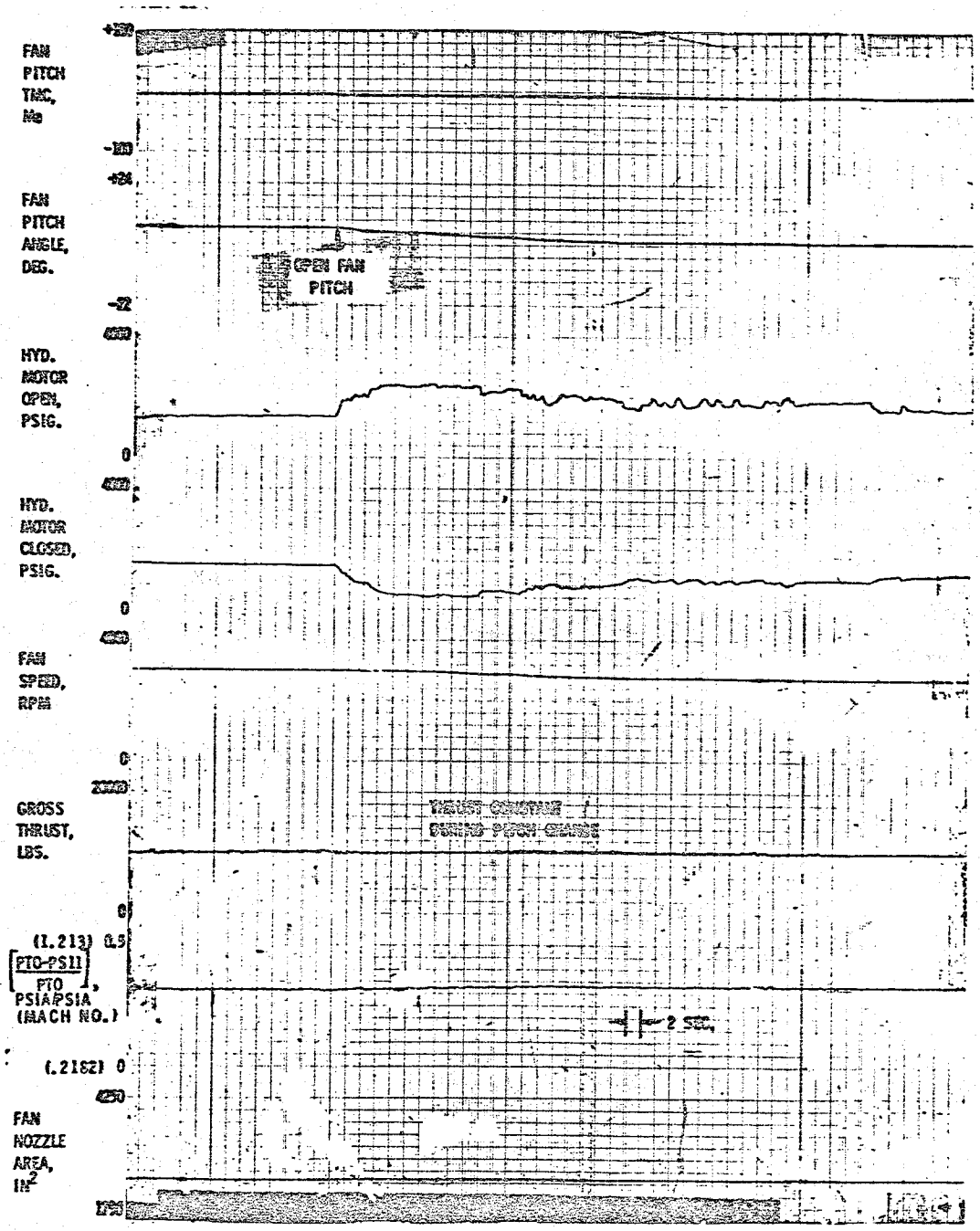

Figure 58(b). Pressure Ratio Control Mode, Fan Pitch Angle Change.

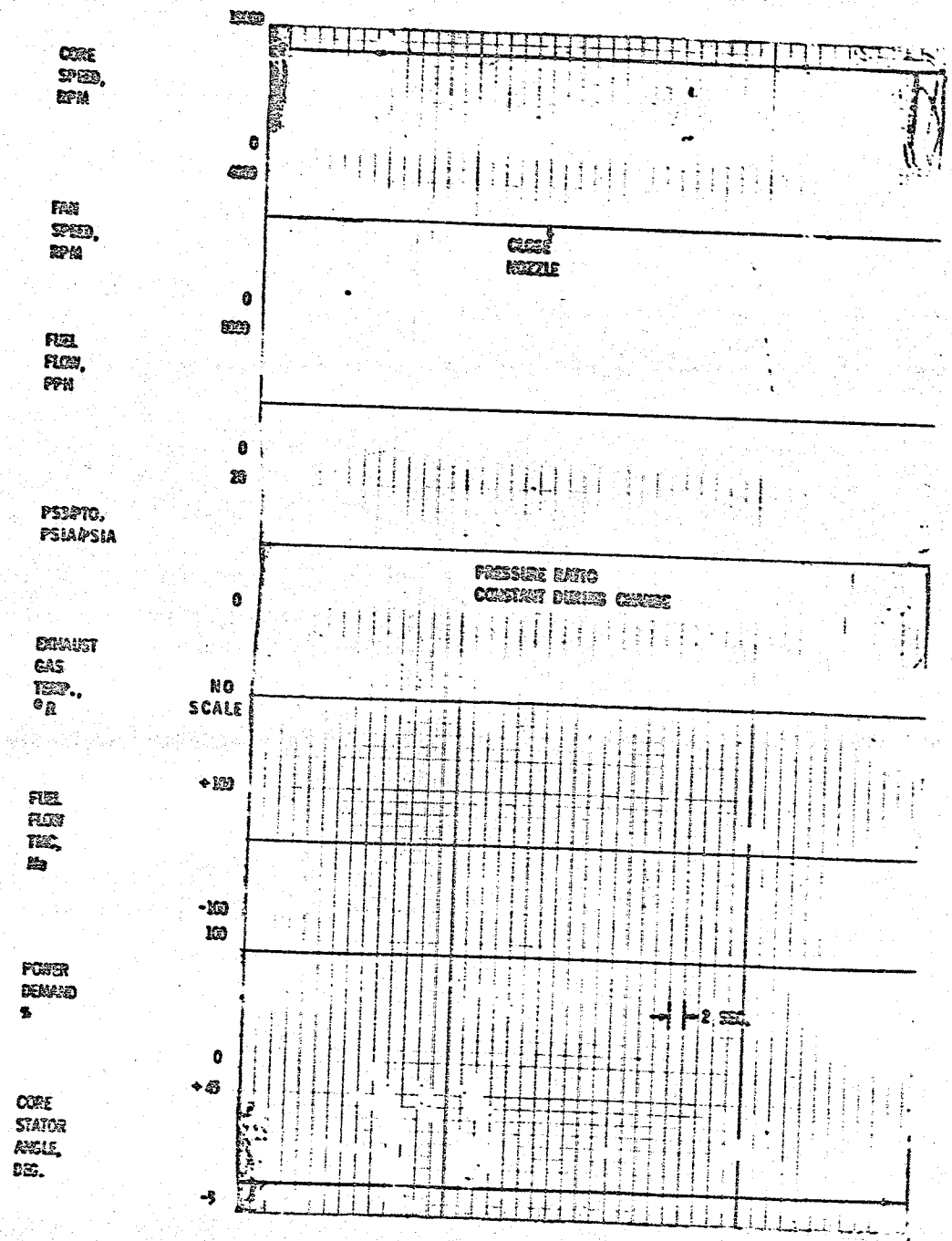

Figure 59(a). Pressure Ratio Control Mode, Fan Nozzle Area Change.

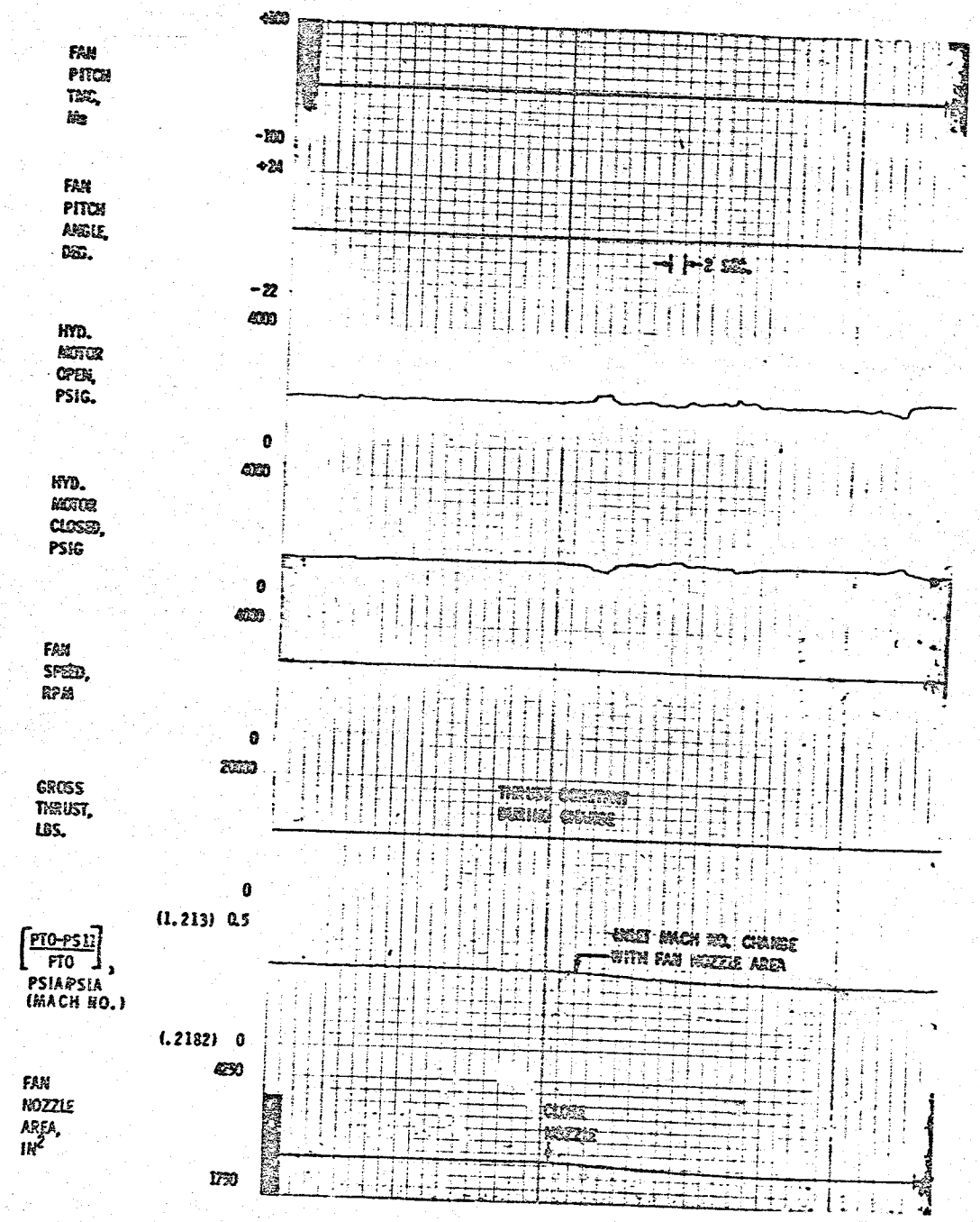

Figure 59(b). Pressure Ratio Control Mode, Fan Nozzle Area Change.

was noted when the nozzle system was being calibrated with the engine shutdown. A simple correction for the problem would be to schedule the nozzle so that the actuator pistons bottom out in the reverse thrust mode.

15.6 AUTOMATIC CONTROL MODE OPERATION

In the automatic control mode, control of the manipulated variables is integrated so that the engine is contrtolled by a single power demand input. In this mode, the control system basically manipulates fuel flow to control thrust, exhaust area to control inlet throat air velocity, and fan pitch to control fan rpm. The ratio of compressor discharge static pressure to free-stream total pressure (PS3/PTO) serves as the thrust parameter so that it is actually the parameter controlled by fuel flow. Overrides are applied to each of the manipulated variables under certain conditions for safety or operational reasons.

Because the integrated control concept just described had not been tested previously on an engine, automatic operation was introduced gradually. One test run was made in the partial automatic mode referred to as Manual A18/βF. In this mode, fuel flow is manipulated to control PS3/PTO in response to the power demand input while fan pitch and nozzle area are controlled manually. In this run, the engine was switched from the full manual mode to the manual A18/βF mode at idle and accelerated in increments using the power demand input with pitch and area constant.

Engine operation proved to be quite stable and satisfactory with oscillations in PS3/PTO less than ±0.05 ratio units which is equivalent to less than ±0.5 percent thrust at takeoff.

At high power, fan pitch and nozzle area were independently varied to determine the effect on PS3/PTO. A 6° pitch change caused PS3/PTO to change less than 0.2 percent and a 2600 sq cm (400 $in.^2$) area change cause less than 0.5 percent pressure ratio change.

Figures 57, 58, and 59 are data traces showing operation in the Manual A18/βF mode.

Another run was made in the partial automatic mode referred to as Manual βF. In this mode, fuel flow is manipulated to control PS3/PTO in response to power demand, nozzle area modulates to set a fixed inlet Mach number (except as limited by maximum and minimum area limits), and fan pitch remains under manual control. The control system was switched into the Manual βF mode at idle. At this point, airflow and inlet Mach number were low and nozzle area was on the maximum limit of 1.87 square meters (2900 $in.^2$). Power demand was then advanced into the high power region where inlet Mach number would be above the desired level if the nozzle remained on the maximum limit. The control system reacted properly and reduced area to maintain the correct Mach number. Operation in this condition was quite stable with fuel flow

controlling PS3/PTO and nozzle area controlling inlet Mach number. Oscillations in PS3/PTO were less than ±0.05 units as they were in the Manual A18/SF mode and inlet Mach number oscillations were less than ±0.005 units at a base level of 0.8. A steady-state data trace of this operation is shown on Figure 60.

While operating in the mode just described, inlet Mach number adjustments were made to demonstrate the area to Mach number relationship at constant thrust. Data from three different adjustment settings checked during this experiment are plotted on Figure 61. The spread in each of the three groups of points gives an indication of the Mach number control accuracy. Another aspect of inlet Mach number control accuracy is shown in Figure 62 which compares the inlet Mach numbers indicated by the control system and the performance data measuring system. The control system read consistently high by approximately 0.015 units. This variation was caused by an error in the empirical equation which converts sensed ΔP/P into throat Mach number.

Subsequent to the two partial automatic control mode runs described above, the engine was run in the fully automatic mode with fuel flow modulating to control PS3/PTO, area modulating within maximum and minimum limits to control inlet Mach number, and fan pitch modulating between maximum closed and maximum open limits to control fan rpm. Operation in this mode was hampered somewhat because of a digital control programming error which caused the manual mode fan rpm schedule (versus power demand) to remain in effect in the automatic mode and conflict under some conditions with the PS3/PTO schedule.

The applicable control system schedules for the automatic control mode run are shown on Figure 63. The key schedule is the PS3/PTO schedule. Fuel flow is manipulated to set PS3/PTO in accordance with this schedule unless the erroneously included fan rpm schedule interferes. The fan nozzle basically tries to set takeoff inlet Mach number; but at low power demand airflow is not high enough to achieve this Mach number so the area runs at the maximum open (roof) schedule shown. Similarly, fan pitch tries to set takeoff fan rpm; but this, likewise, cannot be achieved at low power; therefore, pitch runs on the maximum closed (floor) schedule.

Operating characteristics in the automatic mode are shown on Figure 64. If the fan rpm schedule had not been mistakenly incorporated, PS3/PTO would simply follow the normal schedule, line (1). Instead, it followed the heavy dotted line. At low power, fuel flow was basically controlled by the fan rpm schedule; except that below about 37 percent, the minimum core engine idle limit was in effect. With the PS3/PTO schedule adjusted to line (2) the engine was accelerated in increments on the fan rpm schedule (heavy dotted line) until the adjusted PS3/PTO was encountered at about 82 percent power demand. When power demand was advanced further, full automatic operation was achieved. Figure 65 is a trace showing steady-state operation in this condition. (Note: At this point a PS3/PTO adjustment had been made to

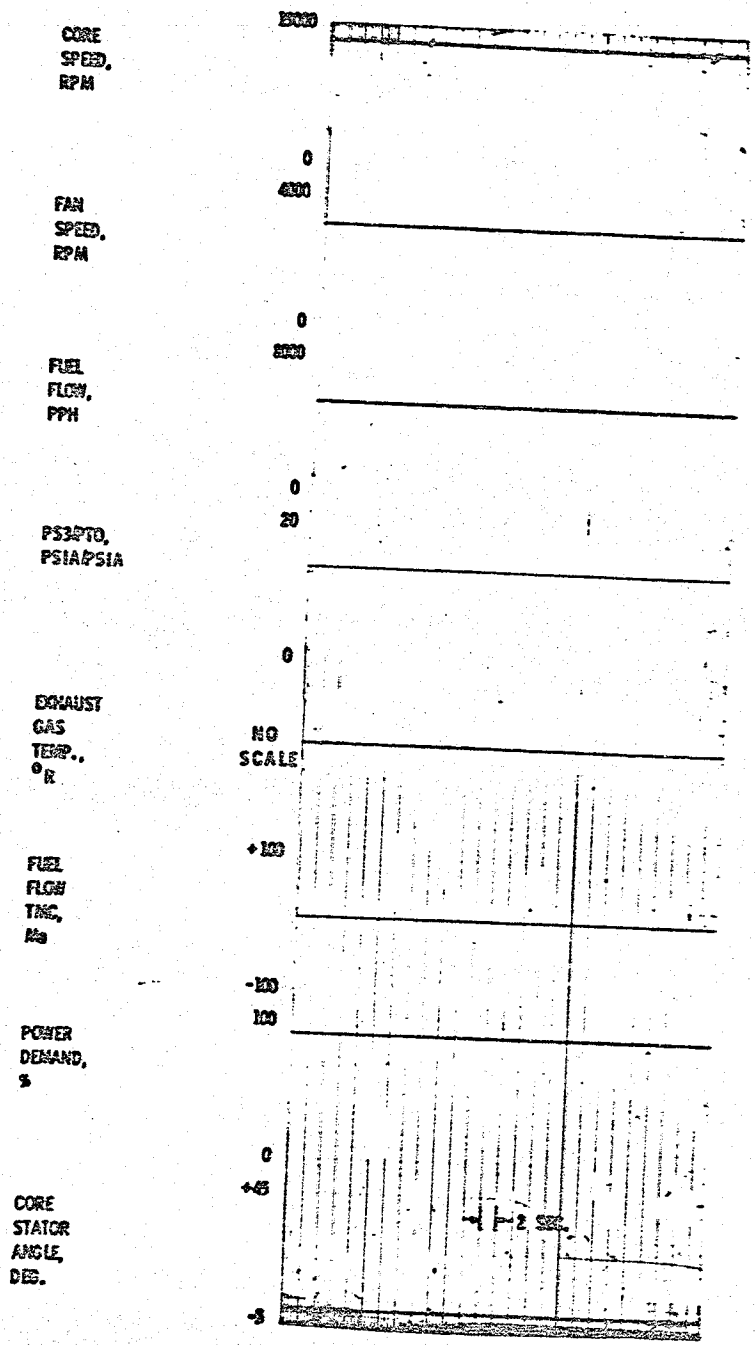

Figure 60(a). Mach Number Control Mode (Position 19 Set to 0.80).

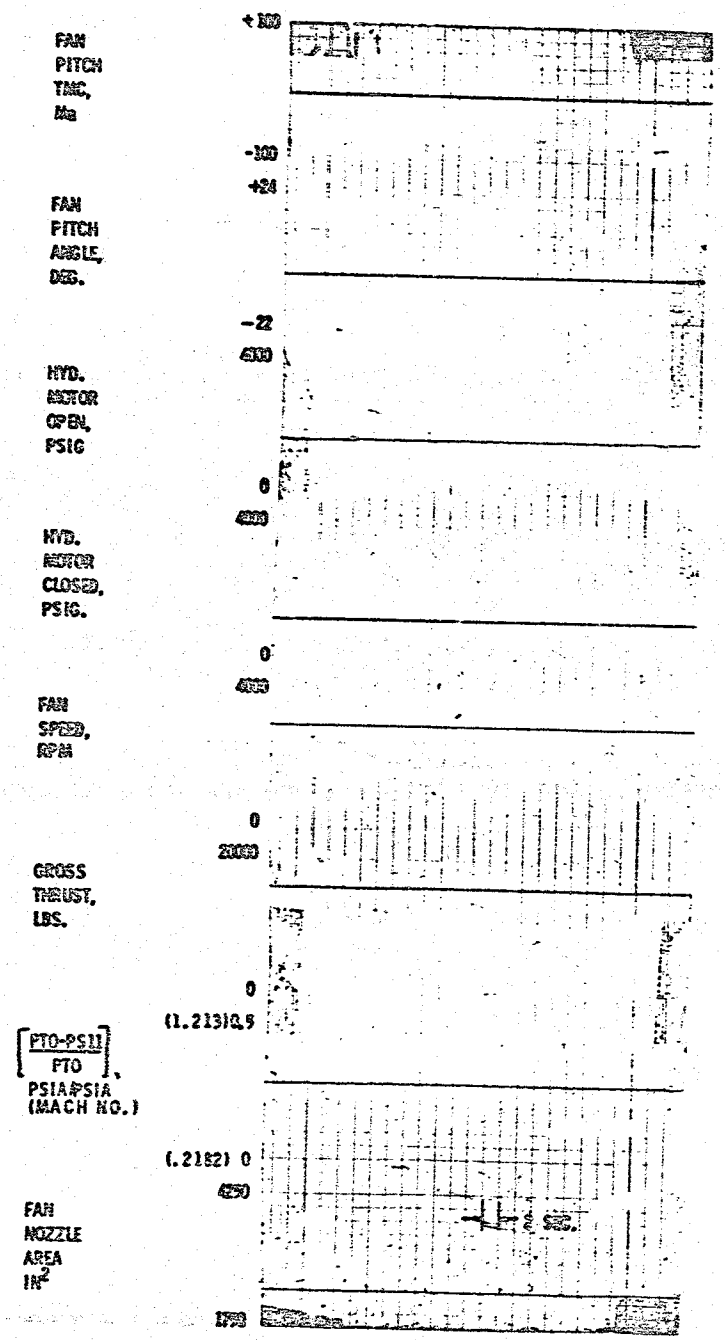

Figure 60(b). Mach Number Control Mode (Position 19 Set to 0.80).

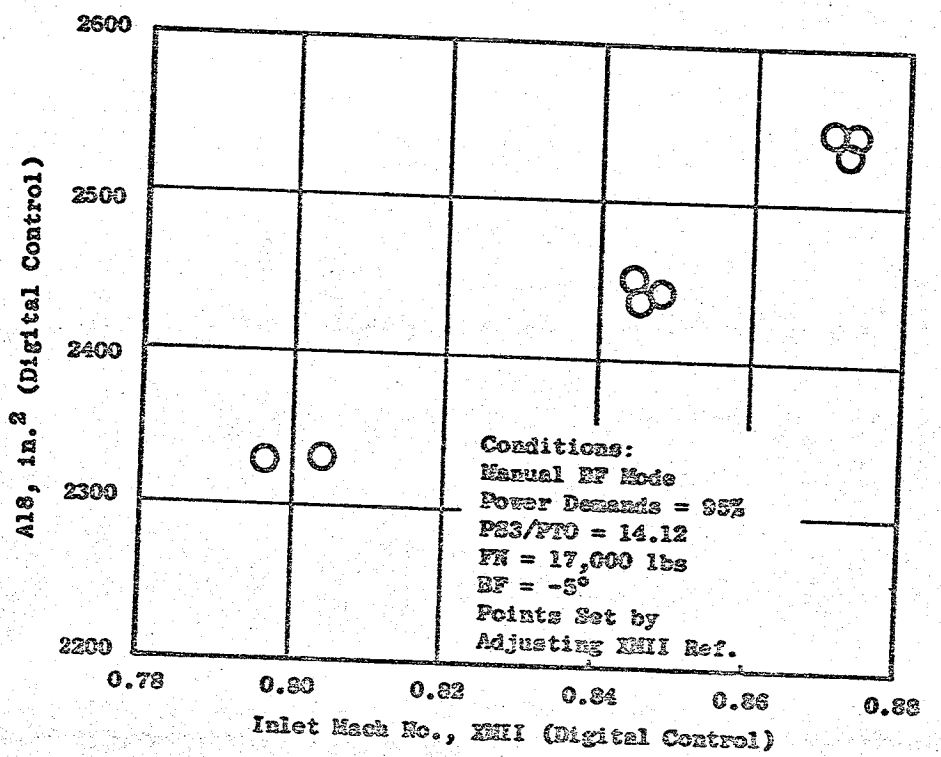

Figure 61. A18 Versus Inlet Mach No. at Constant Power Demand, QCSEE UTW 507-001/2.

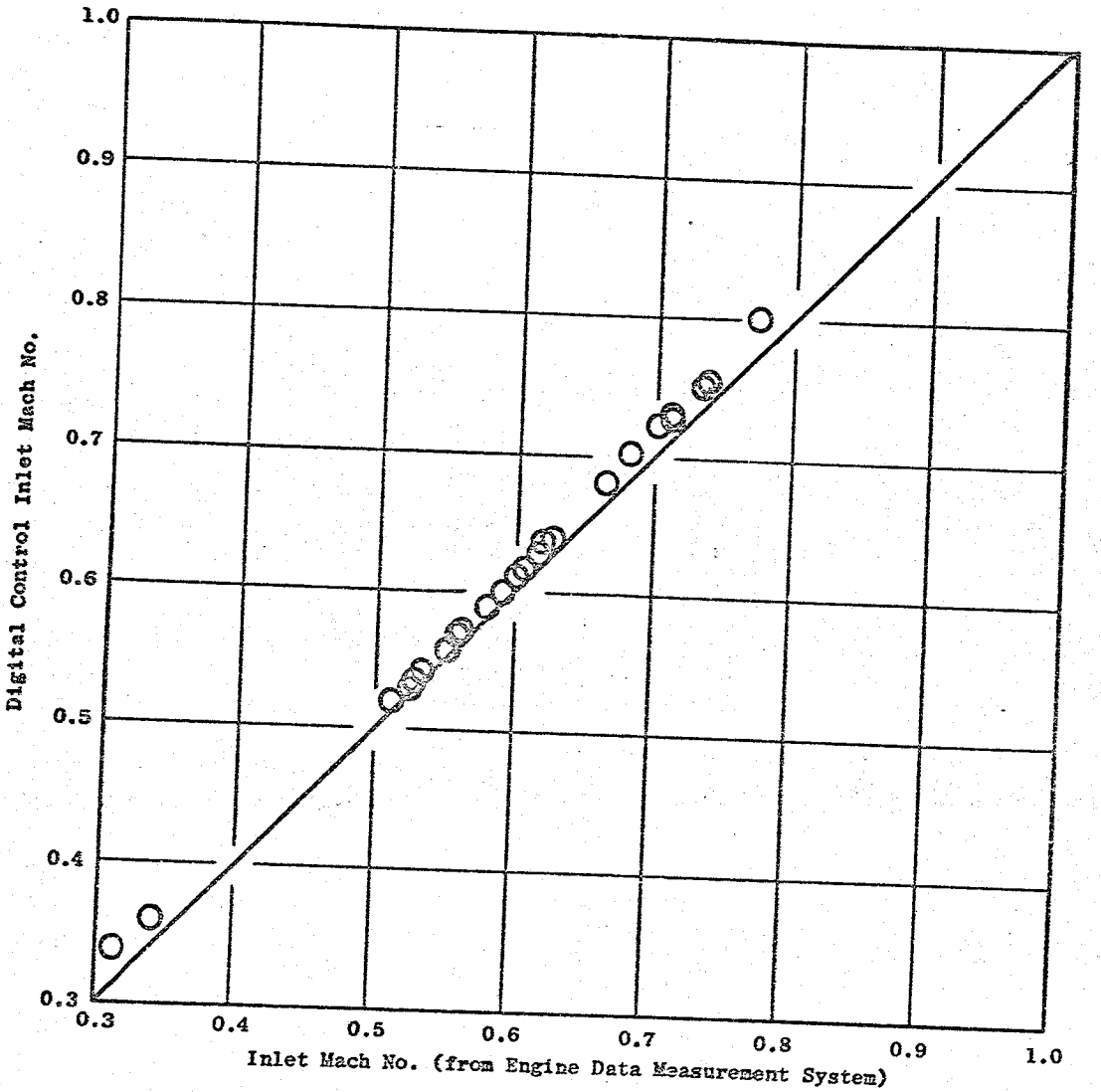

Figure 62. QCSEE Flight Inlet Data, Engine 507-001/2.

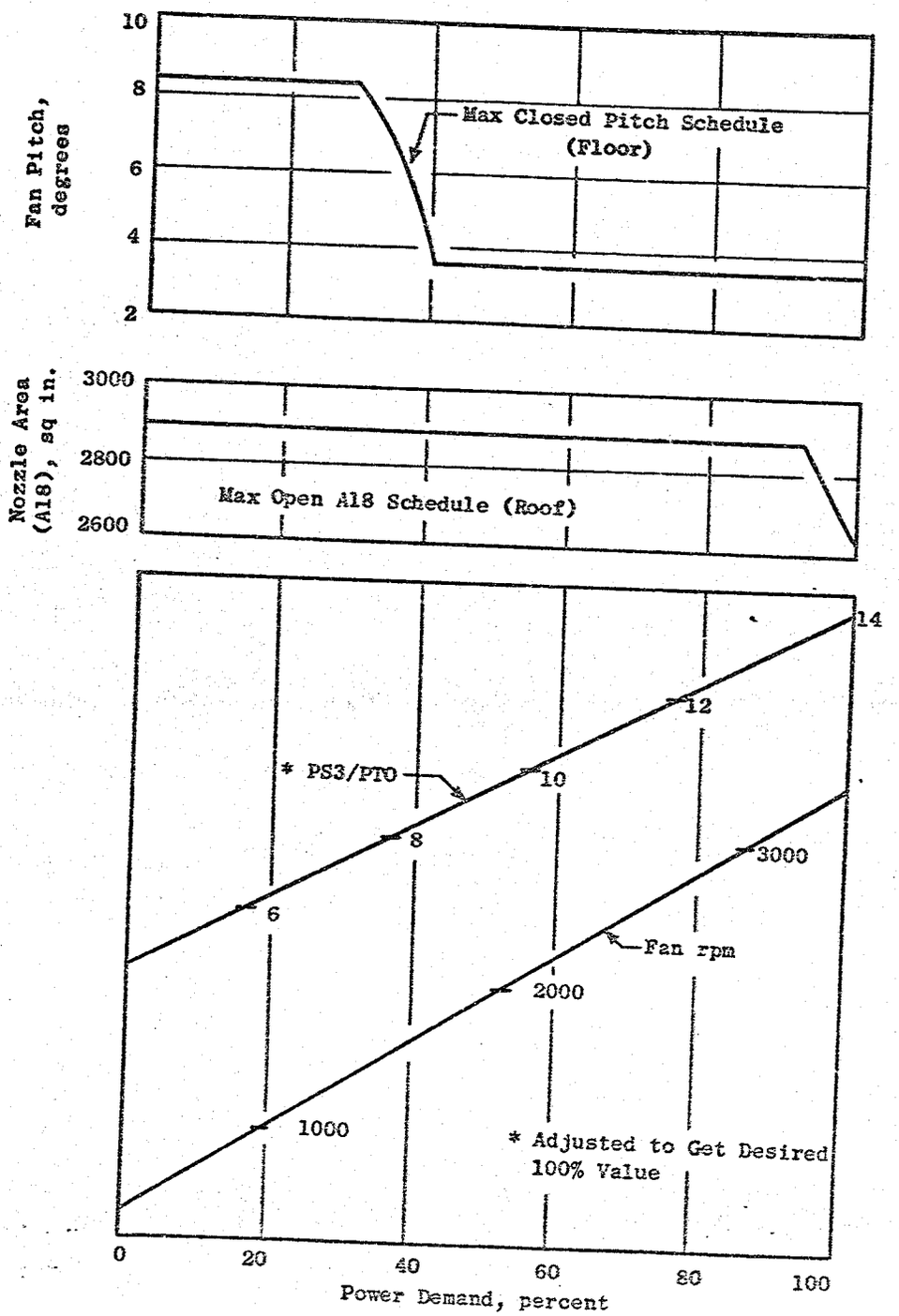

Figure 63. Automatic Control Mode Power Demand Schedules, QCSEE UTW 507-001/2.

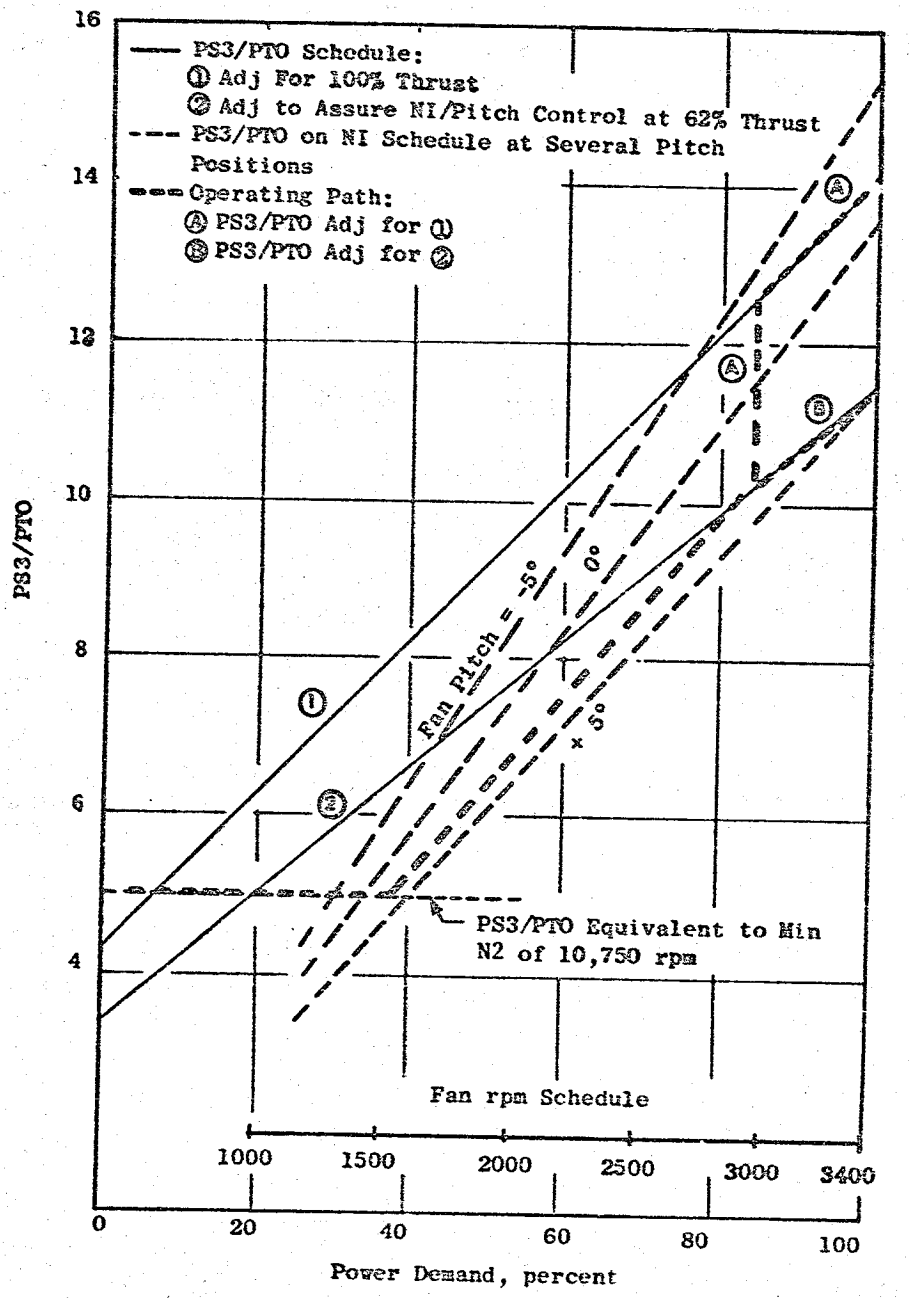

Figure 64. Power Demand Characteristics in Automatic Control Mode, QCSEE UTW 507-001/2.

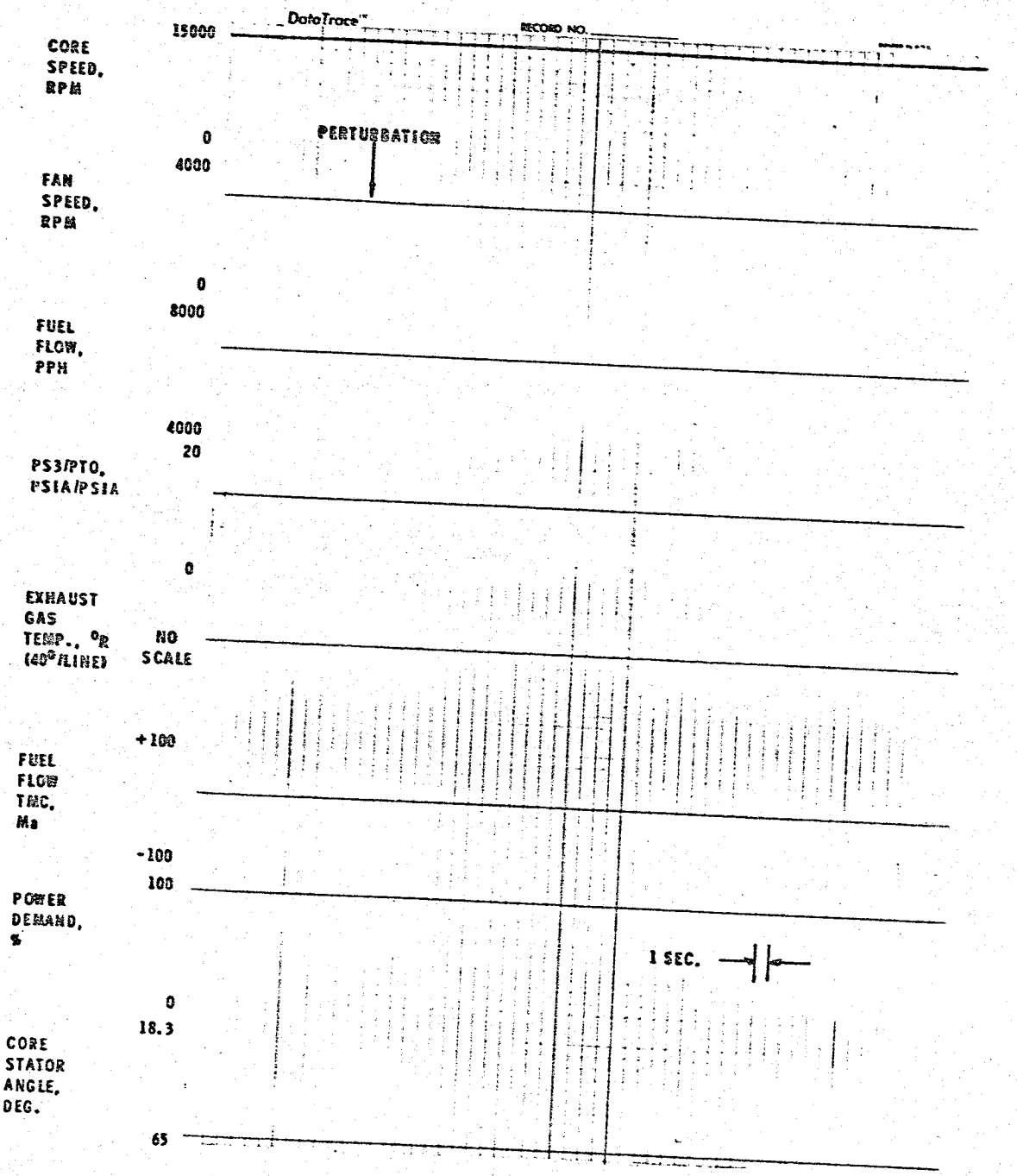

Figure 65(a). Automatic Control Mode Stability Check at 100% Power Setting.

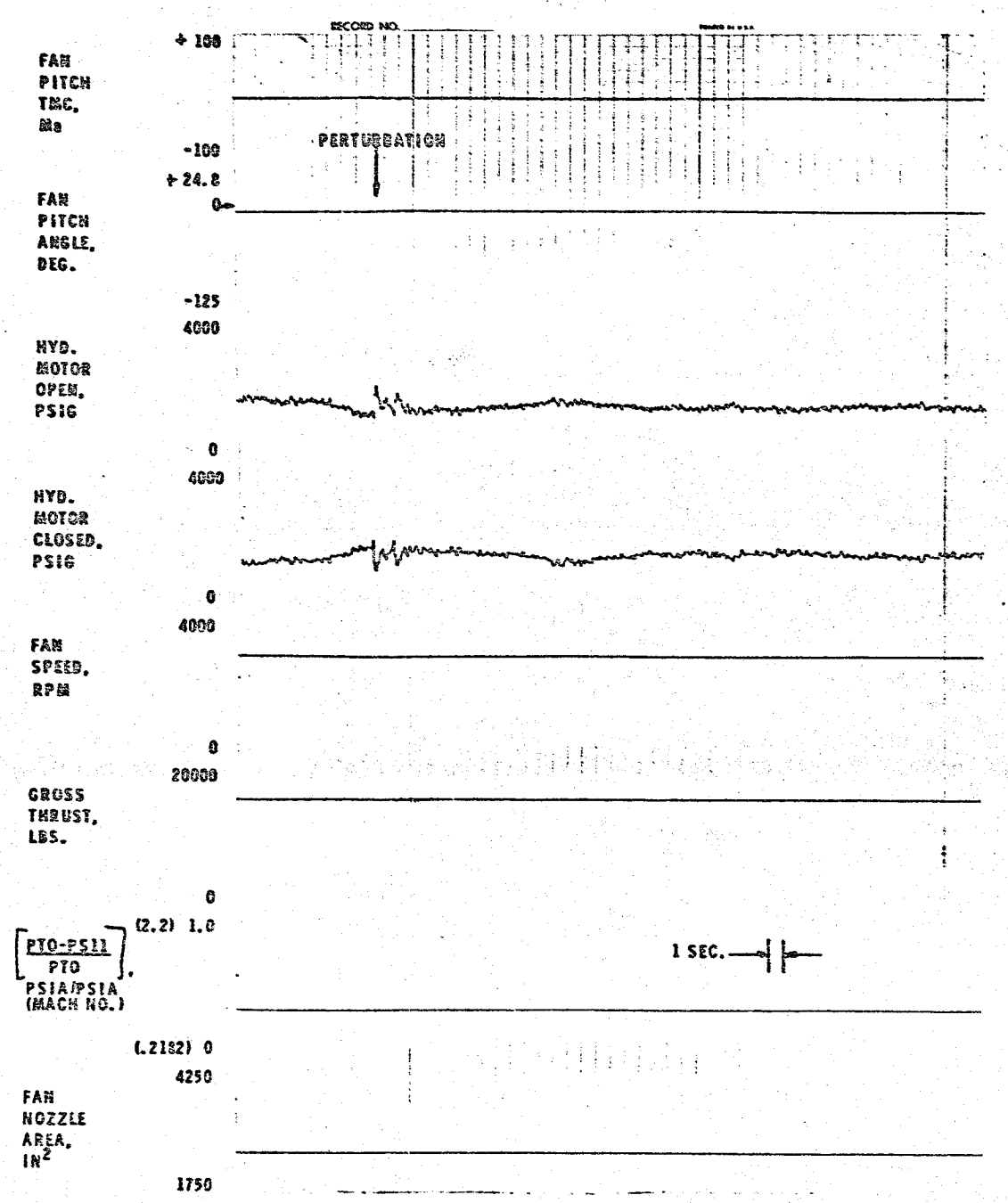

Figure 65(b). Automatic Control Mode Stability Check at 100% Power Setting.

get 100 percent thrust resulting in operation at 100 percent power demand between line (A) and (B) on Figure 64). Stability was excellent with oscillations less than ±0.05 units PS3/PTO, ±0.005 inlet Mach number units, and ±20 rpm fan speed.

The steady-state operating characteristics of the control loop which controls fan speed by manipulating fan pitch in the automatic mode are shown on Figure 66. The slope change in the fan pitch characteristics is associated with interaction between fan pitch and nozzle area. Below 90 percent power demand, the fan nozzle is opened to the roof limit and relatively large fan pitch change is required to maintain fan speed. Above 90 percent, the nozzle is further closed and smaller pitch changes are required to maintain fan speed.

A series of automatic mode transients were run on the engine, starting with small magnitude (5 percent thrust) power demand chops and bursts. These are shown in Figures 67 through 70. In addition, a chop and a burst were made between 62 and 80 percent thrust. These are shown in Figures 71 and 72. Times for the latter two transients (for 95 percent of the total thrust change) were 0.5 second for the chop and 1.0 second for the burst. During the burst, an excessive fan speed overshoot occurred with speed going to 3200 rpm before setting back to the scheduled level of 2900. Fan pitch should have opened faster than it did to prevent this speed overshoot. The trace indicates that the control began increasing pressure to the pitch actuation system when rpm first began to increase, but the pressure built up gradually and the actuation system did not move immediately. It is probable that internal leakage in the actuation motor, which was known to be somewhat high (1.5 gpm versus 0.3 gpm when new), combined with the relatively low control loop gain and high actuation loads caused the slow response.

No further transients were run on the engine because the engine test program was terminated at this point, before the overshoot problem could be investigated and corrected. Thus the original program objective calling for a 1 second acceleration from 62 to 95 percent thrust was not demonstrated. Also, transients between forward and reverse thrust were not demonstrated. Nevertheless, the automatic control mode testing was considered a success because it demonstrated the feasibility of the unique QCSEE UTW three-variable power control concept.

15.7 CALCULATED TURBINE TEMPERATURE FUNCTIONS

The QCSEE control system includes two calculated turbine temperature functions which are made possible by the computational capabilities of the digital control and which offer the potential for improved temperature sensing relative to current engine control systems.

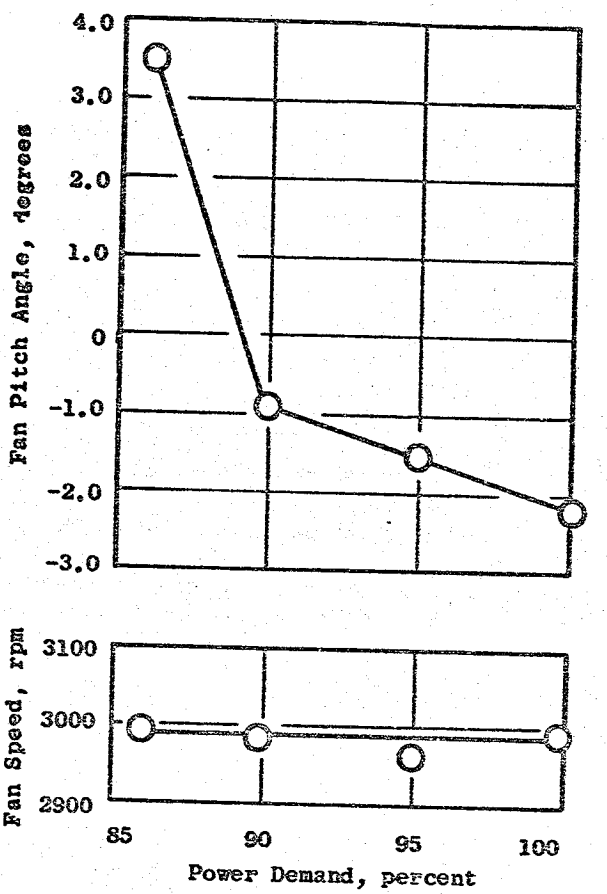

Figure 66. Fan Speed Control, Engine 507-001/2.

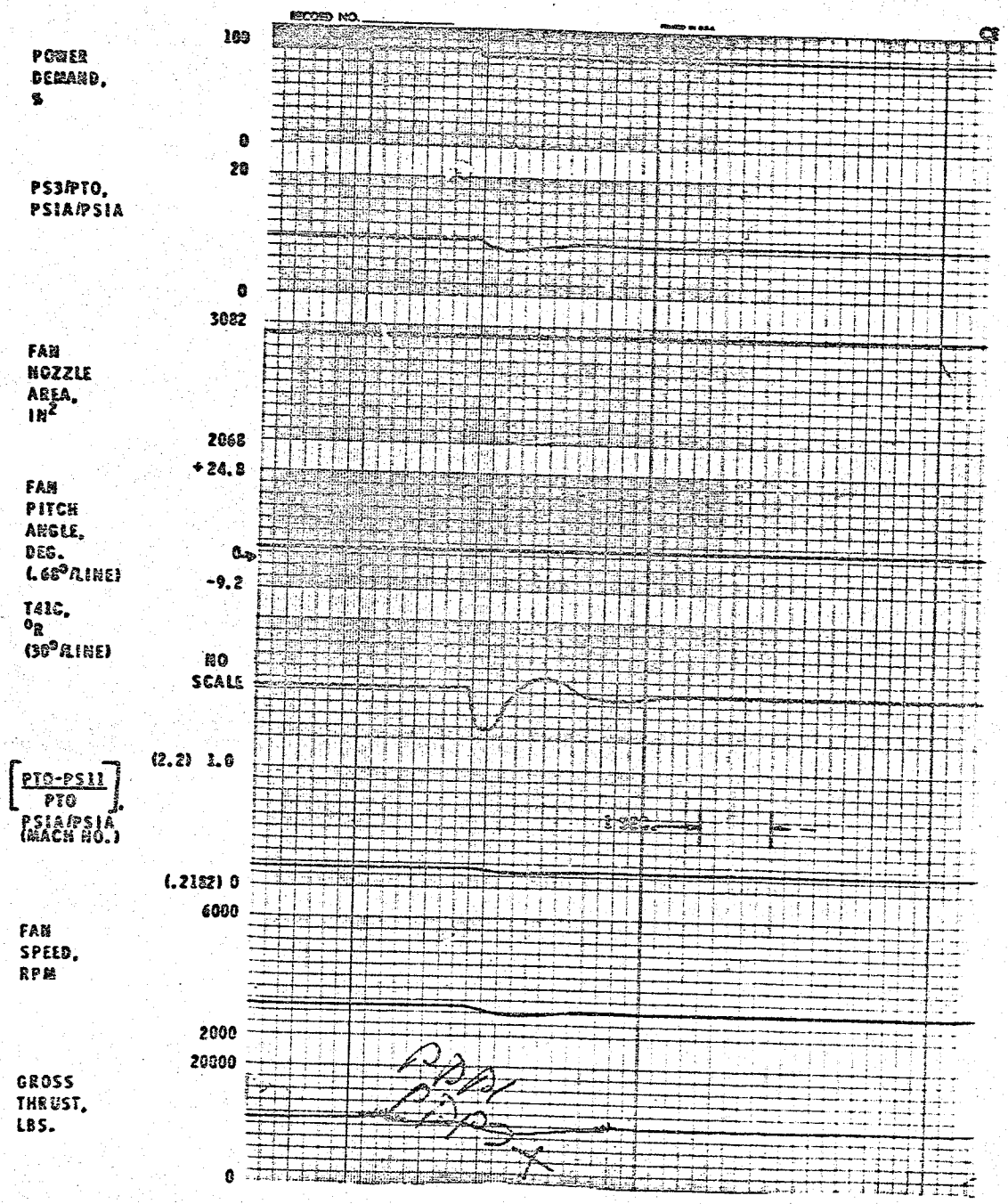

Figure 67. Automatic Control Mode Throttle Chop from 65% to 60% F_N.

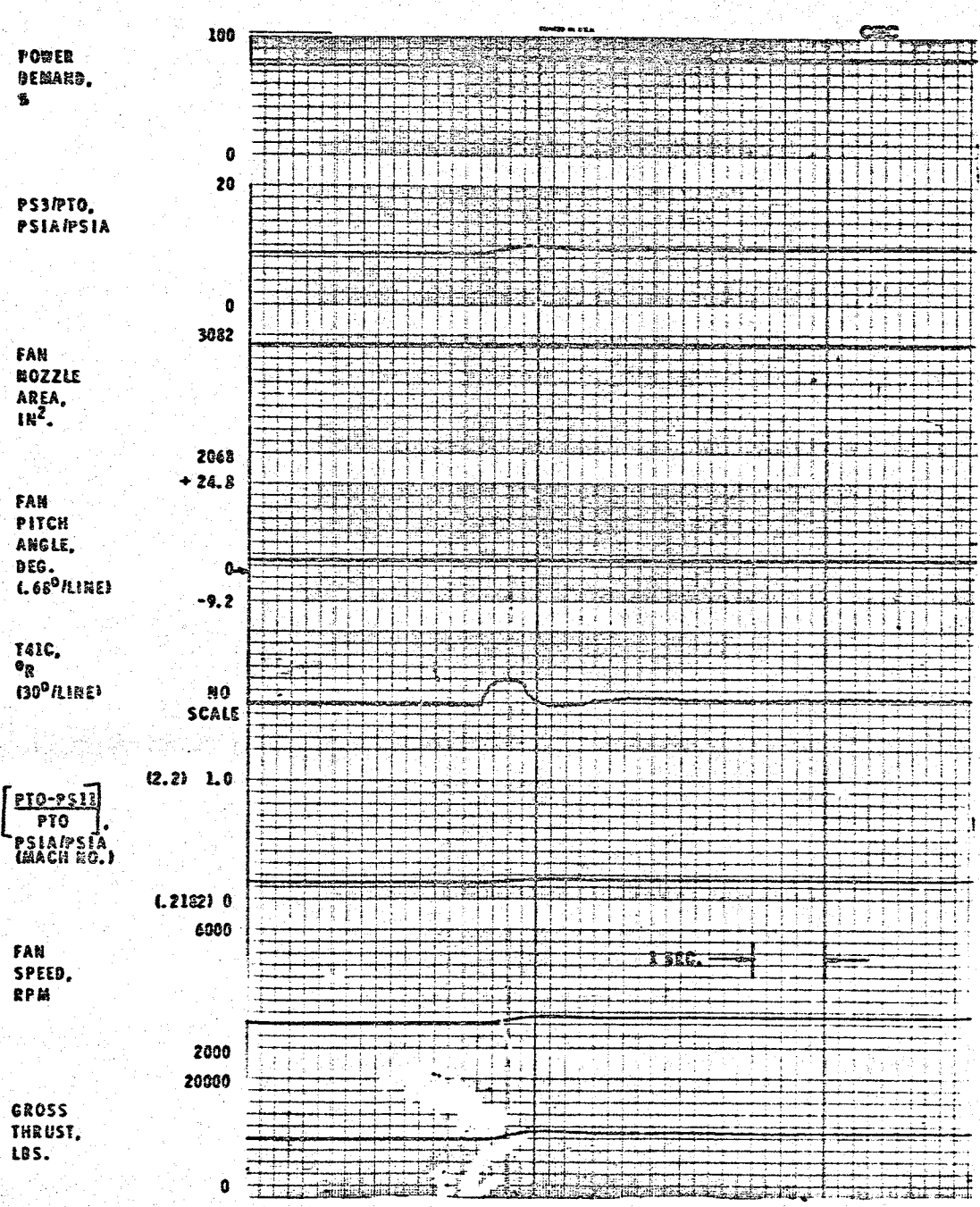

Figure 68. Automatic Control Mode Throttle Burst from 60% to 65% F_N.

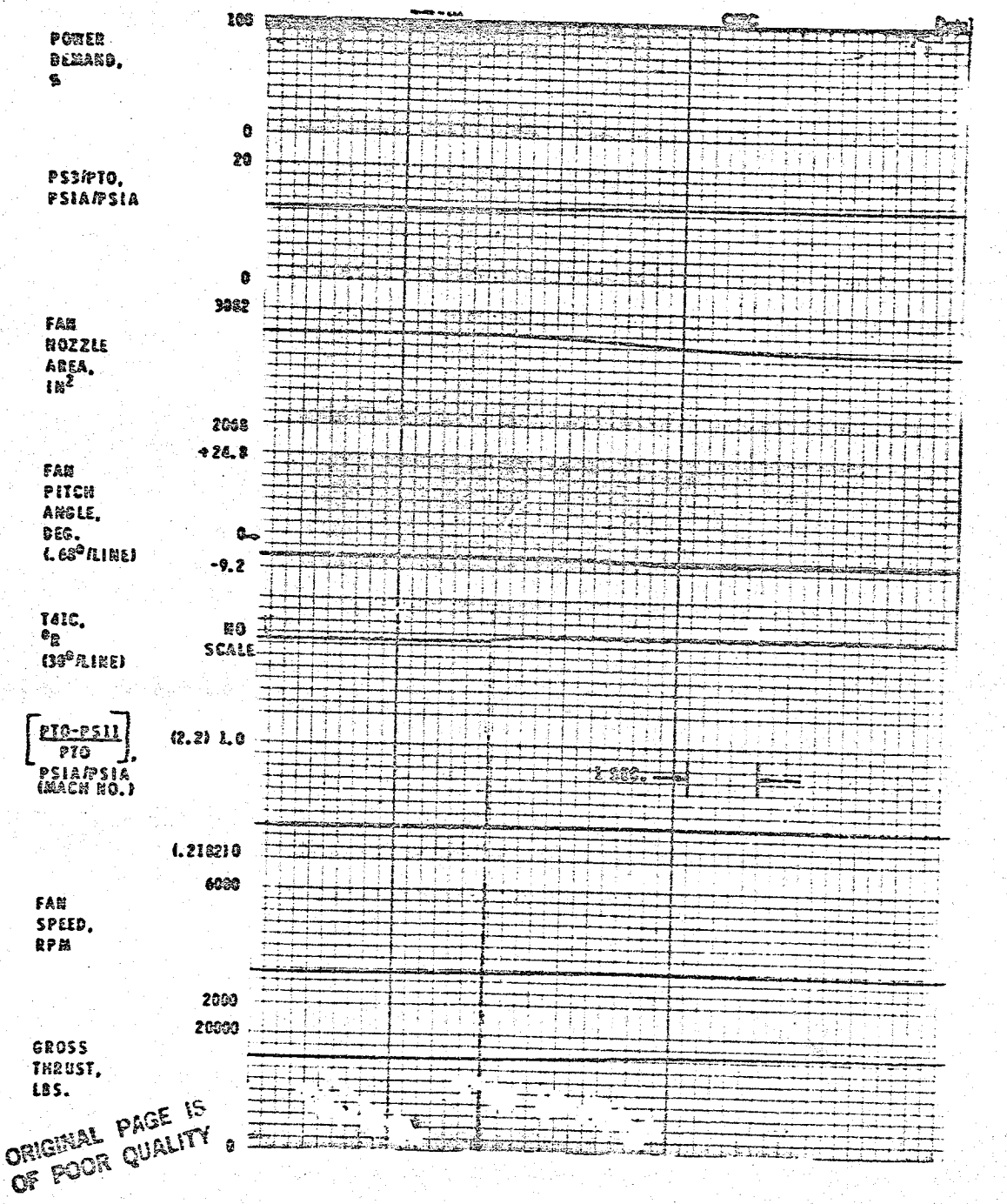

Figure 69. Automatic Control Mode Throttle Burst from 95% to 100% F_N.

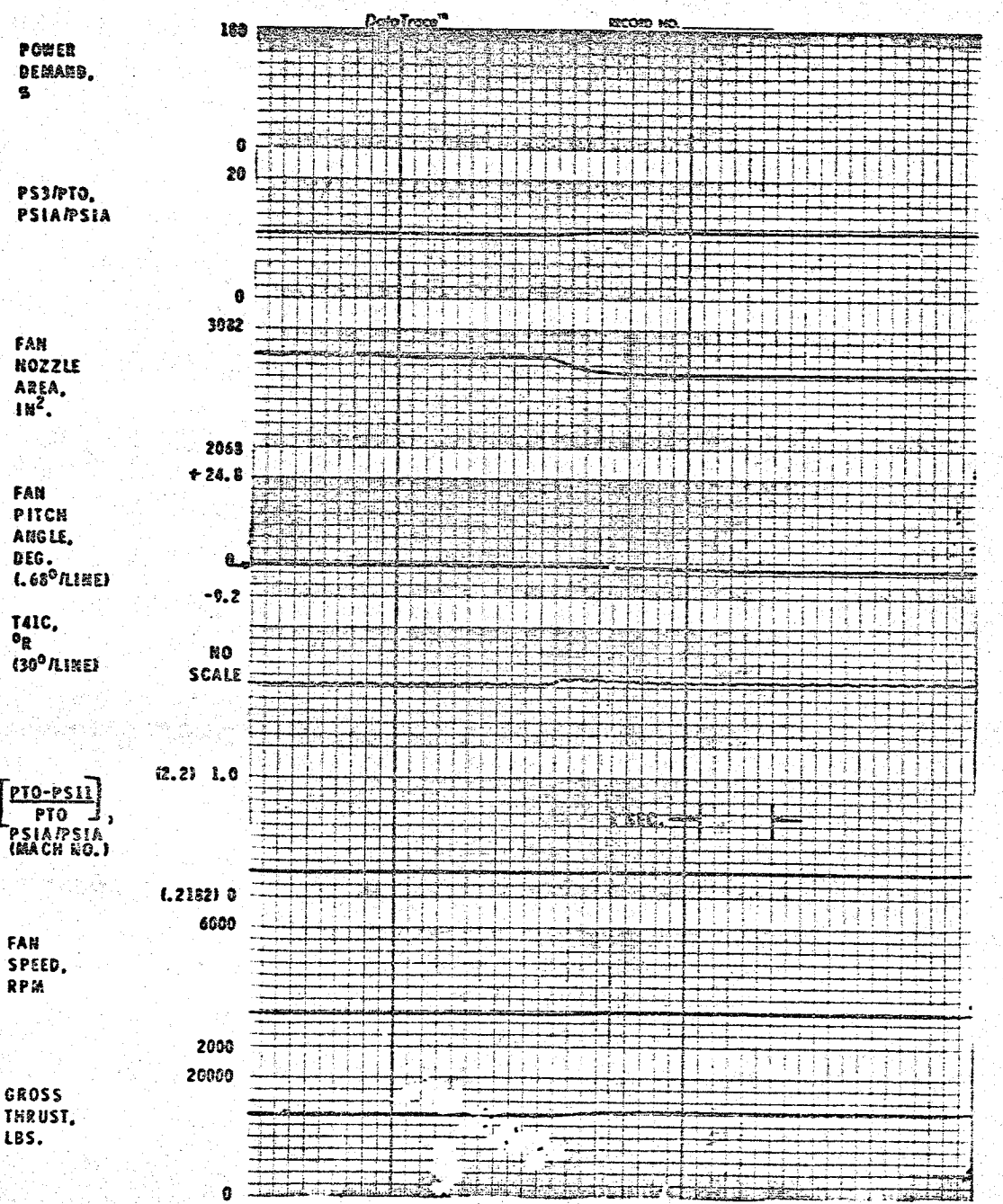

Figure 70. Automatic Control Mode Throttle Burst from 80% to 85% F_N.

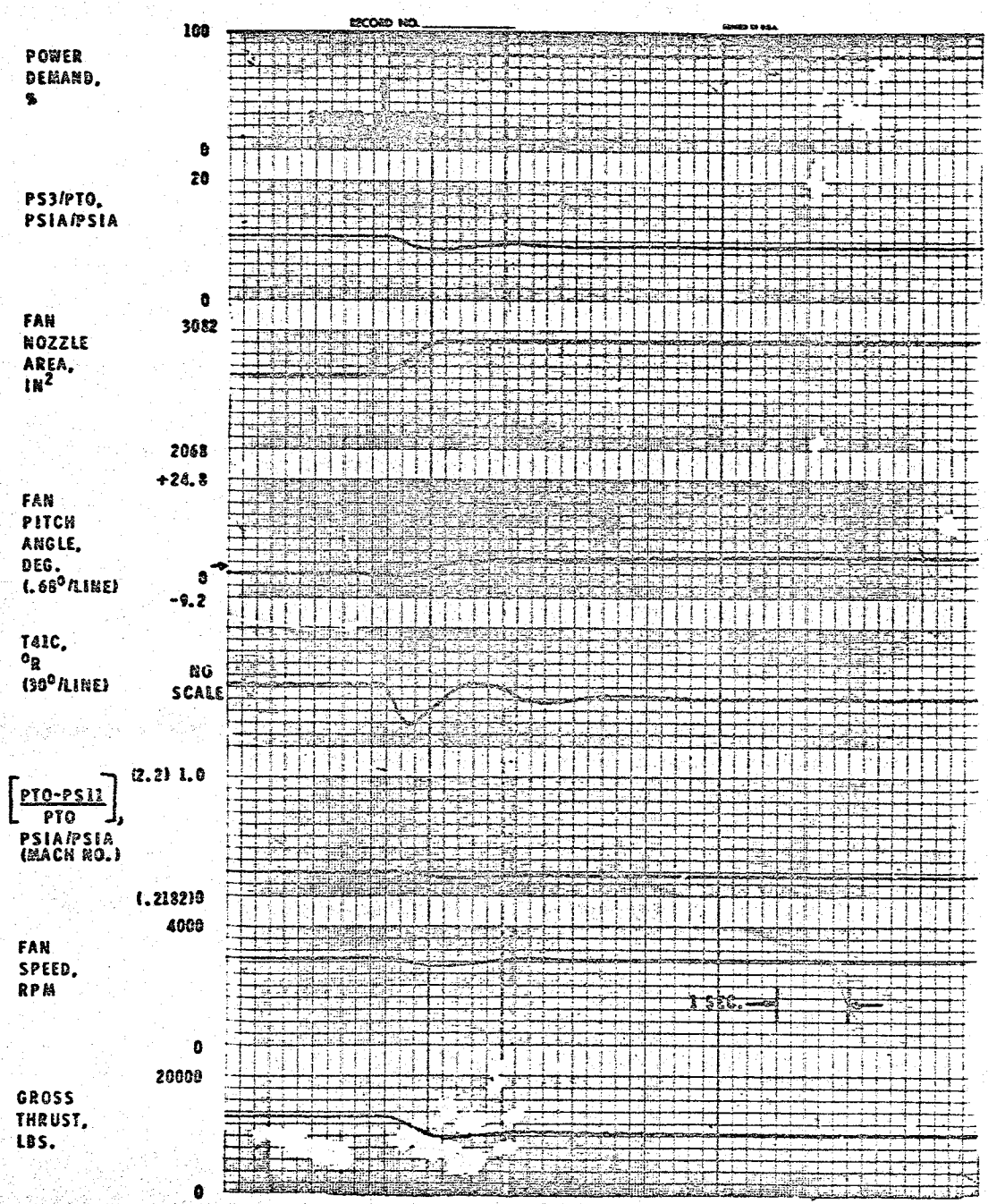

Figure 71(a). Automatic Control Mode Throttle Chop from 80% to 62% F_N.

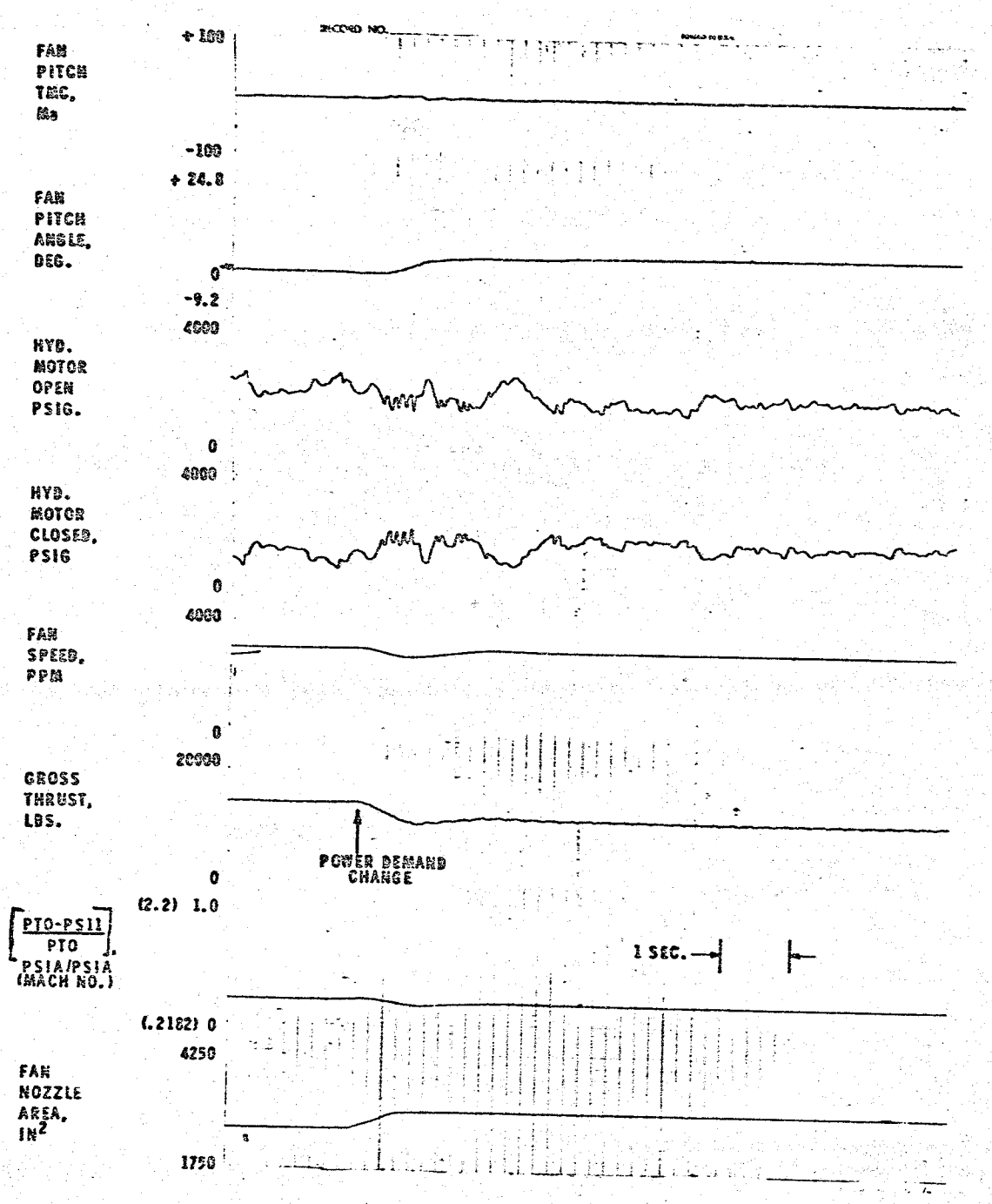

Figure 71(b). Automatic Control Mode Throttle Chop from 80% to 62% F_N.

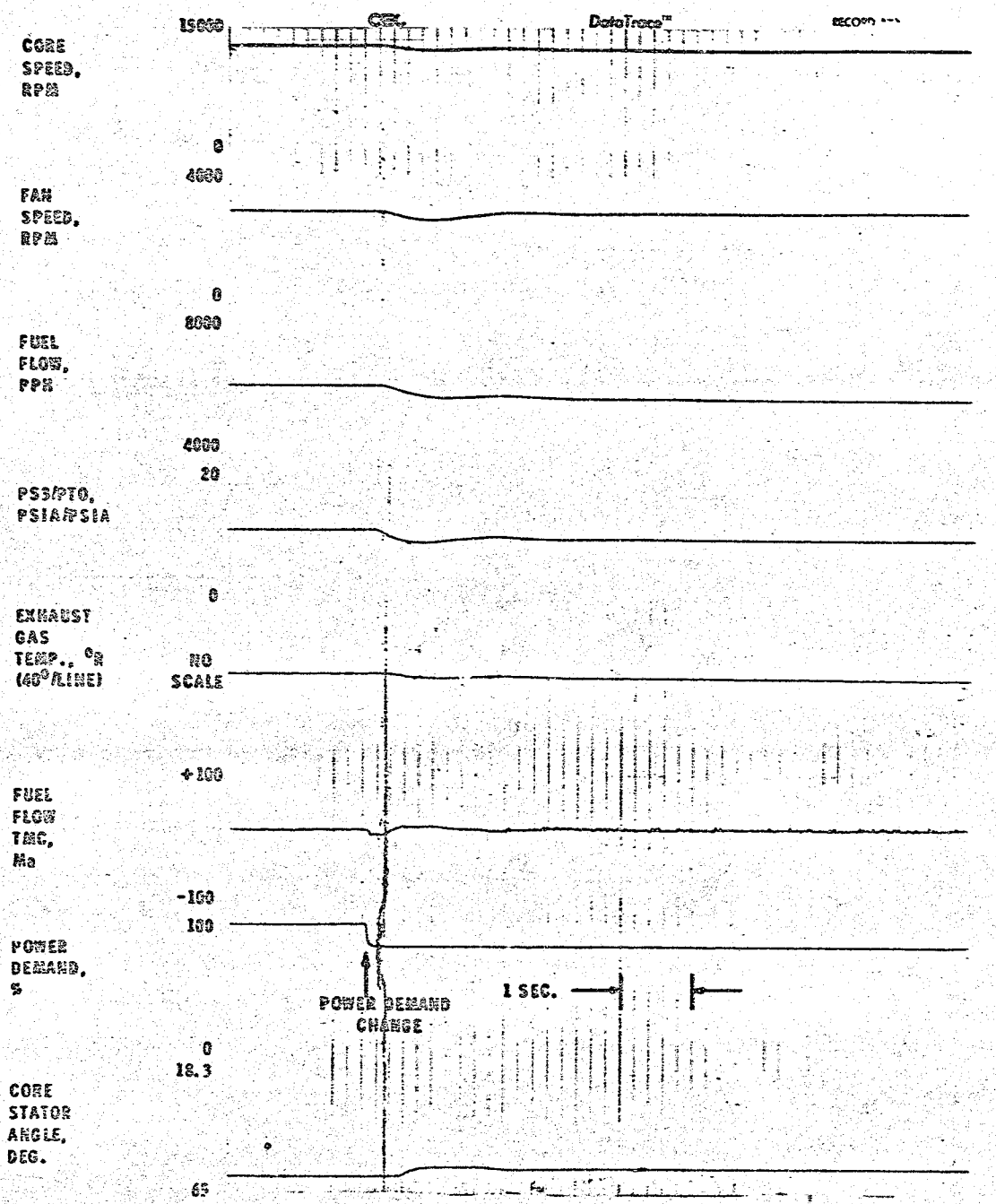

Figure 71(c). Automatic Control Mode Throttle Chop from 80% to 62% F_N.

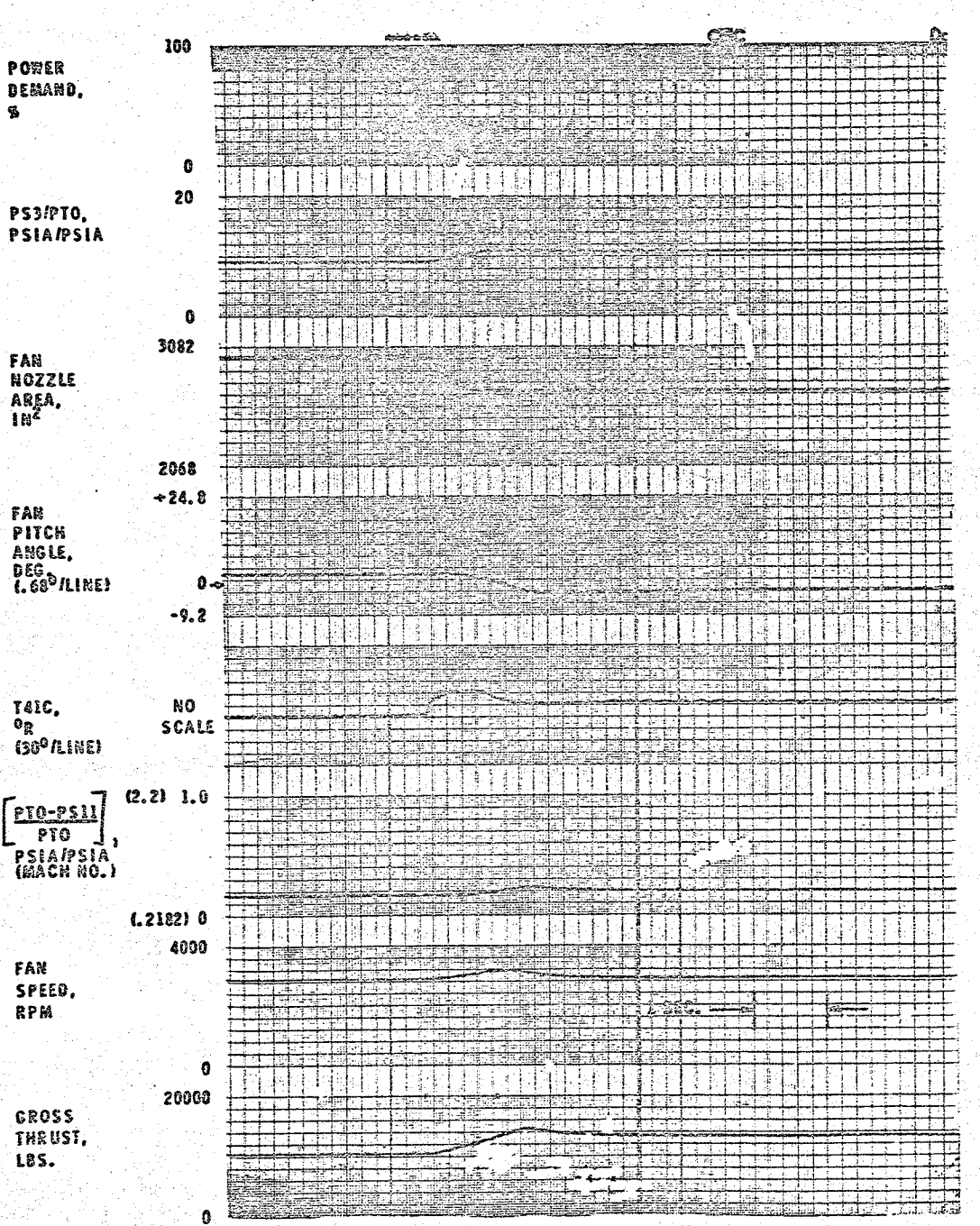

Figure 72(a). Automatic Control Mode Throttle Burst from 62% to 80% F_N.

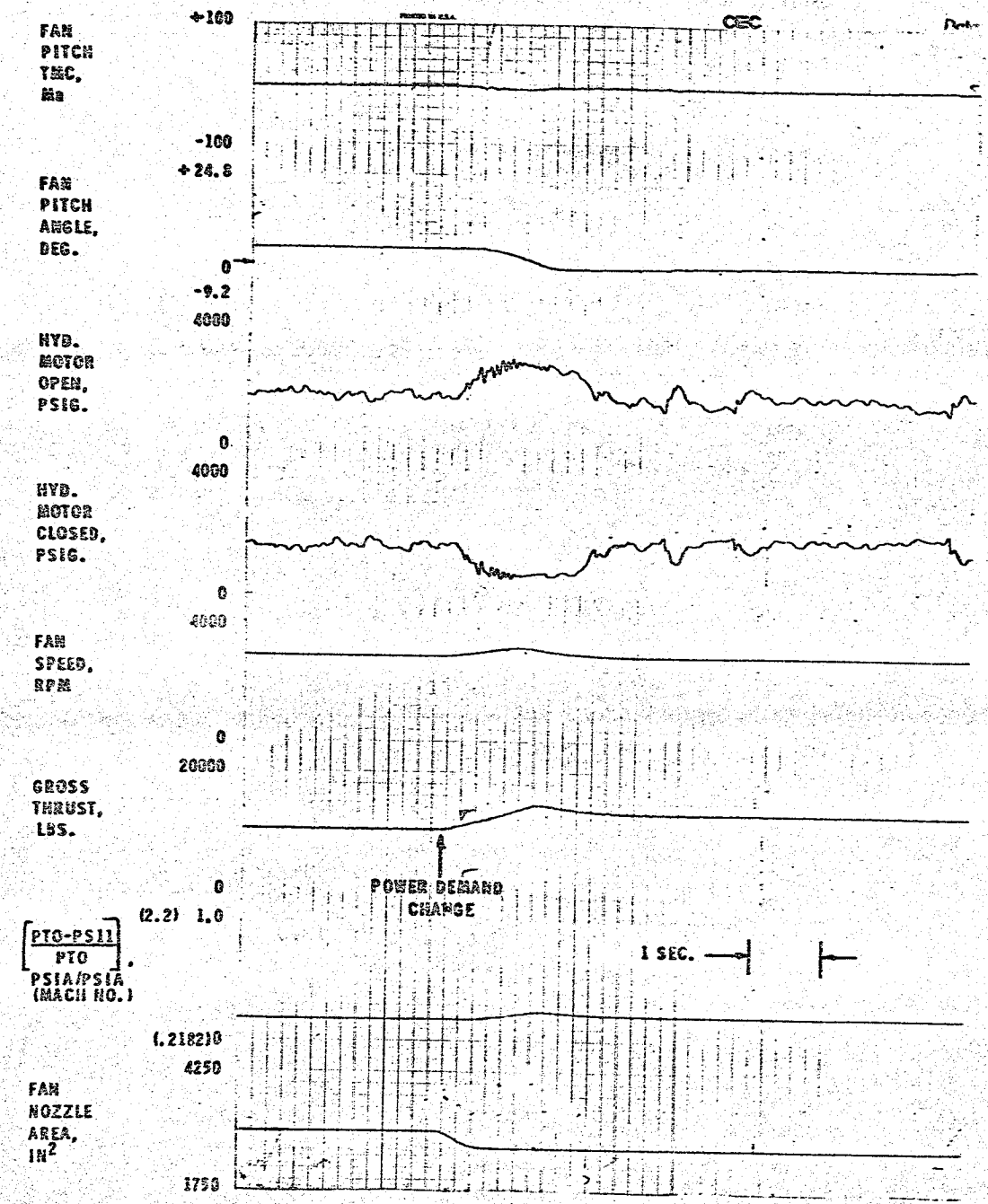

Figure 72(b). Automatic Control Mode Throttle Burst from 62% to 80% F_N.

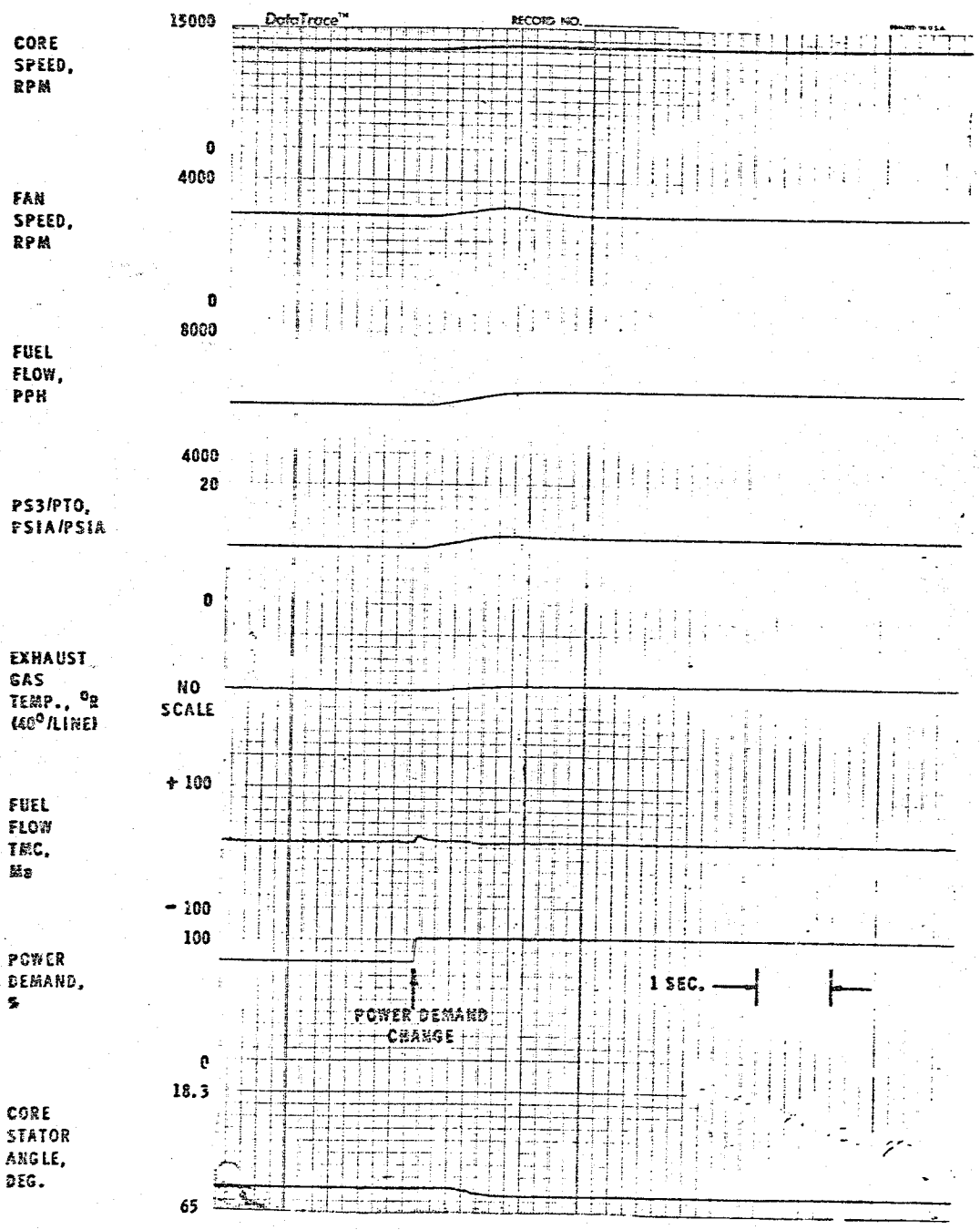

Figure 72(c). Automatic Control Mode Throttle Burst from 62% to 80% F_N.

C - 3

One of the functions calculates turbine inlet temperature (T41C) from compressor discharge temperature (T3), compressor discharge pressure (PS3), and fuel flow (WF) as indicated by the fuel metering valve position. The formula in the digital control for this function was:

$$T41C = 14.6 + 1.06468\ (T3) + 23.9437\ (WF/PS3)1.245$$

Testing showed this temperature to be 60° to 150° F higher than T41 as calculated from engine performance data. This is shown on Figure 73. Investigation revealed that most of this error was caused by an apparent calibration error in the fuel metering valve position sensing elements resulting in an indicated fuel flow in the digital control 114 to 160 kg per hour (250 to 350 pounds per hour) above the flow measured by the engine flow meter. It appears that a recalibration of the metering valve sensing system would correct most of the error and provide an accurate T41C.

The second calculated temperature function calculates turbine inlet temperature from exhaust gas temperature (T5) as measured by thermocouple downstream of the low pressure turbine compressor discharge pressure (PS3), fan inlet temperature (T12), and freestream total pressure (PTO) in accordance with the following formula:

$$T41CB = \left[\frac{T5}{(\theta_{12}).16}\right]^{1.0407} + T12\left[\left(\frac{PS3}{PTO}\right).276\right] - 1$$

Data from the engine on this calculated turbine temperature is shown on Figure 74. Here the error appears to be in the formula and it appears that a new formula based on empirical data could provide an accurate turbine inlet temperature calculation. Considerably more data at different operating conditions would be required to prove this point.

15.8 DATA MONITORING

The QCSEE control system includes a data monitor feature which exploits the inherent capability in the digital control to process data and transmit them to a remote location. The control is capable of processing and transmitting 48 data items. Many of these are control-system items for which no corresponding engine instrumentation was available for data correlation. However, it was possible to correlate several key variables as described below.

15.8.1 Fan Inlet Temperature (T12)

On the engine, T12 was measured with four 5-element thermocouple rakes and data from these rakes averaged (after elimination of obvious bad readings) by the engine test data system. A comparison of data from this source with T12 data from the control system, which utilizes a single, resistance-type

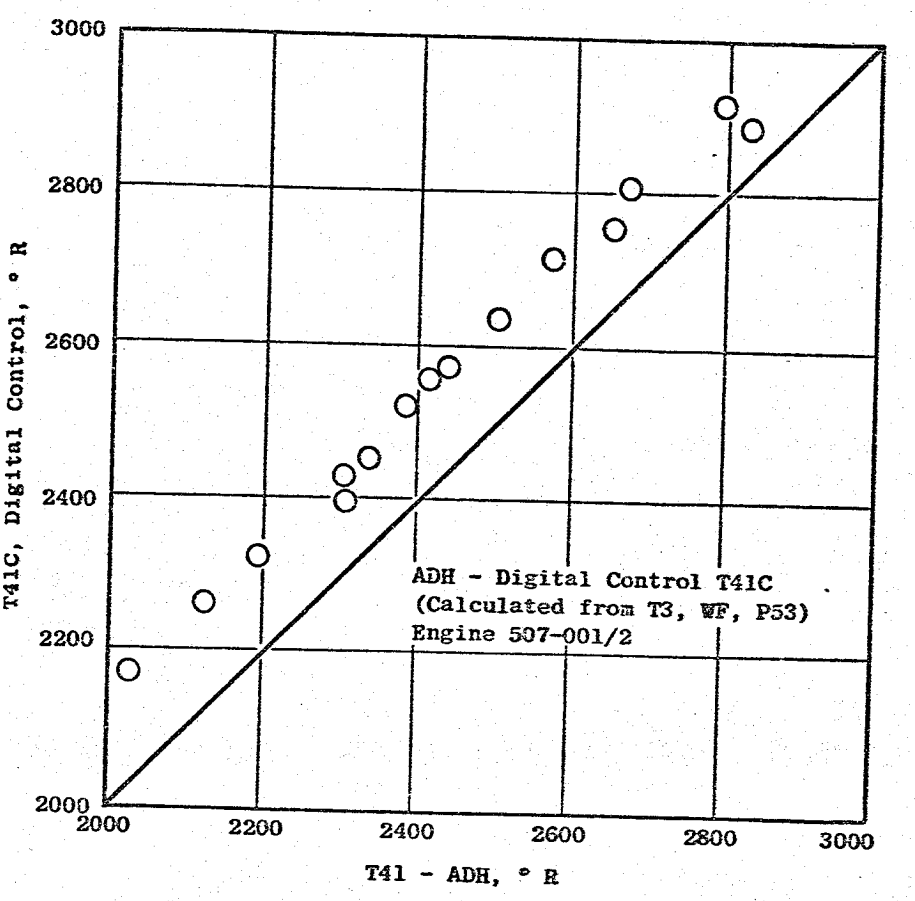

Figure 73. Data System Check.

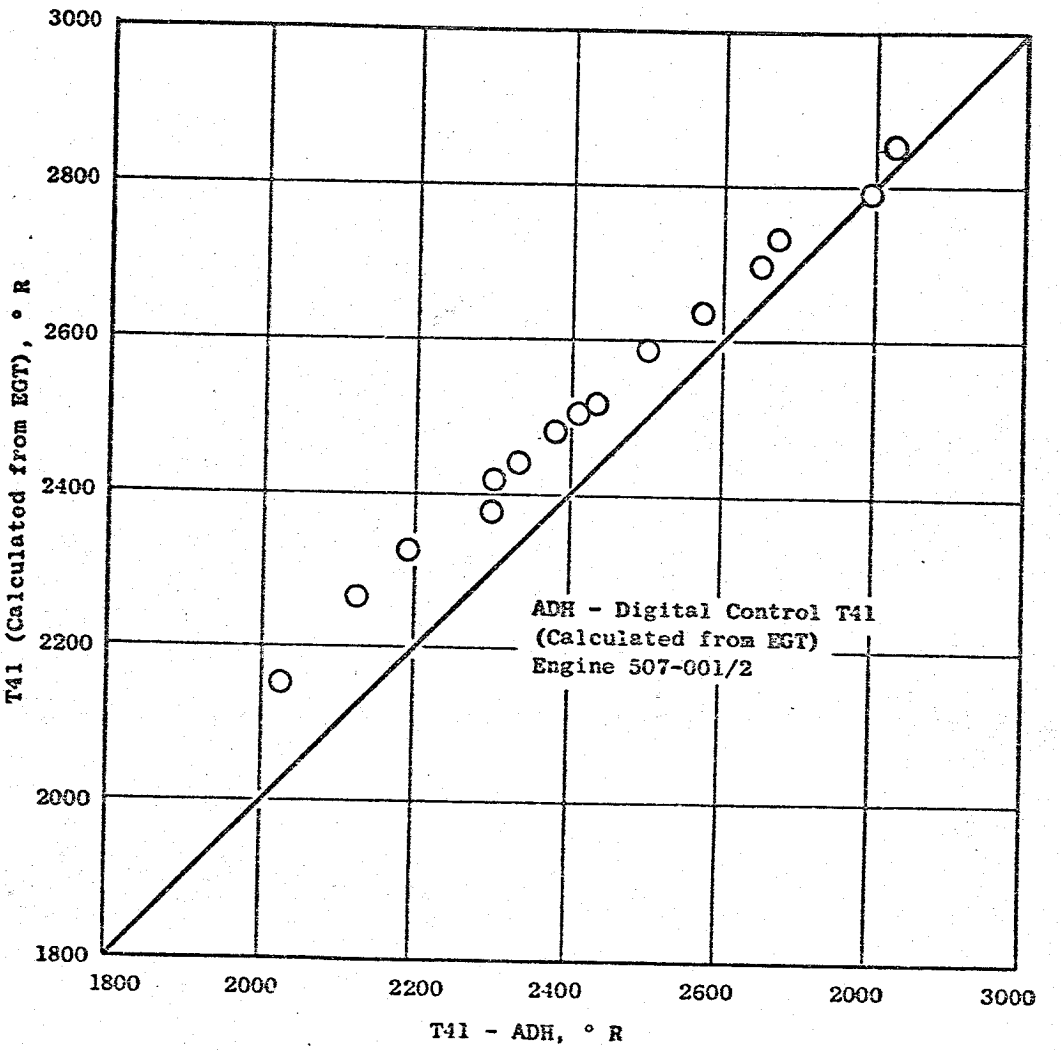

Figure 74. Data System Check.

temperature detector in the inlet at the 11 o'clock position, is shown on Figure 75. Maximum deviation of the control sensed T12 was 1.6° R.

15.8.2 Freestream Total Pressure (PT0)

For this engine test, which was all done at sea level static conditions, the control PT0 values were compared with barometric pressure data. Comparison of a large number of data points showed the control PT0 to be from 0.09 to 0.14 psi higher than the barometric reading, a consistent error for which compensation could be provided.

15.8.3 Inlet Static Pressure (PS11)

Here, engine data based on 8-pressure tap average in the engine inlet was compared with control PS11 as sensed on both sides of the inlet at the horizontal centerline. This comparison is shown in Figure 76. Again, the error is small and consistent so that compensation could be applied.

15.8.4 Compressor Discharge Temperature (T3)

A comparison of T3 as sensed by the engine data system from a single thermocouple within the engine with control system T3 as sensed by a separate, single thermocouple probe, is shown on Figure 77. Control system T3 was consistently low by 0.5 to 2 percent.

15.8.5 Compressor Discharge Pressure (PS3)

The control sensed value of PS3 proved to be consistently above the engine data system PS3, the errors varying from 0.7 to 2.0 percent. It is suspected that there was a leak in the engine sensing system because similar data from the digital control on the QCSEE OTW engine was within 0.4 percent.

15.8.6 Fuel Flow

As noted above in the calculated turbine temperature discussion, the fuel flow level determined by the control system from fuel metering valve position suffered from an apparent calibration error and was consistently higher than engine test flow meter readings, the error varying from 114 to 160 kg (250 to 350 pounds) per hour. Recalibration would have produced an accuracy within 1 percent for this sea level static testing.

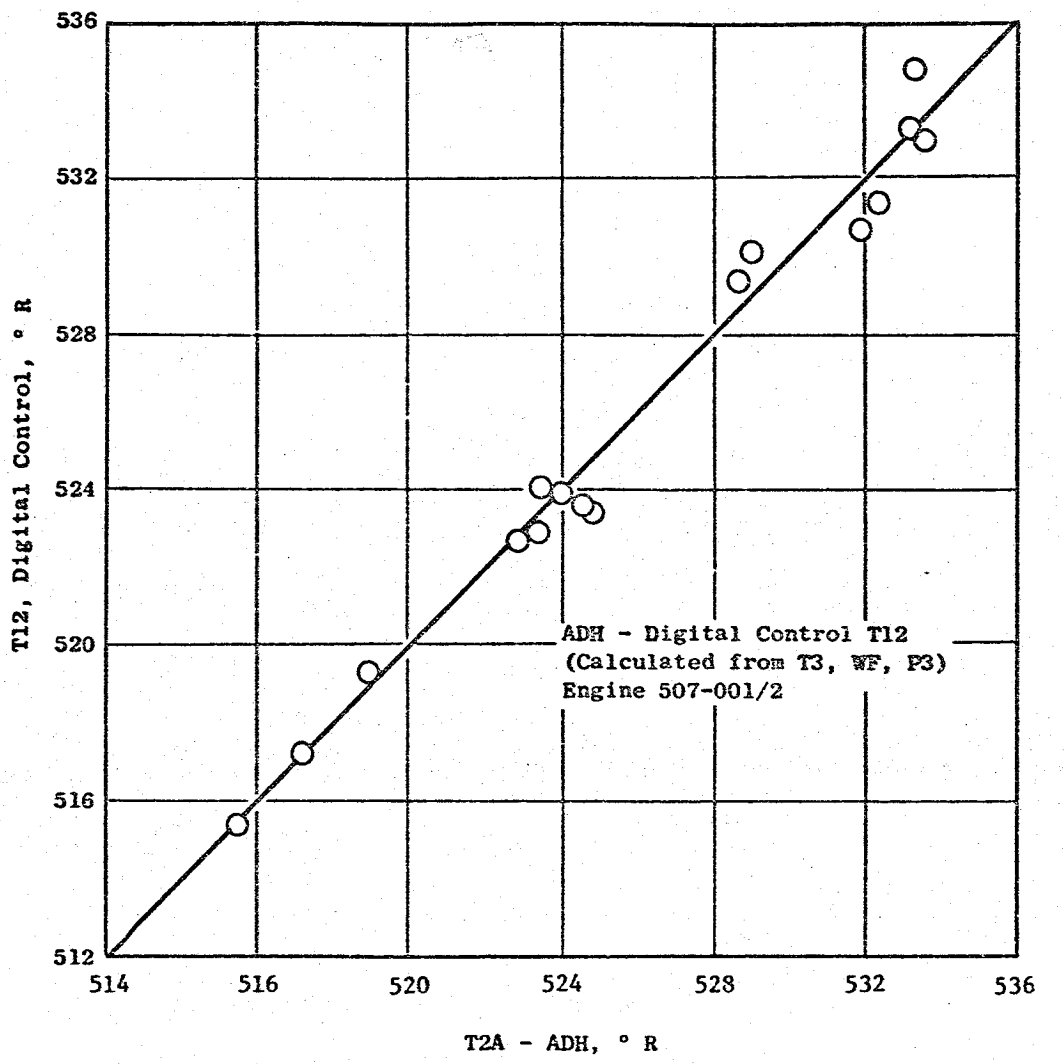

Figure 75. Data System Check.

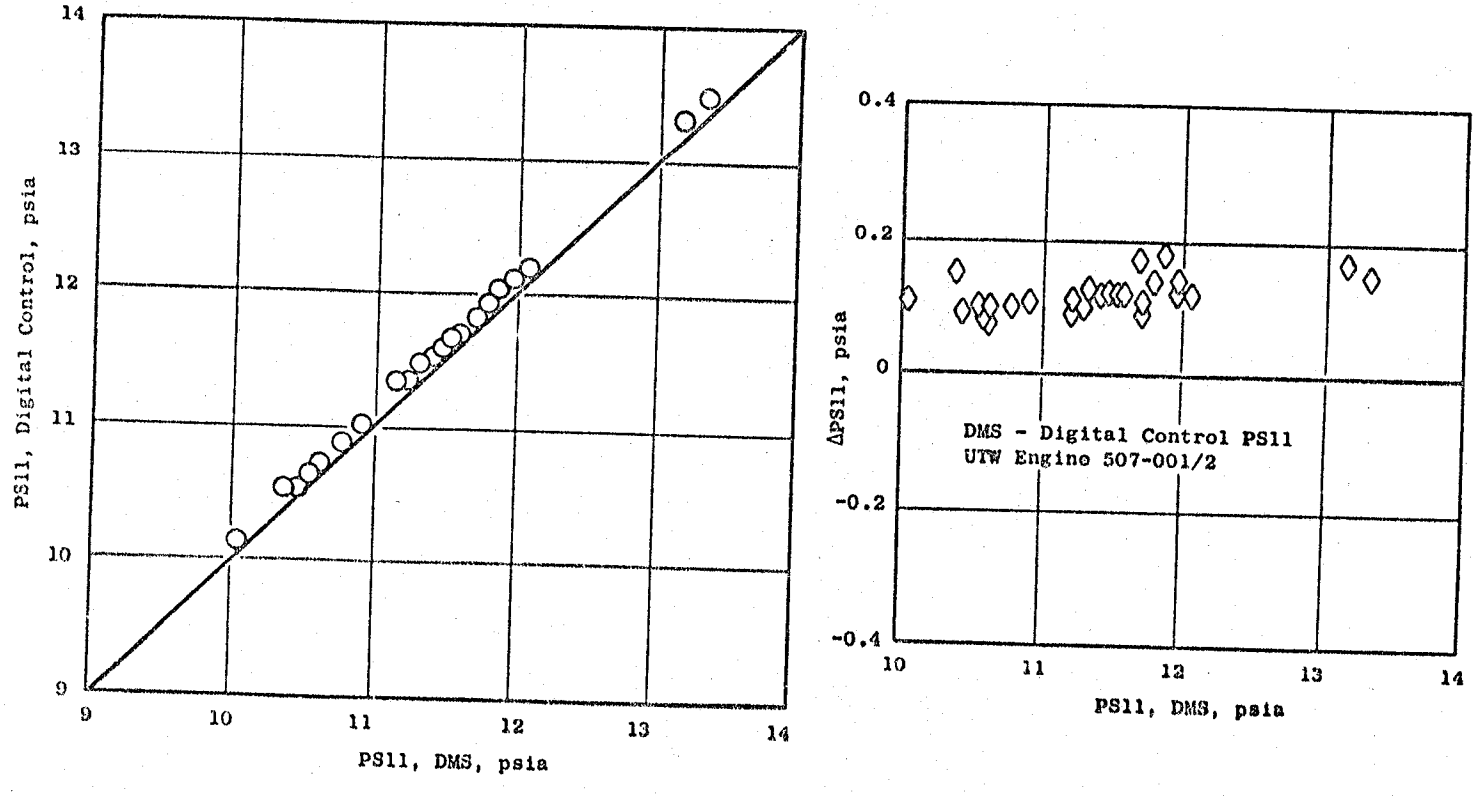

Figure 76. Data System Check.

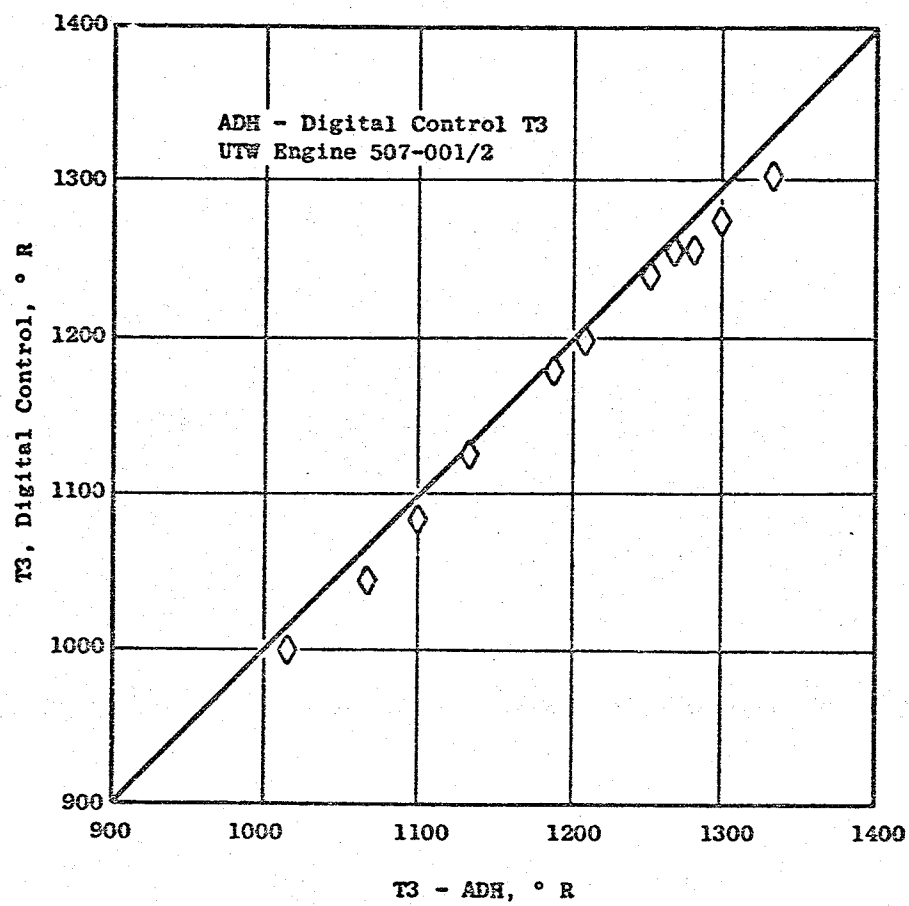

Figure 77. Data System Control.

16.0 VARIABLE PITCH ACTUATION SYSTEM

In the second build of the QCSEE UTW engine, the Hamilton Standard cam/harmonic drive actuator was replaced with the General Electric ball spline actuator. This actuator, shown in Figure 78, operates in the following manner.

A hydrualic motor located on the fan centerline drives a ball screw actuator through a differential gear and no-back. Linear motion of the ball nut of the ball screw causes the translating sleeve (middle member) of a ball spline to move in a fore or aft direction. The ball spline is a double-acting member with helical ball tracks between the translating sleeve and inner member and straight ball tracks between the sleeve and the outer ball spline member. The inner member is attached to the aft ring gear while the outer member is attached to the forward ring gear. Translation of the ball spline sleeve fore and aft drives the two ring gears in tangentially opposite directions. The ring gears, in turn, are mated to 18 pinion gears that are splined to the corresponding fan blade trunnion.

Gear ratio between the hydraulic motor and the fan blade is 479/1. Two LVDT's driven by the hydraulic motor provide a blade angle feedback to the engine digital control system.

This actuator had been whirligig tested (see Reference 6) using a 7.21 cm^3/rev (0.44 $in.^3$/rev) motor which was changed to a 8.52 cm^3/rev (0.52 $in.^3$/rev) motor for the engine build. This was done to obtain more torque capability for actuating the blades since problems were encountered in the first build above 2654 rpm using the Hamilton Standard actuator. The General Electric actuation system actuated blades at the maximum fan speed of 3130 rpm (95 percent speed). At this speed, actuations were made from blade angles of +9° closed to -5° open and the motor ΔP was 1875.4 N/cm^2 (2720 psid).

16.1 ACTUATOR PROBLEMS

16.1.1 Gear Shimming

Early in the testing of the QCSEE UTW Build 2 engine, it was found that the actuator was shifting, which caused engine vibration problems. A shim which controls the clamp-up on the 18 pinion gears was reduced by 0.38 mm (0.015 inch) to increase the clamp-up on the gears. All subsequent testing showed no indication of actuator shift.

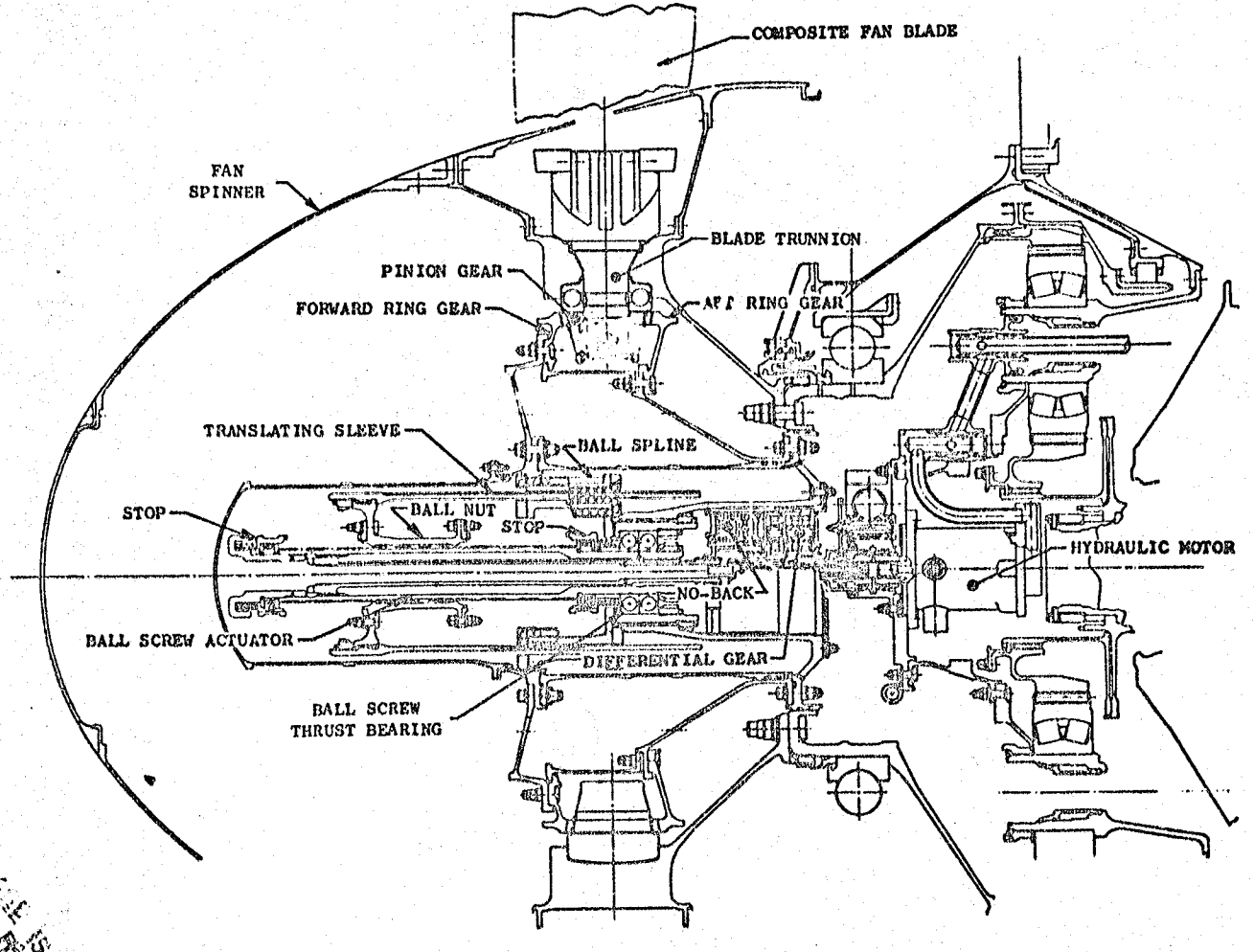

Figure 78. General Electric Ball Spline Actuation System.

16.1.2 Backlash

The apparent backlash of 5° in the actuator is more than originally calculated. When the actuator was reshimmed to improve the engine vibration problem, various checks were made to determine the location of this backlash. The majority of the backlash was found to be in the ball spline. This backlash has not been a major problem in testing at the Peebles Test Site.

16.1.3 Differential Gear Failure

On March 10, 1978, a failure of the differential gear in the variable pitch mechanism occurred. This is shown in Figure 79. Because of the physical condition of the failed parts within the differential assembly, it was not possible to conclusively define the failure cause or sequence. The most likely areas of failure initiation were:

- Aft sun gear bearing
- Planet bearings in the first stage
- Plane bearing carrier

With these areas identified, new hardware was obtained and the differential was rebuilt with the following changes:

- Additional oil was added to the aft sun gear bearing.
- A scoop was added to the differential coverplate so more oil could be introduced into the differential gearing.
- The original three-planet differential design was replaced with a five-planet design to reduce the individual planet bearing and gear loading to 60 percent of original loading.
- The planet bearing carrier material was changed from aluminum to steel for additional strength.
- The differential output ring gear was modified to let additional oil into the differential gearing.

While changes were being made, engine testing continued with a device installed to "lock out" the differential gear where blade angles were changed by manual actuation.

The new differential hardware was installed and a mechanical checkout was made with no problems.

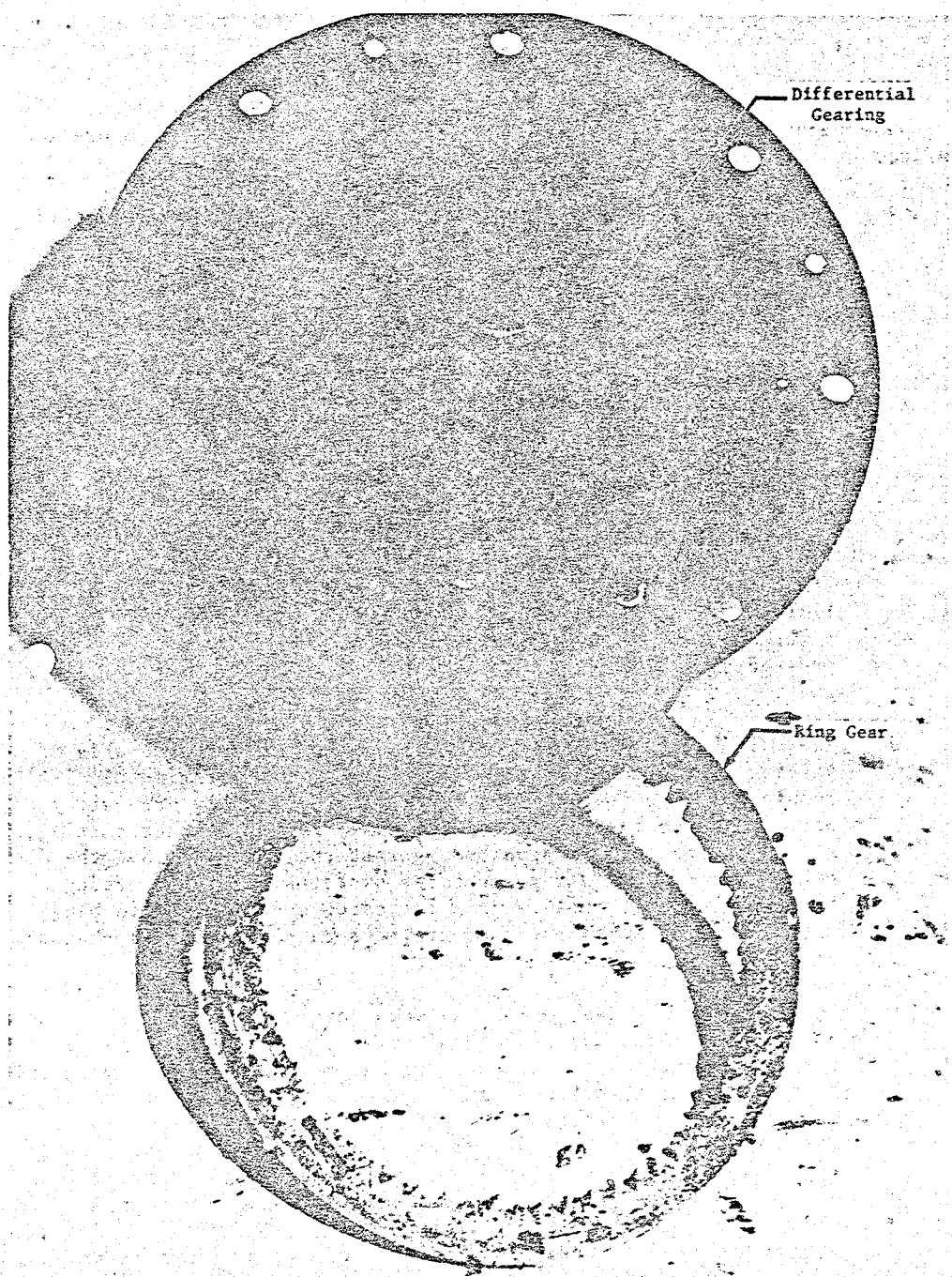

Figure 79. Variable Pitch Differential Gearing.

17.0 TEST RESULTS

The major results of testing the QCSEE UTW propulsion system are summarized as follows:

- In the forward thrust mode, unsuppressed source noise exceeded estimates. The reasons for this are not fully understood, and further testing with noise probes is suggested to determine the exact source. The acoustic suppression system performed as expected, so that the suppressed noise slightly exceeded the 95 EPNdB goal as follows:

  152.4 m (500 ft) Sideline Noise Level
  Based on Four-Engine 58,968 kg (130,000 lb) Aircraft

Takeoff	97.2 EPNdB
Approach	95.7 EPNdB

- In the reverse thrust mode, 27 percent of maximum forward installed thrust was achieved with -100° open blade angle. The T5 limit was reached at this point, preventing further increase in power setting. At the maximum reverse thrust point, the peak suppressed sideline noise level was 105 PNdB compared to the 100 PNdB goal.

- The ball spline variable pitch actuation system was capable of varying fan blade angles at all fan speeds. Approximately 1.4° of running hysteresis existed in the system, probably due partly to ball clearance in the spline tracks. For steady-state testing, blade settings were approached against the load, so that the blade twisting moments would prevent the hysteresis from affecting the blade angle. Performance data indicated a difference in blade angle of about 2° compared to previous data with the cam-harmonic pitch actuation system.

- The composite blades, which had been damaged by ingestion of an exhaust nozzle flap during Build 1 reverse thrust testing, were replaced with blades of the same design, although it was recognized that this design was incapable of meeting FAA bird strike requirements, and had exhibited a vibratory sensitivity in the range of the two-per-rev/first flex crossover. The vibratory problem was aggravated by high crosswinds and tailwinds. During Build 2 testing, delays were caused on a number of occasions by adverse wind conditions. Previous plans to test the engine in the crosswind facility were abandoned, and forward to reverse thrust transients were not attempted.

- The digital control system functioned very well during all steady-state testing. Stability and accuracy in holding all engine variables were excellent in the manual mode of operation. Two semi-automatic modes were demonstrated: inlet Mach number control and engine pressure ratio control. No problems were encountered during these demonstrations. The fully automatic control mode, in which the operator calls for a percent rated thrust and the control sets all variables, operated well at steady-state conditions, and over small thrust transients (5%), but allowed a 300 rpm overshoot in attempting to accelerate from 62 to 85% thrust. This was believed to be a result of internal leakage in the hydraulic motor, and future testing should include acceleration tests with the electrical gain of the control circuit increased.

- The main reduction gear continued to operate very satisfactorily. Further development is warranted, however, to develop the lube system to reduce oil churning and achieve the design levels of gear efficiency.

- Composite nacelle components and the composite fan frame were very satisfactory. Some delamination occurred in the frame vanes and in the exhaust nozzle flaps, but parts were readily repaired without removal from the engine.

- At 43:37 hours, the radial accessory drive shaft failed, losing driving power to the accessories. The failure occurred in the top spline with conclusive indication of fatigue propagation. Analysis showed that the spline design was marginal, and that the method of aligning the accessory gearbox was unsatisfactory. A replacement shaft was procured, with a modified spline. It was installed with an improved gearbox alignment technique and no further trouble was experienced.

- After 59 hours of engine testing, the differential planetary gears in the pitch actuation system failed. This failure apparently originated in the bearings. Replacement parts were ordered with several design changes to reduce bearing loads and improve lubrication. While these parts were being procured, an adapter was fabricated to permit enine testing to continue with the fan pitch fixed. The replacement differential parts were installed and checked out before the end of the test period.

18.0 REFERENCES

1. The General Electric Company, "QCSEE Under-The-Wing (UTW) Engine Boilerplate Nacelle Test Report," Volumes I - III, NASA CR-135249, 250, and 251, December 1977.

2. The General Electric Company, "Quiet Clean Short-Haul Experimental Engine Under-The-Wing Final Design Report," NASA CR-134847, June 1977.

3. The General Electric Company, "Aerodynamic and Aeromechanical Performance of a 50.8 cm (20 in.) Diameter 1.34 Pressure Ratio Variable Pitch Fan with Core Flow," NASA CR-135017, August 1977.

4. The General Electric Company, "QCSEE UTW Engine Composite Blade Design," NASA CR-134840, May 1975.

5. The General Electric Company, "QCSEE UTW Engine Composite Fan Blade Final Design Test Report," NASA CR-135046, February 1977.

6. The General Electric Company, "Ball Spline Pitch Change Mechanism Test Report," NASA CR-135354, October 1978.

End of Document